Systems Biotechnology of *Pseudomonas putida* for the enhanced production of Polyhydroxyalkanoates: a rational approach for strain and bioprocess engineering

Von der Fakulät fur Lebenswissenschaften
der Technischen Universwität Carolo-Wilhelmina
zu Braunschweig
zur Erlangung des Grades eines
Doktors der Naturwissenschften
(Dr. rer. nat.)
genehmigte
Dissertation

von Ignacio Andrés Poblete Castro
aus Santiago, Chile

1. Referent: Prof. Dr. Christoph Wittmann
2. Referent: Prof. Dr. Dieter Jahn
3. Referent: Prof. Dr.-Ing. Vitor Martins dos Santos

eingereicht am: April 16th 2012
mündliche Prüfung (Disputation) am: July 16th 2012

Druckjahr 2012

Vorveröffentlichungen der Dissertation

Teilergebnisse aus dieser Arbeit wurden mit Genehmigung der Fakultät für Lebenswissenschften, vertreten durch den Mentor der Arbeit, in folgen Beiträgen vorab veröffentlicht:

Publikationen:

Poblete-Castro I, Becker J, Dohnt K, dos Santos V, Wittmann C. 2012. Industrial biotechnology of *Pseudomonas putida* and related species. Applied Microbiology and Biotechnology 93(6):2279-2290.

Poblete-Castro I, Escapa I, Jager C, Puchalka J, Lam C, Shomburg D, Prieto MA, dos Santos VAP. 2012. The metabolic response of *Pseudomonas putida* KT2442 producing high levels of polyhydroxyalkanoates under single- and multiple-nutrient-limited growth: Highlights from a multi-level omics approach. Microbial Cell Factories 11:34.

Poblete-Castro I, Binger D, Rodriguez A, Becker J, dos Santos VAP, Wittmann C. 2012. In-silico-driven metabolic engineering of *Pseudomonas putida* for enhanced production of poly-hydroxyalkanoates. Metabolic Engineering.

Tagungsbeiträge:

Poblete-Castro I. 2008. Systems analysis of stress response on poly-hydroxyalkanoates production in *Pseudomonas putida* with relative and non-relative carbon sources. 2nd International PhD symposium, Braunschweig. Germany. (Poster)

Poblete-Castro I, Fernandez I, Prieto MA, Jager C, Schomburg D, Puchalka J, dos Santos VAP. 2009. Omics analysis of mcl-poyhydroxyalkanoates in *Pseudomonas putida* KT2442 under different nutrient limitations. 12th International Conference on Pseudomonas, Hannover. Germany. (Poster)

Poblete-Castro I, Janus D, Puchalka J, dos Santos VAP, & Wittmann C. 2011. Model-driven enhancement of PHA synthesis in *Pseudomonas putida* KT2440: Reprogramming the cell for industrial biocatalysis. 13th International Conference on Pseudomonas, Sydney. Australia. (Speaker)

Lo que puede el sentimiento no lo ha podido el saber, ni el más claro proceder, ni el más ancho pensamiento (Violeta Parra).

Dedicada a todos mis seres queridos, especialmente a mi vieja

TABLE OF CONTENTS

Ackwnoledgments ..... **ix**

Abstract ..... **xi**

Zusammenfassung ..... **xiii**

CHAPTER I. General Introduction **1**

1.1 Background **1**

1.2 Industrial production of PHAs **5**

1.3 Project Rationale **8**

1.4 References **9**

CHAPTER II. Industrial biotechnology of *Pseudomonas putida* and related species **11**

2.1 Background **12**

2.2 Carbon core metabolism of *Pseudomonas putida* **12**

2.2.1 Substrate uptake 13

2.2.2 Catabolic metabolism 14

2.2.3 Redox metabolism 15

2.2.4 Bio-conversion and degradation of non-natural chemicals 15

2.3 Genetic engineering **16**

2.4 In silico modeling of metabolism **16**

2.5 Systems-level profiling by omics technologies **17**

2.5.1 Transcriptomics 18

2.5.2 Proteomics 18

2.5.3 Metabolomics 19

2.5.4 Fluxomics 19

2.6 Industrial applications of *P. putida* strains **20**

2.6.1 Bio-based materials 20

2.6.2 Bioconversion and de-novo synthesis of chemicals 22
2.6.3 Pharmaceuticals and agrochemicals 27

2.7 Conclusions and future perspectives 28

2.8 Acknowledgements 30

2.9 References 31

CHAPTER III. The metabolic response of *P. putida* KT2442 producing high levels of polyhydroxyalkanoate under single- and multiple-nutrient-limited growth: Highlights from a multi-level omics approach 42

3.1 Abstract 42

3.2 Background 44

3.3 Material and Methods 46

3.4 Results and Discussion 54
3.4.1 Physiological response of *Pseudomonas putida* under nutrient-limited conditions 54
3.4.2 PHA accumulation *versus* nutrient availability 59
3.4.3 Global multi-omics analysis of *P. putida* response under various nutrient limitations 60
3.4.4 Integrated analysis of the various "omics" results under different nutrient limitations 69
3.4.5 Process optimization for increasing PHA synthesis in chemostat culture based on a "top-down" approach 84

3.5 Conclusions 87

3.6 Acknowledgments 88

3.7 References 89

CHAPTER IV. *In silico*-driven metabolic engineering of *Pseudomonas putida* for enhanced production of poly-hydroxyalkanoates 104

4.1 Abstract 104

4.2 Introduction 105

4.3 Materials and methods 107

4.4 Results 114

4.4.1 Growth and PHA production performance of the *Pseudomonas putida* wild type on glucose as carbon source 114

4.4.2 *In silico* network modeling of PHA production in the *Pseudomonas putida* wild type 114

4.4.3 *In silico* flux design for superior PHA production 116

4.4.4 Construction and evaluation of PHA-producing capacity of different metabolically enginnered *P. putida* strains 118

4.4.5 Transcriptome profiling of the designed producing strains P. putida Δ*gcd* and *Δgcd-pgl* 120

4.4.6 Evaluation of the designed PHA hyper-producer *P. putida* Δ*gcd* in batch bioreactors 124

4.4.7 Characteristics of *P. putida* strains deficient in 6-phosphoglucolactonase 126

4.5 Discussion 127

4.6 Conclusion 130

4.7 Acknowledgments 131

4.8 References 132

CHAPTER V. Production of mcl(PHA) in high-cell-density cultures of metabolically engineered *P. putida* strains. 136

5.1 Abstract 136

5.2 Materials and methods 137

5.3 Results 139

5.3.1 High-cell-density culture of *P. putida* KT2440 139

5.3.2 Nitrogen limitation along with a linear feeding strategy induces PHA synthesis 139

5.3.3 High-cell-density cultures of mutant strains 141

5.4 Discussion 143

5.5 Acknowledgments 145

5.6 References 145

CHAPTER VI. Summary and outlook 147

CHAPTER VII. Supplementary material 152

Curriculum vitae.....166

Ackwnoledgments

First of all I would like to thank to Prof. Dr. Vitor Martins dos Santos who gave me the opportunity to start my PhD work in his group at the Helmholtz Centre for Infection Research and allows me always to follow my ideas in every stage of the project. To Prof. Dr. Christoph Wittmann who since the very beginning supported my scientific approach and who has been a source of knowledge and a perfect match as a scientific partner. To my partnerships from Madrid, Auxi and Ife, who introduced me to this challenging world of PHAs and extended me a hand whenever I needed it. To Dr. Roberto Bobadilla who was the first to show me how fascinating is to be devoted to the pursuit of new knowledge. It has been a privilege to work with all of you.

I couldn't miss the opportunity to be grateful to all my friends from the former SSBI group with whom I have exchanged so many experiences; happiness, sadness, discussions, supports, and learning moments. Audrey, Carolyn, Danielle, Joost, Petra, Jacek, Agata, Bianka, Blair, Guru, Christoph, Pioter, Andrew, Maria, Jörg, and Alex, thank to all of you that in one way or another contributed to the achievement of this research project. Sagra and Monica, even though you belonged to another group you always give me the time for deep scientific discussions and support in the toughest moments (gracias amigas son las mejores).

To all my friends from the HZI with whom I shared so many parties, grills, dinners, lab space, and greats moments in these four years in Germany; Maca, Dieco, Andreia, Chema, Jenya, Angi, Tobi, Rolf, Daia, Marcia, Juergen, Christian, Maira, Marcela, Marcelo, Christina, Cristina, Andre, Baraham, Diego, Maxi, Alejandra, and Amelia.

A mi familia y amigos de Chile, que a pesar de la distancia los sentí cerca y como siempre un infinito apoyo en este proyecto, sin ustedes no lo hubiera logrado. A Alex, a quien siento mi mejor amigo en Alemania. Gracias *Scarlett* por todo el apoyo y comprensión, y sobre todo la buena onda.

A ti Eve, que te sumaste al final de este proceso y me has apoyado de sobre manera, gracias amor por toda tu comprensión y paciencia.

Abstract

Oil-based plastic production processes have given rise to several environmental problems and energy availability. Over the past 30 years, polyhydroxyalkanoates (PHA) have become one of the main sustainable alternatives to replace petroleum-base commodities. These biopolymers have superior features than synthetic plastics since they are produced from biobased sources and their intrinsic chemical composition make them biodegradable, biocompatible, and part of the carbon cycle of the earth. Although there is a vast knowledge base for synthesizing eco-friendly biopolymers, the industrial production of PHAs is still 5-10 more expensive to obtain than conventional plastics.

Therefore, the present research addresses this critical issue by using *Pseudomonas putida* as a cell factory along with a systems biotechnology approach with the aim of enhancing the production of PHAs. First, it was shown that *P. putida* and related species are suitable as whole-cell biocatalyzers for the production of several value-added industrial compounds. To highlight differences among various nutrient limitations and their influence on PHA synthesis in *P. putida* KT2442, chemostat cultures were employed to perform well-controlled nutrient limitations. Strict nitrogen-limiting condition reached the highest PHA productivity in standard continuous cultivation ever reported. To gain insight into the PHA machinery, transcriptome, proteome, and metabolome analyses were employed to investigate the metabolic responses under such limiting conditions. Dual limitation showed different expression patterns in comparison to those observed under strict carbon- or nitrogen-limiting conditions. Energy metabolism, fatty acids metabolism, stress response, and proteins belonging to the transport system were the components of the cell which were highly affected by the imposed nutrient limitation. Driven by the systems biology approach, it was possible to increase the PHA accumulation under dual limitation, which shows to use the carbon source in the most efficient and economic manner among all tested conditions.

In order to reduce the production costs for PHA synthesis, *P. putida* KT2440 and *in silico*-driven metabolically engineered strains were subjected to PHA-producing conditions using the inexpensive

carbon source glucose. Indeed, the created Δ*gcd* mutant strain exhibited 60% increase in PHA accumulation as compared to the parental wild-type strain. The mutant maintained a high specific growth rate and exhibited an almost unaffected gene expression profile. To further develop an industrial-scale PHA production process, the *P. putida* strains were subjected to the industrial process of choice — the fed-batch cultivation. After the application of an exponential-feeding strategy for biomass synthesis, the PHA accumulation stage should be promoted by applying a pulse-feeding instead of a linear-feeding approach, which appears to be more appropriated for PHA synthesis in *P. putida* within high cell cultivations. In conclusion, the results described in this thesis have shown the strength of *in silico* modeling and integration of omics measurements to lead metabolic engineering works towards optimal performance of the cell and reengineering processes for the synthesis of polyhydroxyalkanoates.

Zusammenfassung

Die Produktion von Kunststoffen aus Erdöl ist mit erheblichen Umweltproblemen verbunden. Darüber hinaus stellt sich die Frage nach der zukünftigen Verfügbarkeit des nicht erneuerbaren Rohstoffs. Während der letzten 30 Jahre haben sich Polyhydroxyalkanoate (PHA) als nachhaltige Alternative zu Erdöl-basierten Produkten durchgesetzt. Im Gegensatz zu synthetischen Kunststoffen haben diese Biopolymere den Vorzug, dass ihre chemische Zusammensetzung sie biokompatibel und zugänglich für Biodegradation macht. Als Teil des natürlichen Kohlenstoffzyklus ist ihre Verwendung CO_2-neutral. Trotz einer enormen Wissensbasis über die Synthese umweltfreundlicher Biopolymere ist die industrielle Produktion von PHA immer noch fünf bis zehnmal teurer als die herkömmlicher Kunststoffe.

Die vorliegende Arbeit widmet sich diesem wichtigen Thema mit dem Ziel die Produktionsrate von PHAs durch einen systembiotechnologischen Ansatz in *Pseudomonas putida* als Zellfabrik zu steigern. Zunächst wurde gezeigt, dass lebende Zellen von *P. putida* und verwandter Spezies als Biokatalysatoren für die Herstellung verschiedener industriell relevanter Grundstoffe geeignet sind. Während kontinuierlicher Kultivierungen in der kontrollierten Umgebung eines Chemostats wurde der Einfluss verschiedener Nährstoff-Limitierungen auf den Stamm *P. putida* KT2442 sowie dessen Produktion von PHA untersucht. Unter strikter Stickstoff-Limitierung wurden die höchsten PHA-Konzentrationen erreicht, die bisher in kontinuierlichen Kulturen gemessen wurden. Um einen Einblick in die Biosynthese von PHA unter verschiedenen limitierenden Bedingungen zu erhalten, wurden Transkriptom-, Proteom- und Metabolom-Studien durchgeführt. Gleichzeitige Stickstoff- und Kohlenstoff-Limitierung zeigte dabei im Vergleich zu den einzelnen Limitierungen ein stark unterschiedliches Expressionsprofil. Unter den zellulären Komponenten, die am stärksten durch die Nährstoff-Limitierungen beeinflusst waren fanden sich der Energie-Metabolismus, der Fettsäure-Metabolismus, die Stressantwort sowie Bestandteile des Transportsystems. Mit Hilfe des Systembiologischen Ansatzes war es möglich, die PHA Biosynthese unter beiden Limitierungen zu erhöhen. Unter dieser Bedingung wurde die Kohlenstoffquelle am

effizientesten und ökonomischsten genutzt. Um die Produktionskosten für PHA weiter zu minimieren, wurden *P. putida* KT2440 und *in silco* abgeleitete Stämme unter Bedingungen kultiviert, die eine PHA-Produktion mit der kostengünstigen Kohlenstoffquelle Glukose begünstigen. Der Stamm mit einer Δgcd-Mutation zeigte eine um 60% erhöhte PHA-Akkumulation im Vergleich zum Wildtyp-Stamm. Dabei zeigte dieser Stamm eine hohe spezifische Wachstumsrate und ein Genexpressionsprofil, das durch die Mutation kaum beeinflusst wurde. Um die PHA-Produktion im Industrie-Maßstab weiterzuentwickeln wurde die *P. putida*-Stämme mit der Methode der Wahl aus der Industrie kultiviert – dem „Fed-batch Process“. Nach der Anwendung eines exponentiellen Fütterungsansatzes, um die Bildung von Biomasse zu optimieren sollte die Bildung von PHA über eine gepulste statt lineare Fütterungsstrategie angeregt werden. Diese stellte sich während der Hochdichte-Zellkultivierung als wesentlich geeigneter für die maximale PHA-Biosynthese heraus.

Zusammenfassend zeigen die in dieser Arbeit vorgestellten Resultate die Stärke von *in silco* basierten Methoden der Integration von „Omics“-Daten und Modellierung für die Optimierung von Stämmen für die Biosynthese von polyhydroxyalkanoaten.

CHAPTER I. General Introduction

1.1 Background

Increasing generation of petroleum-based commodities has given rise to sever energy and environmental problems. The U.S. Energy Information Administration (EIA) estimates that more than 4% of the worldwide oil consumption is used for plastic production, which reflects approximately a consumption rate of 155 million tons of petroleum annually. Biotechnological processes offer the potential to sustainable manufacturing such products, which benifits society and environment by reducing demands on fossil resources. Since the rapid increase and high fluctuation of the oil price in recent years (Fig.1), not only biofuel, but also the synthesis of renewable bio-derived polymers has advanced towards large-scale production.

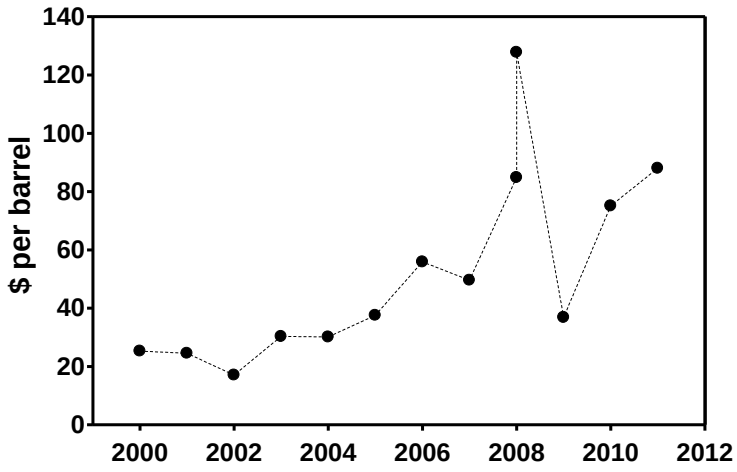

Figure 1. Development of the crude oil prices per barrel (U.S. Energy Information Administration, 2012).

Biopolymers can substitute oil-based plastics due to their similar physical and mechanical properties to conventional plastics. Among them, polyhydroxyalkanoates (PHAs) and polylactic acid (PLA) are promising biopolymers since they can be synthesized from several renewable feedstocks e.g., biomass, industrial wastes. PHAs comprise a large class of polyesters. These accumulate in the bacterial cell in

response to fluctuation of nutrient availability in the environment, specifically when carbon is in excess accompanied by the limitation of one or several inorganic nutrients such as nitrogen, phosphorus, oxygen, etc. There have been more than 150 different types of identified PHAs (Steinbüchel and Valentin 1995) which the number of newly identified PHAs has gone beyond expectation in the last decade.

PHAs can be classified into two groups according to the length of the side chain (Hazer and Steinbüchel 2007); (i) short-chain-length (scl), having an alkyl side chain up to two carbons, and (ii) medium-chain-length (mcl), with an alkyl chain consisting of at least three carbons (Fig. 2). Several bacteria have the capability to naturally produce PHAs. *Cupriavidus necator* (formerly known as *Ralstonia eutropha*) and *Alcaligenes latus* synthesize scl-PHAs such as poly-(*R*)-3-hydroxybutyrate (PHB), and poly((*R*)-3-hydroxybutyrate-co-(*R*)-3-hydroxyvalerate) (PHBV). *Pseudomonas*, belonging to the rRNA homology group I accumulate mcl-PHAs in the presence of fatty acids and sugars (Huijberts et al. 1994b). The monomer composition of the resulting mcl-PHA depends on many factors such as the supplied carbon source, cultivation conditions, and the affinity of the PHA synthase (PhaC) for the substrate (Steinbüchel and Valentin 1995).

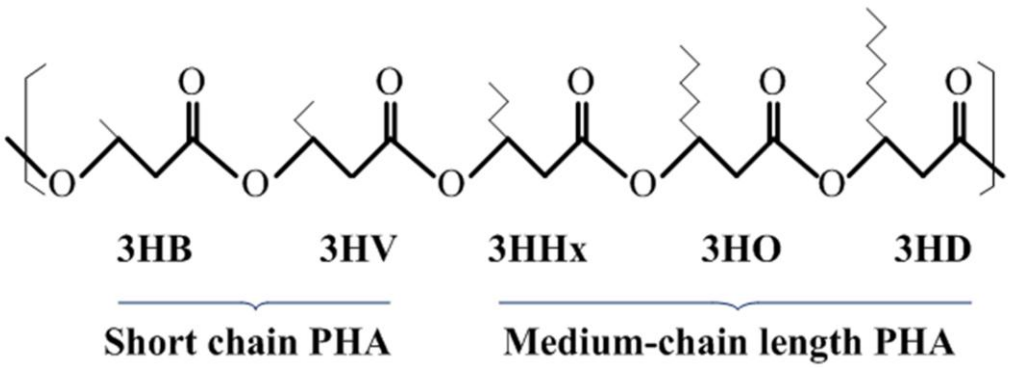

Figure 2. Chemical structure of various PHAs (Adapted from Chen and Chen 2010).

P. putida KT2440 and its rifampisin-resistant derivate KT2442 (Bagdasarian et al. 1981) have been used as laboratory workhorses to investigate PHA formation at the molecular level as well as the pathway organizations and their regulations. PHA precursors can be formed via the *β*-oxidation pathway, *de novo* fatty acid biosynthesis, and elongation of 3-hydroxyalkanoates by acetyl-CoA molecules (Huijberts et al. 1994b). The substrates that activate each pathway for PHA formation in *Pseudomonas* are shown in Figure 3. Fatty acids are oxidized in several steps trough the *β*-oxidation route yielding several precursors towards the formation of (*R*)-3-hydrxyacyl-CoA the substrate of PHA polymerase (PhaC). When glucose or gluconate are employed as carbon sources the route of de novo fatty acid biosynthesis is active. The key enzyme to turn (*R*)-3-hydroxyacyl-ACP into (*R*)-3-hydrxyacyl-CoA was identified as a 3-hydroxyacyl-ACP-CoA transacilase (PhaG) (Rehm et al. 1998).

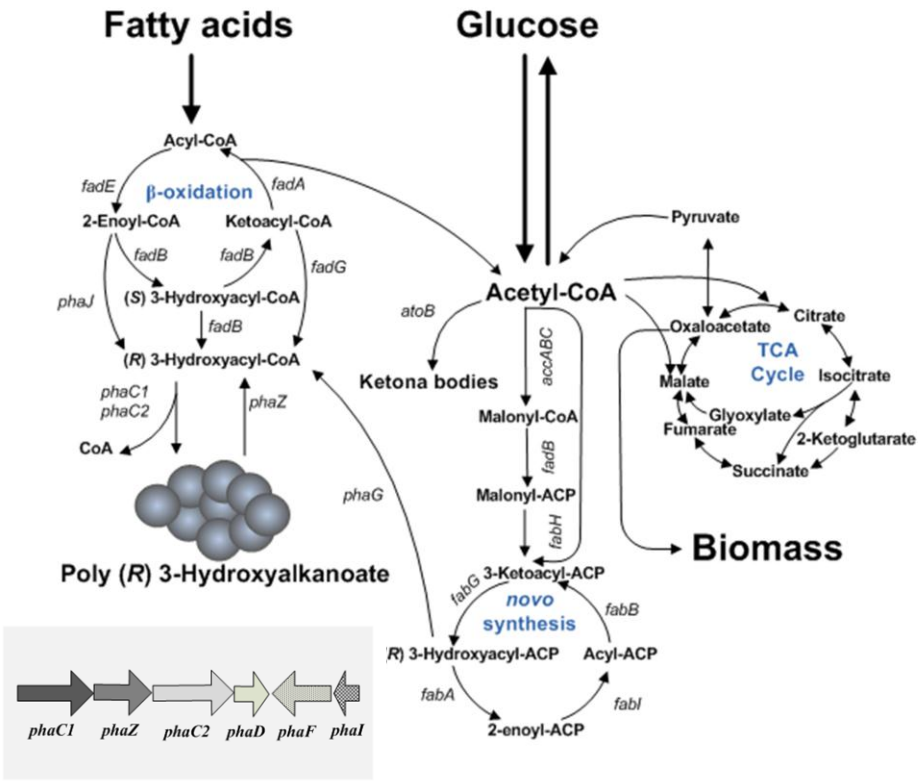

Figure 3. Linkages between PHA biosynthetic pathways in *Pseudomonas putida* KT2440.

The regulation of PHAs pathways has been extensively studied in the genus *Pseudomonas*. Besides PHA synthases (PhaC1 and PhaC2), the *pha* operon has two additional genes, *phaZ* and *phaD*. PhaZ is a depolimerase (lipase) which participates in the degradation process of the granule, releasing hydroxyacyl-CoA derivates from PHAs (Luengo et al. 2003). An additional cluster, which also encodes genes related to PHAs synthesis, is located downstream of the *pha* operon (Fig. 3). PhaI and PhaF are phasins which participate in granule formation and localization within the cell (Galan et al. 2011; Prieto et al. 1999). Interestingly, PhaF plays a role as regulator since it seems to repress transcription of the polyester synthase gene (*phaC1*) and the transacylase gene (*phaG*) (Hoffmann and Rehm 2004). On the other hand, PhaF protein also has a structural function giving stabilization to the granule by creating a phospholipid monolayer between the hydrophobic polymer and the hydrophilic cytoplasm (Kessler and Witholt 2001).

Recently, it was shown that P(I) and P(C1) are the most active promoters of the *pha* cluster (de Eugenio et al. 2010c). Their transcription explain the simultaneous production of PHA depolymerase and synthase. In the same study, *phaD* gene was proved to be a transcriptional regulator, which behaves as a carbon-source-dependent activator of the *pha* cluster. An important external component of the PHA synthesis is the sigma factor σ^{54} encoded by *rpoN*. This regulates at the transcriptional level the PHA biosynthetic genes in *P. aeruginosa* when gluconate is the carbon source (Madison and Huisman 1999) whereas the pathway from fatty acid is completely σ^{54}-independent (Timm and Steinbuhel 1992). The *rpoN* is also suggested as a negative regulator of *phaF* transcription. On the other hand, transcription of *phaC*1 in *P. putida* is not affected by this regulator (Hoffmann and Rehm 2004). The phosphoenolpyruvate-carbohydrate transferase system in *P. putida* KT2440 has five enzymes. It was found that the genes encoding for the proteins EI^{Ntr}, NP^{r}, and EII^{Ntr}, act in concert to modulate the accumulation of PHA (Velazquez et al. 2007).

1.2 Industrial production of PHAs

The industrial production of PHAs began in the 80's when Biopol® —a copolymer made from PHBV— was created by the British's Imperial Chemical Industry (Shah et al. 2008). A two-stage fermentation method was applied to obtain a high PHBV productivity. In 1992 the Boston-based company Metabolix (formerly known as Monsanto) purchased the rights to produce and commercialize Biopol®. Nowadays, Metabolix markets its PHA under the commercial name Mirel® (Chen and Chen 2010). Microbial fermentation is the process of choice for industrial production of PHAs. As many bacteria naturally accumulate PHAs, high cell density fermentation processes were developed to reach PHB productivities up to 4.5 (g/L·h) in the presence of sugar (Table. 1). Nevertheless, only PHB and PHBV are obtained when *C. necator*, *Bacillus spp*, and *A. latus* are used as microbial factories. By applying metabolic engineering strategies, several heterolougus genes have been integrated into *E. coli* — the most employed industrial organism — to obtain different copolymers thus expanding the range of the mechanical as well as the physical properties of the synthesized polyester (Chen 2009).

Table 1. Wild types and industrial bacterial strains for the production of scl-PHA.

Strain	DNA manipulation	PHA type	Productivity (g/L·h)	C-source	Reference
Alcaligenes eutrophus	NO	PHB	3.14	Glucose	Ryu et al. 1997
Escherichia coli	*phbCAB*	PHB	3.2	Glucose	Wang and Lee 1997
Alcaligenes latus	NO	PHB	4.58	Sucrose	Wang and Lee 1997
Bacillus megaterium BA-019	NO	PHB	1.27	Sugars	Kulprescha 2009

At present *P. putida* strains seems not to be used to produce mcl-PHA at industrial scale. In the research field vast information has been generated concerning pathway organization and fermentation strategies to obtain tailored-made mcl-PHAs. It is important to highlight that commercial processes for the production

of PHAs should have volumetric productivities ranging from 0.7 to 2.4 (g/L·h) (Huijberts et al. 1994b). As it is observed in Table 2 many fermentation strategies have achieved such productivity values, positioning *P. putida* as an appropriate industrial strain.

Table 2. *P. putida* strains for the production of mcl-PHA.

Strain	Fermentation mode	Productivity (g/L·h)	C-source	Reference
P. putida GPo1	Continuous	1.06	Octane	(Jung et al. 2001)
P. putida KT2442	Fed-Batch	1.91	Oleic acid	(Lee et al. 2000)
P. putida KT2442	Fed-Batch	1.44	Nonanoic acid	(Sun et al. 2007b)
P. putida IPT046	Fed-Batch	0.80	Glucose + Fructose	(Diniz et al. 2004)
P. putida KT2442	Fed-Batch	0.68	Corn oil hydrolysate	(Shang et al. 2008)

PHA production has several drawbacks as compared to established oil-based plastic production, especially regarding the high cost associated with the synthesis of PHAs. To make them competitive against petrochemical polymers, the use of inexpensive carbon sources such as sugars, PHA-producer bacterial communities in waste water treatments, and systems metabolic engineering of natural producer, have been proposed as possible paths to overcome the high cost issue. The pricing for raw meterials contribute most among the costs in PHA production (Yamane 1993).Therefore, the straightforward approach is to select an appropriate carbon source. In this concern, *P. putida* species are efficient cell factories for such aim (Poblete-Castro et al. 2012a), since their versatility and robustness make them capable to catabolize a broad range of compounds as well as resisting adverse environmental conditions as high substrate toxicity, temperature, pH, among others. Inexpensive substrates have been already tested in different *P. putida* strains, where their metabolic repertoires funneled resources towards PHAs synthesis.

Table 3. Physical properties of different PHAs and polypropylene (PP).

Polyester	T*g* (°C)[a]	T*m* (°C)[b]	Cristallinity	Elongation to break	Reference
PHB	15	175	70	5	(Doi 1990)
PHV	0	118	N.A.	N.A.	(Madison and Huisman 1999)
PHBV	-1	145	56	50	(Sudesh et al. 2000)
P(3HO-3HH)	-36	61	30	300	(Doi 1990)
P3HD	-37	72	N.A.	313	(Liu et al. 2011)
PP	-15	176	50	400	(Doi 1990)

N.A. Data not available

P(3HO-3HH): Poly(3-hydroxyoctanoate-co-3-hydroxyhexanoate), P3HD: Poly(3-hydroxydecanoate).

[a] glass transition temperature

[b] melting temperature

All tested *P. putida* strains produced a heteropolymer in the presence of glycerol (Wang and Nomura 2010), lignocellulosic-derivatives (Diniz et al. 2004), and residual oil from plant (Fuchtenbusch et al. 2000). Due to structural differences, the physical properties mcl-PHA are quite different from PHB and other scl-PHA (Table. 3). In addition, by applying continuous cultivation the monomer composition of the produced PHA can be exactly defined (Hartmann et al. 2004). Furthermore, metabolic engineering of the *β*-oxidation reactions has allowed synthesizing different kind of homopolymers (Liu et al. 2011) as well as novel PHA containing thioester group in the side chain, making them suitable for further chemical modifications (Escapa et al. 2011a). Taking all together, mcl-PHAs have potentially a broader application range than scl-PHAs (Madison and Huisman 1999) as environmentally friendly polymers as well as functional biomaterials for the medical field (Kim et al. 2007).

1.3 Project Rationale

The production of petroleum-based plastics has severe impacts on the environment in terms of soil and atmosphere quality, which are reflected by an increasing accumulation of non-degradable material in the ground as well as a rising global emission of greenhouse gases. Hence, the present work pursues the aims of developing metabolically engineered strains and efficient processes which enhance the production of feedstock bio-based polymer using *Pseudomonas putida* as a cell factory. As *P. putida* KT2440 and KT2442 are natural producers of one of the most promising biopolymers for plastic production *e.g.* PHAs, their metabolic network structure can be redesigned to systematically develop a superior strain.

This work aims at exploring the metabolic response at transcriptome, proteome, and metabolome level, while *P. putida* KT2442 grows in decanoic acid, a well-known precursor for PHA synthesis. Using the chemostat, a valuable tool to perform well-controlled conditions, it is possible to achieve desirable nutrient limitations. In addition, continuous culture has been proved being a good system to achieve a high PHA productivity. Little is known concerning the metabolic response under the carbon-nitrogen limitation regime, and whether this condition is more similar to strict carbon limitation or strict nitrogen limitation is not yet clear. Furthermore, carbon-nitrogen limitation has been proposed as an extremely efficient process since the carbon source is utilized in the most economical manner. Therefore, based on the top-down approach we expect to find insights of the whole-cell metabolic response that drive us to devolope a more efficient process in order to increase the PHA productivity.

The second goal is to develop an engineered *P. putida* strain based upon model-predictions, which target several genes that should increase the pool of acetyl-CoA towards PHA biosynthesis, using non-alkanoic substrates as carbon sources. This systematic analysis may provide a solid framework to optimize the production of PHA within the cell without severely impacting growth features. In order to investigate the microbial production of biopolymers, the developed strain and the parental strain (*P. putida* KT2440) will be subjected to different processes (batch and fed-batch). In addition, transcriptome analysis will be

applied to cells from PHA-producing conditions to unravel more accurately the highly complex metabolic networks that govern the cell under PHA production and non-production conditions.

1.4 References

Bagdasarian M, Lurz R, Ruckert B. 1981. Specific-purpose plasmid cloning vectors. II. Broad host range, high copy number, RSF 1010-derived vectors, and a host-vector system for gene cloning in Pseudomonas. Gene 16(1-3):237-247.

Chen G-Q. 2009. A microbial polyhydroxyalkanoates (PHA) based bio- and materials industry. Chemical Society Reviews 38(8).

Chen G-Q, Chen GG-Q. 2010. Industrial Production of PHA Plastics from Bacteria. Springer Berlin / Heidelberg. p 121-132.

de Eugenio LI, Galán B, Escapa IF, Maestro B, Sanz JM, García JL, Prieto MA. 2010. The PhaD regulator controls the simultaneous expression of the pha genes involved in polyhydroxyalkanoate metabolism and turnover in *Pseudomonas putida* KT2442. Environmental Microbiology 12(6):1591-1603.

Diniz S, Taciro M, Cabrera Gomez J, Pradella J. 2004. High-Cell-Density cultivation of *Pseudomonas putida* IPT 046 and medium-chain-length polyhydroxyalkanoate production from sugarcane carbohydrates. Applied Biochemistry and Biotechnology 119(1):51-69.

Doi Y. 1990. Microbial polyesters. VCH, New York.

Escapa I, Morales V, Martino V, Pollet E, Averous L, Garcia J, Prieto M. 2011. Disruption of B-oxidation pathway in *Pseudomonas putida* KT2442 to produce new functionalized PHAs with thioester groups. Applied Microbiology and Biotechnology 89(5):1583-1598.

Fuchtenbusch B, Wullbrandt D, Steinbuchel A. 2000. Production of polyhydroxyalkanoic acids by *Ralstonia eutropha* and *Pseudomonas oleovorans* from an oil remaining from biotechnological rhamnose production. Applied Microbiology and Biotechnology 53(2):167-172.

Hartmann R, Hany R, Geiger T, Egli T, Witholt B, Zinn M. 2004. Tailored Biosynthesis of Olefinic Medium-Chain-Length Poly[(R)-3-hydroxyalkanoates] in *Pseudomonas putida* GPo1 with Improved Thermal Properties. Macromolecules 37(18):6780-6785.

Hazer B, Steinbüchel A. 2007. Increased diversification of polyhydroxyalkanoates by modification reactions for industrial and medical applications. Applied Microbiology and Biotechnology 74(1):1-12.

Hoffmann N, Rehm BHA. 2004. Regulation of polyhydroxyalkanoate biosynthesis in *Pseudomonas putida* and *Pseudomonas aeruginosa*. FEMS Microbiology Letters 237(1):1-7.

Huijberts GNM, De Rijk TC, De Waard P, Eggink G. 1994. 13C nuclear magnetic resonance studies of *Pseudomonas putida* fatty acid metabolic routes involved in poly(3-hydroxyalkanoate) synthesis. Journal of Bacteriology 176(6):1661-1666.

Jung K, Hazenberg W, Prieto M, Witholt B. 2001. Two-stage continuous process development for the production of medium-chain-length poly(3-hydroxyalkanoates). Biotechnology and Bioengineering 72(1):19-24.

Kessler B, Witholt B. 2001. Factors involved in the regulatory network of polyhydroxyalkanoate metabolism. Journal of Biotechnology 86(2):97-104.

Kim DY, Hyung WK, Moon GC, Young HR. 2007. Biosynthesis, modification, and biodegradation of bacterial medium-chain-length polyhydroxyalkanoates. Journal of Microbiology 45(2):87-97.

Lee SY, Wong HH, Choi JI, Lee SH, Lee SC, Han CS. 2000. Production of medium-chain-length polyhydroxyalkanoates by high-cell- density cultivation *Pseudomonas putida* under phosphorus limitation. Biotechnology and Bioengineering 68(4):466-470.

Liu Q, Luo G, Zhou XR, Chen GQ. 2011. Biosynthesis of poly(3-hydroxydecanoate) and 3-hydroxydodecanoate dominating polyhydroxyalkanoates by β-oxidation pathway inhibited *Pseudomonas putida*. Metabolic Engineering 13(1):11-17.

Luengo JM, Garcia B, Sandoval A, Naharro G, Olivera ER. 2003. Bioplastics from microorganisms. Current Opinion in Microbiology 6(3):251-260.

Madison LL, Huisman GW. 1999. Metabolic engineering of poly(3-hydroxyalkanoates): From DNA to plastic. Microbiology and Molecular Biology Reviews 63(1):21-53.

Poblete-Castro I, Becker J, Dohnt K, dos Santos V, Wittmann C. 2012a. Industrial biotechnology of *Pseudomonas putida* and related species. Applied Microbiology and Biotechnology 93(6):2279-2290.

Poblete-Castro I, Escapa I, Jager C, Puchalka J, Lam CMC, Schomburg D, Prieto MA, Martins dos Santos V. 2012b. The metabolic response of *P. putida* KT2442 producing high levels of polyhydroxyalkanoate under single- and multiple-nutrient-limited growth: Highlights from a multi-level omics approach. Microbial Cell Factories 11(1):34.

Rehm BHA, Krüger N, Steinbüchel A. 1998. A new metabolic link between fatty acid de novo synthesis and polyhydroxyalkanoic acid synthesis. The phaG gene from *Pseudomonas putida* KT2440 encodes a 3-hydroxyacyl-acyl carrier protein-coenzyme a transferase. Journal of Biological Chemistry 273(37):24044-24051.

Shah AA, Hasan F, Hameed A, Ahmed S. 2008. Biological degradation of plastics: A comprehensive review. Biotechnology Advances 26(3):246-265.

Shang L, Jiang M, Yun Z, Yan HQ, Chang HN. 2008. Mass production of mcl(PHAs) from hydrolyzed corn oil by fed-batch culture of *P. putida*. Worl J Microbiology and Biotechnology 24:2783-2787.

Steinbüchel A, Valentin HE. 1995. Diversity of bacterial polyhydroxyalkanoic acids. FEMS Microbiology Letters 128(3):219-228.

Sudesh K, Abe H, Doi Y. 2000. Synthesis, structure and properties of polyhydroxyalkanoates: Biological polyesters. Progress in Polymer Science (Oxford) 25(10):1503-1555.

Sun Z, Ramsay JA, Guay M, Ramsay BA. 2007. Carbon-limited fed-batch production of medium-chain-length polyhydroxyalkanoates from nonanoic acid by *Pseudomonas putida* KT2440. Applied Microbiology and Biotechnology 74(1):69-77.

Timm A, Steinbuhel A. 1992. Cloning and molecular analysis of the poly(3-hydroxyalkanoic acid) gene locus of *Pseudomonas aeruginosa* PAO1. European Journal of Biochemistry 209(1):15-30.

Velazquez F, Pfluger K, Cases I, De Eugenio LI, de Lorenzo V. 2007. The Phosphotransferase System Formed by PtsP, PtsO, and PtsN Proteins Controls Production of Polyhydroxyalkanoates in *Pseudomonas putida*. Journal of Bacteriology 189(12):4529-4533.

Wang Q, Nomura CT. 2010. Monitoring differences in gene expression levels and polyhydroxyalkanoate (PHA) production in *Pseudomonas putida* KT2440 grown on different carbon sources. Journal of Bioscience and Bioengineering 110(6):653-659.

Yamane T. 1993. Yield of poly-D(-)-3-hydroxybutyrate from various carbon sources: A theoretical study. Biotechnology and Bioengineering 41(1):165-170.

CHAPTER II. Industrial biotechnology of *Pseudomonas putida* and related species

This chapter has been published: **Ignacio Poblete-Castro**, Judith Becker, Kathrin Dohnt, Vitor A. P. Martins dos Santos, Christoph Wittmann. Applied Microbiology and Biotechnology (2012) 93:2279-2290.

Abstract

Since their discovery many decades ago, *Pseudomonas putida* and related subspecies have been intensively studied with regard to their potential application in industrial biotechnology. Today, these gram-negative soil bacteria, traditionally known as well-performing xenobiotic degraders are becoming efficient cell factories for various products of industrial relevance including a full range of unnatural chemicals. This development is strongly driven by systems biotechnology, integrating systems metabolic engineering approaches with novel concepts from bioprocess engineering, including novel reactor designs and renewable feedstocks.

Keywords

Pseudomonas putida, cell factory, bio-catalysis, biofilm, systems metabolic engineering, synthetic biology, bioeconomy

2.1 Background

Pseudomonas putida is a Gram-negative road-shaped bacterium occurring in various environmental niches, due to its metabolic versatility, and low nutritional requirements (Timmis 2002). Initiated by the pioneering discovery of its high capability to degrade rather recalcitrant and inhibiting xenobiotics, extensive biochemical analysis of this bacterium has been carried out in the recent years. In addition, *P. putida* shows a very high robustness against extreme environmental conditions such as high temperature, extreme pH or the presence of toxins or inhibiting solvents. Additionally, it is genetically accessible and grows fast with simple nutrient demand (Martins Dos Santos et al. 2004). Meanwhile, *P. putid*a is successfully used for the production of bio-based polymers and a broad range of chemicals, far beyond its initial purpose for the degradation of various toxic compounds. The sequencing of its genomic repertoire (Nelson et al. 2002) and genome-wide pathway modeling (Puchalka et al. 2008) now provide novel possibilities to further engineer this bacterium into a flexible cell factory for bio-industrial application. Hereby, different species of *P. putida* vary to some extent in their genetic repertoire and phenotypic behavior creating a high range of industrial application possibilities. This review highlights fundamental aspects of the cellular physiology of *P. putida* together with recent achievements in systems biology and systems metabolic engineering.

2.2 Carbon core metabolism of *Pseudomonas putida*

Of particular interest for industrial application of *P. putida* are the central routes of carbon metabolism, receiving carbon from the various converging pathways of substrate utilization and supplying building blocks, cofactors and energy for the added-value products of interest. It is interesting to note that *P. putida* differs in key aspects from the generally much conserved central catabolic pathways of many other prokaryotic cells, making its pathway repertoire and usage quite unique (Figure 1). Its fast growth, high biomass yield and low maintenance demands are additional features important for industrial application (Table 1).

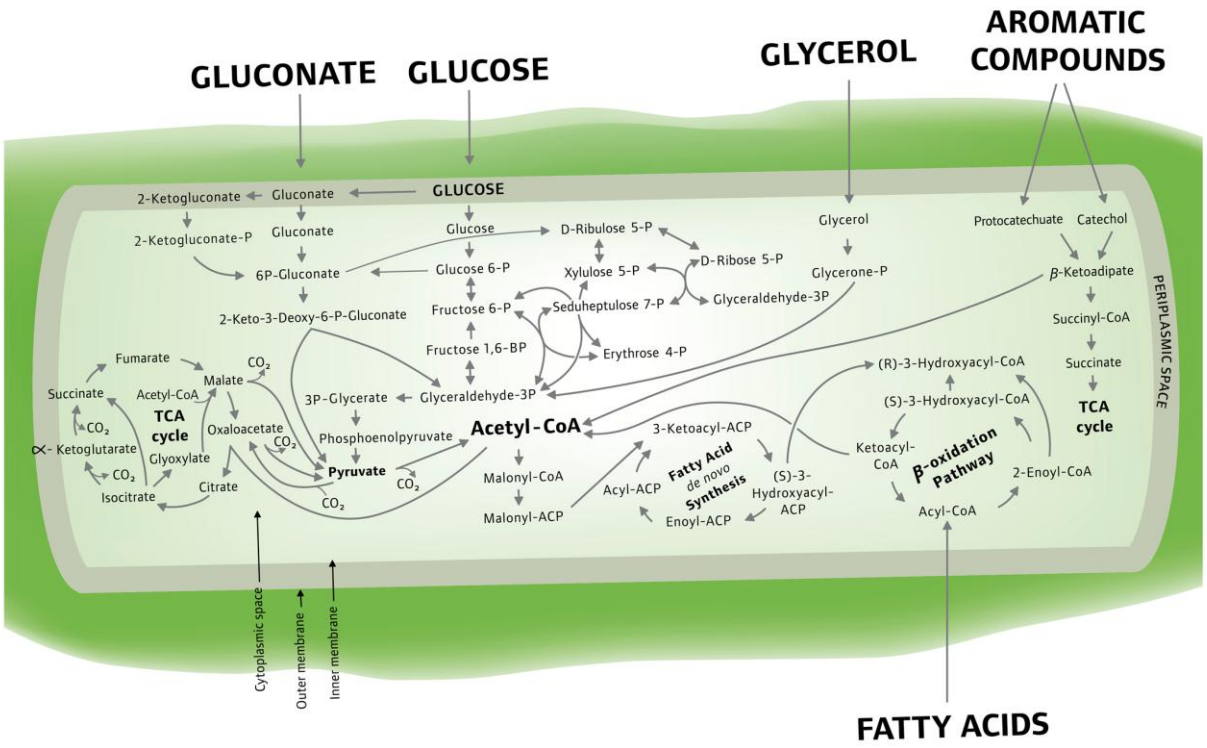

Figure 1. Metabolic pathways in the carbon core metabolism of *Pseudomonas putida*

2.2.1 Substrate uptake

In contrast to various other industrial microorganisms, including e.g. *E. coli, C. glutamicum or B. subtilis*, glucose is not the preferred carbon substrate for pseudomonads. In the presence of succinate and other intermediates of the tricarboxylic acid (TCA) cycle, carbon catabolic repression suppresses the assimilation of glucose (Wolff et al. 1991). It is interesting to note that also some of the mechanisms of substrate up-take vary from those of other bacteria. Differing from the typically observed phosphoenolpyruvate-carbohydrate phosphotransferase system (PTS), *P. putida* assimilates glucose by facilitated diffusion via the specific porin OprB. Concerning the use of industrial substrates, *P. putida* is capable to use raw glycerol, a technical by-product from the biodiesel industry (Ciesielski et al. 2010). Naturally, it cannot grow on carbon five sugars such as D-xylose or L-arabinose, but has been recently

engineered towards utilization of these sugars (Meijnen et al. 2008; Meijnen et al. 2009), important as major constituents of lignocellulosic biomass (Lee 1997),

Table 1. Physiological growth data of *Pseudomonas putida* KT2440 on glucose as carbon source. The data comprise maximum specific growth rate (μ), biomass yield ($Y_{X/S}$) and maintenance coefficient (m_X) from batch as well as continuous culture.

μ (h^{-1})	$Y_{X/S}$ (g g^{-1})	m_X (mmol g^{-1} h^{-1})	Reference
[a]0.81	-	-	(Sohn et al. 2010)
[a]0.73	[a]0.56	[b]0.062	(Ebert et al. 2011)
[b]0.59	[b]0.39	[b]0.171	(van Duuren 2011)

[a] Batch culture

[b] Chemostat culture

2.2.2 Catabolic metabolism

Most strikingly, *P. putida* lacks a functional Embden-Meyerhof-Parnas (EMP) pathway due to the absence of a gene for 6-phosphofructokinase (*pfk*) along with the expression of several transcriptional regulators e.g. HexR (del Castillo et al. 2008). For the catabolism of sugars the Entner-Doudoroff pathway is employed instead (Fuhrer et al. 2005). This catabolic route generates two carbon three blocks, i.e. glyceraldehyde 3-phosphate and pyruvate, from break-down of sugars such as glucose. The pentose phosphate pathway, however, only operates in an anabolic mode to generate biomass precursors (Ebert et al. 2011). Once generated, pyruvate enters the so-called pyruvate shunt which yields either oxaloacetate or acetyl-CoA (del Castillo et al. 2007). In addition to sugars and TCA cycle intermediates, *P. putida* KT2440 can metabolize a number of other substrates including fatty acids, polyols such as glycerol, amino acids, and aromatic compounds. The glyoxylate shunt, active in *P. putida* KT2440, is one of the anaplerotic reactions within the metabolic network. (Ebert et al. 2011).

2.2.3 Redox metabolism

The intracellular glucose provides a huge flexibility for *P. putida* to channel the sugar into different pathways. First, glucose can be either phosphorylated to glucose-6-phosphate, followed by NADPH coupled oxidation to 6-phosphogluconate to enter into the central energy catabolism. Alternatively, glucose can be subjected to successive oxidation steps which produce gluconate and 2-ketogluconate, respectively, whereby these two intermediates can be either secreted or phosphorylated to 6-phosphogluconate and 2-keto-6-phosphogluconate. The latter can be then also reduced to 6-phosphogluconate so that a complex network of alternative pathways is formed. In *P. putida* KT2440 all three possible route towards 6-phosphogluconate work simultaneously (del Castillo et al. 2007). The derived 6-phosphogluconate is the key intermediate of the major catabolic route in pseudomonads, the Entner-Doudoroff pathway. It should be noted that the network of glucose catabolism with multiple reduction and oxidation steps is efficient the supply of redox power, an important feature for whole cell applications in industrial bio-catalysis. The challenge of an elevated NADH oxidation rate did not affect the metabolic performance of *P. putida* KT2440 NADH oxidation rate (Ebert et al. 2011), taking the specific substrate uptake rate as a measure. This differs from e.g. *E. coli and S. cerevisiae*, underscoring the remarkable potential of *P. putida* as a suitable strain for efficient NADH-demanding production of chemicals.

2.2.4 Bio-conversion and degradation of non-natural chemicals

With regard to its environmental applications, huge interest focused on the degradation pathways and the underlying mechanisms from early on (Nakazawa and Yokota 1973). In summary, five major degradation pathways have been found and characterized in Pseudomonas strains, namely; the β-ketoadipate, the phenylacetyl-CoA, the homogentisate, the gentisate, and the homo-proto-catechuate pathway, respectively. Hereby, *P. putida* shows a naturally high capacity to tolerate and modify aliphatic, aromatic and heterocyclic compounds (Schmid et al. 2001). In different isolates, plasmids could be identified which mediate the genes for the break-down of toluene (3-methyl-benzoate) (Nakazawa and Yokota

1973), naphthalene (Dunn and Gunsalus 1973), 4-chloronitrobenzene (Zhen et al. 2006), 2,4- xylenol (Dean et al. 1989) or phenol (Herrmann et al. 1987). In addition, also chromosomal elements contribute to the degradation of aromatics (Jimenez et al. 2002).

2.3 Genetic engineering

Molecular genetics has enabled the investigation of bacterial phenotypes and pathway manipulation for biotechnological applications in *P. putida* (Reva et al. 2006b). The genetic amenability of this bacterium has been proven to be large, making it suitable for metabolic engineering towards the creation of superior strains. It is an ideal host for heterologous gene expression (Meijnen et al. 2008; Ronchel et al. 1998) and has been certified as first Host-Vector Biosafety strain (HV1) which can be released into the environment. The Tn5-derived mini-transposon system has been the method of choice for genomic integration of DNA fragments in *P. putida* (De Lorenzo 1994; De Lorenzo et al. 1990). This straightforward technology allows several insertions into the same cell (De Lorenzo et al. 1998) and has recently led to the valuable creation of a genome-wide mutant library of *P. putida* KT2440 (Duque et al. 2007) as well as to the streamlining of the P. putida genome by using a combinatorial deletion method based on mini-transposon insertion and Flp-FRT recombination (Leprince et al. 2011). With regard to industrial application mini-transposons are less suitable due to the antibiotic markers often used. This can be overcome by a novel method, that is I-Scel based chromosomal engineering (Martinez-Garcia and de Lorenzo 2011) which enables the precise deletion of multiple genomic segments in *P. putida*.

2.4 In silico modeling of metabolism

Driven by the sequencing of the genome of *P. putida* KT2440 (Nelson et al. 2002), and other species including *P. putida* Idaho (Tao et al. 2011), *P. putida* B6-2 (Tang et al. 2011) or *P. putida* S16 (Yu et al. 2011), the recent years have seen a huge progress in genome scale modeling of this bacterium (Nogales et al. 2008; Puchalka et al. 2008; Sohn et al. 2010). Varying to some extent in complexity and study focus,

the created models display valuable information for systems level analysis of *P. putida* (Table 2), including investigation of the pathway repertoire, gene essentiality, resource distribution as well as model based strain design for the production of PHA (Puchalka et al. 2008). Model based predictions of in silico phenotypes were recently refined by the integration of experimental data on stoichiometric demands for anabolism and cellular maintenance which are crucial to increase the predictive power of computational design. This involved exact measurement of maintenance coefficients using a mini-scale chemostat system (Ebert et al. 2011) as well as growth dependent measurement of cellular composition (van Duuren 2011) (Table 2). These data were found useful to evaluate in silico gene essentiality as compared to gene expression, hereby overcoming inconsistencies from previous models. In addition, recent modeling approaches have aimed at resolving the dynamic behavior of pathways in *P. putida* and their regulation providing a new, interesting view into its metabolism (Koutinas et al. 2011; Koutinas et al. 2010; Silva-Rocha et al. 2011).

Table 2. Genome scale models for *Pseudomonas putida* KT2440.

N° of genes	N° of reactions	N° of metabolites	Reference
746	950	911	(Nogales et al. 2008)
815	877	888	(Puchalka et al. 2008)
900	1071	1044	(Sohn et al. 2010)
746	952	917	(van Duuren 2011)

2.5 Systems-level profiling by omics technologies

The development of quantitative omics technologies has provided a solid basis for systems-wide analysis of metabolic and regulatory features of *P. putida*. Most of these studies so far focused on xenobiotic degradation. However, recent examples have initiated the investigation of this bacterium for the production of value-added chemicals. This also includes a first set of multi-omics studies, combining systems profiling on various levels towards superior strains (Verhoef et al. 2010).

2.5.1 Transcriptomics

Fascinating insights into the cellular program of *P. putida* during xenobiotic degradation could be obtained by transcription profiling. A pioneering study on the response of *P. putida* KT2440 (pWW0) to aromatic compounds (Dominguez-Cuevas et al. 2006) revealed that toluene acts as a stressor rather than as a nutrient, activating stress tolerance genes with the minimum expenditure of energy. Similarly, other studies unraveled the stress response of the cell triggered by different toxic agents (Del Castillo and Ramos 2007; Miyakoshi et al. 2007; Reva et al. 2006a; Yeom et al. 2010) or the functionality of several regulators involved in this process (Fonseca et al. 2008; Hervas et al. 2008; Morales et al. 2006; Moreno et al. 2009; Renzi et al. 2010). More recently, transcriptomics was applied to identify targets in the strain *P. putida* S12 producing p-hydroxybenzoate on glucose and glycerol as carbon sources (Verhoef et al. 2010).

2.5.2 Proteomics

Almost ten years ago, first studies created a comprehensive proteome map for *P. putida* KT2440 and identified about 200 polypeptides using conventional 2D-PAGE and matrix-assisted laser desorption ionization time-of-flight mass spectrometry (Heim et al. 2003). Complementary to the progress on the level of gene expression, the stress response of *P. putida* to different toxins was assessed also on the proteomic level (Krayl et al. 2003), so that we have a good knowledge on proteins involved in membrane composition, stabilization, detoxification or energy production (Benndorf et al. 2006; Santos et al. 2004; Segura et al. 2005; Volkers et al. 2006). In addition, studies included the characterization of aromatic degradation pathways and underlying mechanisms (Kim et al. 2006; Tsirogianni et al. 2006). More recently, also biotechnological production processes were characterized. This involved a study on the proteome of the strain *P. putida* CA-3 during growth on styrene under conditions of pure growth and also polyhydroxyalkanoate accumulation (Nikodinovic-Runic et al. 2009). Via shotgun proteomics it was possible to highlight the dual participation of proteins in stress response and PHA synthesis. *P. putida*

S12 was investigated quite intensively with regard to the effects of the enhanced production of building block chemicals on cellular physiology and regulation (Verhoef et al. 2010; Wierckx et al. 2009; Wierckx et al. 2008).

2.5.3 Metabolomics

Probably the most crucial part in quantitative metabolomics, that is the elucidation of pool sizes of the large set of intracellular metabolites, is related to sampling. In this regard, different sampling methods were tested and validated for their applicability to different catabolic and anabolic pathways in *P. putida* (Bolten et al. 2007). More recently, a comprehensive metabolome study of *P. putida* S12 revealed only minor differences among the pool size of all synthesized metabolites while growing in different carbon sources e. g. fructose, glucose, gluconate or succinate (Van Der Werf et al. 2008). Large differences, however, could be detected among specific metabolites belonging to the intermediary degradation routes of the carbon sources studied.

2.5.4 Fluxomics

On the level pathway fluxes, most close to the phenotype, different ^{13}C flux studies provided valuable insights into the carbon core metabolism of *P. putida*. For glucose-grown cells it was found that the Entner-Doudoroff pathway was the exclusive catabolic route, whereas the pentose phosphate pathway served mainly biosynthetic functions, involving the non-oxidative branch (Fuhrer et al. 2005). A more detailed view into the glucose catabolism in *Pseudomonas putida* revealed the simultaneous operation of three pathways that converge at the level of 6-phosphogluconate, which is then converted by the Entner-Doudoroff pathway to metabolites belonging the central metabolism (del Castillo et al. 2007).With regard to the TCA cycle, most of the oxaloacetate was provided by the pyruvate shunt rather than by the direct oxidation of malate by malate dehydrogenase. At the level of substrate mixtures, *P. putida* exhibits a distinct pattern of internal carbon distribution as shown for simultaneous use of glucose and toluene (Del

Castillo and Ramos 2007). Interestingly, toluene directs a larger amount of carbon than glucose into the TCA cycle, indicating the in vivo control by carbon catabolite repression that toluene exerts over glucose. The central carbon and energy metabolism of solvent tolerant *P. putida* DOT-T1E responded to the drastically increased the energy demands in the presence of toxic solvents and alcohols by an enhanced NAD(P)H regeneration (Blank et al. 2008a; Rühl et al. 2009). This was mediated by an increased specific glucose uptake rate together with a reduced anabolic demand and displays a major feature of this bacterium for industrial applications such as whole-cell redox bio-catalysis. More recently, metabolic flux analysis provided valuable information during metabolic engineering of a phenol overproducer strain derived from *P. putida* S12 (Wierckx et al. 2008) (Wierckx et al. 2009). Beyond experimental applications, flux patterns were also applied to validate mathematical models (Puchalka et al. 2008). In general there was a good agreement between in vivo and in silico data, whereby certain discrepancies were attributed to non-optimal allocation of resources in growing cells, differing from the optimization function imposed in the in silico analysis.

2.6 Industrial applications of *P. putida* strains

Stimulated by their excellent production properties and the advent of genetic engineering, *P. putida* and related strains have been applied and optimized to a meanwhile broad portfolio of industrial products, involving bio-based materials, as well as de novo synthesis and biotransformation of high value chemicals and pharmaceuticals (Table 3).

2.6.1 Bio-based materials

Among bio-based polymers, polyhydroxyalkanoates (PHA) comprise a large class of polyesters. Their excellent biodegradability and biocompatibility is interesting for applications in various areas including tissue engineering or eco-friendly packaging (Khanna and Srivastava 2005; Liu and Chen 2007). Depending on the cultivation conditions, polyhydroxyalkanoates are accumulated as carbon and energy

storage by *P. putida* which has been widely exploited for their targeted biosynthesis in this organism (Hoffmann and Rehm 2004). Their material properties, that is elasticity, crystallinity or rigidness depend on the monomeric composition which can be precisely controlled by fermentation strategies (Albuquerque et al. 2011; Hoffmann and Rehm 2004; Sun et al. 2009) or by metabolic engineering (Liu and Chen 2007). A better understanding on the regulation and processes involved in polymer biosynthesis has enabled targeted metabolic and protein engineering approaches to improve production efficiency of tailor made PHAs (Rehm 2010). As example, the weakening of the competing *β*-oxidation pathway in the strain *P. putida* KT2442 by deletion of FadA and FadB, significantly increased overall production and supported the formation of medium-chain-length polymers (Liu and Chen 2007; Ouyang et al. 2007). Further metabolic engineering of the *β*-oxidation reactions has made possible to synthesis different kinds of homo-polymers such as poly(3-hydroxyhexanoate), poly(3-hydroxyheptanoate) (Wang et al. 2011) , and poly(3-hydroxydecanoate) (Liu et al. 2011), as well as a novel PHA containing thioester groups in the side chain, which make them suitable for tailored chemical modifications (Escapa et al. 2011a). More recently, the substrate specificity of type II PHA synthase was modified by site-directed mutagenesis to accept short-chain-length building blocks for PHA production and further extend the product portfolio of this class of bio-based plastics (Yang et al. 2011). Fed-batch cultivation of *P. putida* GPo1 demonstrated the feasibility of large-scale PHA production (Elbahloul and Steinbüchel 2009). High cell density cultures are also well established in *P. putida* KT2440 (Sun et al. 2006a), enabling efficient accumulation of PHA during carbon-limiting exponential feeding (Sun et al. 2007a). A remarkable step towards straightforward biopolymer recovery has been made via a programmed self–disrupting *P. putida* strain that should significantly reduce the costs of the process (Martínez et al. 2011). This illustrates the great potential of *P. putida* species for an economically attractive production of PHA with diverse composition.

2.6.2 Bioconversion and de-novo synthesis of chemicals

Beyond its more traditional application for xenobiotic degradation and PHA production, *P. putida* is gaining more and more importance as host for whole cell bio-catalysis and de novo synthesis of chemicals (Table 3). This takes significant benefit from its well-known capacity to tolerate and modify aliphatic, aromatic and heterocyclic compounds related to a versatile enzymatic set of mono-oxygenases, di-oxygenases and hydroxylases (Schmid et al. 2001). *P. putida* KT2440 is able to metabolize benzoate which gives access to various interesting intermediates of the degradation route (Jiménez et al. 2002). As example, *cis-cis* muconate, an aromatic intermediate of benzoate degradation, is a suitable precursor for the production of adipic acid opening novel routes towards nylon-6,6 (Draths and Frost 1994). Recently, the generation of a (*catR*) deficient mutant of KT2440 showed high rate and yield of *cis-cis* muconate from the co-metabolization of benzoate in the presence of glucose (Van Duuren et al. 2011c). This overproducer strain was used in a pH-stat fed-batch process which resulted in high specific productivity (Van Duuren et al. 2011b) and promising life cycle characteristics for different feed stocks (Van Duuren et al. 2011a). Hereby, *P. putida* exhibits rather high tolerance as compared to many other industrial production organisms. This appears as an excellent starting point to overcome a major bottleneck, that is, substrate and product toxicity to the often unnatural chemical compounds. Indeed, solvent-tolerant strains of *P. putida* were successfully used for stereospecific epoxidation of styrene by the strain DOT-T1E (Blank et al. 2008b), o-cresol formation from toluene with *P. putida* T-57 (Faizal et al. 2005) or de novo synthesis of p-coumarate (Nijkamp et al. 2007), p-hydroxybenzoate (Verhoef et al. 2007) or p-hydroxystyrene (Verhoef et al. 2009), all using *P. putida* S12. These successful developments also recruited metabolic engineering strategies. Reprogramming of the p-coumarate producing strain S12 for p-hydroxy-styrene production was possible by introducing the genes pal and pdc encoding L-phenylalanine/L-tyrosine ammonia lyase and p-coumaric acid decarboxylase, respectively. Degradation of the p-coumarate intermediate was prevented by inactivating the *fcs* gene encoding feruloyl-coenzyme A synthetase (Verhoef et al. 2009). In addition novel reactor configurations have been developed in recent years, showing advantage with regard to toxicity effects. This comprised two-phase-liquid-liquid-

cultivation systems with an aqueous and an organic phase (Schmid et al. 2001; Verhoef et al. 2009; Wierckx et al. 2005). Beyond this, alternative concepts involving catalytically active biofilms came into focus because of their inherent characteristics of self-immobilization, high resistance to reactants and long-term activity, which all facilitate continuous processing (Rosche et al. 2009). Using the biofilm-forming and engineered *Pseudomonas* strain VLB120ΔC, a stable and highly efficient continuous (S)-styrene oxide production process was recently established (Gross et al. 2010) and optimized (Halan et al. 2010). This profited from a high volumetric productivity in situ substrate feed and product recovery (Halan et al. 2010), and improved tolerance and robustness as compared to planktonic cultures (Halan et al. 2011).

Table 3: Overview on biotechnology products derived by natural and recombinant strains of *Pseudomonas putida*.

Product	Parent strain	Production strain	Comment	Reference
PHA hetero-polymer	KT2442	KT2442		Ouyang 2007
PHA hetero-polymer with modified monomer composition	KT2442	KTOY06	Altered *β*-oxidation	Ouyang 2007
PHA hetero-polymer with high-content of 3-hydroxytetradecanoate	KT2442	KTOY06		Liu 2007
PHA C_6 and C_7 homo-polymers	KT2442	KTHH03	Modified *β*-oxidation; feeding of hexanoate and heptanoate	Wang 2011
PHA C_5 homo-polymer	KTHH03	KTHH08	Deletion of mcl PHA synthase genes (*phaC*), plasmid-based expression of the PHA synthesis operon (*phaPCJ*) from Aeromonas hydrophila; valerate used as carbon source	Wang 2011
PHA C_3 and C_4 homo-polymer	KTHH03	KTHH06	Replacement of endogenous *phaC* by *phaC* from *Ralstonia eutropha*; *β*-butyrolactone as precursor	Wang 2011
Myxochromide S	KT2440	P.putida::CMch37a	Heterologous expression of myxochromide S biosynthetic gene cluster from *Stigmatella aurantiaca*	Stephan 2006
--	KT2440	FG2005	Integration of methyl-malonyl-CoA	Gross 2006

			pathway from *Sorangium cellulosum*	
Myxothiazol	FG2005	FG2005::Pm-mta	Integration of myxothiazol synthesis cluster from *Stigmatella aurantiaca*	Gross 2006
p-Hydroxysterene	S12	S12 427Δfcs pJNTpalpdc	Introduction of *pal* (*R. glutinis*) and *pdc* (*L. plantarum*), inactivating *fcs* genes	Verhoef 2009
D-Glucosaminic acid	GNA5	GNA5	D-glucosaminic acid accumulated during oxidative fermentation process	Wu 2010
Phenol	S12	S12	Introduction of *tpl* gene from *Pantea agglomeran*, overexpression of the *aroF-1* gene	Wierckx 2005
p-Coumarate	S12	S12 C3	Inactivation of fcs, construction of phenylalanine auxothrophic mutant	Nijkamp 2007
3-Nitrocatechol	F1	F1	Process optimization for bio-catalytic production	Prakash 2010
3-Methylcatechol	F1 and F107	MC1 and MC2	F107 as a 3-methylcatechol accumulating mutant of F1 with expression of *todC1C2BAD* under control of an inducible regulatory region	Hüsken 2001
o-Cresol	T-57	TODD1	*todD* knockout mutant of T-57	Faizal 2005
Aliphatic alcohols	PpS81	PpS8141	Introduction of the *alk* regulon (*alkBFGH/alkST*) from *Pseudomonas oleovorany*	Bosetti 1992

4-Valerolactone	KT2440	KT2440	Introduction of *tesB* (*E. coli* G1655) to secrete 4-hydroxyvalerate and pon1 (human paraoxonase I), expressed extra-cytosolic to catalyze the utilization the intermediate 4-hydroxyvalerate	Martin 2010
p-Hydroxybenzoate	S12	S12pal_xylB7	Additional copy of *aroF-1* gene, introduction of *xylAB_FGH* genes (*E.coli*) and the *pal* gene (*R. toruloides*)	Meijnen 2011
2-Alkyl-4(1H)-quinolones and related derivates	KT2440	KT2440 [pBBR-pqsABCD]	Insertion of *pqsABCD* from *P. aeruginosa*	Niewerth 2011
Styreneoxide	DOT-T1E	DOT-T1E [pTEZ240]	Heterologous expression of styrene monooxygenase StyAB from *P. spec*. VLB120	Blank 2008
4-Hydroxyquinaldine	KT2440	KT2440 (pKP1)	Inserted genes *qoxLMS* (*Arthrobacter nitroguajoccolicus* Rü61a)	Ütkür 2011
Biodesulfurization	S12	DS23	Insertion of desulfurizing gene cluster (*dszABCD)* (*P. putida* A4)	Tao 2011
Bioconversion of limonin	G7	G7	Use of whole cells permeabilized with EDTA and lysozyme	Malik 2011

2.6.3 Pharmaceuticals and agrochemicals

Natural products of microbial origin are widely used as pharmaceuticals and in agro-chemistry. These compounds are often biosynthesized by multifunctional mega-synthetases whose genetic engineering and heterologous expression offer considerable promise, especially if the natural hosts are genetically difficult to handle, slow growing, unculturable, or even unknown (Wenzel et al. 2005). In this regard, *P. putida* has shown to be capable to express and activate biosynthetic proteins of complex natural products from myxobacteria (Gross et al. 2005; Gross et al. 2006; Wenzel et al. 2005). This has enabled production of high-value pharmaceuticals in this bacterium (Table 3). Using *P. putida* KT2440 as heterologous host, myxochromide S production was successfully established (Stephan et al. 2006). Specific feeding strategies unraveled metabolic bottlenecks for the supply of myxochromid building blocks suggesting process optimization by metabolite feeding (Stephan et al. 2006) or metabolic engineering toward improved supply of the required compounds. In addition *P. putida* FG2005 was used as production host for heterologous myxothiazol production (Gross et al. 2006). More recently, transposition was established for genetic engineering of *P. putida* allowing efficient transfer of extremely large gene clusters which in general build the basis for biosynthesis of natural products (Fu et al. 2008). In another study, the insertion heterologous genes into *P. putida* KT2440 allowed the biosynthesis of valuable carotenoids such as zeaxanthin (Beuttler et al. 2011). Hence, previous size problems for transformation of *P. putida* appear to be solved and offer novel possibilities to further exploit *P. putida* as production platform for high-value natural products.

Table 4. Industrial processes based on *Pseudomonas* strains

Product	Biocatalyst	Applicability	Company	Source
2-quinoxalinecarboxylic acid	*P. putida* ATCC 33015	Biological activity	Pfizer (USA)	(Wong et al. 2002)
5-methylpirazine-2-carboxylic acid	*P. putida* ATCC 33015	Pharmaceutical	Lonza (Switzerland)	(Kiener 1992)
Chiral amines	*Pseudomonas* DSM 8246	Biological activity	BASF (Germany)	(Schulze and Wubbolts 1999)
5-cyanopentanamide	*P. putida*	Catalysis	DuPont (USA)	(Stieglitz et al. 1996)
(S)-2-Chloropropionoc acid	*Pseudomonas*	Herbicides	Astra Zeneca (USA)	(Schulze and Wubbolts 1999)
D-*p*-hydroxyphenyl glycine	*P. putida*	Pharmaceutical	Several companies	(Schulze and Wubbolts 1999)
Chiral compounds	*P. putida* ATCC 12633	Pharmaceutical	DSM (The Netherlands)	(Hermes et al. 1993)
4-[6-hydroxypyridin-3-yl]-4-oxobutyrate	*Pseudomonas* DSM 8653	Pharmaceutical	Lonza (Switzerland)	(Schmid et al. 2001)
Paclitaxel	*Pseudomonas* lipase AK	Pharmaceutical	Bristol-Myers Squibb	(Patel et al. 1994)

2.7 Conclusions and future perspectives

Similar to other industrial microorganisms, the product portfolio of *P. putida* has strongly evolved in recent years (Table 3). Its good genetic accessibility and the naturally high tolerance appear as desirable features to overcome the toxic and harsh conditions typically linked to industrial bio-catalysis and de-novo synthesis of often unnatural chemicals. It interesting to note, that quite a few commercial processes in biotechnology are based on this versatile bacterium (Table 4). *P. putida* and its enzyme repertoire are involved in the industrial synthesis of chiral compounds (Hermes et al. 1993; Schulze and Wubbolts 1999), paclitaxel (Patel et al. 1994), 5-methylpirazine-2-carboxylic acid (Kiener 1992) among others, involving large chemical and biotechnological companies such as Pfizer (USA), Lonza (Switzerland), DSM (The Netherlands), DuPont (USA), or BASF (Germany) (Schulze

and Wubbolts 1999). The application range of *P. putida* in industrial biotechnology has good chances to further grow and expand in the future considering the interesting pipeline of novel products becoming available via efficient *P. putida* cell factories.

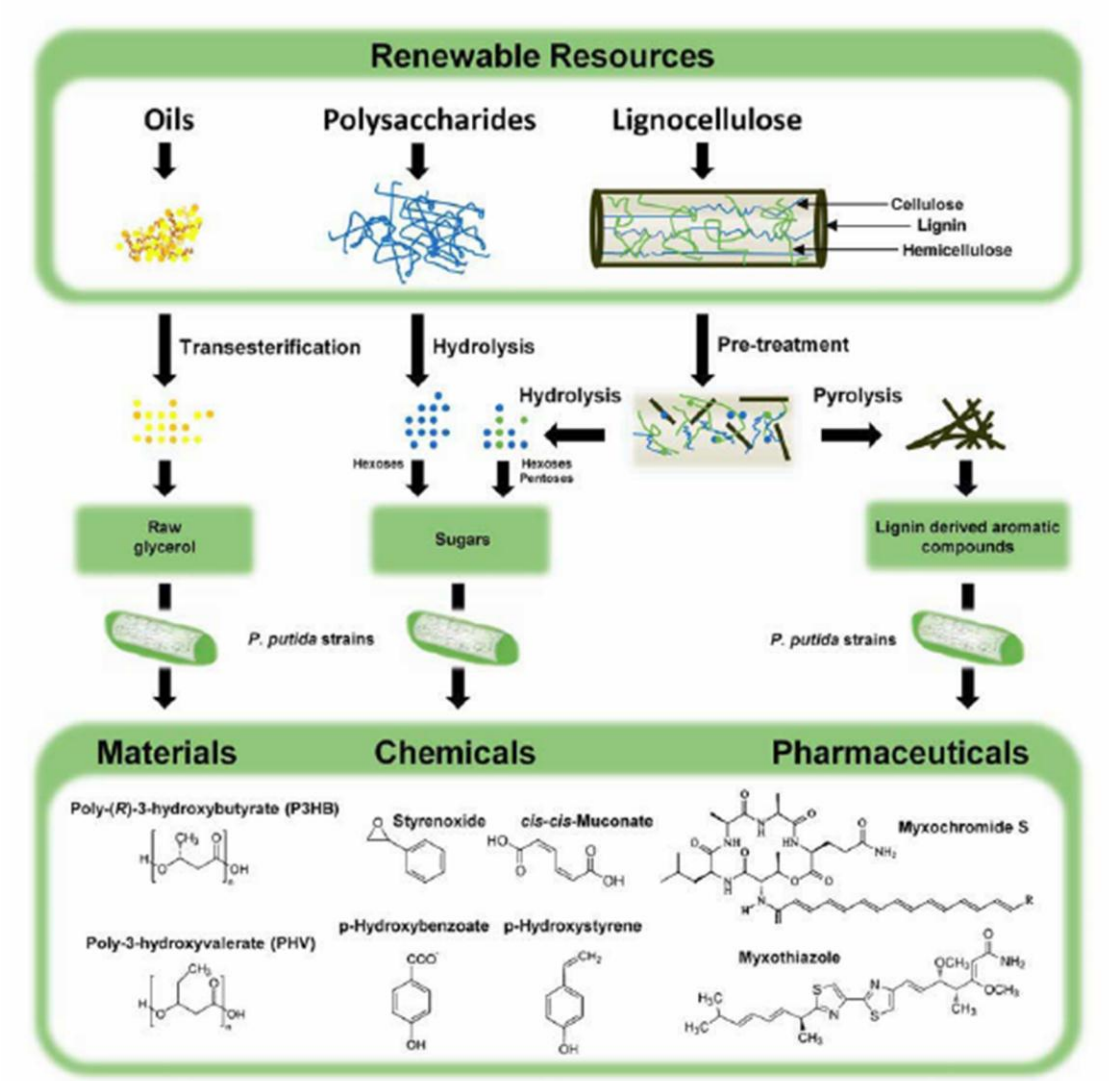

Figure 2. Integration of *Pseudomonas putida* as cell factory in the bio-based production pipelines from renewable resources.

Interesting future developments might consider the integration of *P. putida* into existing or currently developed pipelines of utilizing renewable feedstocks or industrial wastes for sustainable bio-production as visualized in Figure 2. The rich intrinsic pathway repertory enables *P. putida* to degrade and metabolize a broad range of compounds, including also complex aromatics. Together with its

natural high tolerance to harsh and toxic conditions this seems beneficial to couple *P. putida* to various streams of renewable feedstocks. As example, lignocellulosic biomass from catalytic pyrolysis containing also aromatic compounds (Bu et al. 2011) could be converted by *P. putida* capable to utilize such substrates into added value products such as as *cis-cis* muconate, an excellent precursor for the synthesis of adipic acid. Also in the sugar pipeline, *P. putida* seem valuable to create novel chemicals or materials. Hereby, the naturally high tolerance of *P. putida* to harsh and toxic conditions together with flexible genetic modifications displays an excellent starting point of further developing it into a production platform for other, non-natural chemicals which are not accessible so far. This will require experimental and computational systems level strategies to disentangle the complexity of the *Pseudomonas putida* central and peripheral metabolic pathways towards their targeted optimization. Synthetic biology will add a next level of design space to reshape metabolism for enhanced bio-production, e.g. via fine-modulated expression and control of regulation networks or the integration of complex heterologous pathways Rational strain engineering will be further completed by novel concepts or evolutionary engineering, boosting industrial implementation of *Pseudomonas* strains via novel phenotypes with even enhanced tolerance to industrial environments, a promising perspective for *P. putida.*

2.8 Acknowledgements

Ignacio Poblete-Castro and Vitor Martins dos Santos acknowledge financial support by the German Federal Ministry of Education (BMBF) via the project “PSysMo” within the ERA-NET initiative “Systems Biology of Microorganisms” as well as the EU-FP7 project “Microme”. Christoph Wittmann, Judith Becker and Kathrin Dohnt acknowledge support by the German Federal Ministry of Education (BMBF) initiative “Infection Genomics“ for financing of the project “Urogenomics - Systems biology of Pseudomonas and other uropathogenic bacteria” (FKZ 0315833D). All authors thank Evelyn Groschopp for design and creation of the pathway figure.

2.9 References

Albuquerque MGE, Martino V, Pollet E, AvErous L, Reis MAM. 2011. Mixed culture polyhydroxyalkanoate (PHA) production from volatile fatty acid (VFA)-rich streams: Effect of substrate composition and feeding regime on PHA productivity, composition and properties. Journal of Biotechnology 151(1):66-76.

Bagdasarian M, Lurz R, Ruckert B. 1981. Specific-purpose plasmid cloning vectors. II. Broad host range, high copy number, RSF 1010-derived vectors, and a host-vector system for gene cloning in Pseudomonas. Gene 16(1-3):237-247.

Bell A, Bains M, Hancock REW. 1991. *Pseudomonas aeruginosa* outer membrane protein OprH: Expression from the cloned gene and function in EDTA and gentamicin resistance. Journal of Bacteriology 173(21):6657-6664.

Bellido F, Martin NL, Siehnel RJ, Hancock REW. 1992. Reevaluation, using intact cells, of the exclusion limit and role of porin OprF in *Pseudomonas aeruginosa* outer membrane permeability. Journal of Bacteriology 174(16):5196-5203.

Benndorf D, Thiersch M, Loffhagen N, Kunath C, Harms H. 2006. *Pseudomonas putida* KT2440 responds specifically to chlorophenoxy herbicides and their initial metabolites. Proteomics 6(11):3319-3329.

Beuttler H, Hoffmann J, Jeske M, Hauer B, Schmid R, Altenbuchner J, Urlacher V. 2011. Biosynthesis of zeaxanthin in recombinant *Pseudomonas putida*. Applied Microbiology and Biotechnology 89(4):1137-1147.

Blank LM, Ionidis G, Ebert BE, Buhler B, Schmid A. 2008a. Metabolic response of *Pseudomonas putida* during redox biocatalysis in the presence of a second octanol phase. FEBS Journal 275(20):5173-5190.

Blank LM, Ionidis G, Ebert BE, Bühler B, Schmid A. 2008b. Metabolic response of *Pseudomonas putida* during redox biocatalysis in the presence of a second octanol phase. FEBS Journal 275(20):5173-5190.

Bolten CJ, Kiefer P, Letisse F, Portais JC, Wittmann C. 2007. Sampling for metabolome analysis of microorganisms. Analytical Chemistry 79(10):3843-3849.

Bu Q, Lei H, Ren S, Wang L, Holladay J, Zhang Q, Tang J, Ruan R. 2011. Phenol and phenolics from lignocellulosic biomass by catalytic microwave pyrolysis. Bioresource Technology 102(13):7004-7007.

Burne RA, Chen YYM. 2000. Bacterial ureases in infectious diseases. Microbes and Infection 2(5):533-542.

Caldas TD, El Yaagoubi A, Richarme G. 1998. Chaperone properties of bacterial elongation factor EF-Tu. Journal of Biological Chemistry 273(19):11478-11482.

Carter IS, Dawes EA. 1979. Effect of oxygen concentration and growth rate on glucose metabolism, Poly-B-hydroxybutyrate biosynthesis and respiration of *Azotobacter beijerinckii*. Journal of General Microbiology 110(2):393-400.

Chen G-Q. 2009. A microbial polyhydroxyalkanoates (PHA) based bio- and materials industry. Chemical Society Reviews 38(8).

Chen G-Q, Chen GG-Q. 2010. Industrial Production of PHA Plastics from Bacteria. Springer Berlin / Heidelberg. p 121-132.

Ciesielski S, Pokoj T, Klimiuk E. 2010. Cultivation-dependent and -independent characterization of microbial community producing polyhydroxyalkanoates from raw glycerol. Journal of Microbiology and Biotechnology 20(5):853-861.

Dauner M, Storni T, Sauer U. 2001. *Bacillus subtilis* metabolism and energetics in carbon-limited and excess-carbon chemostat culture. Journal of Bacteriology 183(24):7308-7317.

de Eugenio LI, Galán B, Escapa IF, Maestro B, Sanz JM, García JL, Prieto MA. 2010. The PhaD regulator controls the simultaneous expression of the pha genes involved in polyhydroxyalkanoate metabolism and turnover in *Pseudomonas putida* KT2442. Environmental Microbiology 12(6):1591-1603.

De Lorenzo V. 1994. Designing microbial systems for gene expression in the field. Trends in Biotechnology 12(9):365-371.

De Lorenzo V, Herrero M, Jakubzik U, Timmis KN. 1990. Mini-Tn5 transposoon derivatives for insertion mutagenesis, promoter probing, and chromosomal insertion of cloned DNA in gram-negative eubacteria. Journal of Bacteriology 172(11):6568-6572.

De Lorenzo V, Herrero M, Sanchez JM, Timmis KN. 1998. Mini-transposons in microbial ecology and environmental biotechnology. FEMS Microbiology Ecology 27(3):211-224.

Dean HF, Cheevadhanarak S, Skurray RA, Bayly RC. 1989. Characterisation of a degradative plasmid in *Pseudomonas putida* that controls the expression of 2,4-xylenol degradative genes. FEMS Microbiology Letters 61(1-2):153-157.

del Castillo T, Duque E, Ramos JL. 2008. A Set of Activators and Repressors Control Peripheral Glucose Pathways in *Pseudomonas putida* To Yield a Common Central Intermediate. Journal of Bacteriology 190(7):2331-2339.

Del Castillo T, Ramos JL. 2007. Simultaneous catabolite repression between glucose and toluene metabolism in *Pseudomonas putida* is channeled through different signaling pathways. Journal of Bacteriology 189(18):6602-6610.

del Castillo T, Ramos JL, Rodriguez-Herva JJ, Fuhrer T, Sauer U, Duque E. 2007. Convergent peripheral pathways catalyze initial glucose catabolism in *Pseudomonas putida*: Genomic and flux analysis. Journal of Bacteriology 189(14):5142-5152.

Dinamarca MA, Aranda-Olmedo I, Puyet A, Rojo F. 2003. Expression of the *Pseudomonas putida* OCT plasmid alkane degradation pathway is modulated by two different global control signals: Evidence from continuous cultures. Journal of Bacteriology 185(16):4772-4778.

Diniz S, Taciro M, Cabrera Gomez J, Pradella J. 2004. High-Cell-Density cultivation of *Pseudomonas putida* IPT 046 and medium-chain-length polyhydroxyalkanoate production from sugarcane carbohydrates. Applied Biochemistry and Biotechnology 119(1):51-69.

Doi Y. 1990. Microbial polyesters. VCH, New York.

Dominguez-Cuevas P, Gonzalez-Pastor JE, Marques S, Ramos JL, De Lorenzo V. 2006. Transcriptional tradeoff between metabolic and stress-response programs in Pseudomonas putida KT2440 cells exposed to toluene. Journal of Biological Chemistry 281(17):11981-11991.

Draths KM, Frost JW. 1994. Environmentally compatible synthesis of adipic acid from D-glucose [16]. Journal of the American Chemical Society 116(1):399-400.

Dunn NW, Gunsalus IC. 1973. Transmissible plasmid coding early enzymes of naphthalene oxidation in *Pseudomonas putida*. Journal of Bacteriology 114(3):974-979.

Duque E, Molina-Henares AJ, Torre Jdl, Molina-Henares MA, Castillo Td, Lam J, Ramos JL, Ramos J-L, Filloux A. 2007. Towards a Genome-Wide Mutant Library of *Pseudomonas putida* Strain KT2440

Pseudomonas. Springer Netherlands. p 227-251.

Ebert BE, Kurth F, Grund M, Blank LM, Schmid A. 2011. Response of Pseudomonas putida KT2440 to increased NADH and ATP demand. Applied and Environmental Microbiology 77(18):6597-6605.

Elbahloul Y, Steinbüchel A. 2009. Large-scale production of poly(3-hydroxyoctanoic acid) by *Pseudomonas putida* GPo1 and a simplified downstream process. Applied and Environmental Microbiology 75(3):643-651.

Escapa I, Morales V, Martino V, Pollet E, Averous L, Garcia J, Prieto M. 2011a. Disruption of B-oxidation pathway in *Pseudomonas putida* KT2442 to produce new functionalized PHAs with thioester groups. Applied Microbiology and Biotechnology 89(5):1583-1598.

Faizal I, Dozen K, Hong CS, Kuroda A, Takiguchi N, Ohtake H, Takeda K, Tsunekawa H, Kato J. 2005. Isolation and characterization of solvent-tolerant *Pseudomonas putida* strain T-57, and its application to biotransformation of toluene to cresol in a two-phase (organic-aqueous) system. Journal of Industrial Microbiology and Biotechnology 32(11-12):542-547.

Fonseca P, Moreno R, Rojo F. 2008. Genomic analysis of the role of RNase R in the turnover of *Pseudomonas putida* mRNAs. Journal of Bacteriology 190(18):6258-6263.

Fu J, Wenzel SC, Perlova O, Wang J, Gross F, Tang Z, Yin Y, Stewart AF, Müller R, Zhang Y. 2008. Efficient transfer of two large secondary metabolite pathway gene clusters into heterologous hosts by transposition. Nucleic acids research 36(17).

Fuchtenbusch B, Wullbrandt D, Steinbuchel A. 2000. Production of polyhydroxyalkanoic acids by *Ralstonia eutropha* and *Pseudomonas oleovorans* from an oil remaining from biotechnological rhamnose production. Applied Microbiology and Biotechnology 53(2):167-172.

Fuhrer T, Fischer E, Sauer U. 2005. Experimental identification and quantification of glucose metabolism in seven bacterial species. Journal of Bacteriology 187(5):1581-1590.

Galan B, Dinjaski N, Maestro B, De Eugenio LI, Escapa IF, Sanz JM, Garcia JL, Prieto MA. 2011. Nucleoid-associated PhaF phasin drives intracellular location and segregation of polyhydroxyalkanoate granules in *Pseudomonas putida* KT2442. Molecular Microbiology 79(2):402-418.

Gross F, Gottschalk D, Müller R. 2005. Posttranslational modification of myxobacterial carrier protein domains in Pseudomonas sp. by an intrinsic phosphopantetheinyl transferase. Applied Microbiology and Biotechnology 68(1):66-74.

Gross F, Ring MW, Perlova O, Fu J, Schneider S, Gerth K, Kuhlmann S, Stewart AF, Zhang Y, Müller R. 2006. Metabolic Engineering of *Pseudomonas putida* for Methylmalonyl-CoA Biosynthesis to Enable Complex Heterologous Secondary Metabolite Formation. Chemistry and Biology 13(12):1253-1264.

Gross R, Lang K, Bühler K, Schmid A. 2010. Characterization of a biofilm membrane reactor and its prospects for fine chemical synthesis. Biotechnology and Bioengineering 105(4):705-717.

Halan B, Schmid A, Buehler K. 2010. Maximizing the productivity of catalytic biofilms on solid supports in membrane aerated reactors. Biotechnology and Bioengineering 106(4):516-527.

Halan B, Schmid A, Buehler K. 2011. Real-time solvent tolerance analysis of *Pseudomonas sp*. Strain VLB120ΔC catalytic biofilms. Applied and Environmental Microbiology 77(5):1563-1571.

Han MJ, Sang Sun Y, Sang Yup L. 2001. Proteome analysis of metabolically engineered *Escherichia coli* producing poly(3-hydroxybutyrate). Journal of Bacteriology 183(1):301-308.

Hancock REW, Decad GM, Nikaido H. 1979. Identification of the protein producing transmembrane diffusion pores in the outer membranes of *Pseudomonas aeruginosa* PA01. Biochimica et Biophysica Acta 554(2):323-331.

Hartmann R, Hany R, Geiger T, Egli T, Witholt B, Zinn M. 2004. Tailored Biosynthesis of Olefinic Medium-Chain-Length Poly[(R)-3-hydroxyalkanoates] in *Pseudomonas putida* GPo1 with Improved Thermal Properties. Macromolecules 37(18):6780-6785.

Hazer B, Steinbüchel A. 2007. Increased diversification of polyhydroxyalkanoates by modification reactions for industrial and medical applications. Applied Microbiology and Biotechnology 74(1):1-12.

Heim S, Ferrer M, Heuer H, Regenhardt D, Nimtz M, Timmis KN. 2003. Proteome reference map of *Pseudomonas putida* strain KT2440 for genome expression profiling: Distinct responses of KT2440 and *Pseudomonas aeruginosa* strain PAO1 to iron deprivation and a new form of superoxide dismutase. Environmental Microbiology 5(12):1257-1269.

Hermes HFM, Sonke T, Peters PJH, van Balken JAM, Kamphuis J, Dijkhuizen L, Meijer EM. 1993. Purification and Characterization of an l-Aminopeptidase from *Pseudomonas putida* ATCC 12633. Applied and Environmental Microbiology 59(12):4330-4334.

Herrmann H, Janke D, Krejsa S, Kunze I. 1987. Involvement of the plasmid pPGH1 in the phenol degradation of Pseudomonas putida strain H. FEMS Microbiology Letters 43(2):133-137.

Hervas AB, Canosa I, Little R, Dixon R, Santero E. 2009. NtrC-dependent regulatory network for nitrogen assimilation in *Pseudomonas putida*. Journal of Bacteriology 191(19):6123-6135.

Hervas AB, Canosa I, Santero E. 2008. Transcriptome analysis of *Pseudomonas putida* in response to nitrogen availability. Journal of Bacteriology 190(1):416-420.

Hoffmann N, Rehm BHA. 2004. Regulation of polyhydroxyalkanoate biosynthesis in *Pseudomonas putida* and *Pseudomonas aeruginosa*. FEMS Microbiology Letters 237(1):1-7.

Hua Q, Yang C, Baba T, Mori H, Shimizu K. 2003. Responses of the Central Metabolism in *Escherichia coli* to Phosphoglucose Isomerase and Glucose-6-Phosphate Dehydrogenase Knockouts. Journal of Bacteriology 185(24):7053-7067.

Hua Q, Yang C, Oshima T, Mori H, Shimizu K. 2004. Analysis of Gene Expression in *Escherichia coli* in Response to Changes of Growth-Limiting Nutrient in Chemostat Cultures. Applied and Environmental Microbiology 70(4):2354-2366.

Huijberts GNM, De Rijk TC, De Waard P, Eggink G. 1994. 13C nuclear magnetic resonance studies of *Pseudomonas putida* fatty acid metabolic routes involved in poly(3-hydroxyalkanoate) synthesis. Journal of Bacteriology 176(6):1661-1666.

Huijberts GNM, Eggink G, De Waard P, Huisman GW, Witholt B. 1992. *Pseudomonas putida* KT2442 cultivated on glucose accumulates poly(3- hydroxyalkanoates) consisting of saturated and unsaturated monomers. Applied and Environmental Microbiology 58(2):536-544.

Huisman GW, de Leeuw O, Eggink G, Witholt B. 1989. Synthesis of poly-3-hydroxyalkanoates is a common feature of fluorescent pseudomonads. Applied and Environmental Microbiology 55(8):1949-1954.

Huisman GW, Wonink E, De Koning G, Preusting H, Witholt B. 1992. Synthesis of poly(3-hydroxyalkanoates) by mutant and recombinant Pseudomonas strains. Applied Microbiology and Biotechnology 38(1):1-5.

Jackson FA, Dawes EA. 1976. Regulation of the tricarboxylic acid cycle and poly-B-hydroxybutyrate metabolism in *Azotobacter beijerinckii* grown under nitrogen or oxygen limitation. Journal of General Microbiology 97(2):303-312.

Jimenez JI, Miambres B, Garcia JL, Diaz E. 2002. Genomic analysis of the aromatic catabolic pathways from Pseudomonas putida KT2440. Environmental Microbiology 4(12):824-841.

Jiménez JI, Miñambres B, García JL, Díaz E. 2002. Genomic analysis of the aromatic catabolic pathways from *Pseudomonas putida* KT2440. Environmental Microbiology 4(12):824-841.

Jung K, Hazenberg W, Prieto M, Witholt B. 2001. Two-stage continuous process development for the production of medium-chain-length poly(3-hydroxyalkanoates). Biotechnology and Bioengineering 72(1):19-24.

Kang Z, Wang Q, Zhang H, Qi Q. 2008. Construction of a stress-induced system in *Escherichia coli* for efficient polyhydroxyalkanoates production. Applied Microbiology and Biotechnology 79(2):203-208.

Kawakami T, Kuroki M, Ishii M, Igarashi Y, Arai H. 2010. Differential expression of multiple terminal oxidases for aerobic respiration in *Pseudomonas aeruginosa*. Environmental Microbiology 12(6):1399-1412.

Kessler B, Witholt B. 2001. Factors involved in the regulatory network of polyhydroxyalkanoate metabolism. Journal of Biotechnology 86(2):97-104.

Khanna S, Srivastava AK. 2005. Recent advances in microbial polyhydroxyalkanoates. Process Biochemistry 40(2):607-619.

Kiener A. 1992. Enzymatic Oxidation of Methyl Groups on Aromatic Heterocycles: A Versatile Method for the Preparation of Heteroaromatic Carboxylic Acids. Angewandte Chemie International Edition in English 31(6):774-775.

Kim DY, Hyung WK, Moon GC, Young HR. 2007. Biosynthesis, modification, and biodegradation of bacterial medium-chain-length polyhydroxyalkanoates. Journal of Microbiology 45(2):87-97.

Kim YH, Cho K, Yun SH, Kim JY, Kwon KH, Yoo JS, Kim SI. 2006. Analysis of aromatic catabolic pathways in Pseudomonas putida KT 2440 using a combined proteomic approach: 2-DE/MS and cleavable isotope-coded affinity tag analysis. Proteomics 6(4):1301-1318.

Klinke S, Dauner M, Scott G, Kessler B, Witholt B. 2000. Inactivation of isocitrate lyase leads to increased production of medium-chain-length poly(3-hydroxyalkanoates) in *Pseudomonas putida*. Applied and Environmental Microbiology 66(3):909-913.

Kosseva MR, Kennedy JF. 1996. Degradable polymers: Principles and applications. Edited by G. Scott and D. Gilead. Chapman & Hall, London, 1995. pp. xii + 271, price £59.00. ISBN 0-412-59010-7. Polymer International 40(2):151-151.

Koutinas M, Kiparissides A, Lam MC, Silva-Rocha R, Godinho M, de Lorenzo V, Martins dos Santos VAP, Pistikopoulos EN, Mantalaris A. 2011. Improving the prediction of *Pseudomonas putida* mt-2 growth kinetics with the use of a gene expression regulation model of the TOL plasmid. Biochemical Engineering Journal 55(2):108-118.

Koutinas M, Lam MC, Kiparissides A, Silva-Rocha R, Godinho M, Livingston AG, Pistikopoulos EN, de Lorenzo V, Dos Santos VA, Mantalaris A. 2010. The regulatory logic of m-xylene biodegradation by *Pseudomonas putida* mt-2 exposed by dynamic modelling of the principal node Ps/Pr of the TOL plasmid. Environmental Microbiology 12(6):1705-1718.

Krayl M, Benndorf D, Loffhagen N, Babel W. 2003. Use of proteomics and physiological characteristics to elucidate ecotoxic effects of methyl tert-butyl ether in Pseudomonas putida KT2440. Proteomics 3(8):1544-1552.

Lee J. 1997. Biological conversion of lignocellulosic biomass to ethanol. Journal of Biotechnology 56(1):1-24.

Lee SY, Wong HH, Choi JI, Lee SH, Lee SC, Han CS. 2000. Production of medium-chain-length polyhydroxyalkanoates by high-cell- density cultivation *Pseudomonas putida* under phosphorus limitation. Biotechnology and Bioengineering 68(4):466-470.

Leprince A, Janus D, de Lorenzo V, Santos VMd, Weber W, Fussenegger M. 2011. Streamlining of a *Pseudomonas putida* Genome Using a Combinatorial Deletion Method Based on Minitransposon Insertion and the Flp-*FRT* Recombination System

Synthetic Gene Networks. Humana Press. p 249-266.

Liu Q, Luo G, Zhou XR, Chen GQ. 2011. Biosynthesis of poly(3-hydroxydecanoate) and 3-hydroxydodecanoate dominating polyhydroxyalkanoates by β-oxidation pathway inhibited *Pseudomonas putida*. Metabolic Engineering 13(1):11-17.

Liu W, Chen GQ. 2007. Production and characterization of medium-chain-length polyhydroxyalkanoate with high 3-hydroxytetradecanoate monomer content by fadB and fadA knockout mutant of *Pseudomonas putida* KT2442. Applied Microbiology and Biotechnology 76(5):1153-1159.

Luengo JM, Garcia B, Sandoval A, Naharro G, Olivera ER. 2003. Bioplastics from microorganisms. Current Opinion in Microbiology 6(3):251-260.

Madison LL, Huisman GW. 1999. Metabolic engineering of poly(3-hydroxyalkanoates): From DNA to plastic. Microbiology and Molecular Biology Reviews 63(1):21-53.

Martinez-Garcia E, de Lorenzo V. 2011. Engineering multiple genomic deletions in Gram-negative bacteria: Analysis of the multi-resistant antibiotic profile of *Pseudomonas putida* KT2440. Environmental Microbiology 13(10):2702-2716.

Martínez V, García P, García JL, Prieto MA. 2011. Controlled autolysis facilitates the polyhydroxyalkanoate recovery in *Pseudomonas putida* KT2440. Microbial Biotechnology 4(4):533-547.

Martins Dos Santos VAP, Heim S, Moore ERB, Strätz M, Timmis KN. 2004. Insights into the genomic basis of niche specificity of *Pseudomonas putida* KT2440. Environmental Microbiology 6(12):1264-1286.

Meijnen JP, De Winde JH, Ruijssenaars HJ. 2008. Engineering Pseudomonas putida S12 for efficient utilization of D-xylose and L-arabinose. Applied and Environmental Microbiology 74(16):5031-5037.

Meijnen JP, De Winde JH, Ruijssenaars HJ. 2009. Establishment of oxidative D-xylose metabolism in Pseudomonas putida S12. Applied and Environmental Microbiology 75(9):2784-2791.

Miyakoshi M, Shintani M, Terabayashi T, Kai S, Yamane H, Nojiri H. 2007. Transcriptome analysis of Pseudomonas putida KT2440 harboring the completely sequenced IncP-7 plasmid pCAR1. Journal of Bacteriology 189(19):6849-6860.

Mobley HLT, Island MD, Hausinger RP. 1995. Molecular biology of microbial ureases. Microbiological Reviews 59(3):451-480.

Morales G, Ugidos A, Rojo F. 2006. Inactivation of the Pseudomonas putida cytochrome o ubiquinol oxidase leads to a significant change in the transcriptome and to increased expression of the CIO and cbb3-1 terminal oxidases. Environmental Microbiology 8(10):1764-1774.

Moreno R, Martinez-Gomariz M, Yuste L, Gil C, Rojo F. 2009. The Pseudomonas putida Crc global regulator controls the hierarchical assimilation of amino acids in a complete medium: Evidence from proteomic and genomic analyses. Proteomics 9(11):2910-2928.

Morgunov IG, Solodovnikova NY, Sharyshev AA, Kamzolova SV, Finogenova TV. 2004. Regulation of NAD+-Dependent isocitrate dehydrogenase in the citrate producing yeast *Yarrowia lipolytica*. Biochemistry (Moscow) 69(12):1391-1398.

Nakazawa T, Yokota T. 1973. Benzoate metabolism in Pseudomonas putida(arvilla) mt 2: Demonstration of two benzoate pathways. Journal of Bacteriology 115(1):262-267.

Nelson KE, Weinel C, Paulsen IT, Dodson RJ, Hilbert H, Martins dos Santos VAP, Fouts DE, Gill SR, Pop M, Holmes M and others. 2002. Complete genome sequence and comparative analysis of the metabolically versatile *Pseudomonas putida* KT2440. Environmental Microbiology 4(12):799-808.

Nijkamp K, Westerhof RGM, Ballerstedt H, De Bont JAM, Wery J. 2007. Optimization of the solvent-tolerant *Pseudomonas putida* S12 as host for the production of p-coumarate from glucose. Applied Microbiology and Biotechnology 74(3):617-624.

Nikodinovic-Runic J, Flanagan M, Hume AR, Cagney G, O'Connor KE. 2009. Analysis of the Pseudomonas putida CA-3 proteome during growth on styrene under nitrogen-limiting and non-limiting conditions. Microbiology 155(10):3348-3361.

Nogales J, Palsson BO, Thiele I. 2008. A genome-scale metabolic reconstruction of *Pseudomonas putida* KT2440: iJN746 as a cell factory. BMC Syst Biol 2:79.

Ochs MM, Lu CD, Hancock REW, Abdelal AT. 1999. Amino acid-mediated induction of the basic amino acid-specific outer membrane porin OprD from *Pseudomonas aeruginosa*. Journal of Bacteriology 181(17):5426-5432.

Olivera ER, Carnicero D, Jodra R, Miambres B, Garcia B, Abraham GA, Gallardo A, Roman JS, Garcia JL, Naharro G and others. 2001. Genetically engineered Pseudomonas: A factory of new bioplastics with broad applications. Environmental Microbiology 3(10):612-618.

Ouyang SP, Luo RC, Chen SS, Liu Q, Chung A, Wu Q, Chen GQ. 2007. Production of polyhydroxyalkanoates with high 3-hydroxydodecanoate monomer content by fadB anf fadA knockout mutant of *Pseudomonas putida* KT2442. Biomacromolecules 8(8):2504-2511.

Patel RN, Banerjee A, Ko RY, Howell JM, Li Wen S, Comezoglu FT, Partyka RA, Szarka L. 1994. Enzymic preparation of (3R-cis)-3-(acetyloxy)-4-phenyl-2-azetidinone: A taxol side-chain synthon. Biotechnology and Applied Biochemistry 20(1):23-33.

Peng X, Xu C, Ren H, Lin X, Wu L, Wang S. 2005. Proteomic analysis of the sarcosine-insoluble outer membrane fraction of *Pseudomonas aeruginosa* responding to ampicilin, kanamycin, and tetracycline resistance. Journal of Proteome Research 4(6):2257-2265.

Puchalka J, Oberhardt MA, Godinho M, Bielecka A, Regenhardt D, Timmis KN, Papin JA, Martins dos Santos VA. 2008. Genome-scale reconstruction and analysis of the *Pseudomonas putida* KT2440 metabolic network facilitates applications in biotechnology. PLoS Comput Biol 4(10):e1000210.

Rehm BHA. 2010. Bacterial polymers: Biosynthesis, modifications and applications. Nature Reviews Microbiology 8(8):578-592.

Rehm BHA, Krüger N, Steinbüchel A. 1998. A new metabolic link between fatty acid de novo synthesis and polyhydroxyalkanoic acid synthesis. The phaG gene from *Pseudomonas putida* KT2440 encodes a 3-hydroxyacyl-acyl carrier protein-coenzyme a transferase. Journal of Biological Chemistry 273(37):24044-24051.

Renzi F, Rescalli E, Galli E, Bertoni G. 2010. Identification of genes regulated by the MvaT-like paralogues TurA and TurB of Pseudomonas putida KT2440. Environmental Microbiology 12(1):254-263.

Reva ON, Weinel C, Weinel M, Bohm K, Stjepandic D, Hoheisel JD, Tummler B. 2006a. Functional genomics of stress response in Pseudomonas putida KT2440. Journal of Bacteriology 188(11):4079-4092.

Reva ON, Weinel C, Weinel M, Bohm K, Stjepandic D, Hoheisel JD, Tümmler B. 2006b. Functional genomics of stress response in Pseudomonas putida KT2440. Journal of Bacteriology 188(11):4079-4092.

Rodnina MV, Savelsbergh A, Katunin VI, Wintermeyer W. 1997. Hydrolysis of GTP by elongation factor G drives tRNA movement on the ribosome. Nature 385(6611):37-41.

Rojo F. 2010. Carbon catabolite repression in Pseudomonas: Optimizing metabolic versatility and interactions with the environment. FEMS Microbiology Reviews 34(5):658-684.

Ronchel MC, Molina L, Witte A, Lutbiz W, Molin S, Ramos JL, Ramos C. 1998. Characterization of cell lysis in Pseudomonas putida induced upon expression of heterologous killing genes. Applied and Environmental Microbiology 64(12):4904-4911.

Rosche B, Li XZ, Hauer B, Schmid A, Buehler K. 2009. Microbial biofilms: a concept for industrial catalysis? Trends in Biotechnology 27(11):636-643.

Rühl J, Schmid A, Blank LM. 2009. Selected Pseudomonas putida strains able to grow in the presence of high butanol concentrations. Applied and Environmental Microbiology 75(13):4653-4656.

Saito K, Matsuda F. 2010. Metabolomics for functional genomics, systems biology, and biotechnology. Annual Review of Plant Biology. p 463-489.

Santos PM, Benndorf D, Sa-Correia I. 2004. Insights into Pseudomonas putida KT2440 response to phenol-induced stress by quantitative proteomics. Proteomics 4(9):2640-2652.

Schmid A, Dordick JS, Hauer B, Kiener A, Wubbolts M, Witholt B. 2001. Industrial biocatalysis today and tomorrow. Nature 409(6817):258-268.

Schulze B, Wubbolts MG. 1999. Biocatalysis for industrial production of fine chemicals. Current Opinion in Biotechnology 10(6):609-615.

Segura A, Godoy P, Van Dillewijn P, Hurtado A, Arroyo N, Santacruz S, Ramos JL. 2005. Proteomic analysis reveals the participation of energy- and stress-related proteins in the response of Pseudomonas putida DOT-T1E to toluene. Journal of Bacteriology 187(17):5937-5945.

Senior PJ, Beech GA, Ritchie GA, Dawes EA. 1972. The role of oxygen limitation in the formation of poly- -hydroxybutyrate during batch and continuous culture of *Azotobacter beijerinckii*. Biochemical Journal 128(5):1193-1201.

Shah AA, Hasan F, Hameed A, Ahmed S. 2008. Biological degradation of plastics: A comprehensive review. Biotechnology Advances 26(3):246-265.

Silva-Rocha R, de Jong H, Tamames J, de Lorenzo V. 2011. The logic layout of the TOL network of *Pseudomonas putida* pWW0 plasmid stems from a metabolic amplifier motif (MAM) that optimizes biodegradation of m-xylene. BMC Systems Biology:191.

Sohn SB, Kim TY, Park JM, Lee SY. 2010. In silico genome-scale metabolic analysis of Pseudomonas putida KT2440 for polyhydroxyalkanoate synthesis, degradation of aromatics and anaerobic survival. Biotechnology Journal 5(7):739-750.

Sonawane A, Klöppner U, Derst C, Röhm KH. 2003a. Utilization of acidic amino acids and their amides by pseudomonads: Role of periplasmic glutaminase-asparaginase. Archives of Microbiology 179(3):151-159.

Sonawane A, Kloppner U, Hovel S, Volker U, Rohm KH. 2003b. Identification of Pseudomonas proteins coordinately induced by acidic amino acids and their amides: A two-dimensional electrophoresis study. Microbiology 149(10):2909-2918.

Steinbüchel A, Lutke-Eversloh T. 2003. Metabolic engineering and pathway construction for biotechnological production of relevant polyhydroxyalkanoates in microorganisms. Biochemical Engineering Journal 16(2):81-96.

Steinbüchel A, Valentin HE. 1995. Diversity of bacterial polyhydroxyalkanoic acids. FEMS Microbiology Letters 128(3):219-228.

Stephan S, Heinzle E, Wenzel SC, Krug D, Müller R, Wittmann C. 2006. Metabolic physiology of *Pseudomonas putida* for heterologous production of myxochromide. Process Biochemistry 41(10):2146-2152.

Sudesh K, Abe H, Doi Y. 2000. Synthesis, structure and properties of polyhydroxyalkanoates: Biological polyesters. Progress in Polymer Science (Oxford) 25(10):1503-1555.

Sun Z, Ramsay J, Guay M, Ramsay B. 2006. Automated feeding strategies for high-cell-density fed-batch cultivation of *Pseudomonas putida* KT2440. Applied Microbiology and Biotechnology 71(4):423-431.

Sun Z, Ramsay J, Guay M, Ramsay B. 2007a. Carbon-limited fed-batch production of medium-chain-length polyhydroxyalkanoates from nonanoic acid by *Pseudomonas putida* KT2440. Applied Microbiology and Biotechnology 74(1):69-77.

Sun Z, Ramsay J, Guay M, Ramsay B. 2009. Fed-batch production of unsaturated medium-chain-length polyhydroxyalkanoates with controlled composition by *Pseudomonas putida* KT2440. Applied Microbiology and Biotechnology 82(4):657-662.

Sun Z, Ramsay JA, Guay M, Ramsay BA. 2007b. Carbon-limited fed-batch production of medium-chain-length polyhydroxyalkanoates from nonanoic acid by *Pseudomonas putida* KT2440. Applied Microbiology and Biotechnology 74(1):69-77.

Tang H, Yu H, Li Q, Wang X, Gai Z, Yin G, Su F, Tao F, Ma C, Xu P. 2011. Genome Sequence of *Pseudomonas putida* Strain B6-2, a Superdegrader of Polycyclic Aromatic Hydrocarbons and Dioxin-Like Compounds. Journal of Bacteriology 193(23):6789-6790.

Tao F, Tang H, Gai Z, Su F, Wang X, He X, Xu P. 2011. Genome Sequence of *Pseudomonas putida* Idaho, a Unique Organic-Solvent-Tolerant Bacterium. Journal of Bacteriology 193(24):7011-7012.

Tessmer N, König S, Malkus U, Reichelt R, Pötter M, Steinbüchel A. 2007. Heat-shock protein HspA mimics the function of phasins sensu stricto in recombinant strains of *Escherichia coli* accumulating polythioesters or polyhydroxyalkanoates. Microbiology 153(2):366-374.

Timm A, Steinbuhel A. 1992. Cloning and molecular analysis of the poly(3-hydroxyalkanoic acid) gene locus of *Pseudomonas aeruginosa* PAO1. European Journal of Biochemistry 209(1):15-30.

Timmis KN. 2002. *Pseudomonas putida*: A cosmopolitan opportunist par excellence. Environmental Microbiology 4(12):779-781.

Trias J, Nikaido H. 1990. Protein D2 channel of the *Pseudomonas aeruginosa* outer membrane has a binding site for basic amino acids and peptides. Journal of Biological Chemistry 265(26):15680-15684.

Tsirogianni E, Aivaliotis M, Papasotiriou DG, Karas M, Tsiotis G. 2006. Identification of inducible protein complexes in the phenol degrader Pseudomonas sp. strain phDV1 by blue native gel electrophoresis and mass spectrometry. Amino Acids 30(1):63-72.

Van Der Werf MJ, Overkamp KM, Muilwijk B, Koek MM, Van Der Werff-Van Der Vat BJC, Jellema RH, Coulier L, Hankemeier T. 2008. Comprehensive analysis of the metabolome of Pseudomonas putida S12 grown on different carbon sources. Molecular BioSystems 4(4):315-327.

van Duuren JBJH. 2011. Optimization of *Pseudomonas putida* KT2440 as host for the production of cis, cis-muconate from benzoate. Wageningen: Wageningen.

Van Duuren JBJH, Brehmer B, Mars AE, Eggink G, dos Santos VM, Sanders JPM. 2011a. A limited LCA of bio-adipic acid: Manufacturing the nylon-6,6 precursor adipic acid using the benzoic acid degradation pathway from different feedstocks. Biotechnology and Bioengineering 108(6):1298-1306.

Van Duuren JBJH, Wijte D, Karge B, Martins dos Santos VA, Yang Y, Mars AE, Eggink G. 2011b. pH-stat fed-batch process to enhance the production of *cis, cis*-muconate from benzoate by *Pseudomonas putida* KT2440-JD1. Biotechnology Progress.

Van Duuren JBJH, Wijte D, Leprince A, Karge B, Puchalka J, Wery J, Dos Santos VAPM, Eggink G, Mars AE. 2011c. Generation of a *catR* deficient mutant of *P. putida* KT2440 that produces *cis, cis*-muconate from benzoate at high rate and yield. Journal of Biotechnology 156(3):163-172.

Velazquez F, Pfluger K, Cases I, De Eugenio LI, de Lorenzo V. 2007. The Phosphotransferase System Formed by PtsP, PtsO, and PtsN Proteins Controls Production of Polyhydroxyalkanoates in *Pseudomonas putida*. Journal of Bacteriology 189(12):4529-4533.

Verhoef S, Ballerstedt H, Volkers RJM, De Winde JH, Ruijssenaars HJ. 2010. Comparative transcriptomics and proteomics of p-hydroxybenzoate producing *Pseudomonas putida* S12: Novel responses and implications for strain improvement. Applied Microbiology and Biotechnology 87(2):679-690.

Verhoef S, Ruijssenaars HJ, de Bont JAM, Wery J. 2007. Bioproduction of p-hydroxybenzoate from renewable feedstock by solvent-tolerant *Pseudomonas putida* S12. Journal of Biotechnology 132(1):49-56.

Verhoef S, Wierckx N, Westerhof RGM, De Winde JH, Ruijssenaars HJ. 2009. Bioproduction of p-hydroxystyrene from glucose by the solvent-tolerant bacterium *Pseudomonas putida* S12 in a two-phase water-decanol fermentation. Applied and Environmental Microbiology 75(4):931-936.

Volkers RJM, De Jong AL, Hulst AG, Van Baar BLM, De Bont JAM, Wery J. 2006. Chemostat-based proteomic analysis of toluene-affected *Pseudomonas putida* S12. Environmental Microbiology 8(9):1674-1679.

Wang HH, Zhou XR, Liu Q, Chen GQ. 2011. Biosynthesis of polyhydroxyalkanoate homopolymers by *Pseudomonas putida*. Applied Microbiology and Biotechnology 89(5):1497-1507.

Wang Q, Nomura CT. 2010. Monitoring differences in gene expression levels and polyhydroxyalkanoate (PHA) production in *Pseudomonas putida* KT2440 grown on different carbon sources. Journal of Bioscience and Bioengineering 110(6):653-659.

Wenzel SC, Gross F, Zhang Y, Fu J, Stewart AF, Müller R. 2005. Heterologous expression of a myxobacterial natural products assembly line in Pseudomonads via Red/ET recombineering. Chemistry and Biology 12(3):349-356.

Wierckx N, Ruijssenaars HJ, de Winde JH, Schmid A, Blank LM. 2009. Metabolic flux analysis of a phenol producing mutant of Pseudomonas putida S12: Verification and complementation of hypotheses derived from transcriptomics. Journal of Biotechnology 143(2):124-129.

Wierckx NJP, Ballerstedt H, De Bont JAM, De Winde JH, Ruijssenaars HJ, Wery J. 2008. Transcriptome analysis of a phenol-producing *Pseudomonas putida* S12 construct: Genetic and physiological basis for improved production. Journal of Bacteriology 190(8):2822-2830.

Wierckx NJP, Ballerstedt H, De Bont JAM, Wery J. 2005. Engineering of solvent-tolerant *Pseudomonas putida* S12 for bioproduction of phenol from glucose. Applied and Environmental Microbiology 71(12):8221-8227.

Wolff JA, MacGregor CH, Eisenberg RC, Phibbs Jr PV. 1991. Isolation and characterization of catabolite repression control mutants of pseudomonas aeruginosa pao. Journal of Bacteriology 173(15):4700-4706.

Wong JW, Watson HA, Bouressa JF, Burns MP, Cawley JJ, Doro AE, Guzek DB, Hintz MA, McCormick EL, Scully DA and others. 2002. Biocatalytic Oxidation of 2-Methylquinoxaline to 2-Quinoxalinecarboxylic Acid. Organic Process Research & Development 6(4):477-481.

Yamane T. 1993. Yield of poly-D(-)-3-hydroxybutyrate from various carbon sources: A theoretical study. Biotechnology and Bioengineering 41(1):165-170.

Yang T, Jung Y, Kang H, Kim T, Park S, Lee S. 2011. Tailor-made type II *Pseudomonas* PHA synthases and their use for the biosynthesis of polylactic acid and its copolymer in recombinant *Escherichia coli*. Applied Microbiology and Biotechnology 90(2):603-614.

Yeom S, Yeom J, Park W. 2010. NtrC-sensed nitrogen availability is important for oxidative stress defense in Pseudomonas putida KT2440. Journal of Microbiology 48(2):153-159.

Yu H, Tang H, Wang L, Yao Y, Wu G, Xu P. 2011. Complete genome sequence of the nicotine-degrading *Pseudomonas putida* strain S16. Journal of Bacteriology 193(19):5541-5542.

Zhao YH, Li HM, Qin LF, Wang HH, Chen GQ. 2007. Disruption of the polyhydroxyalkanoate synthase gene in *Aeromonas hydrophila* reduces its survival ability under stress conditions. FEMS Microbiology Letters 276(1):34-41.

Zhen D, Liu H, Wang SJ, Zhang JJ, Zhao F, Zhou NY. 2006. Plasmid-mediated degradation of 4-chloronitrobenzene by newly isolated *Pseudomonas putida* strain ZWL73. Applied Microbiology and Biotechnology 72(4):797-803.

CHAPTER III. The metabolic response of *P. putida* KT2442 producing high levels of polyhydroxyalkanoate under single- and multiple-nutrient-limited growth: Highlights from a multi-level omics approach

3.

This chapter has been published: **Ignacio Poblete-Castro**, Isabel F. Escapa, Christian Jäger, Jacek Puchalka, Carolyn Ming Chi Lam, Dietmar Schomburg, María Auxiliadora Prieto, Vítor A. P. Martins dos Santos. Microbial Cell Factories (2012) 11: 34.

3.1 Abstract

Background

Pseudomonas putida KT2442 is a natural producer of polyhydroxyalkanoates (PHAs), which can substitute petroleum-based non-renewable plastics and form the basis for the production of tailor-made biopolymers. However, despite the substantial body of work on PHA production by *P. putida* strains, it is not yet clear how the bacterium re-arranges its whole metabolism when it senses the limitation of nitrogen and the excess of fatty acids as carbon source, to result in a large accumulation of PHAs within the cell. In the present study we investigated the metabolic response of KT2442 using a systems biology approach to highlight the differences between single- and multiple-nutrient-limited growth in chemostat cultures.

Results

We found that 26, 62, and 81% of the cell dry weight consist of PHA under conditions of carbon, dual, and nitrogen limitation, respectively. Under nitrogen limitation a specific PHA production rate of 0.43 $(g \cdot (g \cdot h)^{-1})$ was obtained. The residual biomass was not constant for dual- and strict nitrogen-limiting growth, showing a different feature in comparison to other *P. putida* strains. Dual limitation resulted in patterns of gene expression, protein level, and metabolite concentrations that substantially differ from those observed under exclusive carbon or nitrogen limitation. The most pronounced differences were

found in the energy metabolism, fatty acid metabolism, as well as stress proteins and enzymes belonging to the transport system.

Conclusion

This is the first study where the interrelationship between nutrient limitations and PHA synthesis has been investigated under well-controlled conditions using a system level approach. The knowledge generated will be of great assistance for the development of bioprocesses and further metabolic engineering work in this versatile organism to both enhance and diversify the industrial production of PHAs.

Keywords

P. putida KT2442, Nutrient limitation, Systems biology, Polyhydroxyalkanoates

3.2 Background

Microorganisms constantly face fluctuations of nutrient concentrations in their natural environments. One of the common evoked responses by bacteria is the storage of carbon and energy sources, as shown by the considerable increase in the accumulation of various compounds, such as glycogen, polyesters, and polyphosphates etc. (Wilson et al. 2010). The primary feature of these compounds is that they can be readily degraded by the cell to satisfy metabolic demands, thus ensuring its survival during famine. *Pseudomonas putida* KT2440 is a metabolically versatile bacterium (Nelson et al. 2002) normally found in aerobic and semi-aerobic soil and water habitats (Timmis 2002), which has become an efficient cell factory for the biotechnological production of value-added compounds (Poblete-Castro et al. 2012a). It synthesizes medium-chain-length polyhydroxyalkanoate (PHA) that exhibit different physical properties than those of the first discovered polyester polyhydroxybutyrate (PHB) (Kim et al. 2007; Prieto et al. 2007). PHAs can substitute petroleum-based non-renewable plastics and form the basis for the production of tailor-made biopolymers for medical applications (Rehm 2010), where fermentation strategies (Sun et al. 2009) and the supplied carbon sources (Hartmann et al. 2004) highly influence the final monomer composition of the PHA. However, despite the substantial body of work on PHA production by *P. putida* strains, it is not yet clear how the bacterium re-arranges its whole metabolism when it senses the limitation of an inorganic (N, S, P, or O) nutrient and the excess of fatty acids as carbon source, resulting in a large accumulation of PHAs within the cell. Recently, we demonstrated that this pathway acts as an important energy and carbon buffer under nutrient-limiting conditions that guarantee efficient growth (de Eugenio et al. 2010a). Inactivation of the pathway for PHA accumulation under low nitrogen growth conditions resulted in oxidation of the excess carbon source, rather than transforming it into biomass or secretable compounds, which could be further reused as carbon or energy sources (Escapa et al. 2012). Chemostat operation allows the single limitation of carbon or of any desirable nutrient in the culture. It is as well the best alternative to perform controlled and highly reproducible cultivation for studying the phenotype of a given organism (Hoskisson and Hobbs 2005), especially when applying hightroughput technology to capture the transcriptome, proteome, or metabolome of the cell for a given phenotype.

Using continuous cultivation, Egli and Quayle demonstrated that varying the ratio of carbon/nitrogen in the feed medium had a significant influence in the cellular and enzymatic composition on the yeast *H. polymorpha* (Egli and Quayle 1986). In addition, three distinct growth regimes were recognized: namely carbon-, carbon-nitrogen-, and strict nitrogen-limiting growth. By applying those fermentation strategies, *P. putida* GPo1 (formerly known as *P. oleovorans*) was investigated for its capacity to accumulate PHAs from different carbon sources (Durner et al. 2000; Durner et al. 2001; Hartmann et al. 2004), proving the high metabolic flexibility of GPo1 which was reflected in part by the broad dual-limiting area between the two single-nutrient limitation (for excellent review, see (Egli 1991)). One of the most interesting findings is that the dual-nutrient-limiting regime can result in the accumulation of PHA at levels comparable to those under strict nitrogen limitation (Zinn et al. 2004). As this results in less amounts of carbon used for comparable levels of PHA, this can substantially reduce the production costs.

The release of the *P. putida* KT2440 genome sequence in 2002 (Nelson et al. 2002) has enabled researchers to gain deeper and broader insights into the mechanisms underlying PHA biosynthesis (de Eugenio et al. 2010b; Escapa et al. 2011b; Liu et al. 2011; Ouyang et al. 2007). The progress in high-throughput technologies such as transcriptomics, proteomics, and metabolomics has expanded greatly the understanding of the genotype-phenotype relationships in *Pseudomonas*. As a result, several constrain-based metabolic models of this versatile organism have been developed (Nogales et al. 2008; Puchalka et al. 2008; Sohn et al. 2010). These models are useful to improve the production of PHAs, especially since the metabolic responses for PHA synthesis, which takes place preferably under the limitation of several nutrients, are complex and so far not well-understood. The work herein described aims to unravel the differences between carbon-, carbon-nitrogen-, and nitrogen-limited cultures, where omic-wide measurements were integrated to interpret the resulting phenotype for each condition in terms of PHA/biomass production in *P. putida* KT2442. This can contribute to set a basis for further development of new biocatalysts and processes that can contribute to reducing the production cost, which remains the biggest obstacle for the economically viable industrial production of PHAs.

3.3 Material and Methods

Culture conditions and bacterial strain. *Pseudomonas putida* KT2442 (Bagdasarian et al. 1981) was grown in a defined mineral medium (MM) consisting of (per liter) 12.8 g $Na_2HPO_4.7H_2O$, 3 g KH_2O_4, 1 g NH_4Cl, 0.5 g NaCl, supplemented with 0.12 g of $MgSO_4.H_2O$, and trace elements ($mg \cdot l^{-1}$): 6.0 $FeSO_4.7H_2O$, 2.7 $CaCO_3$, 2.0 $ZnSO_4.H2O$, 1.16 $MnSO_4.H_2O$, 0.37 $CoSO_4.7H_2O$, 0.33 $CuSO_4.5H_2O$, 0.08 H_3BO_3 and 0.1% (v/v) TEGO antifoam D 2310 (EVONIK Industries, Essen, Germany). Sodium decanoate (98% purity, Sigma-Aldrich) was used as a single carbon source in concentrations ranging from 1.90 to 8.70 $g \cdot l^{-1}$ (Table 1). For the preparation of the feeding solution, MM was mixed with sodium decanoate and TEGO antifoam. After mixing it, the solution was autoclaved for 25 min at 121°C. Once the bottle reached room temperature, it was placed into the clean bench where sterile trace elements solution and $MgSO_4.H_2O$ (by filtration) were added. Continuous cultivations were carried out under aerobic conditions at a dilution rate (*D)* of 0.1 h^{-1}, working volume of 0.8 liter in 1 liter top-bench BIOSTAT B1 bioreactor (Sartorius B Systems GmbH, Melsungen, Germany) at 30°C, constant stirring speed 700 r.p.m., and the pH was maintained at 7.0 by adding 2 M H_2SO_4. The working volume was kept constant by removing the fermentation broth through a peristaltic pump and recording the weight with a balance placed under the bioreactor. The aeration rate was set at 1 $l \cdot min^{-1}$ using a mass flow controller (PR4000, MKS Instruments, Wilmington, MA, USA), a mixture of air and pure oxygen was used to ensure that the dissolved oxygen was above 30% of air saturation. A paramagnetic gas analyzer (Servomex Xentra 4100, USA) to record online the concentrations of carbon dioxide and oxygen in the course of the process was coupled to the gas outlet of the bioreactor.

Analytical procedures. Once the considered steady state was attained, - *i.e*. that the optical density of the biomass, dissolved oxygen concentration, and exhaust gas concentration remained constant for at least four residence times - samples from chemostat cultures were taken using a peristaltic pump and processed as follows:

Cell and ammonium concentration. Cellular dry weight was determined by centrifuging 5 ml samples of the culture broth for 10 min at 4°C and 10,000 rpm (centrifuge 5810 R, Eppendorf, Germany) in pre-weighed tubes, washing the cell pellets once with distilled water and drying them at 80°C until a constant weight was obtained. Cell growth was recorded by measuring the optical density at 600_{nm} (Ultraspect 2000 UV/VIS, Hitachi, Japan). The ammonium concentration in the cell-free supernatant was measured using the LCK 303 kit of Hach Lange (Danaher, USA). The detection limit of this method was 1.9 mg of N/liter.

Fatty acid and PHA analysis. PHA compositions of the polymer produced, as well as the cellular PHA content and fatty acid concentration were determined by gas chromatography (GC) and mass spectrometry (MS) of the methanolyzed fatty acid and polyester. Methanolysis procedure was carried out by suspending 5–10 mg of lyophilized aliquots in 2 ml of chloroform and 2 ml of methanol containing 15% sulfuric acid and 0.5 mg ml^{-1} 3-methylbenzoic acid (internal standard) and then incubated at 100°C for 4 h. After cooling, 1 ml of demineralized water was added and the organic phase containing the resulting methyl esters of monomers was analysed by GC-MS (Lageveen et al. 1988). An Agilent (Waldbronn, Germany) series 7890A coupled with a 5975C MS detector (EI, 70 eV) and a split–splitless injector were used for analysis. An aliquot (1 ml) of organic phase was injected into the gas chromatograph at a split ratio of 1:50. Separation of compounds was achieved using a HP-5 MS capillary column (5% phenyl-95% methyl siloxane, 30 m X 0.25 mm i.d. X 0.25 mm film thickness). Helium was used as carrier gas at a flow rate of 0.9 ml min^{-1}. The injector and transfer line temperature were set at 275°C and 300°Crespectively. The oven temperature programme was: initial temperature 80°C for 2 min, then from 80°C up 150°C at a rate of 5°C min^{-1} and finally up 200°C at a rate of 10°C min^{-1}. EI mass spectra were recorded in full scan mode (*m/z* 40-550).

Exometabolite profile. 1D ^{1}H nuclear magnetic resonance spectra were recorded on a Bruker AVANCE DMX600 NMR spectrometer at 300 K of aqueous centrifuged supernatant containing 10% D_2O to give a final volume of 0.66 ml. The water signal was suppressed using standard Bruker software. For

comparison purposes, spectra of solutions of initial medium containing antifoam and sodium decanoate were recorded. In order to acquire an appropriate signal-to-noise ratio, spectra were recorded under standard conditions (sweep width: 20 ppm, acquisition time: 1.36 s, pulse delay: 1 s, number of scans: 1400, Bruker program noesypr1d).

Transcriptomics. Aliquots of 10 ml of culture broth were placed in RNAprotect buffer (Qiagen), cell pellets were further frozen at -80°C. Isolation of total RNA was performed using RNeasy kits (Qiagen), according to the instructions provided by the manufacturer. Progenika Biopharma (Vizcaya, Spain) *P. putida* Oligonucleotides Arrays were used for all transcriptional analyses. Fluorescently labelled cDNA for microarray hybridizations was obtained by using the SuperScript Indirect cDNA Labeling System (Invitrogen), as recommended by the supplier. In brief, 20 µg of total RNA was transformed to cDNA with Superscript III reverse transcriptase using random hexamers as primers, and including aminoallyl-modified nucleotides in the reaction mixture. After cDNA purification, the Cy3 or Cy5 fluorescent dyes (Amersham Biosciences) were coupled to the amino-modified first-strand cDNA. Labeling efficiency was assessed using a NanoDrop ND1000 spectrophotometer (NanoDropTechnologies). Equal amounts of Cy3- or Cy5-labelled cDNAs, one of them corresponding to the control and the other one to the condition to be analyzed, were mixed and dried in a Speed-Vac. The scanning was done with a GenePix 400B Scanner (Molecular Devices Corporation, Sunnyvale, California, USA.) at a 10 µm resolution. The images were quantified with GenePix Pro 5.1. Images from Cy3 and Cy5 channels were equilibrated and captured with a GenePix 4000B (Axon) and spots were quantified using GenPix Pro 5.1 software (Axon). The microarrays were analyzed using various packages from the Bioconductor suite (Gentleman et al. 2004). The results of image analysis were read in using the 'limma' package. The quality of the chips was analyzed with the 'arrayQualityMetrics' package (Kauffmann et al. 2009). The intensity values were background-corrected using the "'normexp" method of the limma package (Ritchie et al. 2007) and normalized with the variance stabilization method (Huber et al. 2002). The significantly differentially expressed genes were identified by fitting the linear model (using the functions 'lmFit' and 'eBayes' from

the 'limma' package) (Smyth 2004). Genes for which the adjusted p-value (by Benjamini-Hochberg method) was lower than 0.05 and the fold change exceeded 2 in either direction were assumed to be significantly expressed.

Proteomics. For protein extraction, cells were centrifuged at 8000 *g* for 15 minutes (centrifuge 5810 R, Eppendorf, Germany), the pellet was washed twice with PBS solution (pH 7.4). The resulting pellet was resuspended in lysis buffer consisting of 7 M urea, 2 M thiourea, 4% w/v CHAPS, 20 mM Tris base and 30 mM 1.4 dithiothreitol (DTT), together with protease inhibitor cocktail tablets. The lysis was complemented by sonication (Labsonic U, B. Braun, Germany. The resulting solution was ultracentrifuged (Sorval ultracentrifuge OTD-Combi, Thermo Electron, Germany) at 12000 *g*, 4°C for 30 min. The supernatant, corresponding to the soluble protein fraction, was aliquoted and further precipitated by using the 2-D Clean-Up Kit (GE Healthcare, USA). Analytical determinations were carried out with 100 mg of protein mixture determined by Bradford (Bio-Rad protein assay, Bio-Rad, USA), diluted up to 300 ml with rehydration solution (7 M urea; 5% w/v Serdolit; 2 M thio-urea; 4% w/v CHAPS; 20 mM Trizma base) in the presence of ampholytes and under reducing conditions, on ReadyStrip IPG strips, 17 cm, pH 3–10 (Bio-Rad, USA). Passive rehydration was carried out for 2 h at 20°C on the focusing tray. Samples were covered with silicon oil to avoid dehydration. Active rehydration was performed at 50 V for 12 h. Isoelectric focusing was done at a final voltage of 10 000 V on ProteanIEF cell (Bio-Rad, USA) until reaching 75 kVh. Focused samples were stored at -70°C until the second dimension step. Focused ReadyStrip IPG strips were equilibrated first in equilibration buffer containing 6 M urea, 0.375 M Trizma base (pH 8.6), 30% v/v glycerin, 2% w/v SDS and 2% w/v DTT and later in the same buffer replacing DTT with 2.5% w/v iodoacetamide. After equilibration, second-dimension separation was performed on 12–15% gradient SDS-polyacrylamide 20 X 20 cm gels with the focused sample embedded in 0.5% IEF agarose in a Protean Plus Dodeca Cell (Bio-Rad, USA) at 100 V overnight. The gels were fixed in 10% trichloroacetic acid solution for a minimum of 3 h, stained with 0.1% w/v Coomassie Brilliant Blue G-250 solution overnight and finally de-stained with distilled water. Images of the 2-DE gels were captured

with a molecular imager GS-800 calibrated densitometer (Bio-Rad, USA) and processed using Phoretix 2D image analysis software version 2004 (NonLinear Dynamics, UK) for protein DE analysis. Differential expression was defined as the ratio of spot protein expression in a comparative image to the expression of a corresponding spot in a reference image. Up- and down-regulation of protein expression were considered when the *p* value was less than 0.05, and twofold (or higher), and 0.5-fold (or lower) DE values, correspondingly. Protein spots were excised manually from the gels. Spots were de-stained and digested overnight using sequence grade modified trypsin (Promega, USA). The peptides were eluted and desalted with ZipTip (Millipore, USA). For MALDI-TOF analysis, the samples were loaded along with a-cyano-4-hydroxycinnamic acid matrix. The target was then analyzed using an Ultraflex II ToF (Bruker Daltonics, USA). The resulting spectra were used for Peptide Mass Fingerprint (PMF) and analyzed using FlexAnalysis 2.0 and Biotools 2.2 software (Bruker Daltonics). Proteins were identified using an in-house-licensed Mascot search engine (version 2.1.0, Matrix Science, U.K.). The P. putida KT2440 database was searched using the MALDI TOF-MS data with carbamidomethyl cysteine as a fixed modification and oxidized methionine as a variable modification. Trypsin was specified as the proteolytic enzyme and up to two missed cleavages were allowed.

Metabolomics. For metabolite extraction, cells were centrifuged at 4629 *g*, 4 °C for 3 minutes (centrifuge 5810 R, Eppendorf, Germany). The supernatant was discarded and the cell pellet was resuspended in 10 ml pre-cooled 0.9% NaCl (w/v). After further centrifugation the supernatant was discarded to complete the washing step. Furthermore, the resulting cell pellet was resupended in 1.5 ml cold methanol containing 60 µl ribitol (0.2 $g \cdot l^{-1}$) as internal standard. To achieve cell lysis the tubes were incubated in an ultrasonic bath (15 min, 70 °C). After the samples were cooled down for 2 min by placing them on ice, 1.5 ml of deionized H_2O was added and vortexed for 30 s. The addition of 1 ml chloroform was followed by mixing and centrifugation (9000 *g*, 4 °C, 5 min); 1 ml of the polar phase was subjected to a centrifugal-vacuum concentrator to allow evaporation. For derivatization, dried pellets were redissolved in 20 µl pyridine, containing 20 mg ml^{-1} methoxyamine hydrochloride, at 30 °C for 90 min under shaking.

After adding 32 µl N-methyl-N-trimethylsilyltrifluoroacetamide, samples were incubated at 37 °C for 30 min, followed by incubation at room temperature for 90 min under continuous shaking. Finally, the samples were centrifuged at 14 000 *g* for 5 min and the supernatant was used for GC-MS analysis. All samples were analysed within 24 h after derivatization. A retention index marker (n-alkanes ranging from C10...C36 in cyclohexane) was used to convert retention times to retention indices.

GC-MS analysis was performed on a FinniganTrace mass spectrometer (ThermoFinnigan, San Jose, USA). In summary, 1 µl of the derivatized samples was injected in randomized sequence into a programmed temperature vaporizer in split mode (1:25) at 70 °C. After an initial time of 0.2 min the injector was ramped at 14 °C s^{-1} to a final temperature of 280 °C and held for 5 min. The gas chromatograph was equipped with a J&W DB-5MS column (30 m x 0.25 mm ID, 0.25 µm film thickness). The GC was operated at constant flow of 1 ml min^{-1} helium. The temperature program started at 70 °C, held for 1 min, followed by a temperature ramping of 10 °C min^{-1} to a final temperature of 325 °C, which was held constant for 6 min. The transfer line temperature was set to 275 °C. Ion source temperature was adjusted to 200 °C. Full-scan mass spectra of m/z 40...460 were collected at an acquisition rate of 2.5 scans sec^{-1}. Solvent delay time was 4.5 min. For data acquisition Xcalibur 1.2 (Thermo Scientific) was used.

All chromatograms were processed using MetaboliteDetector (Hiller et al. 2009) for targeted analysis. The software supports automatically deconvolution of all mass spectra from a chromatogram and calculates the retention indices. The obtained mass spectra were matched against the reference with a minimum match factor of 0.75. Compounds were annotated by retention index and mass spectra comparison to our in-house library. Selected fragment ions unique for each individual metabolite were used for quantification. Finally, each compound was normalized by peak area from the internal standard (ribitol) and given cell dry weight.

Transcmission electron microscopy

Bacteria were fixed with 2% glutaraldehyde and 3% formaldehyde in cacodylate buffer (0.1 M cacodylate, 0.01 M $CaCl_2$, 0.01 M $MgCl_2$, 0.09 M sucrose, pH 6.9) for 1 hour on ice, washed with cacodylate buffer, and osmificated with 1% aqueous osmium for 1 hour at room temperature. Samples were then dehydrated with a graded series of acetone (10%, 30%, 50%, 70%, 90%, and 100%) for 30 minutes at each step. Dehydration in the 70% acetone step was done with 2% uranyl acetate overnight. Samples were infiltrated with an epoxy resin according to the Spurr formula (Spurr, 1969). Ultrathin sections were cut with a diamond-knife, counterstained with uranyl acetate and lead citrate, and examined in a TEM910 transmission electron microscope (Carl Zeiss, Oberkochen) at an acceleration voltage of 80 kV. Images were taken at calibrated magnifications using a line replica. Images were recorded digitally with a Slow-Scan CCD-Camera (ProScan, 1024x1024, Scheuring, Germany) with ITEM-Software (Olympus Soft Imaging Solutions, Münster, Germany).

Calculations

In the chemostat, the physiological parameters, as well as the PHA productivity where calculated according to the following equations:

$$Y_{X/C} = \frac{\Delta X}{\Delta C} \qquad [g \cdot g^{-1}] \qquad (1)$$

$$Y_{X/N} = \frac{\Delta X}{\Delta N} \qquad [g \cdot g^{-1}] \qquad (2)$$

$$q_{C/\hat{x}} = \frac{\Delta C \cdot D}{X_{(PHA\text{-}free)}} \qquad [g \cdot (g \cdot h)^{-1}] \qquad (3)$$

$$q_{PHA/\hat{x}} = \frac{PHA \cdot D}{X_{(PHA\text{-}free)}} \qquad [g \cdot (g \cdot h)^{-1}] \qquad (4)$$

The nutrient yield coefficient for carbon and nitrogen were used to calculate the boundaries according to the procedure described by Egly and Quayle (1986):

$$\frac{C_0}{N_0} \cong \frac{Y_{X/N} \cdot 14}{Y_{X/C} \cdot 12} \qquad [\text{mol}\cdot\text{mol}^{-1}] \qquad (5)$$

3.4 Results and Discussion

3.4.1 Physiological response of *Pseudomonas putida* under nutrient-limited conditions

In order to evaluate both the capacity of *P. putida* to produce medium-chain-length polyhydroxyalkanoates (mcl-PHAs) and the global cellular responses at the transcriptome, proteome, and metabolome levels, continuous cultivations were conducted under different nutrient-limited conditions. At least three independent experiments for each nutrient limitation were performed under aerobic chemostat conditions. To achieve metabolic steady-state at a dilution rate (*D*) of 0.1 h^{-1}, five to eight times the residence volume were necessary to attain constant macroscopic physiological parameters across the time. From continuous and flask-culture cultivations the maximum specific growth rate (μ_{max}) on decanoate was found to be 0.53 h^{-1} (data not shown). When *D* approaches μ_{max}, the amount of PHA decreases within the cell (Huijberts and Eggink 1996). Therefore, we imposed a low *D* (0.1 h^{-1}) to obtain as much PHA as possible. Decanoate was employed as the unique carbon and energy source, whereas ammonium [NH_4^+] as used as the nitrogen source. We changed the (C_0/N_0) ratios in the feed medium by keeping the nitrogen concentration invariable and increasing the carbon quantity. We were able to establish three specific environments within the chemostat: carbon- (C), carbon-nitrogen- (dual), and strictly nitrogen- (N) limited cultures, which were confirmed by the analytical measurement of the fermentation broth (Table 1). ^1H spectra were recorded from samples taken under all limiting fermentation conditions. In all cases there was no significant accumulation of acetate or any other soluble small molecular weight metabolite.

To obtain insights into the distribution of the metabolized carbon within the cell, we have performed a carbon mass balance analysis for each condition tested (Fig. 1).

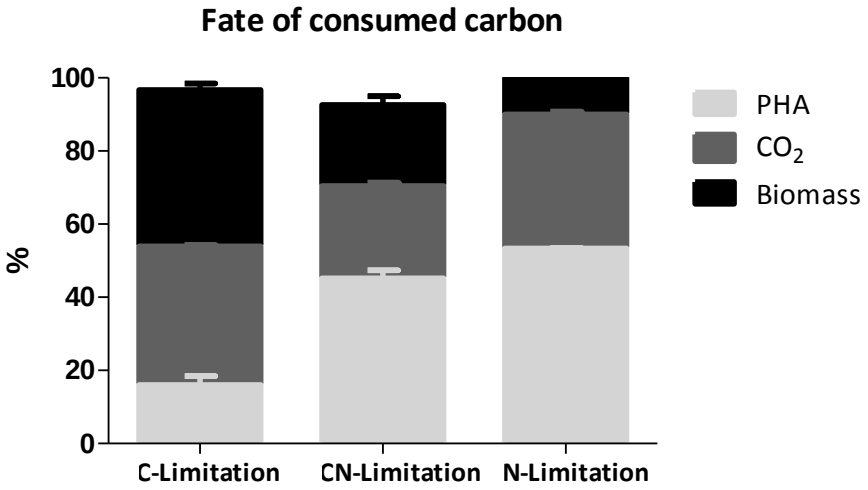

Figure 1. Fate of consumed carbon based on the carbon balance within the chemostat subjected to carbon, carbon-nitrogen, and nitrogen limitation.

This was calculated based on number of moles of carbon consumed and generated within the chemostat. The C-mol content in the biomass (PHA-free) was assumed to be constant which corresponds to a molecular weight of 27 g (C-mol biomass)$^{-1}$ (van Duuren 2011). The environment which is assigned less CO_2 (in terms of percentage) among those tested conditions is the dual limitation. A similar percentage of carbon ended up in PHAs in carbon-nitrogen- and nitrogen-deprived cells. In decanoate and decanoate-ammonium-limited cultures, mass-balances indicated that the entire carbon available in the reaction volume was converted to biomass, CO_2, and PHA (Fig. 1). As shown in (Fig. 2A), the biomass yield on decanoate decreased when the ammonium concentration limited growth, expressing its major effect under strict nitrogen limitation. The physiological response of KT2442 to the nutrient-deprived environments differed in the build-up of biomass for both C-N- and N-limited cultures as compared with the C-limited culture. This might be due to the increased pool of metabolites suitable for PHA accumulation in the β-oxidation pathway, which consequently decreases the buffer of precursor for biomass formation, affecting the energy efficiency not only for strict N-deprived cultures (Follonier et al. 2011), but also for C-N-deprived cells.

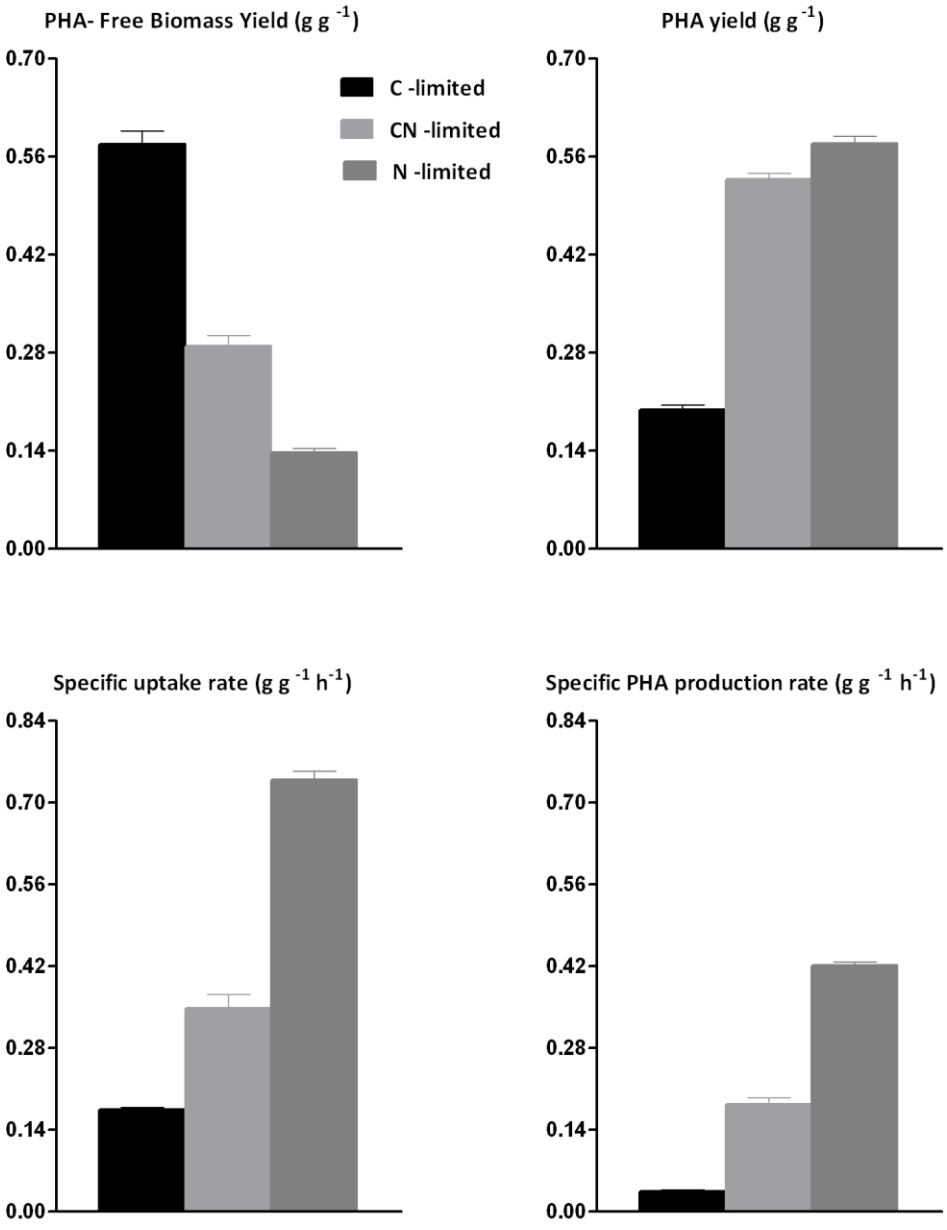

Figure 2. Physiological parameters of chemostat subjected to nutrient limitations. A) Grams of biomass (PHA-free) per gram of decanoate; B) Grams of PHA per gram of decanoate; C) Grams of decanoate per gram of biomass (PHA-free) per hour; D) Grams of PHA per gram of biomass (PHA-free) per hour.

The PHA yield on decanoate was very similar for both dual and strict nitrogen limitation (Fig. 2B). Because of this, the additional carbon source is nearly superfluous, indicating potential for savings on the raw materials. Besides, the imposed carbon/nitrogen ratio to achieve the dual limitation environment (Table 1) was significantly higher than the calculated boundary of this condition, which is known to achieve a higher PHA yield (Durner et al. 2001). Remarkably, *P. putida* KT2442 showed a different behavior compared to *P. putida* GPo1 with regard to the residual biomass, since for KT2442 this was not constant under CN-and N-limiting growth conditions (Table 1). For GPo1, once the growth condition reached the dual limitation area, the residual biomass remained constant while the PHA content increased proportionally with respect to the C_0/N_0 ratio in feed medium (Durner et al. 2000). In our study the maximum specific PHA production rate of KT2442 was obtained when the single nitrogen limitation was imposed to the chemostat (Fig. 2 D), reaching a value of 0.43 $(g \cdot (g\ h)^{-1})$. This productivity is 3.5-fold higher than the one showed by GPo1 with the same dilution rate while growing on octanoate (Durner et al. 2000), and 2-fold higher than the processes using 10-undecenoate as carbon source with also *P. putida* GPo1 (Hartmann et al. 2004).

Table 1. PHA production and relative monomer composition by *P. putida* KT2442 in continuous culture at D = 0.1 h^{-1}

Limitation	(C_0/N_0)*	$Y_{X/C}$	$Y_{X/N}$	**$(C_0/N_0)^b$ Borders**	Residual carbon[a]	Residual nitrogen[a]	CDW[a]	PHA content[a]	Monomer composition (mol %)		
	(mol mol^{-1})	(g g^{-1})	(g g^{-1})	**(mol mol^{-1})**	(g)	(g)	(g l^{-1})	(% CDW)	C6	C8	C10
Carbon	5.83	1.11	9.80	**10.40**	N.D.	0.112 ± 0.01	1.46 ± 0.04	25.78 ± 0.97	3.3	53.4	43.3
Carbon-Nitrogen	16.56	1.16	16.67		N.D.	N.D.	4.35 ± 0.13	61.94 ± 4.95	4.8	42.8	52.4
Nitrogen	26.97	1.01	17.74	**20.50**	1.53 ± 0.04	N.D.	4.63 ± 0.14	80.58 ± 0.24	4.3	40.2	55.5

[a] Standard deviation (±) from at least three independent experiments.

*C_0/N_0: Initial feeding ratio of carbon-nitrogen.

N.D.: Not detectable

[b] According to the procedure described by Egly and Quayle (1986)

3.4.2 PHA accumulation *versus* nutrient availability

To assess the capability of *P. putida* to synthesize mcl-PHAs, we used gas chromatography to quantify intracellular polyester content and characterize the monomer composition from each individual chemostat culture. The heteropolymer was synthesized under each condition, with the accumulation range of the storage compound in the cell increasing when the (C_0/N_0) ratio in the feed medium is higher (see Table 1). *P. putida* KT2442 was capable of synthesizing PHA up to 26% of its total cell dry weight (CDW) in carbon-limited cultures. A similar PHA concentration (20% of CDW) was found when KT2442 was grown in oleic acid with a C-mol/N-mol ratio of 10 in continuous cultures (Huijberts and Eggink 1996). Such polymer accumulation is one of the special characteristics shown by *P. putida* strains under carbon-limiting conditions. Nevertheless, not all of them reach high levels of PHA accumulation. In the case of *P. putida* GPo1 the polyester synthesis yielded 2% of the CDW during carbon-limited growth on heptanoate and octanoate, but with nonanoate PHA accounted for 19 wt% of the biomass (Durner et al. 2001). Under dual limitation 62% of the CDW of KT2442 was composed of PHAs, whereas under strict nitrogen-limitation this was 81%.

We were able to identify three saturated monomers in the polyester (Huijberts et al. 1992; Ouyang et al. 2007) composed of 3.3 mole% of 3-hydroxyhexanoate (C6), 53.4 mole% of 3-hydroxyoctanoate (C8), and 43.3 mole% of 3-hydrodecanoate (C10) when carbon was the limited compound. The monomer composition present in this study is extremely similar when *P. putida* KT2440 was grown in batch cultures supplemented with decanoate (Huijberts et al. 1992). When decanoate is supplied as the only carbon source, the catabolic process occurs through the β-oxidation pathway. This correlates with the chain length structure detected in the heteropolymer showing C10, C8, and C6 hydroxyl-fatty acids as monomers, as consequence of two carbons loss during each round of the metabolic cycle. Comparing all nutrient-limited regimes, no remarkable difference could be observed in the monomer distribution. However, when ammonia was the limiting inorganic nutrient, a slight increase (of approximately 10%) in C10 was observed. When both carbon and nitrogen were bellow the detection limit in the chemostat, the

monomer composition of the polymer was almost the same as the one observed in nitrogen deprived cultures (Table 1). Further discussion is made below (see fatty acid and PHA metabolism).

3.4.3 Global multi-omics analysis of *P. putida* response under various nutrient limitations

Transcriptomics

Employing *genome-wide microarray* technology, we quantified the variation in gene expression levels of all three limiting conditions. As we set up our experiments under *steady-state*, the measurements reflected a snap-shot of the metabolic state under the desirable growth limitation by nitrogen or carbon-nitrogen. Three independent biological replicates were analyzed statistically after hybridization. The conditions of strict nitrogen limitation and carbon-nitrogen limitation were compared independently to carbon limitation, i.e. N vs. C and CN vs. C, respectively. The resulting intensities were treated using a different package from the Bioconductor suite (see material and methods). The classification of the resulting variations in gene expression were based on Cluster of Orthologous Groups (COG) (http://www.ncbi.nlm.nih.gov/COG/grace/cogenome.cgi?g=287) and illustrated in Fig. S1 (supplementary material). In total, 215 genes were differentially expressed ($P < 0.05$), from which 36% of their gene products were assigned as having unknown function (Table S1). The analysis of N vs. C and CN vs. C revealed 42 and 31 upregulated genes, while those that had a fold change less than 0.5-fold were 17 and 125, respectively (Table S1, supplemental material). As such, the N vs. C and CN vs. C comparisons shared 20 Open Reading Frames (in grey background Table. 2), with 11 showing more than 2-fold differential expression (Table 2).

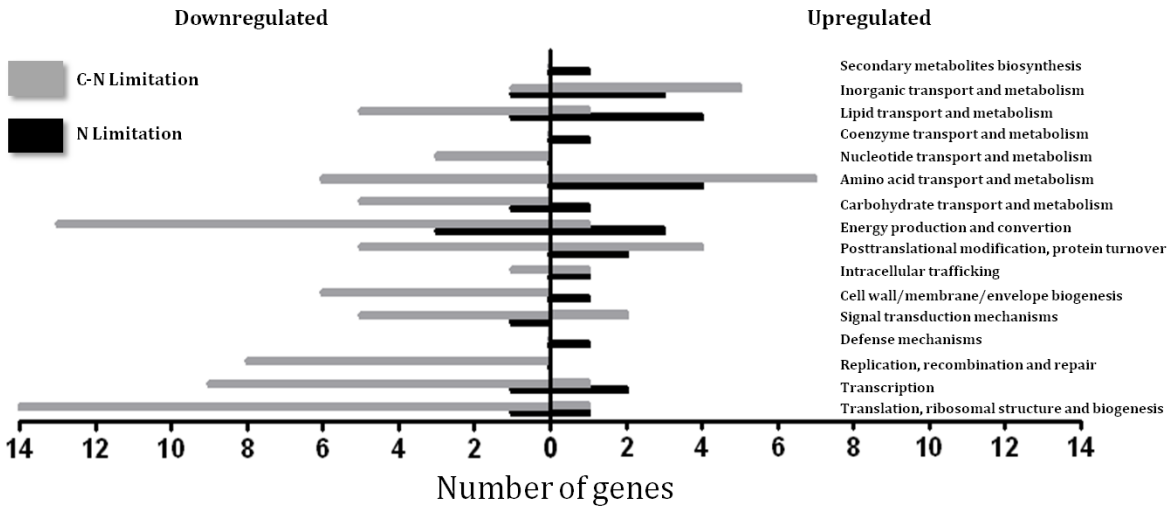

Figure S1. Genes differentially expressed in response to the limitation of nitrogen and carbon-nitrogen limitation. The generated functional categories groups were based on COG data.

Proteomics

Proteome profiling of *Pseudomonas putida* was performed using two-dimensional electrophoresis gels for each limiting condition to gain insight into the PHA accumulation machinery. As performed in the transcriptome analysis the gels from N- and CN-limited conditions were overlapped against the gel of C-limitation (master gel). The proteomic profile for the CN vs. C exhibited only 17 spots with differential expression (DE). A completely different scenario was detected by overlapping the nitrogen limiting growth gel with the master gel, giving 74 spots with differential expression. After searching the sequence similarity for protein identification (see materials and methods), out of these 74 spots, 45 met the requirements for protein identification. The proteins were classified using COGs and JCVI-CMR (http://cmr.jcvi.org/cgi-bin/CMR/CmrHomePage.cgi) and presented in table 3. The transcriptome response based on DNA microarray was compared to the proteome data. For C/N vs. C limitation only 5 proteins matched with their corresponding gene expression, and for N vs. C limitation 6 fell into this category (Table 3, in grey background). Although, 2-D PAGE proteome analysis is one of the most employed techniques in the field, it did not capture the entire proteome of the tested conditions (no identification of PhaC or PhaF), thus having a significant impact on the comparison.

Table 2. Selected genes differentially expressed within nitrogen (N) or carbon-nitrogen (C-N) limited cultures relative to carbon limited chemostat cultures.

Cellular role category	Locus tag	Description	Fold change	
			N	C-N
Energy metabolism				
	PP2638	Cellulose synthase operon C putative	3.9	4.3
	PP0813	Cytochrome *o* ubiquinol oxidase subunit I	5.0	1.2
	PP0814	Cytochrome *o* ubiquinol oxidase subunit III	4.4	-1.1
	PP4050	Glycogen synthase	3.1	1.3
	PP0555	Acetoin dehydrogenase alpha subunit	-6.7	-8.3
	PP0556	Acetoin catabolism protein	-3.7	-4.6
	PP0554	Acetoin dehydrogenase beta subunit	-4.6	-4.2
	PP0553	Acetoin dehydrogenase dihydrolipoamide	-5.3	-4.0
	PP0557	Acetoin catabolism regulatory protein	-3.4	-3.6
	PP2149	Glyceraldehyde 3-phospate dehydrogenase	1.5	-3.7
	PP4715	Triosephosphate isomerase	1.9	-3.3
	PP4737	D-lactate dehydrogenase putative	-2.6*	-3.1
	PP0545	Aldehyde dehydrogenase family protein	-1.9	-3.1
	PP1083	Bacterioferritin-associated ferredoxin putative	1.4	2.9
	PP3071	Acetoacetyl-CoA synthetase putative	1.1	-2.6
	PP4736	L- lactate dehydrogenase	-1.1	-2.5
	PP4192	Succinate dehydrogenase hydrophobic	3.9*	-2.4
	PP4193	Succinate dehydrogenase cytochrome	2.7*	-2.2
Amino acid transport and biosynthesis				
	PP4842	Branched-chain amino acid ABC transport	15.9	5.8
	PP4841	Branched-chain amino acid ABC transport	7.3	4.5
	PP5075	Glutamate synthase small subunit	3.4	1.2
	PP3021	Transporter LysE family	-1.4	2.2
Transport and binding proteins				
	PP4147	Peptide ABC transporter	-1.1	-2.7
	PP1076	Glycerol uptake facilitator protein	1.4	-2.9
	PP3954	Periplasmic binding protein putative	-1.9	-3.2
Nitrogen metabolism				
	PP5234	Nitrogen regulatory protein P-II	25.1	12.2
	PP5233	Ammonium transporter	13.7	2.6
	PP1705	Nitrate reductase	4.1*	5.2
	PP1703	Assimilatory nitrate reductase putative	2.3*	3.6

	PP2094	Nitrate-binding protein	4.5*	2.6
	PP2092	Nitrate transporter	2.3*	3.7
	PP2846	Urease accessory protein UreE	3.1*	2.8
	PP2847	Urease accessory protein UreJ	2.6*	2.5
	PP2843	Urease gamma subunit UreA	2.3	2.2
Polyhydroxyalkanoate				
	PP5008	PHA granule-associated 1 protein (phasin)	6.1	2.5
	PP5007	PHA granule-associated 2 protein (phasin)	3.1*	2.3
	PP5003	PHA polymerase 1	3.4*	1.0
	PP5005	PHA polymerase2	1.2	1.1
Fatty acid and phospholipid metabolism				
	PP2050	Conserved hypothetical protein	28.4	1.2
	PP2051	Acetyl-CoA acetyltransferase	27.9	-1.1
	PP2049	Alcohol dehydrogenase iron-containing	28.3	1.1
	PP2047	3-hydroxyacyl-CoA dehydrogenase family	20.9	1.1
	PP2048	Acyl-CoA dehydrogenase putative	19.8	1.5
	PP4550	Long-chain-fatty-acid-CoA ligase	4.2	1.5
	PP2437	Acyl-CoA dehydrogenase putative	-1.4	-3.2
Stress response				
	PP3781	Oxygen-independent Coproporphyrinogen III	7.5	-1.1
	PP1185	Outer membrane protein H1	6.6	2.0*
	PP1360	Chaperonin, 10 kDa	3.4	-1.1
Other functions				
	PP2141	Hypothetical protein	-4.0	-3.1
	PP1659	Hypothetical protein	-4.8	-2.4
	PP0765	Hypothetical protein	-7.1	-2.8
	PP2685	Hypothetical protein	11.1	4.0
	PP2686	Transglutaminase-like superfamily	6.6	4.6
	PP2687	Conserved hypothetical protein	7.1	2.6
	PP2689	Endoribonuclease putative	1.7	2.5

* 0.1 > *P*-value > 0.05

Gray background indicates matching gene expression of N vs. C and CN vs.

Relationships and discrepancies between transcripts and proteins

The correlation between increased transcripts and their corresponding protein abundance is very poor as shown in Table 3 for CN vs. C and N vs. C comparisons. Earlier studies have previously shown this trend between mRNA and protein levels (Kolkman et al. 2006; Lu et al. 2007; Verhoef et al. 2010). It has

mainly been attributed to post-transcriptional events (Kolkman et al. 2006) e.g. translation efficiency or protein degradation, and/or false-positive results either on the mRNA or protein levels (Resch et al. 2006). The generated gels from the proteome analysis in this study were made in triplicate for each tested condition, giving a confident proteome profile. Therefore, the high discrepancy between the transcript and protein expression levels, for both comparisons, might be evoked by a post-transcriptional regulation. This is supported by the number of differentially expressed genes — especially while comparing CN vs. C limitation — and the matched protein/mRNA abundance. Nevertheless, to fully confirm this hypothesis further studies should be addressed with more accurate techniques by which thousands of proteins can be quantified and compared (Lee et al. 2011). In this study, a surprisingly high number of downregulated genes in CN-limitation relative to C-limitation was found (Fig. S1). This highly differs from the proteome profile (Table 3). In addition, it is interesting to see how *P. putida* KT2442 displays many changes at the transcription level, but at the translation level the final response is quite conservative upon CN limitation. One could propose that under CN-limitation the coupling between anabolism and catabolism is tighter than N-limitation, as it can be seen by the residual biomass formation under the mentioned conditions (Fig. 2). Therefore, it seems that dual limitation is more similar to C-limiting than N-limiting cultures, since the proteome profile —which is a closer link than transcriptome to the final phenotype of the cell — did not have a significant change for the dual limitation relative to strict carbon limitation (Table 3).

Table 3. Change in protein expression in response to nitrogen and carbon-nitrogen limitation in comparison with carbon-limitation.

	Locus tag	Gene symbol	Protein		Transcript	
			D.E	[a]Peptides No.	Fold change	*P*-value
Differential protein expression of CN vs. C						
Energy metabolism						
ATP synthase F1, α-sub	PP5415	*atpA*	***only in CN***	12	ND	ND
Glycogen debranching	PP4055	*glgX*	**4.5**	20	1.9	0.05
Acetolactate synthase	PP3365		**3.5**	15	-1.0	n.s
Isocitrate dehydrogenase	PP4011	*icd*	**-5.0**	28	-1.4	n.s
Acetoin dehydrogenase α-sub	PP0555	*acoA*	**-4.0**	7	-8.3	0
Acetoin dehydrogenase β-sub	PP0554	*acoB*	**-5.6**	23	-4.2	0
Acetoin dehydrogenase	PP0553	*acoC*	**-3.7**	10	-4.0	0
Nitrogen metabolism						
Nitrogen regulatory protein P-II	PP5234	*glnK*	***only in CN***	6	10.4	0
Protein synthesis						
Elongation factor Tu	PP0452	*tuf-2*	***only in CN***	16	-1.6	n.s
Amino acid transport and biosynthesis						
Branched-chain amino acid ABC trans	PP4841	*livK*	**26.4**	22	4.5	0
Glutamine synthetase	PP5046	*glnA*	**2.2**	28	1.0	n.s
Signal transduction						
Response regulator	PP5048	*ntrC*	**6.7**	43	1.7	n.s
Transport and binding protein						
Outer membrane porin	PP1206	*oprD*	**2.7**	11	-1.1	n.s
Outer membrane porin	PP2089	*oprF*	**2.6**	21	1.2	n.s
Purine ribonucleotide biosynthesis						
adenylosuccinate synthetase	PP4889	*purA*	**-4.4**	16	-1.1	n.s
Hypothetical protein	PP2384		**-2.8**	6	1.5	n.s
Protein fate	PP0980	*pepA*	**-2.3**	30	1.0	n.s
Differential protein expression of N vs. C						
Energy metabolism						
Succinyl-CoA synthetase	PP4185	*sucD*	***only in N***	8	1.2	n.s
ATP synthase F1, alpha sub	PP5415	*atpA*	***only in N***	13	ND	ND
Glycogen debranching	PP4055	*glgX*	**12.3**	31	2.4	n.s
Electron transfer flavoprotein	PP4203		**4.5**	36	0.90	n.s
Succinate dehydrogenase	PP4191	*sdhA*	**3.9**	23	2.8	n.s
NADH dehydrogenase I	PP4123	*nuoF*	**2.9**	15	2.4	n.s
Glycosyl hydrolase	PP4053		**2.6**	21	3.0	n.s

Phosphoenolpyruvate synthase	PP2082	*ppsA*	**2.4**	24	1.5	n.s
Acetoin dehydrogenase β-sub	PP0554	*acoB*	***only in C***	23	-4.0	0
Acetoin dehydrogenase	PP0553	*acoC*	***only in C***	10	-5.3	0
Malate synthase	PP0356	*glcB*	**-9.1**	9	-1.2	n.s
Aldehyde dehydrogenase	PP0545	*glcB*	**-5.9**	19	-1.9	n.s
thioredoxin reductase	PP0786	*trxB*	**-5.6**	11	1.3	n.s
Isocitrate lyase	PP4116	*aceA*	**-4.2**	19	1.3	n.s
Isocitrate dehydrogenase	PP4011	*icd*	**-2.1**	14	1.1	n.s
Fatty acid metabolism						
3-hydroxyacyl-CoA dehydrogenase	PP2047		***only in N***	18	20.9	0
Acetyl-CoA acetyltransferase	PP2051	*atoB*	***only in N***	20	27.9	0
acetyl-CoA carboxylase	PP0558	*accC-1*	**8.3**	27	1.3	n.s
Fatty oxidation complex α-sub	PP2136	*fadB*	**3.1**	13	2.3	n.s
3-oxoacyl-CoA thiolase	PP2137	*fadA*	**3.0**	23	2.4	n.s
Fatty-acid CoA ligase	PP0763		**-2.9**	15	-1.1	n.s
Transport and binding protein						
Outer membrane porin	PP2089	*oprF*	**5.4**	17	1.4	n.s
ABC transporter	PP1726		**-25.0**	15	1.2	n.s
Amino acid transport and biosynthesis						
Branched-chain amino acid ABC	PP4864		***only in N***	9	-1.1	n.s
Amino acid biosynthesis	PP5046	*glnA*	**16.0**	17	1.5	n.s
Hydantoin racemase	PP4310		**8.8**	15	1.2	n.s
General amino acid ABC transporter	PP1300	*aapP*	**4.0**	16	1.1	n.s
amino acid ABC transporter	PP1071		***only in C***	23	-2.0	n.s
amino acid ABC transporter	PP0282		**-33.3**	15	-1.2	n.s
Branched-chain amino acid ABC	PP4867		**-16.7**	11	1.8	n.s
Dipeptide ABC transporter	PP0885		**-5.0**	22	1.2	n.s
Amino acid biosynthesis	PP0671	*glyA-2*	**-3.6**	20	-1.3	n.s
Cell envelope						
Outer membrane protein H1	PP1185	*oprH*	***only in N***	8	6.6	0.01
Cellular processes						
Small multidrug resistance	PP4930		**4.9**	216	1.1	n.s
superoxide dismutase	PP0915	*sodB*	**-20.0**	4	-1.3	n.s
DNA interactions						
Transcriptional regulator, LysR	PP5375		**-12.5**	5	-1.5	n.s
C4-type zinc finger protein	PP4693		**-11.1**	5	1.4	n.s
Protein fate						
ATP-dependent Clp protease	PP2300		***only in N***	7	1.2	n.s
Protein synthesis						
Elongation factor-G	PP0451	*fusA-1*	**20.0**	26	1	n.s

Hypotetical protein	PP2050		**9.4**	10	28.4	0
Purine ribonucleotide biosynthesis	PP0722	*prsA*	**6.6**	24	2.0	n.s
Cell division	PP1342	*ftsZ*	**-7.1**	5	1.0	n.s
Nucleoside interconversions	PP0849	*ndK*	**-3.3**	6	1.2	n.s
Biosynthesis of co-factors	PP0842	*iscS-1*	**-2.9**	18	1.3	n.s
Chemotaxis and motility	PP4366	*flil*	**-2.3**	7	1.3	n.s

Gray background indicates matching between protein and transcript changes.
[a]Amount of peptides utilized for protein identification.
ND. Not determined
n.s. *P*-value not significant (> 0.05)

Metabolomics

Applying metabolome analysis, the peak areas of the Entner-Doudoroff-pathway and TCA cycle intermediates, and amino acids were determined and the mass corresponding masses quantified as described in Materials and Methods. The reproducibility of the analytical protocols (technical reproducibility) was determined for every sample set by establishing the relative standard deviation (RSD) among three samples harvested from the same fermentor. An average RSD of 22% was obtained for the technical reproducibility analyzed by GC-MS. In addition, an average RSD was calculated for specific metabolites in cells grown under the same condition in two independent cultivations ($RSD_{C\text{-}limitation}$ 32%, $RSD_{CN\text{-}limitation}$ 28%, $RSD_{N\text{-}limitation}$ 49%). A Pearson correlation factor of 0.97 between measured metabolites in C- and CN-limitation was determined, which indicates slight differences in metabolite levels in the central carbon metabolism. Between C- and N-limitation, a Pearson correlation factor of 0.84 was obtained, but the biological variances were clearly higher in N-limitation within independent cultivations. Because of the high variability of specific metabolites among biological replicates, most probably due to the sampling procedure since we did not have a fast sampling device for quenching samples, their concentration levels could not be determined. Therefore, these metabolites were excluded from the discussion. Globally, 233 intracellular compounds were found in the chromatogram (containing systemic peaks derivates). According to their retention times and mass spectra, 80 metabolites could be identified by comparison to our in-house libraries.

Table 4. Metabolites of known level changes in comparison to carbon-limiting condition.

	CN-limitation	N-limitation
Entner-Doudoroff-pathway		
Glucose	*up*	*up*
2-Keto-3-deoxy-6Pgluconate	*up*	*n.d*
3-Phosphoglycerate	*up*	*n.d*
TCA cycle		
Citrate	*up*	*up*
2-Ketoglutarate	*down*	*down*
Succinate	*up*	*down*
Fumarate	*up*	*down*
Malate	*up*	*down*
Amino acids		
Aspartate	*down*	*down*
Cysteine	*up*	*n.d*
Glutamate	*down*	*down*
Glutamine	*up*	*up*
Glycine	*up*	*up*
Isoleucine	*up*	*n.d.*
Ornithine	*n.d*	*down*
Serine	*n.d*	*up*
Threonine	*n.d*	*up*
Tyrosine	*up*	*down*
Valine	*up*	*up*

n.d, not defined

3.4.4 Integrated analysis of the various "omics" results under different nutrient limitations

The profile of metabolites in a cell at any given moment is closely related to the perturbation of gene expression and the modulation of protein function (Saito and Matsuda 2010). All together, the data from these three levels of cellular response offer a more comprehensive global view of the changes taking place under limitation of carbon and/or nitrogen sources.

Nutrient limitation leads to modulation of several transport systems

Pseudomonas putida KT2440 possesses approximately 370 cytoplasmic membrane transport systems, a feature that confers a greater transport capability to this versatile bacterium (Martins Dos Santos et al. 2004). When comparing N- versus C-limitation, both the ABC transporter that belongs to the ATP-binding cassette superfamily (encoded by PP_4864) and the general amino acid system AapP (encoded by PP_1300) were found, by proteomics, to have increased enzyme levels. In contrast, the genes encoding for proteins responsible for importing specific amino acids, *e.g.* glutamate, aspartate, and other compounds across the membrane, as well as periplasmic ABC transporters (encoded by PP_1071, PP_0282, PP_0112, PP_0885) (Table 3) were clearly downregulated. The dual limitation triggered high induction of only one ABC transporter, LivK (26.4-fold), which is one of the five proteins that form the branched-chain amino acid ABC transporter system and whose transcript level was found also to be induced (Table 2). Another amino acid transporter differentially expressed was LysE (encoded by PP_3021), as well as the urea assimilation system (UreE, UreJ, and UreA). The activation of urease may increase competitive fitness of bacteria under nitrogen-limiting conditions, since urease catalyzes the hydrolysis of urea to yield ammonia and carbamate (Mobley et al. 1995). For instance, many pathogens are able to colonize several niches in the human body due to the capacity of synthesizing nitrogen from urea, which helps them to overcome nitrogen limitation and thereby increase their potential to thrive in the host (Burne and Chen 2000).

The activation of the major porin protein OprF (encoded by PP_2089) in *Pseudomonas,* was indicated by the variation of the protein production by 2.6-fold and 5.4-fold in CN vs. C and N vs. C, respectively. OprF is involved in conferring several degrees of permeability to the cell (Bellido et al. 1992) and has been described as one the intrinsic factors in *P. aeruginosa* that strongly increases its resistance to antibiotics (Hancock et al. 1979; Peng et al. 2005). Another member of the porin family OprD (encoded by PP_1206) was exclusively induced by the dual limitation. The specific porin OprD has been shown to be implicated in the uptake of basic amino acids (Ochs et al. 1999; Trias and Nikaido 1990), facilitating their diffusion across the membrane. Such behavior indicates that the outer membrane composition follows a sensitive response to different signals, *e.g.* nutrient and/or metabolite concentrations, which is reflected in the modulation of specific transporters as needed. Furthermore, based on the high incorporation level of OprH exclusively under N vs. C limitation, it seems that OprH, an outer membrane protein mainly responsible for membrane stabilization (Bell et al. 1991; Volkers et al. 2006), has an important role in KT2442 to cope with such elevated concentrations of decanoate used to reach the strict nitrogen limitation.

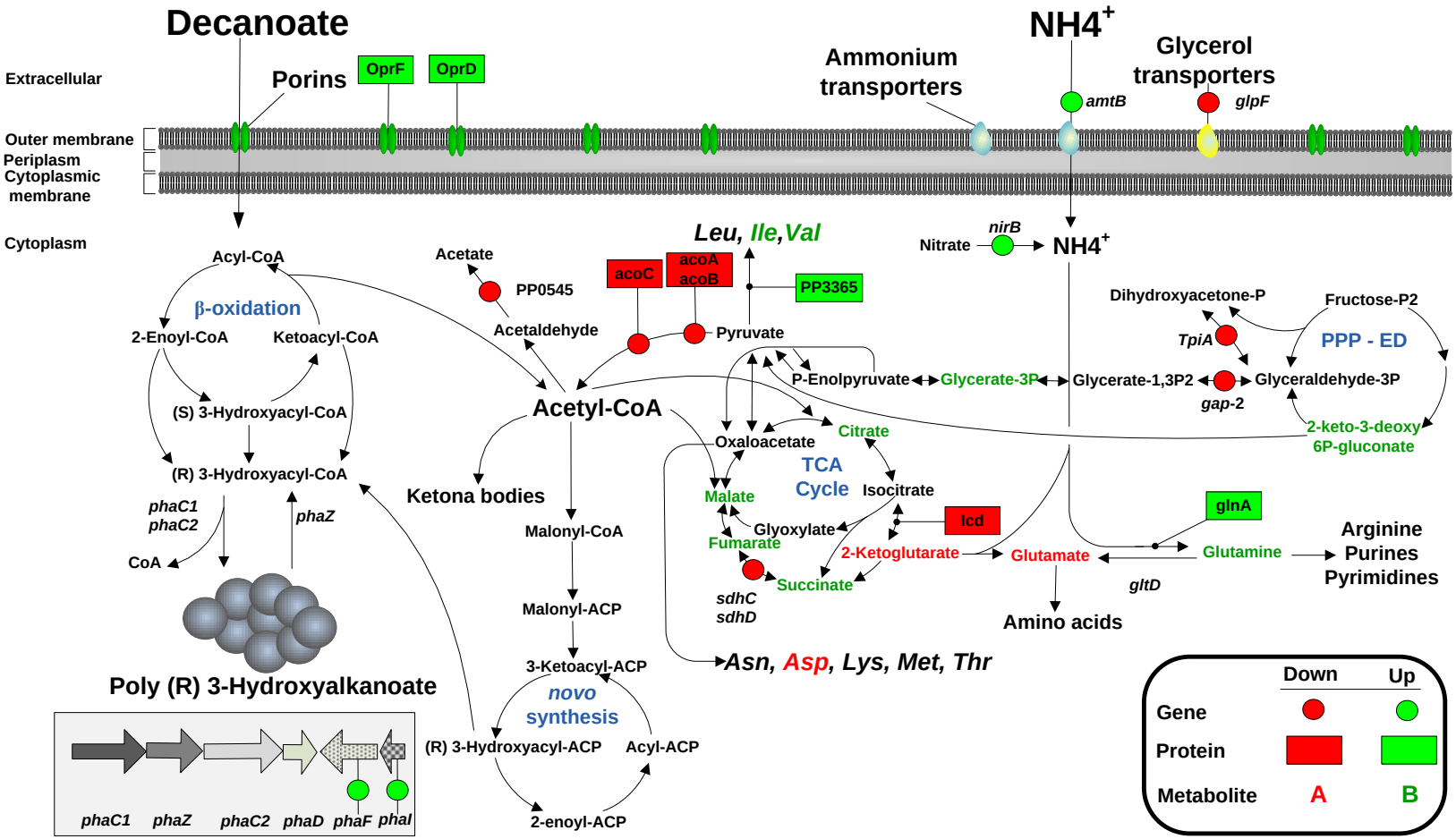

Figure 3. The scheme shows the changes on the metabolic response at gene, protein, and metabolite level, while growing the cells under carbon-nitrogen in comparison to carbon limitation using decanoate as carbon source.

Fatty acid metabolism and PHA synthesis

Fluorescent pseudomonads are able to metabolize a broad range of fatty acids. The cells first convert the fatty acid to the corresponding acyl-CoA thioester, which is further oxidized by the β-oxidation cycle (Steinbüchel and Lutke-Eversloh 2003). In this regard, three sets of FadAB genes have been described in KT2440 (Liu and Chen 2007): FadB and FadA (PP_2136 and PP_2137), FadBx and FadAx (PP_2214 and PP_2215), and PP_2047 and PP_2048, which encode 3-hydroxyacyl-CoA dehydrogenase (FadB-like) and acyl-CoA dehydrogenase (FadE-like), respectively (Escapa et al. 2011b; Liu et al. 2011). Mutations of those genes showed that FadB and FadA played important roles in fatty acid degradation. However, the deletion of these genes could not completely block the β-oxidation pathway and mutant strains produced PHA with longer chain monomers, likely due to a slower or defective β-oxidation pathway (Escapa et al. 2011b; Liu et al. 2011; Olivera et al. 2001). Several intermediates from the cycle, such as 2-*trans*-enoyl CoA, (*S*)-3-hydroxyacyl-CoA, and 3-ketoacyl-CoA, may serve as precursors for PHA synthesis. The latter intermediate is also cleaved by a β-ketothiolase to yield acetyl-CoA and acyl-CoA, which have two less carbons compared with the one that initially entered the cycle. It is still unclear which intermediate contributes the most to produce the PHA polymerase substrate (*R*)-3-OH-acyl-CoA.

Relative to carbon limitation, dual limitation showed no upregulation of enzymes or genes belonging to the β-oxidation pathway (Fig. 3). It was not the case for the PHA gene cluster, where the phasins PhaI and PhaF were found upregulated (Table 2B). The application of non-standard accumulating conditions e.g. all nutrients in excess or carbon limitation, has been reported to lead to the biosynthesis of polyesters (Huisman et al. 1992; Sun et al. 2007b). Nevertheless, a clear explanation of this phenomenon remains unknown. Based on our findings, we argue that *P. putida* KT2442 has a metabolic system in which the constant channeling of precursors for PHA accumulation occurs even under carbon limitation since the activity of the β-oxidation pathway (fatty acid metabolism) and the PHA synthases (PhaC) did not change significantly between dual vs. carbon limitation (Table 2, 2B, and 3). Dual limitation resulted in 60% of the CDW as PHA. In this case the phasins may segregate and distribute more PHA (Galan et al. 2011)

than under carbon limitation, thus explaining their induction. In contrast, one set of proteins that showed a high expression level under N vs. C were related to the β-oxidation cycle (Table 3). Indeed, this is the main route to metabolize aliphatic fatty acids, where the synthesis of two key metabolites, (*S*)-3-hydroxy-acyl-CoA and acetyl-CoA, occurs simultaneously (Steinbüchel and Lutke-Eversloh 2003).

The most over-expressed proteins in the fatty acid group, 3-hydroxyacyl-CoA dehydrogenase (encoded by PP_2047) and acetoacetyl-CoA thiolase (encoded by PP_2051), matched the remarkable induction of the gene cluster (PP_2047-PP_2051) at the mRNA level (Table 3). Recent evidence indicates that the protein product of the PP_2047 and PP_2048 open reading frames play very important roles in defining the PHA composition when fatty acids are the carbon source (Liu *et al.*, 2011). In this respect, the observed enrichment in C10 found in the chemostat subjected to strict nitrogen limitation could be assigned to this dehydrogenase (PP_2047), since a dramatic shift was obtained in the monomer composition when the gene encoding this enzyme was knocked-out in KT2442 (Liu *et al.*, 2011). Nevertheless, under dual limitation a similar monomer composition was found where no overexpression of PP_2047 could be observed at the proteome level. Based on these results, the defined monomer composition is a much more complex mechanism, where nutrients availability seems to be another important factor in controlling the fate of carbon in PHA synthesis. The protein FadA, which is the product of gene PP_2137 (Table 3) that belongs to the first set of genes coding for the *β*-oxidation pathway in *P. putida* converting 3-ketoacyl-CoA into acetyl-CoA and acyl-CoA, is responsible for the last step in the *β*-oxidation pathway and its expression showed a 3.0-fold increase. Furthermore, FadB was identified in two different spots where the average of its protein abundance was about 3-fold. AccC-1 (encoded by PP_0558), an important protein involved in PHA synthesis (Huijberts *et al*., 1992), presented an 8.3-fold induction at N vs. C. It is noteworthy that this enzyme leads the initial step from acetyl-CoA to fatty acid *de novo* synthesis via malonyl-CoA and it is normally activated while growing on non-PHA-related substrates such as sugar and gluconate (Rehm et al. 1998). Taking all together, we could capture the difference at single molecular levels within the *β*-oxidation pathway which is known to generate

intermediates for both biomass and PHA synthesis while fatty acids are supplied as carbon sources (Huijberts and Eggink 1996). Huijbert and co-workers hypothesized that, at certain level of C/N ratio, the catabolic cycle for fatty acids switches its precursor preference, where instead of replenishing its intermediates for further oxidation, they are converted to PHA monomers. The finding in this study, where the residual biomass is not constant for C/N- and N-limited cultures — which was not observed in previous reports using *P. putida* GPo1 — can be explain by the fact that several enzymes (FadB, FadA) and the gene cluster PP_2047-PP_2051 were differentially expressed when comparing N- vs. C-limiting growth. To further investigate which genes contributed most to this difference, we performed a transcriptome analysis comparing N vs. CN limitation using a very strict cut-off (Fold change > 3.5 and a *P* value < 0.03). Only 9 genes fell into this group (Table S3). The gene cluster PP_2047-PP_2051 exhibits more than 10-fold change in expression, and especially 3-hydroxyacyl-CoA dehydrogenase (encoded by PP_2047) was induced by 25-folds (Table S3). Based on this result, we can postulate that these ORFs are responsible for the diminishing on biomass formation, where the generated precursors within the oxidation cycle are redirected to PHA synthesis. On top of this, AtoB (encoded by PP_2051) is an enzyme that converts acetyl-CoA into acetoacetyl-CoA, a competing pathway for the TCA cycle. By a chain elongation process the acetyl-CoA is further condensed to 3-hydroxyacyl-CoA which is finally involved in PHA synthesis (Huijberts et al. 1994a), thus explaining the variation on biomass formation while comparing N vs. CN-limited growth in *P. putida* KT2442. With regard to the degradation system of the PHA granule in *P. putida* strains, recent studies have elucidated its influence on the metabolic balance of the cell. A negative PhaZ mutant strain from *P. putida* KT2442 had shown no increase in PHA yield but a reduction in the biomass concentration relative to the wild-type in batch cultures (de Eugenio et al. 2010a). In the same study, it was demonstrated that PHA metabolism is an ongoing cycle where synthesis and degradation of the polyester is a simultaneous process. The same result was found using *P. putida* U, where the activities of PhaC and PhaZ are concomitantly active (Ren et al. 2010). It is worth to mention that in batch processes the kinetic limitation of a single nutrient takes place. As the present study was

performed using chemostat cultures, the cells are always exponentially growing, and therefore the physiological state of the cells differs from that shown in batch culture. The expression level of the *phaZ* depolymerase gene was not affected by the dual limitation in comparison to carbon limitation (Table 2B). This was not the case when nitrogen was the single limiting nutrient, showing an increase in *phaZ* expression (Table 2B). In agreement with one of our previous reports, the transcription levels of *phaC* and *phaZ* are highly correlated (de Eugenio et al. 2010b), thus indicating that such regulatory system is independent of the cultivation mode. This result supports the postulate that at high production rate of PHAs, the expression of the PhaZ is needed for the efficient production of the polyester (Garcia et al. 1999; Ren et al. 2009).

Energy metabolism

TCA Cycle

Once the fatty acid is oxidized in subsequent steps within the β-oxidization cycle, acetyl-CoA is produced in the TCA cycle for energy generation and to sustain biomass and maintenance of the cell. Little is known about the regulation of this pathway when fatty acids are used as a carbon source and several nutrient limitations are imposed on the system. This is even more complex since intermediates and co-factors of the Krebs cycle inhibit various enzymatic reactions within the cycle itself. For instance, NADH inhibits the isocitrate dehydrogenase, 2-ketoglutarate dehydrogenase, and isocitrate synthase. A crucial question is how the cells orchestres its metabolism to generate the energy for sustaining growth while simultaneously large quantities of PHA is being synthesized. The F0F1 synthase subunit alpha AtpA (encoded by PP_5415) (oxidative phosphorylation) was overproduced in dual and strict nitrogen limitation as compared to the carbon limitation. According to this finding, oxygen may also have an effect on the PHA production capacity in *P. putida* KT2442, but this statement still needs to be tested. The increased expression of the F0F1-type ATP synthase might be necessary for the cell in order to produce ATP molecules via the loss of proton-motive force, since high PHA yields decrease intracellular levels of

ATP (Ruiz et al. 2001). This effect might trigger different expression patterns from enzymes in the TCA cycle which is an important source of ATP generation along with the electron transport chain. As for the activity of the Krebs cycle, several genes were repressed under the dual limitation condition (Table 2). At the protein level only one enzyme, isocitrate dehydrogenase ICD (encoded by PP_4011), showed a fold change less than 2 (Table 3). The deficiency in the TCA cycle was confirmed by the metabolome analysis, where the increase in the pool size of succinate is a direct consequence of the repression of the *sdhC* and *sdhD* genes (Fig. 3, Table 2). The quantitative increase of fumarate and malate was also triggered by the dual limitation. As catabolism and anabolism are tightly coupled under carbon limitation, the cell may coordinate the energy requirement in such a way that no overflow of carbon is present. When both carbon and nitrogen are the limiting nutrients simultaneously, the gluconeogenesis pathway responded by repressing the genes *tpiA* and *gap*-2, which coordinate carbon re-funneling in the Krebs cycle and the conversion rates of dihydroxyacetone phosphate and glyceraldehyde3-phosphate (Fig. 3). The findings suggest that the carbon catabolic repression observed in the TCA cycle can be attributed to the high expression of the nitrogen regulatory protein NtrC (encoded by PP_5048) (Table 3), which is believed to control such an effect under nitrogen limitation (Hervas et al. 2008).

High-energy compounds

The strict nitrogen-limited cultures differ in their response to energy requirement relative to the CN-limited cultures, principally due to the elevated level of enzymes participating in the Krebs cycle. Succinyl-CoA synthase SucD (encoded by PP_4185), which participates in the synthesis of the high-energy compounds ATP and GTP, was identified in cells only under strict nitrogen limitation. Examining the metabolome, we found a decreased pool size of metabolites down- and up-stream of succinate dehydrogenase, namely succinate and fumarate, respectively (Fig. 4).

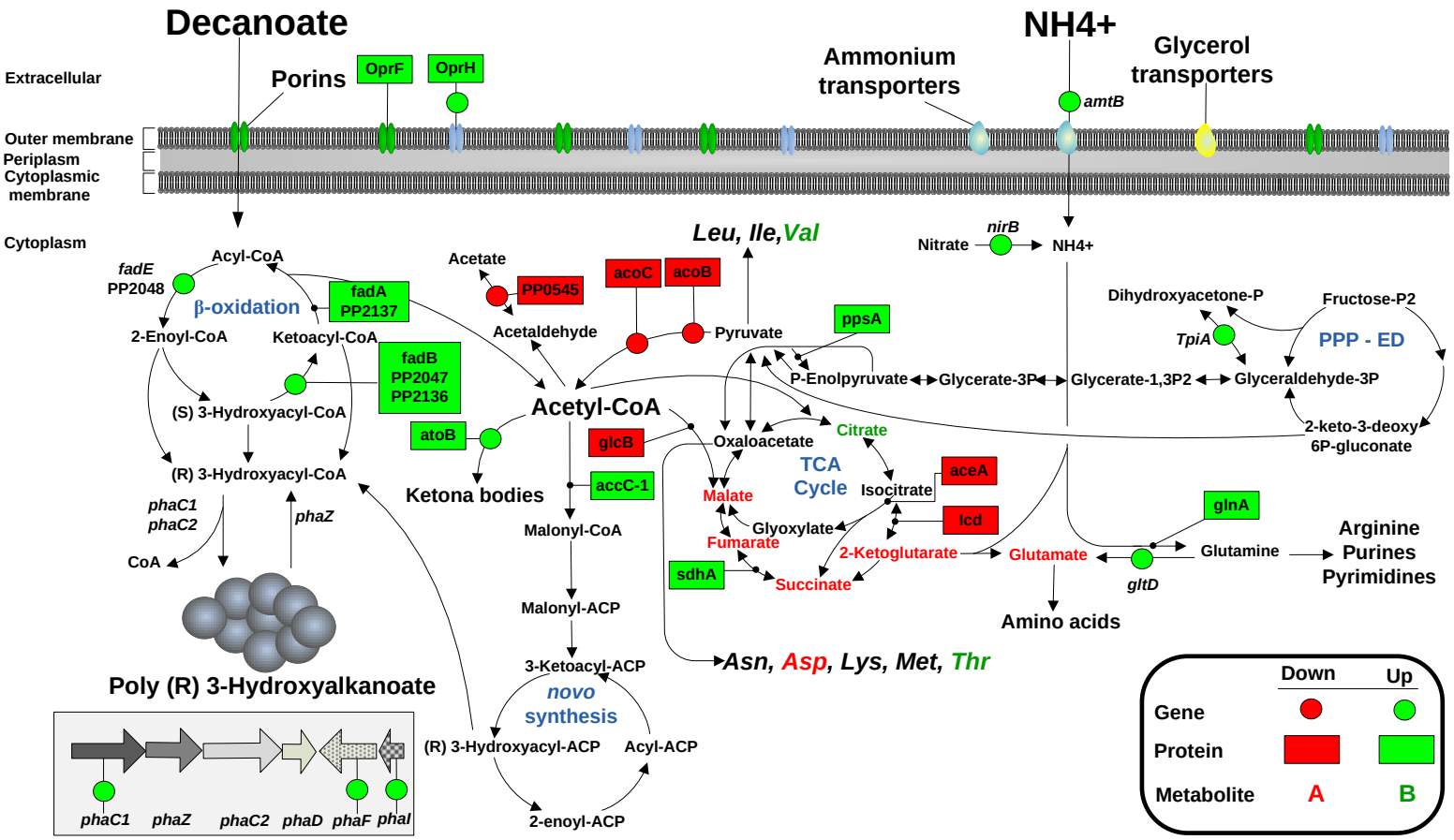

Figure 4. The scheme shows the changes on the metabolic response at gene, protein, and metabolite level, while growing the cells under strict nitrogen in comparison to carbon limitation using decanoate as carbon source.

All together it appears that the TCA cycle plays an important role in providing the necessary energy to the cell when PHAs are accumulated in increased proportion. Employing 2-D gels, we also identified a particular modulation of another important enzyme in the cycle, isocitrate dehydrogenase ICD (encoded by PP_4011), which can be repressed by various mechanisms together with the low expression of ICD, two enzymes of the glyoxylate shunt, isocitrate lyase (encoded by PP_4116) and malate synthase (encoded by PP_0356), were significantly downregulated at strict nitrogen limitation. As such, this phenomenon can be directly related to the repression of the glyoxylate shunt, resulting in the downregulation of malate, which is the main precursor for oxaloacetate synthesis and is known as an essential compound for increasing the flux of acetyl-CoA into the TCA cycle (Klinke et al. 2000). In this sense, the inactivation of isocitrate lyase and isocitrate dehydrogenase in KT2442 led to the enhancement of PHAs when gluconate was used as the carbon source (Klinke et al. 2000). The inactivation of the glyoxylate shunt including the downregulation of malate synthase (GlcB) regulates the concentration of malate. Moreover, downregulation of isocitrate dehydrogenase (ICD) had a direct influence on the pool size of 2-ketoglutarate and consequently on glutamate formation. The cell triggered the activation of glutamine synthase (GlnA) to form glutamine to counteract the decreased pool of precursor for the synthesis of amino acids. In this respect, the metabolome profile showed an increase in the concentration of glutamine under CN vs. C limitation. No change in glutamine concentration was observed at N vs. C limitation, although GlnA was also found upregulated. Another metabolite that is directly regulated by the expression of isocitrate dehydrogenase is citrate. Studies on bacteria and yeast subjected to nitrogen limitation (Hua et al. 2004; Morgunov et al. 2004), have shown repression of isocitrate dehydrogenase. Morgunov and co-workers found an increased concentration of citrate in yeast probably caused by the high ratio of $NADH/NAD^+$, which inhibits isocitrate dehydrogenase. Notably, after comparing N vs. C and CN vs. C, the pool size of citrate increased under both conditions (Table 4). Although the expression of isocitrate dehydrogenase was found to be significantly reduced under dual limitation, the inactivation was not accompanied by a downregulation of enzymes belonging to the glyoxylate pathway, suggesting a distinct regulatory system in this particular environment.

Electron transport chain

Another important finding while comparing N vs. C limitation was the high induction of genes encoding the cytochrome o ubiquinol oxidase Cyo (encoded by PP_0813-0814) (Table 2). Cyo is a terminal oxidase of the electron transport chain which is believed to sense the energetic state of the cell, thus controlling the catabolic pathways and the expression of different genes (Rojo 2010). In addition, terminal oxidases are highly regulated by oxygen concentration (Kawakami et al. 2010; Morales et al. 2006). Due to the high oxygen concentration supplied to the bioreactor in order to keep the oxygen tension above 20%, it is most likely that such an environment affects the composition of the electron transport chain. One possible explanation for the reorganization of the terminal oxidase under strict nitrogen limitation, is to optimize the energy generation in the cell (Morales et al. 2006) since a remarkable energy accumulation in the polyester form is present. In addition, Cyo levels have been shown as being responsible for decreasing the expression level of many promoters *in P. putida* including the PalkB promoter (for alkane assimilation). Furthermore, rather than a carbon catabolic repression, this effect has been postulated as a general physiological control mechanism (Dinamarca et al. 2003). Whether or not Cyo modulates the expression of genes under strict nitrogen limitation is still a question to be answered. There is a clear correlation between the TCA cycle and the electron transport chain, as shown by the high expression of the protein succinate dehydrogenase (4-fold change) which stimulates the cytochrome o ubiquinol oxidase by supplying electrons directly to it.

The overflow metabolism is one of the repeated trends of chemostats subjected to strict nitrogen limitation (Durner et al. 2000). Since the exo-metabolite profile did not contain any secondary metabolites under this condition, *P. putida* KT2442 seems to arrange its metabolism in such a manner that it blocks energy-spilling by strongly repressing enzymes involved in the pyruvate and acetate pathways (*acoA*, *acoB*, *acoC*, PP_0545) (Table 3), thus preventing the shortage of partially oxidized metabolites (Russell and Cook 1995). This may be desirable because of the huge channeling of the consumed carbon (reflected

in energy storage) towards polyester synthesis. Despite the dowregulation of those enzymes in the pyruvate and acetate pathways where acetyl-CoA is needed, there was a high expression of isoacetyl-CoA carboxylase and biosynthetic thiolase, which are the first enzymes responsible for channeling acetyl-CoA to *de novo* fatty acid and ketona bodies biosynthesis, respectively. Interestingly, it seems most likely that *P. putida* KT2442 channels the remaining acetyl-CoA into storage compounds by activating those pathways to save energy for later consumption (Fig. 4).

(iv) Nitrogen and amino acid metabolism

As seen in tables 2 and 3, the nitrogen regulatory protein P-II GnlK (encoded by PP_5234) showed a large change in both mRNA abundance and protein level, when *Pseudomonas putida* was subjected to dual limitation. This was not the case when we examined the proteome profile from strict nitrogen-deprived cells, since the spot for this enzyme did not show differential expression compared to the carbon-limited cultures. The expression of GnlK is led by the nitrogen availability via the nitrogen transcriptional regulator NtrC in *P. putida* KT2442 (Hervas et al. 2009). We also found that KT2442 displays the upregulation of NtrC when both carbon and nitrogen were completely depleted (Table 3). NtrC also modulates the expression of the *glnA* gene (Hua *et al*., 2004), which is positioned upstream in the *glnA-ntrAB* operon in *Escherichia coli*. Hervas and co-workers showed NtrC-dependency for the (*glnA*) gene in KT2442, postulating that it could be part of an operon together with (*ntrB*) and (*ntrC*) genes, like in enterobacteria. Notably, GlnA exhibited the highest levels of induction among the proteins associated to amino acid biosynthesis (Table 3) in the case of strict nitrogen limitation. The condition also caused significant repression of several enzymes that were identified as serine hydroxymethyltransferase GlyA, putative hydantoin racemase (encoded by PP_4310), and branched-chain amino acid aminotransferase Ilv*E*. In the valine, leucine, and isoleucine metabolic pathway IlvE has a double function to either act together with leucine dehydrogenase in the synthesis/degradation of leucine or in the degradation of valine and isoleucine to glutamate by transferring nitrogenous groups. Another

enzyme responsible for the turnover of certain amino acids in the same family is GlyA, which carries out the conversion of glycine by transferring one-carbon group, giving serine as a product. Furthermore, it catalyzes the reaction of glycine with acetaldehyde to form threonine. Particularly, the downregulation of the periplasmic glutaminase-asparaginase protein occurred solely under strict nitrogen limitation. This protein is responsible for the uptake of the acidic amino acids, e.g. aspartate and glutamate (Sonawane et al. 2003b). Carbon catabolite repression of the periplasmic glutamate/aspartate transporter took place when KT2440 was exposed to glucose or mono- and dicarboxylic acids (Sonawane et al. 2003a). However, the metabolome profile showed a decrease in the pool size of fumarate and succinate (Table 4). Therefore, there may be another system which drives the transport selectivity described here.

(v) Stress response proteins

Besides their primary feature as a reservoir of energy and carbon, PHAs have displayed a key role in conferring robustness to the bacteria under unfavorable conditions, such as temperature, UV irradiation, chemicals, and osmotic pressure (Zhao et al. 2007). In contrast, based on the high polyester accumulation within the cell (Table 1), PHAs have also been postulated to act as a stressor, especially concerning protein synthesis and the activation of various protective proteins(Han et al. 2001). It is worth noting that all studies which stated such a stress produced by the polyester inclusion to the cell, have been performed in metabolically engineered *E. coli* (Han et al. 2001; Kang et al. 2008; Tessmer et al. 2007). The use of electron microscopy allows dimensioning how the cytoplasmic space has been occupied by the polymeric inclusion under production conditions (Fig. 5).

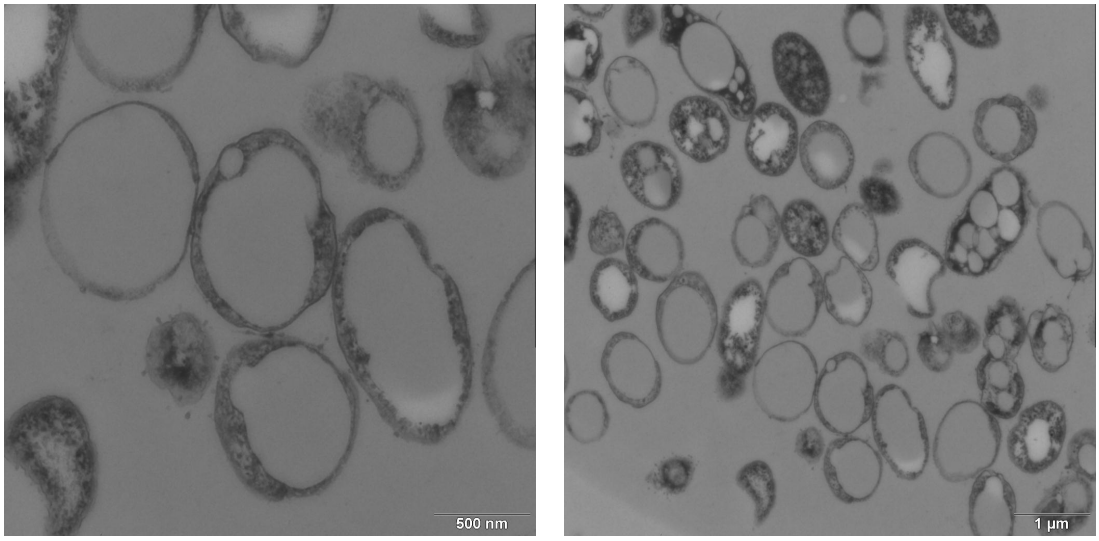

Figure 5. Electron-microscopic pictures of *P. putida* KT2442 when decanoate was in excess in continuous fermentation.

In the current study a stress response of the cell while growing under CN- and N-limitation can be seen. The high expression level of elongation factor enzymes is the first indicator of such an effect. The protein abundance of TuF-2 (encoded by PP_0452, Table 3), one of the Tu- elongation factor enzymes, was extremely high under CN limitation. Besides its primarily role of binding and transporting the proper codon-specified aminoacyl-tRNA to the aminoacyl site of the ribosome, TuF-2 also has chaperon-like functions that enhance protein folding and stress protection(Caldas et al. 1998). Strict nitrogen-limited cultures exhibit overexpression of the elongation factor FusA-1 (encoded by PP_0451, Table 3), which is a GTPase (classified as a G-elongation factor) that is involved in the translocation of bacterial ribosomes along messenger RNA during protein biosynthesis (Rodnina et al. 1997). On the other hand, the protease enzyme PP_2300, which is involved in hydrolysis of proteins to small peptides, was strongly induced in the presence of excess carbon (Table 3). So far, the decreased expression level of Tu-elongation factor has been related to the reduced capability of a metabolically engineered *Escherichia coli* to synthesize proteins (Han *et al.*, 2001). However, *E. coli* does not naturally accumulate PHAs, therefore it is not surprising that KT2442 showed a different proteome pattern for these elongation factor enzymes. Indeed,

the normal protein synthesis machinery is affected by the shortage of nitrogen; thereby the cell may react in such a way that guarantees the biosynthesis of the main building blocks (amino acids) of these macromolecules. In addition, the induction of the gene encoding the chaperonin 10 GroES (Table 2) was another metabolic adaptation against the stress produced by the nitrogen limitation. Han and colleagues also observed a high level expression of several heat shock proteins, arguing that the polyester inclusion disturbs the normal intracellular architecture due to its direct contact with the chromosome, resulting in activation of the heat shock response. Nevertheless, GroES also mediates protein folding. We suggest that this may be the principal reason for its incorporation since the genes coding the phasin enzymes were found to be induced (Table 1). The phasins prevent the disturbance of intracellular architecture by forming a protein layer covering the hydrophobic surface of the PHAs, thus creating a protective barrier between the core of the granule and the cytoplasm (Prieto et al. 2007). Very recently, we have demonstrated that the phasin PhaF is involved in granule cell localization and granule segregation during cell division by interaction with the chromosome (Galan et al. 2011). Based on our results, we cannot elucidate whether or not phasins enzymes, PhaF or PhaI, have an influence on stress protein formation. To address this question, mutants strain deficient of genes encoding for PhaF and PhaI should be generated and assessed, by comparing them against the wild-type strain at the proteomic level under well-defined conditions (chemostat).

3.4.5 Process optimization for increasing PHA synthesis in chemostat culture based on a "top-down" approach

In order to increase the PHA accumulation within the carbon-nitrogen limiting condition, we looked deeply into the most significant changes at the protein and transcriptional levels, which are linked to energy metabolism. As PHA is an energy storage compound its accumulation dependents highly on the energetic state of the cell (Huisman et al. 1989). In the sections 3.4.4 (energy metabolism) was shown that genes belonging to the Electron Transport Chain and TCA cycle were differentially expressed under the tested conditions. Both pathways are modulated by several factors, with special importance being the oxygen availability (Kawakami et al. 2010). Therefore, the fermentor was supplied only with pure air instead of a gas mixture (70% air, 30% O_2, keeping the same aeration rate, see material and methods) and, thus assessing the influence of this parameter on the PHA synthesis. Table 5 demonstrates the final PHA accumulation under the set conditions under strict carbon, dual and strict nitrogen limitation. No difference in PHA accumulation could be observed under carbon limitation. Also, total biomass yield on decanoate did not change at any tested condition (Table 5). Nevertheless, under strict nitrogen limitation the PHA yield drops from 80 to 56% of the cell dry weight. Supplying pure air increased the PHA yield by 21% under dual limitation, resulting in a total accumulation of 71% of CDW as PHA.

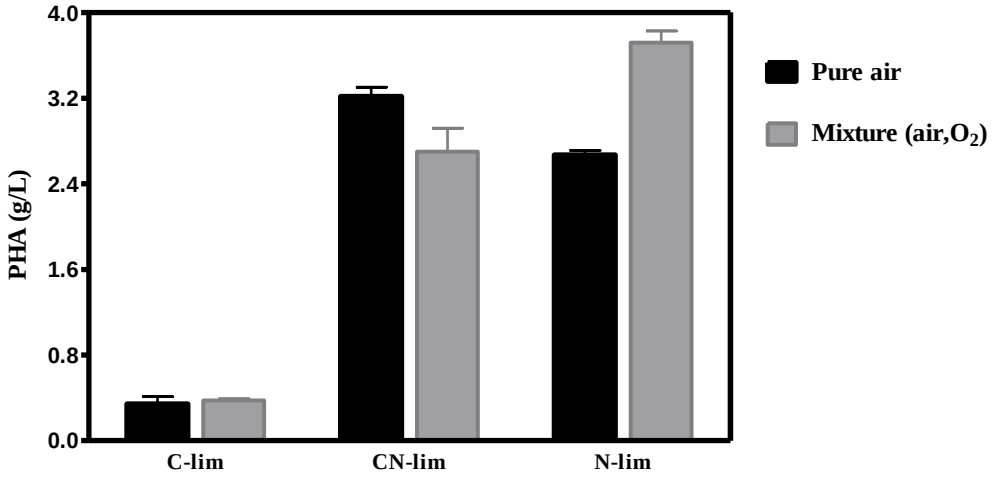

Figure 6. Comparison in the PHA productivity under several nutrient limitations in chemostat cultures.

To our knowledge, this is the highest PHA yield (in terms of percentage) ever reached under dual limitation. In addition, it was possible to increase the PHA yield at the dual limiting condition (Fig. 6), which has proved to be the most efficient way to produce PHA in continuous process. These results clearly prove the importance of oxygen within the process of PHA synthesis. A possible explanation for such changes, when oxygen concentration dropped, is that PHA not only acts as an energy storage compound, but also as an electron-sink (Kosseva and Kennedy 1996). It was first proposed in the early 70s (Senior et al. 1972), where *A. beijerinckii* accumulated higher PHA under oxygen limitation in chemostat cultures either under nitrogen-limited or nitrogen-sufficient environments. Further studies with the same strain showed that NADH oxidase activity is reduced upon oxygen limitation, but the NADH/NAD ratios increase accompanied by the rise in PHA accumulation (Jackson and Dawes 1976). It was finally demonstrated that PHA can partially replace respiration, thus acting in a concert manner with it as an electron-sink (Carter and Dawes 1979).

Table 5. PHA production and relative monomer composition by *P. putida* KT2442 in continuous culture at *D* 0.1 h^{-1} and aeration rate 1(L/min) [pure air].

Limitation	PO_2	Residual carbon	Residual nitrogen	CDW	PHA content	Monomer composition (mol %)		
	(%)	(g)	(g)	(g l^{-1})	(% CDW)	C6	C8	C10
Carbon	66.3	N.D	0.131 ± 0.02	1.41 ± 0.08	24.32 ± 0.60	3.0	52.1	44.8
Carbon-Nitrogen	25.7	N.D	N.D	4.21 ± 0.25	76.40 ± 1.14	4.7	40.8	54.3
Nitrogen	0	1.44 ± 0.25	N.D	4.73 ± 0.18	56.43 ± 0.24	4.6	43.2	52.0

[a] Standard deviation (±) from two independent experiments.

N.D: Not detectable

It is noteworthy that all experiments described above were preformed with glucose as the carbon source. In this study, as decanoate was the unique carbon and energy source, the oxidation process occurred through the β-oxidation route, which replenishes precursors for both PHA and biomass synthesis. Because of the nature of the catabolic pathway, under strict nitrogen-oxygen limitation (Table 5), the PHA accumulation dropped as compared with oxygen-sufficient. Another scenario is governing the dual limitation, because there was enough oxygen, in both conditions, to oxidize the carbon source and make the pathway work efficiently, thus generating the needed precursor for the PHA synthesis. Therefore, the difference could lie at the level of acetyl-CoA, where two pathways, the TCA cycle and the *de novo* fatty acid synthesis, compete for it. A metabolically engineered strain from *P. putida* lacking the *PhaG* gene, which encodes for (R)-3-hydroxydecanoyl-ACP:CoA transacylase —being the main precursor for PHA synthesis from *de novo* synthesis— resulted in a reduction by 30% in the PHA yield compared with the parental strain KT2442 when decanoate was used as the unique carbon source (Liu et al. 2011). Thus, reflecting the key role of this route for the formation of PHA when the fatty acid is the carbon source. The reduction in the oxygen concentration in the culture may affect the respiration system, and as in *A. beijerinckii*, PHA may act to some extend as an electron-sink in *P. putida* KT2442.

3.5 Conclusions

By combining measurements of transcriptomics, proteomics, and metabolomics, under well-controlled nutrient limitations, we have shown that the underlying cellular wiring is remarkably different when two nutrients are limiting at the same time, as compared to those under single limitation. We have captured the response of *P. putida* KT2442 to the shift in resource distribution and how these changes activate/repress several metabolic pathways along with transporter systems. We have found that the modulation of the expression of outer membrane proteins — in particular porins — under nitrogen and dual limitation correlates with the specific uptake rate of decanoate within the chemostat. We have shown that these two conditions also promote the overexpression of many transporters for scavenging nitrogen

sources. The PHA content under nitrogen limitation was found to be the highest, followed by dual limitation and carbon limitation. The residual biomass was not constant for dual- and strict nitrogen-limiting growth, showing a different feature in comparison to other *P. putida* strains. Furthermore, the high accumulation of PHA under carbon limitation is a result of the constant channeling of precursors for PHA biosynthesis since no significant difference could be observed within the *β*-oxidation pathway at any omic level, when compared to dual limitation. Regarding energy generation, genes and proteins belonging to the electron transport chain system were found significantly upregulated when there was a considerable amount of PHA stored in the cell. To overcome the stress caused by the shortening of precursors for amino acid synthesis (nitrogen) and, consequently protein production, elongation factors along with chaperons guarantee the biosynthesis of the main building blocks (amino acids) of these macromolecules.

The systems approach applied in this study has enabled us to gain substantial insights into the metabolic adaptation of *Pseudomonas putida* KT2442 to nutrient limitation. Owing to its comprehensiveness and integration, the knowledge generated will be of great assistance on the development of further metabolic engineering work in this versatile organism to both enhance and diversify the production of PHAs. Our findings, especially concerning the dual limitation that uses both the carbon and nitrogen sources in the most economical manner, have brought an alternative to fulfill one of the remaining gaps in further improving industrial production of PHAs.

3.6 Acknowledgments

We thank Agata Bielecka and Petra Völler for the excellent technical assistance on the sample processing on the proteomic analysis. We also thank Christel Kakoschke and Dr. Victor Wray for NMR analysis. We acknowledge the funding by the BMBF (DE) and MICINN (ES) within the scope of the ERA-NET program on the Systems Biology of Microorganisms (Project PSYSMO: Grant No.0313980).

3.7 References

Albuquerque MGE, Martino V, Pollet E, AvErous L, Reis MAM. 2011. Mixed culture polyhydroxyalkanoate (PHA) production from volatile fatty acid (VFA)-rich streams: Effect of substrate composition and feeding regime on PHA productivity, composition and properties. Journal of Biotechnology 151(1):66-76.

Asadollahi MA, Maury J, Patil KR, Schalk M, Clark A, Nielsen J. 2009. Enhancing sesquiterpene production in *Saccharomyces cerevisiae* through in silico driven metabolic engineering. Metabolic Engineering 11(6):328-334.

Bagdasarian M, Lurz R, Ruckert B. 1981. Specific-purpose plasmid cloning vectors. II. Broad host range, high copy number, RSF 1010-derived vectors, and a host-vector system for gene cloning in Pseudomonas. Gene 16(1-3):237-247.

Becker J, Zelder O, Hafner S, Schroder H, Wittmann C. 2011. From zero to hero - Design-based systems metabolic engineering of *Corynebacterium glutamicum* for l-lysine production. Metabolic Engineering 13(2):159-168.

Bell A, Bains M, Hancock REW. 1991. *Pseudomonas aeruginosa* outer membrane protein OprH: Expression from the cloned gene and function in EDTA and gentamicin resistance. Journal of Bacteriology 173(21):6657-6664.

Bellido F, Martin NL, Siehnel RJ, Hancock REW. 1992. Reevaluation, using intact cells, of the exclusion limit and role of porin OprF in *Pseudomonas aeruginosa* outer membrane permeability. Journal of Bacteriology 174(16):5196-5203.

Benndorf D, Thiersch M, Loffhagen N, Kunath C, Harms H. 2006. *Pseudomonas putida* KT2440 responds specifically to chlorophenoxy herbicides and their initial metabolites. Proteomics 6(11):3319-3329.

Beuttler H, Hoffmann J, Jeske M, Hauer B, Schmid R, Altenbuchner J, Urlacher V. 2011. Biosynthesis of zeaxanthin in recombinant *Pseudomonas putida*. Applied Microbiology and Biotechnology 89(4):1137-1147.

Blank LM, Ionidis G, Ebert BE, Buhler B, Schmid A. 2008a. Metabolic response of *Pseudomonas putida* during redox biocatalysis in the presence of a second octanol phase. FEBS Journal 275(20):5173-5190.

Blank LM, Ionidis G, Ebert BE, Bühler B, Schmid A. 2008b. Metabolic response of *Pseudomonas putida* during redox biocatalysis in the presence of a second octanol phase. FEBS Journal 275(20):5173-5190.

Bolten CJ, Kiefer P, Letisse F, Portais JC, Wittmann C. 2007. Sampling for metabolome analysis of microorganisms. Analytical Chemistry 79(10):3843-3849.

Bro C, Regenberg B, Forster J, Nielsen J. 2006. In silico aided metabolic engineering of *Saccharomyces cerevisiae* for improved bioethanol production. Metabolic Engineering 8(2):102-111.

Bu Q, Lei H, Ren S, Wang L, Holladay J, Zhang Q, Tang J, Ruan R. 2011. Phenol and phenolics from lignocellulosic biomass by catalytic microwave pyrolysis. Bioresource Technology 102(13):7004-7007.

Burgard AP, Pharkya P, Maranas CD. 2003. Optknock: A bilevel programming framework for identifying gene knockout strategies for microbial strain optimization. Biotechnology and Bioengineering 84(6):647-657.

Burne RA, Chen YYM. 2000. Bacterial ureases in infectious diseases. Microbes and Infection 2(5):533-542.

Caldas TD, El Yaagoubi A, Richarme G. 1998. Chaperone properties of bacterial elongation factor EF-Tu. Journal of Biological Chemistry 273(19):11478-11482.

Carter IS, Dawes EA. 1979. Effect of oxygen concentration and growth rate on glucose metabolism, Poly-B-hydroxybutyrate biosynthesis and respiration of *Azotobacter beijerinckii*. Journal of General Microbiology 110(2):393-400.

Chen G-Q. 2009. A microbial polyhydroxyalkanoates (PHA) based bio- and materials industry. Chemical Society Reviews 38(8).

Chen G-Q, Chen GG-Q. 2010. Industrial Production of PHA Plastics from Bacteria. Springer Berlin / Heidelberg. p 121-132.

Chen G-Q, Wu Q. 2005. Microbial production and applications of chiral hydroxyalkanoates. Applied Microbiology and Biotechnology 67(5):592-599.

Ciesielski S, Pokoj T, Klimiuk E. 2010. Cultivation-dependent and -independent characterization of microbial community producing polyhydroxyalkanoates from raw glycerol. Journal of Microbiology and Biotechnology 20(5):853-861.

Cowles CE, Nichols NN, Harwood CS. 2000. BenR, a XylS Homologue, Regulates Three Different Pathways of Aromatic Acid Degradation in *Pseudomonas putida*. Journal of Bacteriology 182(22):6339-6346.

D'mello R, Hill S, Poole RK. 1996. The cytochrome bd quinol oxidase in *Escherichia coli* has an extremely high oxygen affinity and two oxygen-binding haems: implications for regulation of activity in vivo by oxygen inhibition. Microbiology 142(4):755-763.

Daddaoua A, Krell T, Alfonso C, Morel B, Ramos J-L. 2010. Compartmentalized Glucose Metabolism in *Pseudomonas putida* Is Controlled by the PtxS Repressor. Journal of Bacteriology 192(17):4357-4366.

de Eugenio LI, Escapa IF, Morales V, Dinjaski N, Galán B, García JL, Prieto MA. 2010a. The turnover of medium-chain-length polyhydroxyalkanoates in *Pseudomonas putida* KT2442 and the fundamental role of PhaZ depolymerase for the metabolic balance. Environmental Microbiology 12(1):207-221.

de Eugenio LI, Galan B, Escapa IF, Maestro B, Sanz JM, Garcia JL, Prieto MA. 2010b. The PhaD regulator controls the simultaneous expression of the pha genes involved in polyhydroxyalkanoate metabolism and turnover in *Pseudomonas putida* KT2442. Environmental Microbiology 12(6):1591-1603.

de Eugenio LI, Galán B, Escapa IF, Maestro B, Sanz JM, García JL, Prieto MA. 2010c. The PhaD regulator controls the simultaneous expression of the pha genes involved in polyhydroxyalkanoate metabolism and turnover in *Pseudomonas putida* KT2442. Environmental Microbiology 12(6):1591-1603.

De Lorenzo V. 1994. Designing microbial systems for gene expression in the field. Trends in Biotechnology 12(9):365-371.

De Lorenzo V, Herrero M, Jakubzik U, Timmis KN. 1990. Mini-Tn5 transposoon derivatives for insertion mutagenesis, promoter probing, and chromosomal insertion of cloned DNA in gram-negative eubacteria. Journal of Bacteriology 172(11):6568-6572.

De Lorenzo V, Herrero M, Sanchez JM, Timmis KN. 1998. Mini-transposons in microbial ecology and environmental biotechnology. FEMS Microbiology Ecology 27(3):211-224.

de Lorenzo V, Timmis KN. 1994. Analysis and construction of stable phenotypes in gram-negative bacteria with Tn5- and Tn10-derived minitransposons. Methods in Enzymology 235:386-405.

Dean HF, Cheevadhanarak S, Skurray RA, Bayly RC. 1989. Characterisation of a degradative plasmid in *Pseudomonas putida* that controls the expression of 2,4-xylenol degradative genes. FEMS Microbiology Letters 61(1-2):153-157.

del Castillo T, Duque E, Ramos JL. 2008. A Set of Activators and Repressors Control Peripheral Glucose Pathways in *Pseudomonas putida* To Yield a Common Central Intermediate. Journal of Bacteriology 190(7):2331-2339.

Del Castillo T, Ramos JL. 2007. Simultaneous catabolite repression between glucose and toluene metabolism in Pseudomonas putida is channeled through different signaling pathways. Journal of Bacteriology 189(18):6602-6610.

del Castillo T, Ramos JL, Rodriguez-Herva JJ, Fuhrer T, Sauer U, Duque E. 2007. Convergent peripheral pathways catalyze initial glucose catabolism in *Pseudomonas putida*: Genomic and flux analysis. Journal of Bacteriology 189(14):5142-5152.

Dinamarca MA, Aranda-Olmedo I, Puyet A, Rojo F. 2003. Expression of the *Pseudomonas putida* OCT plasmid alkane degradation pathway is modulated by two different global control signals: Evidence from continuous cultures. Journal of Bacteriology 185(16):4772-4778.

Diniz S, Taciro M, Cabrera Gomez J, Pradella J. 2004. High-Cell-Density cultivation of *Pseudomonas putida* IPT 046 and medium-chain-length polyhydroxyalkanoate production from sugarcane carbohydrates. Applied Biochemistry and Biotechnology 119(1):51-69.

Doi Y. 1990. Microbial polyesters. VCH, New York.

Dominguez-Cuevas P, Gonzalez-Pastor JE, Marques S, Ramos JL, De Lorenzo V. 2006. Transcriptional tradeoff between metabolic and stress-response programs in Pseudomonas putida KT2440 cells exposed to toluene. Journal of Biological Chemistry 281(17):11981-11991.

Draths KM, Frost JW. 1994. Environmentally compatible synthesis of adipic acid from D-glucose [16]. Journal of the American Chemical Society 116(1):399-400.

Driouch H, Melzer G, Wittmann C. 2012. Integration of in vivo and in silico metabolic fluxes for improvement of recombinant protein production. Metabolic Engineering 14(1):47-58.

Dunn NW, Gunsalus IC. 1973. Transmissible plasmid coding early enzymes of naphthalene oxidation in *Pseudomonas putida*. Journal of Bacteriology 114(3):974-979.

Duque E, Molina-Henares AJ, Torre Jdl, Molina-Henares MA, Castillo Td, Lam J, Ramos JL, Ramos J-L, Filloux A. 2007. Towards a Genome-Wide Mutant Library of *Pseudomonas putida* Strain KT2440

Pseudomonas. Springer Netherlands. p 227-251.

Durner R, Witholt B, Egli T. 2000. Accumulation of poly[(R)-3-hydroxyalkanoates] in *Pseudomonas oleovorans* during growth with octanoate in continuous culture at different dilution rates. Applied and Environmental Microbiology 66(8):3408-3414.

Durner R, Zinn M, Witholt B, Egli T. 2001. Accumulation of poly[(R)]-3-hydroxyalkanoates] in *Pseudomonas oleovorans* during growth in batch and chemostat culture with different carbon sources. Biotechnology and Bioengineering 72(3):278-288.

Ebert BE, Kurth F, Grund M, Blank LM, Schmid A. 2011. Response of Pseudomonas putida KT2440 to increased NADH and ATP demand. Applied and Environmental Microbiology 77(18):6597-6605.

Egli T. 1991. On multiple-nutrient-limited growth of microorganisms, with special reference to dual limitation by carbon and nitrogen substrates. Antonie Van Leeuwenhoek 60(3):225-234.

Egli T, Quayle JR. 1986. Influence of the carbon: Nitrogen ratio of the growth medium on the cellular composition and the ability of the methylotrophic yeast *Hansenula polymorpha* to utilize mixed carbon sources. Journal of General Microbiology 132(7):1779-1788.

Elbahloul Y, Steinbüchel A. 2009. Large-scale production of poly(3-hydroxyoctanoic acid) by *Pseudomonas putida* GPo1 and a simplified downstream process. Applied and Environmental Microbiology 75(3):643-651.

Escapa I, Morales V, Martino V, Pollet E, Averous L, Garcia J, Prieto M. 2011a. Disruption of B-oxidation pathway in *Pseudomonas putida* KT2442 to produce new functionalized PHAs with thioester groups. Applied Microbiology and Biotechnology 89(5):1583-1598.

Escapa IF, García JL, Bühler B, Blank LM, Prieto MA. 2012. The polyhydroxyalkanoate metabolism controls carbon and energy spillage in *Pseudomonas putida*. Environmental Microbiology:no-no.

Escapa IF, Morales V, Martino VP, Pollet E, Averous L, Garcia JL, Prieto MA. 2011b. Disruption of *B*-oxidation pathway in *Pseudomonas putida* KT2442 to produce new functionalized PHAs with thioester groups. Applied Microbiology and Biotechnology 89(5):1583-1598.

Faizal I, Dozen K, Hong CS, Kuroda A, Takiguchi N, Ohtake H, Takeda K, Tsunekawa H, Kato J. 2005. Isolation and characterization of solvent-tolerant *Pseudomonas putida* strain T-57, and its application to biotransformation of toluene to cresol in a two-phase (organic-aqueous) system. Journal of Industrial Microbiology and Biotechnology 32(11-12):542-547.

Follonier S, Panke S, Zinn M. 2011. A reduction in growth rate of Pseudomonas putida KT2442 counteracts productivity advances in medium-chain-length polyhydroxyalkanoate production from gluconate. Microbial Cell Factories 10(1):25.

Fonseca P, Moreno R, Rojo F. 2008. Genomic analysis of the role of RNase R in the turnover of *Pseudomonas putida* mRNAs. Journal of Bacteriology 190(18):6258-6263.

Fu J, Wenzel SC, Perlova O, Wang J, Gross F, Tang Z, Yin Y, Stewart AF, Müller R, Zhang Y. 2008. Efficient transfer of two large secondary metabolite pathway gene clusters into heterologous hosts by transposition. Nucleic acids research 36(17).

Fuchtenbusch B, Wullbrandt D, Steinbuchel A. 2000. Production of polyhydroxyalkanoic acids by *Ralstonia eutropha* and *Pseudomonas oleovorans* from an oil remaining from biotechnological rhamnose production. Applied Microbiology and Biotechnology 53(2):167-172.

Fuhrer T, Fischer E, Sauer U. 2005. Experimental identification and quantification of glucose metabolism in seven bacterial species. Journal of Bacteriology 187(5):1581-1590.

Galan B, Dinjaski N, Maestro B, De Eugenio LI, Escapa IF, Sanz JM, Garcia JL, Prieto MA. 2011. Nucleoid-associated PhaF phasin drives intracellular location and segregation of polyhydroxyalkanoate granules in *Pseudomonas putida* KT2442. Molecular Microbiology 79(2):402-418.

Garcia B, Olivera ER, Miambres B, Fernandez-Valverde M, Cacedo LM, Prieto MA, Garcia JL, Martinez M, Luengo JM. 1999. Novel Biodegradable Aromatic Plastics from a Bacterial Source. Journal of Biological Chemistry 274(41):29228-29241.

Grage K, Jahns AC, Parlane N, Palanisamy R, Rasiah IA, Atwood JA, Rehm BHA. 2009. Bacterial Polyhydroxyalkanoate Granules: Biogenesis, Structure, and Potential Use as Nano-/Micro-Beads in Biotechnological and Biomedical Applications. Biomacromolecules 10(4):660-669.

Gross F, Gottschalk D, Müller R. 2005. Posttranslational modification of myxobacterial carrier protein domains in Pseudomonas sp. by an intrinsic phosphopantetheinyl transferase. Applied Microbiology and Biotechnology 68(1):66-74.

Gross F, Ring MW, Perlova O, Fu J, Schneider S, Gerth K, Kuhlmann S, Stewart AF, Zhang Y, Müller R. 2006. Metabolic Engineering of *Pseudomonas putida* for Methylmalonyl-CoA Biosynthesis to Enable Complex Heterologous Secondary Metabolite Formation. Chemistry and Biology 13(12):1253-1264.

Gross R, Lang K, Bühler K, Schmid A. 2010. Characterization of a biofilm membrane reactor and its prospects for fine chemical synthesis. Biotechnology and Bioengineering 105(4):705-717.

Halan B, Schmid A, Buehler K. 2010. Maximizing the productivity of catalytic biofilms on solid supports in membrane aerated reactors. Biotechnology and Bioengineering 106(4):516-527.

Halan B, Schmid A, Buehler K. 2011. Real-time solvent tolerance analysis of *Pseudomonas sp*. Strain VLB120ΔC catalytic biofilms. Applied and Environmental Microbiology 77(5):1563-1571.

Han MJ, Sang Sun Y, Sang Yup L. 2001. Proteome analysis of metabolically engineered *Escherichia coli* producing poly(3-hydroxybutyrate). Journal of Bacteriology 183(1):301-308.

Hancock REW, Decad GM, Nikaido H. 1979. Identification of the protein producing transmembrane diffusion pores in the outer membranes of *Pseudomonas aeruginosa* PA01. Biochimica et Biophysica Acta 554(2):323-331.

Hartmann R, Hany R, Geiger T, Egli T, Witholt B, Zinn M. 2004. Tailored Biosynthesis of Olefinic Medium-Chain-Length Poly[(R)-3-hydroxyalkanoates] in *Pseudomonas putida* GPo1 with Improved Thermal Properties. Macromolecules 37(18):6780-6785.

Hartmann R, Hany R, Pletscher E, Ritter A, Witholt B, Zinn M. 2006. Tailor-made olefinic medium-chain-length poly[(R)-3-hydroxyalkanoates] by *Pseudomonas putida* GPo1: Batch versus chemostat production. Biotechnology and Bioengineering 93(4):737-746.

Hazer B, Steinbüchel A. 2007. Increased diversification of polyhydroxyalkanoates by modification reactions for industrial and medical applications. Applied Microbiology and Biotechnology 74(1):1-12.

Heim S, Ferrer M, Heuer H, Regenhardt D, Nimtz M, Timmis KN. 2003. Proteome reference map of *Pseudomonas putida* strain KT2440 for genome expression profiling: Distinct responses of KT2440 and *Pseudomonas aeruginosa* strain PAO1 to iron deprivation and a new form of superoxide dismutase. Environmental Microbiology 5(12):1257-1269.

Hermes HFM, Sonke T, Peters PJH, van Balken JAM, Kamphuis J, Dijkhuizen L, Meijer EM. 1993. Purification and Characterization of an l-Aminopeptidase from *Pseudomonas putida* ATCC 12633. Applied and Environmental Microbiology 59(12):4330-4334.

Herrero M, De Lorenzo V, Timmis KN. 1990. Transposon vectors containing non-antibiotic resistance selection markers for cloning and stable chromosomal insertion of foreign genes in gram-negative bacteria. Journal of Bacteriology 172(11):6557-6567.

Herrmann H, Janke D, Krejsa S, Kunze I. 1987. Involvement of the plasmid pPGH1 in the phenol degradation of Pseudomonas putida strain H. FEMS Microbiology Letters 43(2):133-137.

Hervas AB, Canosa I, Little R, Dixon R, Santero E. 2009. NtrC-dependent regulatory network for nitrogen assimilation in *Pseudomonas putida*. Journal of Bacteriology 191(19):6123-6135.

Hervas AB, Canosa I, Santero E. 2008. Transcriptome analysis of Pseudomonas putida in response to nitrogen availability. Journal of Bacteriology 190(1):416-420.

Hoffmann N, Rehm BHA. 2004. Regulation of polyhydroxyalkanoate biosynthesis in *Pseudomonas putida* and *Pseudomonas aeruginosa*. FEMS Microbiology Letters 237(1):1-7.

Hoskisson PA, Hobbs G. 2005. Continuous culture - Making a comeback? Microbiology 151(10):3153-3159.

Hua Q, Yang C, Oshima T, Mori H, Shimizu K. 2004. Analysis of Gene Expression in *Escherichia coli* in Response to Changes of Growth-Limiting Nutrient in Chemostat Cultures. Applied and Environmental Microbiology 70(4):2354-2366.

Huber W, Von Heydebreck A, Sultmann H, Poustka A, Vingron M. 2002. Variance stabilization applied to microarray data calibration and to the quantification of differential expression. Bioinformatics 18(SUPPL. 1):S96-S104.

Huijberts GN, de Rijk TC, de Waard P, Eggink G. 1994a. 13C nuclear magnetic resonance studies of *Pseudomonas putida* fatty acid metabolic routes involved in poly(3-hydroxyalkanoate) synthesis. Journal of Bacteriology 176(6):1661-1666.

Huijberts GNM, De Rijk TC, De Waard P, Eggink G. 1994b. 13C nuclear magnetic resonance studies of *Pseudomonas putida* fatty acid metabolic routes involved in poly(3-hydroxyalkanoate) synthesis. Journal of Bacteriology 176(6):1661-1666.

Huijberts GNM, Eggink G. 1996. Production of poly(3-hydroxyalkanoates) by *Pseudomonas putida* KT2442 in continuous cultures. Applied Microbiology and Biotechnology 46(3):233-239.

Huijberts GNM, Eggink G, De Waard P, Huisman GW, Witholt B. 1992. *Pseudomonas putida* KT2442 cultivated on glucose accumulates poly(3- hydroxyalkanoates) consisting of saturated and unsaturated monomers. Applied and Environmental Microbiology 58(2):536-544.

Huisman GW, de Leeuw O, Eggink G, Witholt B. 1989. Synthesis of poly-3-hydroxyalkanoates is a common feature of fluorescent pseudomonads. Applied and Environmental Microbiology 55(8):1949-1954.

Huisman GW, Wonink E, De Koning G, Preusting H, Witholt B. 1992. Synthesis of poly(3-hydroxyalkanoates) by mutant and recombinant Pseudomonas strains. Applied Microbiology and Biotechnology 38(1):1-5.

Jackson FA, Dawes EA. 1976. Regulation of the tricarboxylic acid cycle and poly-B-hydroxybutyrate metabolism in *Azotobacter beijerinckii* grown under nitrogen or oxygen limitation. Journal of General Microbiology 97(2):303-312.

Jimenez JI, Miambres B, Garcia JL, Diaz E. 2002. Genomic analysis of the aromatic catabolic pathways from Pseudomonas putida KT2440. Environmental Microbiology 4(12):824-841.

Jiménez JI, Miñambres B, García JL, Díaz E. 2002. Genomic analysis of the aromatic catabolic pathways from *Pseudomonas putida* KT2440. Environmental Microbiology 4(12):824-841.

Jung K, Hazenberg W, Prieto M, Witholt B. 2001. Two-stage continuous process development for the production of medium-chain-length poly(3-hydroxyalkanoates). Biotechnology and Bioengineering 72(1):19-24.

Kang Z, Wang Q, Zhang H, Qi Q. 2008. Construction of a stress-induced system in *Escherichia coli* for efficient polyhydroxyalkanoates production. Applied Microbiology and Biotechnology 79(2):203-208.

Kauffmann A, Gentleman R, Huber W. 2009. arrayQualityMetrics - A bioconductor package for quality assessment of microarray data. Bioinformatics 25(3):415-416.

Kawakami T, Kuroki M, Ishii M, Igarashi Y, Arai H. 2010. Differential expression of multiple terminal oxidases for aerobic respiration in *Pseudomonas aeruginosa*. Environmental Microbiology 12(6):1399-1412.

Kellerhals MB, Kessler B, Witholt B, Tchouboukov A, Brandl H. 2000. Renewable Long-Chain Fatty Acids for Production of Biodegradable Medium-Chain-Length Polyhydroxyalkanoates (mcl-PHAs) at Laboratory and Pilot Plant Scales. Macromolecules 33(13):4690-4698.

Kessler B, Witholt B. 2001. Factors involved in the regulatory network of polyhydroxyalkanoate metabolism. Journal of Biotechnology 86(2):97-104.

Khanna S, Srivastava AK. 2005. Recent advances in microbial polyhydroxyalkanoates. Process Biochemistry 40(2):607-619.

Kiener A. 1992. Enzymatic Oxidation of Methyl Groups on Aromatic Heterocycles: A Versatile Method for the Preparation of Heteroaromatic Carboxylic Acids. Angewandte Chemie International Edition in English 31(6):774-775.

Kim DY, Hyung WK, Moon GC, Young HR. 2007. Biosynthesis, modification, and biodegradation of bacterial medium-chain-length polyhydroxyalkanoates. Journal of Microbiology 45(2):87-97.

Kim YH, Cho K, Yun SH, Kim JY, Kwon KH, Yoo JS, Kim SI. 2006. Analysis of aromatic catabolic pathways in Pseudomonas putida KT 2440 using a combined proteomic approach: 2-DE/MS and cleavable isotope-coded affinity tag analysis. Proteomics 6(4):1301-1318.

Klinke S, Dauner M, Scott G, Kessler B, Witholt B. 2000. Inactivation of isocitrate lyase leads to increased production of medium-chain-length poly(3-hydroxyalkanoates) in *Pseudomonas putida*. Applied and Environmental Microbiology 66(3):909-913.

Kolkman A, Daran-Lapujade P, Fullaondo A, Olsthoorn MMA, Pronk JT, Slijper M, Heck AJR. 2006. Proteome analysis of yeast response to various nutrient limitations. Molecular Systems Biology 2.

Korz DJ, Rinas U, Hellmuth K, Sanders EA, Deckwer WD. 1995. Simple fed-batch technique for high cell density cultivation of *Escherichia coli*. Journal of Biotechnology 39(1):59-65.

Kosseva MR, Kennedy JF. 1996. Degradable polymers: Principles and applications. Edited by G. Scott and D. Gilead. Chapman & Hall, London, 1995. pp. xii + 271, price £59.00. ISBN 0-412-59010-7. Polymer International 40(2):151-151.

Koutinas M, Kiparissides A, Lam MC, Silva-Rocha R, Godinho M, de Lorenzo V, Martins dos Santos VAP, Pistikopoulos EN, Mantalaris A. 2011. Improving the prediction of *Pseudomonas putida* mt-2 growth kinetics with the use of a gene expression regulation model of the TOL plasmid. Biochemical Engineering Journal 55(2):108-118.

Koutinas M, Lam MC, Kiparissides A, Silva-Rocha R, Godinho M, Livingston AG, Pistikopoulos EN, de Lorenzo V, Dos Santos VA, Mantalaris A. 2010. The regulatory logic of m-xylene biodegradation by *Pseudomonas putida* mt-2 exposed by dynamic modelling of the principal node Ps/Pr of the TOL plasmid. Environmental Microbiology 12(6):1705-1718.

Krayl M, Benndorf D, Loffhagen N, Babel W. 2003. Use of proteomics and physiological characteristics to elucidate ecotoxic effects of methyl tert-butyl ether in Pseudomonas putida KT2440. Proteomics 3(8):1544-1552.

Lee J. 1997. Biological conversion of lignocellulosic biomass to ethanol. Journal of Biotechnology 56(1):1-24.

Lee MV, Topper SE, Hubler SL, Hose J, Wenger CD, Coon JJ, Gasch AP. 2011. A dynamic model of proteome changes reveals new roles for transcript alteration in yeast. Mol Syst Biol 7.

Lee SJ, Song H, Lee SY. 2006. Genome-Based Metabolic Engineering of *Mannheimia succiniciproducens* for Succinic Acid Production. Applied and Environmental Microbiology 72(3):1939-1948.

Lee SY, Choi J-i, Wong HH. 1999. Recent advances in polyhydroxyalkanoate production by bacterial fermentation: mini-review. International Journal of Biological Macromolecules 25(1-3):31-36.

Lee SY, Wong HH, Choi JI, Lee SH, Lee SC, Han CS. 2000. Production of medium-chain-length polyhydroxyalkanoates by high-cell- density cultivation *Pseudomonas putida* under phosphorus limitation. Biotechnology and Bioengineering 68(4):466-470.

Leprince A, Janus D, de Lorenzo V, Santos VMd, Weber W, Fussenegger M. 2011. Streamlining of a *Pseudomonas putida* Genome Using a Combinatorial Deletion Method Based on Minitransposon Insertion and the Flp-*FRT* Recombination System

Synthetic Gene Networks. Humana Press. p 249-266.

Liu Q, Luo G, Zhou XR, Chen GQ. 2011. Biosynthesis of poly(3-hydroxydecanoate) and 3-hydroxydodecanoate dominating polyhydroxyalkanoates by β-oxidation pathway inhibited *Pseudomonas putida*. Metabolic Engineering 13(1):11-17.

Liu W, Chen GQ. 2007. Production and characterization of medium-chain-length polyhydroxyalkanoate with high 3-hydroxytetradecanoate monomer content by fadB and fadA knockout mutant of *Pseudomonas putida* KT2442. Applied Microbiology and Biotechnology 76(5):1153-1159.

Lu P, Vogel C, Wang R, Yao X, Marcotte EM. 2007. Absolute protein expression profiling estimates the relative contributions of transcriptional and translational regulation. Nat Biotech 25(1):117-124.

Luengo JM, Garcia B, Sandoval A, Naharro G, Olivera ER. 2003. Bioplastics from microorganisms. Current Opinion in Microbiology 6(3):251-260.

Madison LL, Huisman GW. 1999. Metabolic engineering of poly(3-hydroxyalkanoates): From DNA to plastic. Microbiology and Molecular Biology Reviews 63(1):21-53.

Martinez-Garcia E, de Lorenzo V. 2011. Engineering multiple genomic deletions in Gram-negative bacteria: Analysis of the multi-resistant antibiotic profile of *Pseudomonas putida* KT2440. Environmental Microbiology 13(10):2702-2716.

Martínez V, García P, García JL, Prieto MA. 2011. Controlled autolysis facilitates the polyhydroxyalkanoate recovery in *Pseudomonas putida* KT2440. Microbial Biotechnology 4(4):533-547.

Martins Dos Santos VAP, Heim S, Moore ERB, Strätz M, Timmis KN. 2004. Insights into the genomic basis of niche specificity of *Pseudomonas putida* KT2440. Environmental Microbiology 6(12):1264-1286.

Meijnen JP, De Winde JH, Ruijssenaars HJ. 2008. Engineering Pseudomonas putida S12 for efficient utilization of D-xylose and L-arabinose. Applied and Environmental Microbiology 74(16):5031-5037.

Meijnen JP, De Winde JH, Ruijssenaars HJ. 2009. Establishment of oxidative D-xylose metabolism in Pseudomonas putida S12. Applied and Environmental Microbiology 75(9):2784-2791.

Melzer G, Esfandabadi M, Franco-Lara E, Wittmann C. 2009. Flux Design: In silico design of cell factories based on correlation of pathway fluxes to desired properties. BMC Systems Biology 3(1):120.

Miyakoshi M, Shintani M, Terabayashi T, Kai S, Yamane H, Nojiri H. 2007. Transcriptome analysis of Pseudomonas putida KT2440 harboring the completely sequenced IncP-7 plasmid pCAR1. Journal of Bacteriology 189(19):6849-6860.

Mobley HLT, Island MD, Hausinger RP. 1995. Molecular biology of microbial ureases. Microbiological Reviews 59(3):451-480.

Morales G, Ugidos A, Rojo F. 2006. Inactivation of the Pseudomonas putida cytochrome o ubiquinol oxidase leads to a significant change in the transcriptome and to increased expression of the CIO and cbb3-1 terminal oxidases. Environmental Microbiology 8(10):1764-1774.

Moreno R, Martinez-Gomariz M, Yuste L, Gil C, Rojo F. 2009. The Pseudomonas putida Crc global regulator controls the hierarchical assimilation of amino acids in a complete medium: Evidence from proteomic and genomic analyses. Proteomics 9(11):2910-2928.

Morgunov IG, Solodovnikova NY, Sharyshev AA, Kamzolova SV, Finogenova TV. 2004. Regulation of NAD+-Dependent isocitrate dehydrogenase in the citrate producing yeast *Yarrowia lipolytica*. Biochemistry (Moscow) 69(12):1391-1398.

Nakazawa T, Yokota T. 1973. Benzoate metabolism in Pseudomonas putida(arvilla) mt 2: Demonstration of two benzoate pathways. Journal of Bacteriology 115(1):262-267.

Nelson KE, Weinel C, Paulsen IT, Dodson RJ, Hilbert H, Martins dos Santos VAP, Fouts DE, Gill SR, Pop M, Holmes M and others. 2002. Complete genome sequence and comparative analysis of the metabolically versatile *Pseudomonas putida* KT2440. Environmental Microbiology 4(12):799-808.

Nijkamp K, Westerhof RGM, Ballerstedt H, De Bont JAM, Wery J. 2007. Optimization of the solvent-tolerant *Pseudomonas putida* S12 as host for the production of p-coumarate from glucose. Applied Microbiology and Biotechnology 74(3):617-624.

Nikodinovic-Runic J, Flanagan M, Hume AR, Cagney G, O'Connor KE. 2009. Analysis of the Pseudomonas putida CA-3 proteome during growth on styrene under nitrogen-limiting and non-limiting conditions. Microbiology 155(10):3348-3361.

Nogales J, Palsson BO, Thiele I. 2008. A genome-scale metabolic reconstruction of *Pseudomonas putida* KT2440: iJN746 as a cell factory. BMC Syst Biol 2:79.

Ochs MM, Lu CD, Hancock REW, Abdelal AT. 1999. Amino acid-mediated induction of the basic amino acid-specific outer membrane porin OprD from *Pseudomonas aeruginosa*. Journal of Bacteriology 181(17):5426-5432.

Olivera ER, Carnicero D, Jodra R, Miambres B, Garcia B, Abraham GA, Gallardo A, Roman JS, Garcia JL, Naharro G and others. 2001. Genetically engineered Pseudomonas: A factory of new bioplastics with broad applications. Environmental Microbiology 3(10):612-618.

Ouyang SP, Luo RC, Chen SS, Liu Q, Chung A, Wu Q, Chen GQ. 2007. Production of polyhydroxyalkanoates with high 3-hydroxydodecanoate monomer content by fadB anf fadA knockout mutant of *Pseudomonas putida* KT2442. Biomacromolecules 8(8):2504-2511.

Park JH, Lee KH, Kim TY, Lee SY. 2007. Metabolic engineering of *Escherichia coli* for the production of l-valine based on transcriptome analysis and in silico gene knockout simulation. Proceedings of the National Academy of Sciences 104(19):7797-7802.

Patel RN, Banerjee A, Ko RY, Howell JM, Li Wen S, Comezoglu FT, Partyka RA, Szarka L. 1994. Enzymic preparation of (3R-cis)-3-(acetyloxy)-4-phenyl-2-azetidinone: A taxol side-chain synthon. Biotechnology and Applied Biochemistry 20(1):23-33.

Peng X, Xu C, Ren H, Lin X, Wu L, Wang S. 2005. Proteomic analysis of the sarcosine-insoluble outer membrane fraction of *Pseudomonas aeruginosa* responding to ampicilin, kanamycin, and tetracycline resistance. Journal of Proteome Research 4(6):2257-2265.

Poblete-Castro I, Becker J, Dohnt K, dos Santos V, Wittmann C. 2012a. Industrial biotechnology of *Pseudomonas putida* and related species. Applied Microbiology and Biotechnology 93(6):2279-2290.

Prieto MA, De Eugenio LI, Galan B, Luengo JM, Witholt B. 2007. Synthesis and degradation of polyhydroxyalkanoates. In: Ramos J-L, Filloux A, editors. Pseudomonas --- A Model in Systems Biology: Springer. p 409-410.

Puchalka J, Oberhardt MA, Godinho M, Bielecka A, Regenhardt D, Timmis KN, Papin JA, Martins dos Santos VA. 2008. Genome-scale reconstruction and analysis of the *Pseudomonas putida* KT2440 metabolic network facilitates applications in biotechnology. PLoS Comput Biol 4(10):e1000210.

Regenhardt D, Heuer H, Heim S, Fernandez DU, Strömpl C, Moore ERB, Timmis KN. 2002. Pedigree and taxonomic credentials of *Pseudomonas putida strain* KT2440. Environmental Microbiology 4(12):912-915.

Rehm BHA. 2003. Polyester synthases: Natural catalysts for plastics. Biochemical Journal 376(1):15-33.

Rehm BHA. 2007. Biogenesis of microbial polyhydroxyalkanoate granules: A platform technology for the production of tailor-made bioparticles. Current Issues in Molecular Biology 9(1):41-62.

Rehm BHA. 2010. Bacterial polymers: Biosynthesis, modifications and applications. Nature Reviews Microbiology 8(8):578-592.

Rehm BHA, Krüger N, Steinbüchel A. 1998. A new metabolic link between fatty acid de novo synthesis and polyhydroxyalkanoic acid synthesis. The phaG gene from *Pseudomonas putida* KT2440 encodes a 3-hydroxyacyl-acyl carrier protein-coenzyme a transferase. Journal of Biological Chemistry 273(37):24044-24051.

Ren Q, de Roo G, Ruth K, Witholt B, Zinn M, Thony-Meyer L. 2009. Simultaneous Accumulation and Degradation of Polyhydroxyalkanoates: Futile Cycle or Clever Regulation? Biomacromolecules 10(4):916-922.

Ren Q, de Roo G, Witholt B, Zinn M, Thony-Meyer L. 2010. Influence of growth stage on activities of polyhydroxyalkanoate (PHA) polymerase and PHA depolymerase in *Pseudomonas putida* U. BMC Microbiology 10(1):254.

Renzi F, Rescalli E, Galli E, Bertoni G. 2010. Identification of genes regulated by the MvaT-like paralogues TurA and TurB of Pseudomonas putida KT2440. Environmental Microbiology 12(1):254-263.

Resch A, Leicht S, Saric M, Pásztor L, Jakob A, Götz F, Nordheim A. 2006. Comparative proteome analysis of *Staphylococcus aureus* biofilm and planktonic cells and correlation with transcriptome profiling. Proteomics 6(6):1867-1877.

Reva ON, Weinel C, Weinel M, Bohm K, Stjepandic D, Hoheisel JD, Tummler B. 2006a. Functional genomics of stress response in Pseudomonas putida KT2440. Journal of Bacteriology 188(11):4079-4092.

Reva ON, Weinel C, Weinel M, Bohm K, Stjepandic D, Hoheisel JD, Tümmler B. 2006b. Functional genomics of stress response in Pseudomonas putida KT2440. Journal of Bacteriology 188(11):4079-4092.

Ritchie ME, Silver J, Oshlack A, Holmes M, Diyagama D, Holloway A, Smyth GK. 2007. A comparison of background correction methods for two-colour microarrays. Bioinformatics 23(20):2700-2707.

Rodnina MV, Savelsbergh A, Katunin VI, Wintermeyer W. 1997. Hydrolysis of GTP by elongation factor G drives tRNA movement on the ribosome. Nature 385(6611):37-41.

Rojo F. 2010. Carbon catabolite repression in Pseudomonas: Optimizing metabolic versatility and interactions with the environment. FEMS Microbiology Reviews 34(5):658-684.

Ronchel MC, Molina L, Witte A, Lutbiz W, Molin S, Ramos JL, Ramos C. 1998. Characterization of cell lysis in Pseudomonas putida induced upon expression of heterologous killing genes. Applied and Environmental Microbiology 64(12):4904-4911.

Rosche B, Li XZ, Hauer B, Schmid A, Buehler K. 2009. Microbial biofilms: a concept for industrial catalysis? Trends in Biotechnology 27(11):636-643.

Rothmel RK, Aldrich TL, Houghton JE, Coco WM, Ornston LN, Chakrabarty AM. 1990. Nucleotide sequencing and characterization of *Pseudomonas putida* catR: A positive regulator of the catBC operon is a member of the LysR family. Journal of Bacteriology 172(2):922-931.

Rühl J, Schmid A, Blank LM. 2009. Selected Pseudomonas putida strains able to grow in the presence of high butanol concentrations. Applied and Environmental Microbiology 75(13):4653-4656.

Ruiz JA, Lopez NI, Fernandez RO, Medez BS. 2001. Polyhydroxyalkanoate degradation is associated with nucleotide accumulation and enhances stress resistance and survival of *Pseudomonas oleovorans* in natural water microcosms. Applied and Environmental Microbiology 67(1):225-230.

Russell JB, Cook GM. 1995. Energetics of bacterial growth: Balance of anabolic and catabolic reactions. Microbiological Reviews 59(1):48-62.

Ryu HW, Hahn SK, Chang YK, Chang HN. 1997. Production of poly(3-hydroxybutyrate) by high cell density fed-batch culture of *Alcaligenes eutrophus* with phospate limitation. Biotechnology and Bioengineering 55(1):28-32.

Saito K, Matsuda F. 2010. Metabolomics for functional genomics, systems biology, and biotechnology. Annual Review of Plant Biology. p 463-489.

Santos PM, Benndorf D, Sa-Correia I. 2004. Insights into Pseudomonas putida KT2440 response to phenol-induced stress by quantitative proteomics. Proteomics 4(9):2640-2652.

Schmid A, Dordick JS, Hauer B, Kiener A, Wubbolts M, Witholt B. 2001. Industrial biocatalysis today and tomorrow. Nature 409(6817):258-268.

Schulze B, Wubbolts MG. 1999. Biocatalysis for industrial production of fine chemicals. Current Opinion in Biotechnology 10(6):609-615.

Segre D, Vitkup D, Church GM. 2002. Analysis of optimality in natural and perturbed metabolic networks. Proceedings of the National Academy of Sciences 99(23):15112-15117.

Segura A, Godoy P, Van Dillewijn P, Hurtado A, Arroyo N, Santacruz S, Ramos JL. 2005. Proteomic analysis reveals the participation of energy- and stress-related proteins in the response of Pseudomonas putida DOT-T1E to toluene. Journal of Bacteriology 187(17):5937-5945.

Senior PJ, Beech GA, Ritchie GA, Dawes EA. 1972. The role of oxygen limitation in the formation of poly- -hydroxybutyrate during batch and continuous culture of *Azotobacter beijerinckii*. Biochemical Journal 128(5):1193-1201.

Shah AA, Hasan F, Hameed A, Ahmed S. 2008. Biological degradation of plastics: A comprehensive review. Biotechnology Advances 26(3):246-265.

Shevchuk NA, Bryksin AV, Nusinovich YA, Cabello FC, Sutherland M, Ladisch S. 2004. Construction of long DNA molecules using long PCR-based fusion of several fragments simultaneously. Nucleic acids research 32(2):e19.

Silva-Rocha R, de Jong H, Tamames J, de Lorenzo V. 2011. The logic layout of the TOL network of *Pseudomonas putida* pWW0 plasmid stems from a metabolic amplifier motif (MAM) that optimizes biodegradation of m-xylene. BMC Systems Biology:191.

Smyth GK. 2004. Linear models and empirical bayes methods for assessing differential expression in microarray experiments. Statistical Applications in Genetics and Molecular Biology 3(1).

Sohn SB, Kim TY, Park JM, Lee SY. 2010. In silico genome-scale metabolic analysis of Pseudomonas putida KT2440 for polyhydroxyalkanoate synthesis, degradation of aromatics and anaerobic survival. Biotechnology Journal 5(7):739-750.

Sonawane A, Klöppner U, Derst C, Röhm KH. 2003a. Utilization of acidic amino acids and their amides by pseudomonads: Role of periplasmic glutaminase-asparaginase. Archives of Microbiology 179(3):151-159.

Sonawane A, Kloppner U, Hovel S, Volker U, Rohm KH. 2003b. Identification of Pseudomonas proteins coordinately induced by acidic amino acids and their amides: A two-dimensional electrophoresis study. Microbiology 149(10):2909-2918.

Steinbüchel A, Lutke-Eversloh T. 2003. Metabolic engineering and pathway construction for biotechnological production of relevant polyhydroxyalkanoates in microorganisms. Biochemical Engineering Journal 16(2):81-96.

Steinbüchel A, Valentin HE. 1995. Diversity of bacterial polyhydroxyalkanoic acids. FEMS Microbiology Letters 128(3):219-228.

Stephan S, Heinzle E, Wenzel SC, Krug D, Müller R, Wittmann C. 2006. Metabolic physiology of *Pseudomonas putida* for heterologous production of myxochromide. Process Biochemistry 41(10):2146-2152.

Straathof AJJ, Panke S, Schmid A. 2002. The production of fine chemicals by biotransformations. Current Opinion in Biotechnology 13(6):548-556.

Sudesh K, Abe H, Doi Y. 2000. Synthesis, structure and properties of polyhydroxyalkanoates: Biological polyesters. Progress in Polymer Science (Oxford) 25(10):1503-1555.

Sun Z, Ramsay J, Guay M, Ramsay B. 2006a. Automated feeding strategies for high-cell-density fed-batch cultivation of *Pseudomonas putida* KT2440. Applied Microbiology and Biotechnology 71(4):423-431.

Sun Z, Ramsay J, Guay M, Ramsay B. 2007a. Carbon-limited fed-batch production of medium-chain-length polyhydroxyalkanoates from nonanoic acid by *Pseudomonas putida* KT2440. Applied Microbiology and Biotechnology 74(1):69-77.

Sun Z, Ramsay J, Guay M, Ramsay B. 2009. Fed-batch production of unsaturated medium-chain-length polyhydroxyalkanoates with controlled composition by *Pseudomonas putida* KT2440. Applied Microbiology and Biotechnology 82(4):657-662.

Sun Z, Ramsay JA, Guay M, Ramsay BA. 2006b. Automated feeding strategies for high-cell-density fed-batch cultivation of *Pseudomonas putida* KT2440. Applied Microbiology and Biotechnology 71(4):423-431.

Sun Z, Ramsay JA, Guay M, Ramsay BA. 2007b. Carbon-limited fed-batch production of medium-chain-length polyhydroxyalkanoates from nonanoic acid by *Pseudomonas putida* KT2440. Applied Microbiology and Biotechnology 74(1):69-77.

Sun Z, Ramsay JA, Guay M, Ramsay BA. 2007c. Fermentation process development for the production of medium-chain-length poly-3-hyroxyalkanoates. Applied Microbiology and Biotechnology 75(3):475-485.

Tang H, Yu H, Li Q, Wang X, Gai Z, Yin G, Su F, Tao F, Ma C, Xu P. 2011. Genome Sequence of *Pseudomonas putida* Strain B6-2, a Superdegrader of Polycyclic Aromatic Hydrocarbons and Dioxin-Like Compounds. Journal of Bacteriology 193(23):6789-6790.

Tao F, Tang H, Gai Z, Su F, Wang X, He X, Xu P. 2011. Genome Sequence of *Pseudomonas putida* Idaho, a Unique Organic-Solvent-Tolerant Bacterium. Journal of Bacteriology 193(24):7011-7012.

Tessmer N, König S, Malkus U, Reichelt R, Pötter M, Steinbüchel A. 2007. Heat-shock protein HspA mimics the function of phasins sensu stricto in recombinant strains of *Escherichia coli* accumulating polythioesters or polyhydroxyalkanoates. Microbiology 153(2):366-374.

Timm A, Steinbuhel A. 1992. Cloning and molecular analysis of the poly(3-hydroxyalkanoic acid) gene locus of *Pseudomonas aeruginosa* PAO1. European Journal of Biochemistry 209(1):15-30.

Timmis KN. 2002. *Pseudomonas putida*: A cosmopolitan opportunist par excellence. Environmental Microbiology 4(12):779-781.

Trias J, Nikaido H. 1990. Protein D2 channel of the *Pseudomonas aeruginosa* outer membrane has a binding site for basic amino acids and peptides. Journal of Biological Chemistry 265(26):15680-15684.

Tropel D, van der Meer JR. 2004. Bacterial Transcriptional Regulators for Degradation Pathways of Aromatic Compounds. Microbiology and Molecular Biology Reviews 68(3):474-500.

Tsirogianni E, Aivaliotis M, Papasotiriou DG, Karas M, Tsiotis G. 2006. Identification of inducible protein complexes in the phenol degrader Pseudomonas sp. strain phDV1 by blue native gel electrophoresis and mass spectrometry. Amino Acids 30(1):63-72.

Van Der Werf MJ, Overkamp KM, Muilwijk B, Koek MM, Van Der Werff-Van Der Vat BJC, Jellema RH, Coulier L, Hankemeier T. 2008. Comprehensive analysis of the metabolome of Pseudomonas putida S12 grown on different carbon sources. Molecular BioSystems 4(4):315-327.

van Duuren JBJH. 2011. Optimization of *Pseudomonas putida* KT2440 as host for the production of cis, cis-muconate from benzoate. Wageningen: Wageningen.

Van Duuren JBJH, Brehmer B, Mars AE, Eggink G, dos Santos VM, Sanders JPM. 2011a. A limited LCA of bio-adipic acid: Manufacturing the nylon-6,6 precursor adipic acid using the benzoic acid degradation pathway from different feedstocks. Biotechnology and Bioengineering 108(6):1298-1306.

Van Duuren JBJH, Wijte D, Karge B, Martins dos Santos VA, Yang Y, Mars AE, Eggink G. 2011b. pH-stat fed-batch process to enhance the production of *cis, cis*-muconate from benzoate by *Pseudomonas putida* KT2440-JD1. Biotechnology Progress.

Van Duuren JBJH, Wijte D, Leprince A, Karge B, Puchalka J, Wery J, Dos Santos VAPM, Eggink G, Mars AE. 2011c. Generation of a *catR* deficient mutant of *P. putida* KT2440 that produces *cis, cis*-muconate from benzoate at high rate and yield. Journal of Biotechnology 156(3):163-172.

Velazquez F, Pfluger K, Cases I, De Eugenio LI, de Lorenzo V. 2007. The Phosphotransferase System Formed by PtsP, PtsO, and PtsN Proteins Controls Production of Polyhydroxyalkanoates in *Pseudomonas putida*. Journal of Bacteriology 189(12):4529-4533.

Verhoef S, Ballerstedt H, Volkers RJM, De Winde JH, Ruijssenaars HJ. 2010. Comparative transcriptomics and proteomics of p-hydroxybenzoate producing *Pseudomonas putida* S12: Novel responses and implications for strain improvement. Applied Microbiology and Biotechnology 87(2):679-690.

Verhoef S, Ruijssenaars HJ, de Bont JAM, Wery J. 2007. Bioproduction of p-hydroxybenzoate from renewable feedstock by solvent-tolerant *Pseudomonas putida* S12. Journal of Biotechnology 132(1):49-56.

Verhoef S, Wierckx N, Westerhof RGM, De Winde JH, Ruijssenaars HJ. 2009. Bioproduction of p-hydroxystyrene from glucose by the solvent-tolerant bacterium *Pseudomonas putida* S12 in a two-phase water-decanol fermentation. Applied and Environmental Microbiology 75(4):931-936.

Volkers RJM, De Jong AL, Hulst AG, Van Baar BLM, De Bont JAM, Wery J. 2006. Chemostat-based proteomic analysis of toluene-affected *Pseudomonas putida* S12. Environmental Microbiology 8(9):1674-1679.

Wang F, Lee SY. 1997. Poly(3-hydroxybutyrate) production with high productivity and high polymer content by a fed-batch culture of *Alcaligenes latus* under nitrogen limitation. Applied and Environmental Microbiology 63(9):3703-3706.

Wang HH, Zhou XR, Liu Q, Chen GQ. 2011. Biosynthesis of polyhydroxyalkanoate homopolymers by *Pseudomonas putida*. Applied Microbiology and Biotechnology 89(5):1497-1507.

Wang Q, Nomura CT. 2010. Monitoring differences in gene expression levels and polyhydroxyalkanoate (PHA) production in *Pseudomonas putida* KT2440 grown on different carbon sources. Journal of Bioscience and Bioengineering 110(6):653-659.

Wenzel SC, Gross F, Zhang Y, Fu J, Stewart AF, Müller R. 2005. Heterologous expression of a myxobacterial natural products assembly line in Pseudomonads via Red/ET recombineering. Chemistry and Biology 12(3):349-356.

Wierckx N, Ruijssenaars HJ, de Winde JH, Schmid A, Blank LM. 2009. Metabolic flux analysis of a phenol producing mutant of *Pseudomonas putida* S12: Verification and complementation of hypotheses derived from transcriptomics. Journal of Biotechnology 143(2):124-129.

Wierckx NJP, Ballerstedt H, De Bont JAM, De Winde JH, Ruijssenaars HJ, Wery J. 2008. Transcriptome analysis of a phenol-producing *Pseudomonas putida* S12 construct: Genetic and physiological basis for improved production. Journal of Bacteriology 190(8):2822-2830.

Wierckx NJP, Ballerstedt H, De Bont JAM, Wery J. 2005. Engineering of solvent-tolerant *Pseudomonas putida* S12 for bioproduction of phenol from glucose. Applied and Environmental Microbiology 71(12):8221-8227.

Wilson WA, Roach PJ, Montero M, Baroja-Fernandez E, Munoz FJ, Eydallin G, Viale AM, Pozueta-Romero J. 2010. Regulation of glycogen metabolism in yeast and bacteria. FEMS Microbiology Reviews 34(6):952-985.

Wolff JA, MacGregor CH, Eisenberg RC, Phibbs Jr PV. 1991. Isolation and characterization of catabolite repression control mutants of pseudomonas aeruginosa pao. Journal of Bacteriology 173(15):4700-4706.

Wong JW, Watson HA, Bouressa JF, Burns MP, Cawley JJ, Doro AE, Guzek DB, Hintz MA, McCormick EL, Scully DA and others. 2002. Biocatalytic Oxidation of 2-Methylquinoxaline to 2-Quinoxalinecarboxylic Acid. Organic Process Research & Development 6(4):477-481.

Yamaguchi M, Takechi K, Myouga F, Imura S, Sato H, Takio S, Shinozaki K, Takano H. 2011. Loss of the plastid envelope protein AtLrgB causes spontaneous chlorotic cell death in *Arabidopsis thaliana*. Plant and Cell Physiology.

Yamane T. 1993. Yield of poly-D(-)-3-hydroxybutyrate from various carbon sources: A theoretical study. Biotechnology and Bioengineering 41(1):165-170.

Yang T, Jung Y, Kang H, Kim T, Park S, Lee S. 2011. Tailor-made type II *Pseudomonas* PHA synthases and their use for the biosynthesis of polylactic acid and its copolymer in recombinant *Escherichia coli*. Applied Microbiology and Biotechnology 90(2):603-614.

Yeom S, Yeom J, Park W. 2010. NtrC-sensed nitrogen availability is important for oxidative stress defense in Pseudomonas putida KT2440. Journal of Microbiology 48(2):153-159.

Yim H, Haselbeck R, Niu W, Pujol-Baxley C, Burgard A, Boldt J, Khandurina J, Trawick JD, Osterhout RE, Stephen R and others. 2011. Metabolic engineering of *Escherichia coli* for direct production of 1,4-butanediol. Nature Chemical Biology 7(7):445-452.

Yu H, Tang H, Wang L, Yao Y, Wu G, Xu P. 2011. Complete genome sequence of the nicotine-degrading *Pseudomonas putida* strain S16. Journal of Bacteriology 193(19):5541-5542.

Zhao YH, Li HM, Qin LF, Wang HH, Chen GQ. 2007. Disruption of the polyhydroxyalkanoate synthase gene in *Aeromonas hydrophila* reduces its survival ability under stress conditions. FEMS Microbiology Letters 276(1):34-41.

Zhen D, Liu H, Wang SJ, Zhang JJ, Zhao F, Zhou NY. 2006. Plasmid-mediated degradation of 4-chloronitrobenzene by newly isolated *Pseudomonas putida* strain ZWL73. Applied Microbiology and Biotechnology 72(4):797-803.

Zinn M, Witholt B, Egli T. 2001. Occurrence, synthesis and medical application of bacterial polyhydroxyalkanoate. Adv Drug Deliv Rev 53(1):5-21.

Zinn M, Witholt B, Egli T. 2004. Dual nutrient limited growth: Models, experimental observations, and applications. Journal of Biotechnology 113(1-3):263-279.

CHAPTER IV. *In silico*-driven metabolic engineering of *Pseudomonas putida* for enhanced production of poly-hydroxyalkanoates

This chapter has been published: **Ignacio Poblete-Castro**, Danielle Binger, Andre Rodrigues, Judith Becker, Vitor A. P. Martins dos Santos and Christoph Wittmann. Metabolic Engineering (2012).

4.1 Abstract

Here, we present systems metabolic engineering driven by in-silico modeling to tailor *Pseudomonas putida* for synthesis of medium chain length PHAs on glucose. Using physiological properties of the parent wild type as constraints, elementary flux mode analysis of a large-scale model of the metabolism of *P. putida* was used to predict genetic targets for strain engineering. Among a set of priority ranked targets, glucose dehydrogenase (encoded by *gcd*) was predicted as most promising deletion target. The mutant *P. putida* Δ*gcd*, generated on basis of the computational design, exhibited 100% increased PHA accumulation as compared to the parent wild type, maintained a high specific growth rate and exhibited an almost unaffected gene expression profile, which excluded detrimental side effects of the modification. A second mutant strain, *P. putida* Δ*pgl*, that lacked 6-phosphogluconolactonase, exhibited a substantially decreased PHA synthesis, as was also predicted by the model. The production potential of *P. putida* Δ*gcd* was assessed in batch bioreactors. The novel strain showed an increase of the PHA yield (+ 80%), the PHA titer (+ 100%) and cellular PHA content (+ 50%) and revealed almost unaffected growth and diminished by-product formation. It was thus found superior in all relevant criteria towards industrial production. Beyond the contribution to more efficient PHA production processes at reduced costs that might replace petrochemical plastics in the future, the study illustrates the power of computational prediction to tailor microbial strains for enhanced biosynthesis of added-value compounds.

Key Words: elementary flux modes; pathway engineering; phosphogluconolactonase; glucose dehydrogenase; polyhydroxyalkanoates; in-silico design, *Pseudomonas putida* KT2440, systems metabolic engineering; bio-polymer; transcriptome

4.2 Introduction

Bio-based plastic materials are among the most important products to overcome the shortage of fossil resources and the environmental burden linked to conventional plastics produced from petroleum. Particularly, poly-hydroxyalkanoates (PHAs) have proven valuable to replace common oil-based polymers because of their similar mechanical and physical properties (Madison and Huisman, 1999). Through the past decades, short-chain-length PHAs such as poly(3-hydroxybutyrate) and related co-polymers have been commercialized in the biopolymer market because of a well-established production process (Ryu et al., 1997; Wang and Lee, 1997), supported by knowledge on the underlying biosynthetic pathway at the molecular level (Rehm, 2003). However, these short-chain-length polymers reveal rather poor physical properties which restricts them to the production of soft plastic such as packaging films (Chen, 2009). This has recently shifted the interest to medium-chain-length PHAs with superior properties that promise a broader spectrum of applications (Kim et al., 2007) in the chemical industry (Chen and Wu, 2005), but also as material for medical purposes (Zinn et al., 2001), protein purification (Rehm, 2007), and drug delivery (Grage et al., 2009). *Pseudomonas putida* KT2440 and related strains produce such medium-chain-length PHAs (Huijberts et al., 1992). Most of the investigations with this bacterium have focused on the use of fatty acids as carbon source, since these promote high accumulation of the biopolymer up to 80% of the cell dry weight (Poblete-Castro et al. 2012). The production of medium-chain-length PHAs on fatty acids has meanwhile been complemented by the identification of PHA regulatory factors (de Eugenio et al., 2010a; de Eugenio et al., 2010b), the generation of new co-polymers (Liu et al., 2011) and process development (Kellerhals et al., 2000; Sun et al., 2007). As the raw material accounts for the most part of the production costs for PHAs (Yamane, 1993), one step ahead

towards a cost-effective process is the use of substrates, such as glucose, which are cheaper than fatty acids. Nevertheless, a previous report has shown that glucose-grown *P. putida* accumulates much less of the desired biopolymer as compared to other substrates, including fatty acids (Huijberts et al., 1992), which places sugar-based production as economically not viable against the conventional oil-based route.

In this regard, systems metabolic engineering now opens novel avenues to enhance the synthesis of value-added products. As the genomic repertoire of *P. putida* comprises the entire set of enzymes to synthesize PHAs, there seems no direct need to insert heterologous genes in first instance. In fact, a re-engineering of its metabolic pathway network towards improved PHA production appears more straightforward. Hereby, the sequenced genomes of different *P. putida* strains (Nelson et al., 2002; Tang et al., 2011; Tao et al., 2011) and the genome-scale networks created (Nogales et al., 2008; Puchalka et al., 2008; Sohn et al., 2010) now enable a next level of strain design, i.e. design-based systems metabolic engineering, which recruits systems-wide network modeling to predict genetic targets. The beauty of this approach was successfully demonstrated by model-based design of a bacterial strain that then accumulated 120 g L^{-1} lysine with only 12 defined genomic traits (Becker et al., 2011). Design-based strain engineering is supported by powerful software tools such as Minimization of Metabolic Adjustments (MOMA) (Segre et al., 2002), and Optknock (Burgard et al., 2003), and more recently FluxDesign (Melzer et al., 2009). The latter is based on elementary flux modes and thus enables the simultaneous prediction of amplification, attenuation and deletion targets for any biological system of interest (Melzer et al., 2009). Here, we rationally re-designed *P. putida* KT2440 towards enhanced production of medium-chain-length PHAs using glucose as carbon source. Translating the computational design guided by FluxDesign into the laboratory, the metabolically engineered strain that carried only one predicted key mutation, revealed a 100 % increase in the final PHA titer, a 50 % increase of the cellular PHA content and a 80 % in the PHA yield, relative to its parent strain, *P. putida* KT2440. This displays an important step towards industrial production of medium-chain-length PHAs using *P. putida* as a cell factory.

4.3 Materials and methods

Strains and plasmids.

The parent strain *P. putida* KT2440 (DSM 6125) was obtained from the German Collection of Microorganisms and Cell Cultures (DSMZ, Braunschweig, Germany). All PCR fragments generated for the construction of plasmids were sub-cloned into the plasmid pCR®2.1 (Invitrogen, CA, USA), transformed into *E. coli* DH5 (Invitrogen, CA, USA), and validated by sequencing. The plasmid pEMG (Martinez-Garcia and de Lorenzo, 2011) was used for the construction of pEMG_PP1023 and pEMG_PP1444. In the first case, about 600 bp of the upstream and downstream regions of the *P. putida* gene PP1023, i.e. *pgl* that encodes for 6-phosphogluconolactonase, were amplified using Taq DNA polymerase (Qiagen, Venlo, The Netherlands) with primers UP1023XbaIF and UP1023ClaIR, as well as DOWN1023ClaIF and DOWN1023XmaIR (Table 1) and genomic DNA from strain *P. putida* KT2440. Both PCR fragments were inserted into the *Xma*I-*Xba*I restriction sites of pEMG, which generated pEMG_PP1023. In case of vector pEMG_PP1444, the 600 bp upstream and downstream regions of the gene PP1444, i.e. *gcd* that encodes glucose dehydrogenase, were amplified using the primers UP1444KpnIF and UP1444R, as well as DOWN1444F and DOWN1444EcoRIR (Table 1). Both PCR fragments were fused by PCR (Shevchuk et al., 2004). The resulting fragment was integrated into pEMG via the *Eco*RI-*Kpn*I restriction sites to generate pEMG_PP1444. pEMG derivatives were then transformed into *E. coli* CC118λ*pir* (Herrero et al., 1990) to generate donor cells for the later tri-parental mating with *P. putida* KT2440 (Bagdasarian et al., 1981; Regenhardt et al., 2002) and the helper strain *E. coli* HB101 as described by (de Lorenzo and Timmis, 1994).

Genetic engineering of *P. putida*

To generate single and double deletion mutants of *Pseudomonas putida* KT2440, genome editing was applied (Martinez-Garcia and de Lorenzo, 2011). For this purpose, the pEMG derivatives were first co-integrated by a single crossover into the chromosome of *P. putida* KT2440 using tri-parental mating with *E. coli* HB101 as helper strain, as well as the donor strains *E. coli* CC118λ*pir* pEMG_PP1023 and *E. coli* CC118λ*pir* pEMG_PP1444, respectively. Successful homologous integration of the vector DNA was confirmed by PCR (data not shown). The successful genomic deletions were confirmed by PCR.

Table 1. Primers used in this study

Primer	**Sequence (5'-3')**
UP1023XbaIF	TCTAGACGGCCAGTACATTGCCGGCT
UP1023ClaIR	ATCGATGGTCCGCCAGTTCATGAGCCTT
DOWN1023ClaIF	ATCGATGGCCTGTCGATGACCCGTTCGCT
DOWN1023XmaIR	CCCGGGGGCGGTAGCCCAGGGCATAGC
UP1444KpnIF	GGTACCGGTTTCAAGCTCAGCGGCAG
UP1444R	CGACCGAAACGCGACACAAGGGTTAGAAACTGCTCTGGATCTTCAGG
DOWN1444F	GATCCAGAGCAGTTTCTAACCCTTGTGTCGCGTTTCGGTCGCGCAGC
DOWN1444EcoRIR	GAATTCGACCTCGTCGGTCGGCTCGG

Medium

P. putida strains were grown in a defined mineral medium (M9) consisting of (per liter) 12.8 g $Na_2HPO_4 \cdot 7H_2O$, 3 g KH_2O_4, 1 g NH_4Cl, and 0.5 g NaCl. This basic solution was autoclaved and subsequently supplemented with 0.12 g of $MgSO_4 \cdot H_2O$, trace elements (mg L^{-1}): 6.0 $FeSO_4 \cdot 7H_2O$, 2.7 $CaCO_3$, 2.0 $ZnSO_4 \cdot H2O$, 1.16 $MnSO_4 \cdot H_2O$, 0.37 $CoSO_4 \cdot 7H_2O$, 0.33 $CuSO_4 \cdot 5H_2O$, 0.08 H_3BO_3, and 18.5 g L^{-1} glucose (all filter-sterilized).

Cultivations

Flask experiments

P. putida strains, kept as frozen stock in 25 % glycerol at -80°C, were streaked on Luria Bertani agar plates and incubated for one day at 30 °C. Single colonies were then picked from the plate and inoculated it into a 50 mL shake flask containing 10 ml of the above described medium and incubated overnight under aerobic conditions at 30 °C and 180 rpm (Innova, Enfield, USA) set. By taking a calculated volume of the obtained cell suspension from the pre-culture (to begin the PHA-accumulating process with an initial OD of 0.05), 1000 mL baffled shake flasks containing 200 mL of culture medium were inoculated and placed in a rotary shaker under aerobic conditions at 30 °C. Each culture was carried out by triplicate.

Batch fermentations

Batch fermentations were carried out in a 2L top-bench BIOSTAT B1 bioreactor (Sartorius B Systems GmbH, Melsungen, Germany) with a working volume of 1.5 L, at 30°C. The aeration rate was set to 0.5 L L^{-1} min^{-1} using a mass flow controller (PR4000, MKS Instruments, Wilmington, MA, USA). The dissolved oxygen level was kept above 20% of air saturation by control of the agitation speed up to a maximum of 900 rpm. The pH was maintained at 7.0 by automatic addition of 0.5 M H_2SO_4 and 1 M of KOH.

Analytics of substrates and products

Cell growth was recorded as optical density (OD) at 600_{nm} (Ultraspec 2000, Hitachi, Japan). The cell dry weight was determined gravimetrically after collection of 10 mL culture broth for 10 min at 4°C and 3,800 x *g* (Eppendorf 5810 R, Hamburg, Germany) in pre-weighed tubes, including a washing step with distilled water, and drying of the obtained pellet at 100 °C until constant weight. The ammonium concentration in cell-free supernatant was measured by a photometric test (LCK 303 kit, Hach Lange, Danaher, USA). The glucose concentration in cultivation supernatant and medium was analyzed after appropriate dilution by enzymatic analysis (2300 STAT Plus, Yellow Spring Instrument, Ohio, USA). Gluconate and 2-keto-gluconate were quantified by HPLC (Hitachi Elite LaChrom, Krefeld, Germany) equipped with an Aminex HPX 87 H column (Biorad, Hercules, CA, USA) as the stationary phase and 12.5 mM H_2SO_4 as the mobile phase at 0.5 mL min^{-1} and 45 °C, and UV detection at 220 nm.

PHA characterization and quantification

PHA was first characterized by NMR to confirm its basic structure. For this purpose, 30 mL of culture were harvested (3,800 x*g*, 15 min, 4°C, (Eppendorf 5810 R, Hamburg, Germany). Then, the pellet was washed with deionized water, frozen at -20°C, and lyophilized in a freeze-dryer Alpha 1-4 LCS (Christ, Osterode, Germany). The obtained lyophilizate was suspended in 10 mL chloroform and kept for 3 h at 80 °C to extract the PHA. The chloroform solution was filtered to remove cell debris and then concentrated by rotary evaporation. Subsequently, the PHA was isolated and purified by precipitation through drop wise addition into cold methanol. The methanol-chloroform mixture was decanted and the pure polymer was stored under nitrogen at -20 °C. For ^{1}H-NMR analysis, 5-10 mg of polymer was dissolved in 0.7 mL deuterated chloroform ($CDCl_3$), whereas 15-20 mg of polymer was used for recording the ^{13}C spectra. ^{1}H and ^{13}C NMR spectra were recorded at 300K on a Bruker DPX-300 NMR Spectrometer (Bricker, Billerica, MA, USA) locked to the deuterium resonance of the solvent ($CDCl_3$).

Chemical shifts are given in ppm relative to the signal of the solvent (^{1}H: 7.26, ^{13}C: 77.3) and a coupling constant in Hz. Standard Bruker pulse programs were used throughout.

PHA compositions of the polymer produced, as well as the cellular PHA content concentration were determined by gas chromatography (GC) and mass spectrometry (MS) of the methanolyzed polyester. Methanolysis was carried out by suspending 5–10 mg of lyophilized aliquots (see above) in 2 mL of chloroform and 2 mL of methanol containing 15 % sulfuric acid and 0.5 mg mL^{-1} 3-methylbenzoic acid as internal standard, respectively, followed by incubation at 100 °C for 4 h. After cooling, 1 mL of demineralized water was added and the organic phase containing the resulting methyl esters of monomers was analyzed by GC-MS. Analysis was performed in Varian GC-MS system 450GC/240MS ion trap mass spectrometer (Varian Inc., Agilent Technologies) and operated by the software MS Workstation 6.9.3 (Varian Inc., Agilent Technologies). An aliquot (1 mL) of the organic phase was injected into the gas chromatograph at a split ratio of 1:10. Separation of the analytes of interest (i.e. the methyl esters of 3-hydroxyexanoate, 3-hydroxyoctanoate, 3-hydroxydecanoate, 3-hydroxydodecanoate, 3-hydroxy-5-cis-dodecanoate, 3-hydroxytetradecanoate) was achieved by a FactorFour VF-5ms capillary column (30 m X 0.25 mm i.d. X 0.25 mm film thickness). Helium was used as carrier gas at a flow rate of 0.9 mL min^{-1}. The injector and transfer line temperature were 275°C and 300°C respectively. The oven temperature program was: initial temperature 40°C for 2 min, then from 40°C up 150°C at a rate of 5°C min^{-1} and finally up to 280°C at a rate of 10°C min^{-1}. Positive ions were obtained using electron ionization at 70 eV and the mass spectra were generated by scanning ions of *m/z* 50 to *m/z* 650. The PHA content (wt%) was defined as the percentage of the CDW represented by the polyhydroxyalkanoate.

Transcriptome analysis

Aliquots of 10 mL of culture broth were transferred into RNA protect buffer (Qiagen, Hilden, Germany), and 5 mL of cold methanol (-80°C) was added to the tube and further centrifuge after which the supernatant was discarded. Cell pellets were stored at -80°C for further RNA extraction. Isolation of total RNA was performed using the RNeasy kit (Qiagen, Venlo, The Netherlands), according to the instructions provided by the manufacturer. An amount of 2 µg total RNA was then labeled, either with Cy3 or with Cy5 using the ULS-system (Kreatech, Amsterdam, The Netherlands) according to the manufacturers manual. Equal amounts of Cy3 or Cy5-labelled RNA, one corresponding to the control and the other one to the condition to be analyzed, were then mixed by pipetting. A 600-ng weight of labeled RNA was fragmented and hybridized to the microarray. Agilent 8x15K two-color microarrays (Agilent Technologies, USA), designed for *Pseudomonas putida* KT2440, were used for all transcriptional analyses. The microarrays were scanned using a GenePix Pro 4001 scanner and the GenePix 4.0 software (Axon Instruments, Foster City, USA). The microarrays were analyzed using various packages (see below) from the Bioconductor suite. The results from the image analysis were read in by the 'limma' package. The quality of the chips was analyzed with the 'arrayQualityMetrics' package (Kauffmann et al., 2009). The intensity values were background-corrected using the “'normexp” method of the limma package (Ritchie et al., 2007) and normalized with the variance stabilization method (Huber et al., 2002). The significantly differentially expressed genes were identified by fitting the linear model (using the functions 'lmFit' and 'eBayes' from the 'limma' package) (Smyth, 2004). Genes for which the adjusted p-value (by Benjamini-Hochberg method) was lower than 0.05 and the fold change exceeded 2.00 in either direction were considered to be differentially expressed.

Elementary flux mode analysis

For elementary flux mode analysis, the genome-scale network of *P. putida* KT2440 (Sohn et al., 2010) was condensed into a large-scale network comprising the central catabolic reactions, energy metabolism, the entire set of anabolic pathways to biomass, as well as the biosynthetic routes to the desired product PHA, and by-products such as gluconate or 2-ketogluconate. The list of reactions is provided in the supplement. Considering the monomeric composition of the PHA homo-polymer obtained by *P. putida* from glucose, carbon ten acyl CoA monomers were regarded as building blocks (Nogales et al., 2008). The network comprised different compartments for gluconate and 2-ketogluconate formation (periplasm) and all other reactions (cytosol) (Daddaoua et al., 2010). Elementary flux modes were calculated as described previously (Melzer et al., 2009). Evaluation of the obtained modes was carried out in Excel (MS Office, Windows, 2007) and provided relative pathway fluxes and yields for each of the modes as well as the theoretical maximum yield for PHA among all modes. In addition, the data set was used to predict deletion, attenuation and amplification targets for rational strain engineering based on metabolic pathway correlations, i. e. flux correlation coefficients between the target flux (PHA production) and the other fluxes in the network (Driouch et al., 2012; Melzer et al., 2009).

4.4 Results

4.4.1 Growth and PHA production performance of the *Pseudomonas putida* wild type on glucose as carbon source

The performance of the wild type *P. putida* KT2440 was assessed in minimal medium with 18.5 g L^{-1} glucose as carbon source and a limiting amount of 350 mg L^{-1} ammonium as nitrogen source (Figure 1). This aimed at the characterization of its physiological properties to integrate these as realistic constraints into the subsequent model-driven strain design. The cells rapidly consumed glucose and exhibited exponential growth as long as ammonium was present in the medium. Subsequently, growth continued, but slowed down. As observed previously for *P. putida* (del Castillo et al., 2007; Vicente and Canovas, 1973), gluconate was detected as major by-product. Gluconate accumulated in large amounts in the broth and reached a maximum level of about 12 g/L after 35 h of cultivation, when the glucose was completely consumed. The cells then switched to consume gluconate, which led to a further increase of the cell concentration. The final OD value corresponded to about 4 g L^{-1} of cell dry weight. The cells of *P. putida* KT2440 contained about 26 % of the desired polymer at the final harvest (Figure 2). During the process, the formation of 2-ketogluconate was almost negligible. A minor amount appeared only transiently during the first hours. The yield for biomass of 0.25 g (g glucose)$^{-1}$ was relatively low, resulting in an overall PHA yield of 0.07 g (g glucose)$^{-1}$.

4.4.2 *In silico* network modeling of PHA production in the *Pseudomonas putida* wild type

As next step, in silico design was carried out using the software tool FluxDesign to derive predictions for promising genetic targets (Melzer et al., 2009; Driouch et al., 2012). For this purpose, elementary flux mode analysis was carried out for the metabolic network of PHA-producing *P. putida*, which considered glucose and ammonium as nutrients. The calculation yielded 1,029 unique elementary modes that defined the possible solution space for the investigated strain with all theoretically possible metabolic flux distributions. Interestingly, the yields for PHA, biomass and gluconate substantially differed between the

modes. This was obviously reflected by a strongly different pathway use, being a first indication that fluxes are inherently linked to production properties. The most common product, found in 82 % of the modes, was biomass, whereas gluconate was observed for 29 % of the modes. PHA production was found in 24 % of the modes. The maximum product yield, found among all the modes, was 0.4 mol mol^{-1} on basis of the assumed C_{10} building block. This value defined the theoretical optimum of PHA production from glucose in *P. putida*. Taking the molecular weight of the monomer (MW = 170 g mol^{-1}) into account, the resulting optimum yield was 0.37 g (g glucose)$^{-1}$ on a mass basis. Obviously, it was significantly higher as compared to the real value found for the wild type (0.07 g g^{-1}), leaving substantial space for strain improvement.

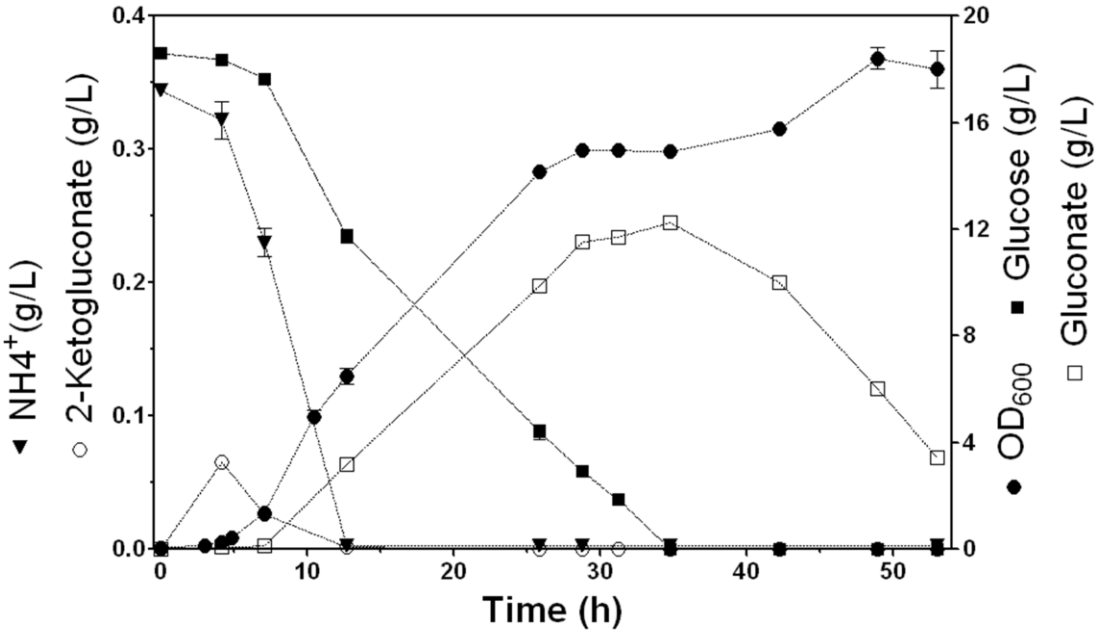

Figure 1. Growth of *P. putida* KT2440 on glucose under PHA-producing conditions.

4.4.3 *In silico* flux design for superior PHA production

The model-driven strain design on basis of these elementary modes was now focused to reflect the actual physiology of the parent strain considered the actually occurring substrates and products of the wild-type based process. To this end, a careful selection of a subset of modes from the total data set was performed. On basis of the obtained cultivation data (Figure 1), we decided to only including modes with simultaneous production of PHA and gluconate, whereas biomass formation was left optional due to the intentionally introduced growth limitation by ammonium. The further pathway analysis therefore focused on a selected set of 54 modes, representing the metabolic state that was most close to the observed production characteristics of the wild type. These modes were now screened for promising genetic targets via flux correlation coefficients between the target reaction towards PHA and all other individual reactions through the network. As illustrated in Figure 2, numerous reactions in the entire network had substantial impact on PHA production. Several reactions exhibited negative flux correlation coefficients and obviously competed with the production, whereas other showed positive correlation and were found supportive. By the concept and algorithm of FluxDesign, this information could be translated and visualized as priority ranked list of deletion, attenuation and amplification target (Melzer et al., 2009; Driouch et al., 2012). Most strikingly, glucose dehydrogenase in the periplasm was predicted as deletion target with the highest priority with regard to PHA production (Figure 2). Glucose 6-phosphate isomerase was predicted as important deletion target. A negative influence was also predicted for the TCA cycle, obviously withdrawing the polymer precursor acetyl-CoA. Selected reactions were found beneficial for PHA synthesis. This was most pronounced for glucose 6-phosphate dehydrogenase, identifying the G6P node as key switch point for rational strain engineering. In addition, pyruvate dehydrogenase appeared as promising amplification target, probably in line with its supply of acetyl-CoA, as also true for all reactions downstream of glyceraldehyde 3-phosphate that lead to this precursor.

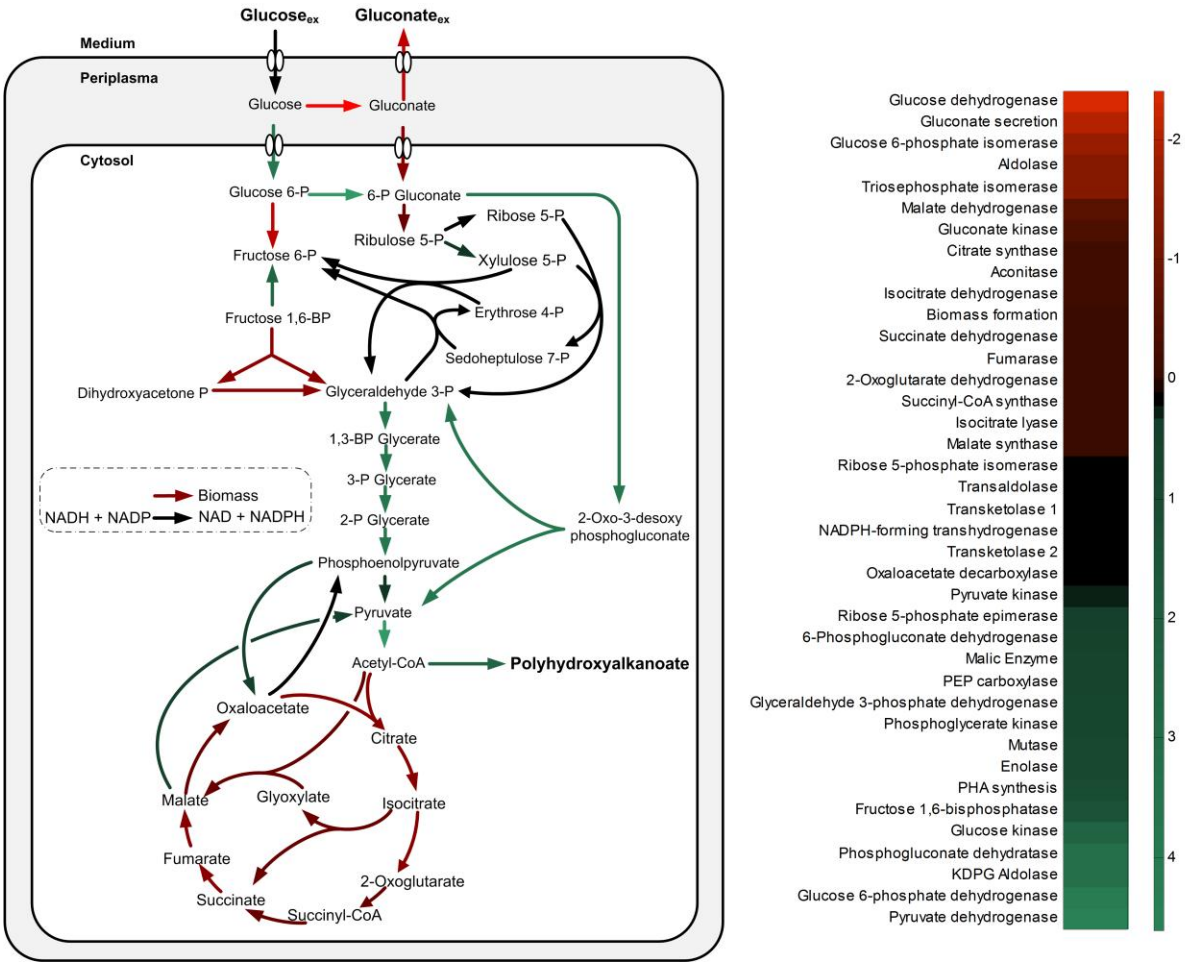

Figure 2. In silico driven metabolic engineering for the prediction of targets towards optimized production of PHA in *Pseudomonas putida*. Pathway correlations were determined from calculated elementary modes and are indicated in green (positive correlation) and red (negative correlation). Reactions with most pronounced correlations represent deletion (red) or amplification (green) targets.

Overall, the model identified glucose dehydrogenase and glucose 6-phosphate dehydrogenase as two key targets for PHA production. The flux of glucose dehydrogenase, linked to gluconate secretion, was negatively coupled to PHA production efficiency, probably due to the competition for carbon (Figure 4 A). An elevated polymer synthesis can be only realized at low or diminished flux through this reaction. The opposite is true for the glucose 6-phosphate dehydrogenase flux. In all the modes, the flux through this reaction obviously supports superior PHA production (Figure 4 B). Based on Flux Design, selected mutants were generated. The deletion strain *P. putida* KT2440 Δ*gcd* that lacked glucose dehydrogenase

aimed at superior PHA production as predicted by the model. In addition, the mutant *P. putida* KT2440 Δ*pgl*, deficient in the PHA supporting pathway via glucose 6-phosphate dehydrogenase, served as interesting and relevant proof-of-concept for the model-based approach. Both mutants did not contain any foreign DNA, which is desirable regarding industrial application due to the non-use of antibiotic markers (Poblete-Castro et al., 2012a).

4.4.4 Construction and evaluation of PHA-producing capacity of different metabolically enginnered *P. putida* strains

The novel strains were first evaluated in batch-flask experiments under PHA-producing conditions. Most beautifully, the design-based strain *P. putida* KT2440 Δ*gcd* revealed a 60 % increase in the final PHA concentration as compared to the parent strain (Figure 2). In line, also the PHA yield of 0.10 g (glucose)$^{-1}$ was substantially higher upon the elimination of *gcd*, thus having an excellent match with the *in silico* prediction. It was also interesting to see that the deletion of *pgl* strongly reduced the PHA formation by almost 50 %, which also nicely matched with the *in silico* design (Figures 3 and 4 B). Cell dry weight as well as PHA synthesis dropped by almost by 50% as compared to the wild type strain (Figure 3). Recently, genome-scale modeling of *P. putida* KT2440 (iJP815) (Puchalka et al., 2008), along with the OptKnock approach (Burgard et al., 2003), predicted that a double mutation (*pgl* and *gcd* genes) in *P. putida* KT2440 would increase PHA production. In contrast Flux Design suggested that only *gcd* should be deleted, whereas *pgl* was identified as important reaction to be amplified. This was also tested in the present work by construction of the double deletion strain *P. putida* KT2440 Δ*gcd-pgl* (see material and methods) and its evaluation for PHA-synthesis. The Δ*gcd-pgl* strain synthesized slightly more PHA than the wild type, but was less efficient than the single mutant *P. putida* KT2440 Δ*gcd* (Figure 3).

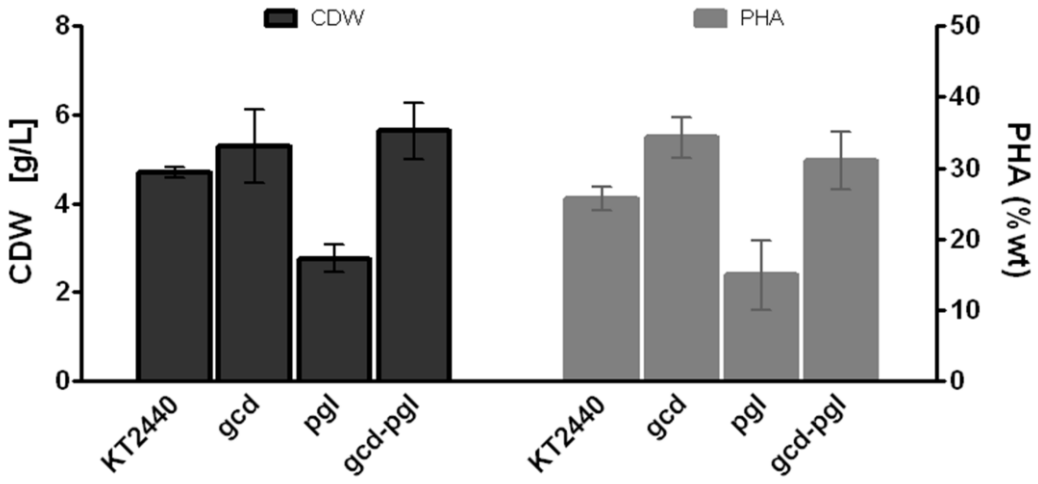

Figure 3. Cell dry weight and PHA content (% wt) of the wild type *P. putida* KT2440 and the deletion mutants *P. putida* KT2440 Δ*gcd*, Δ*pgl*, Δ*gcd-pgl*.

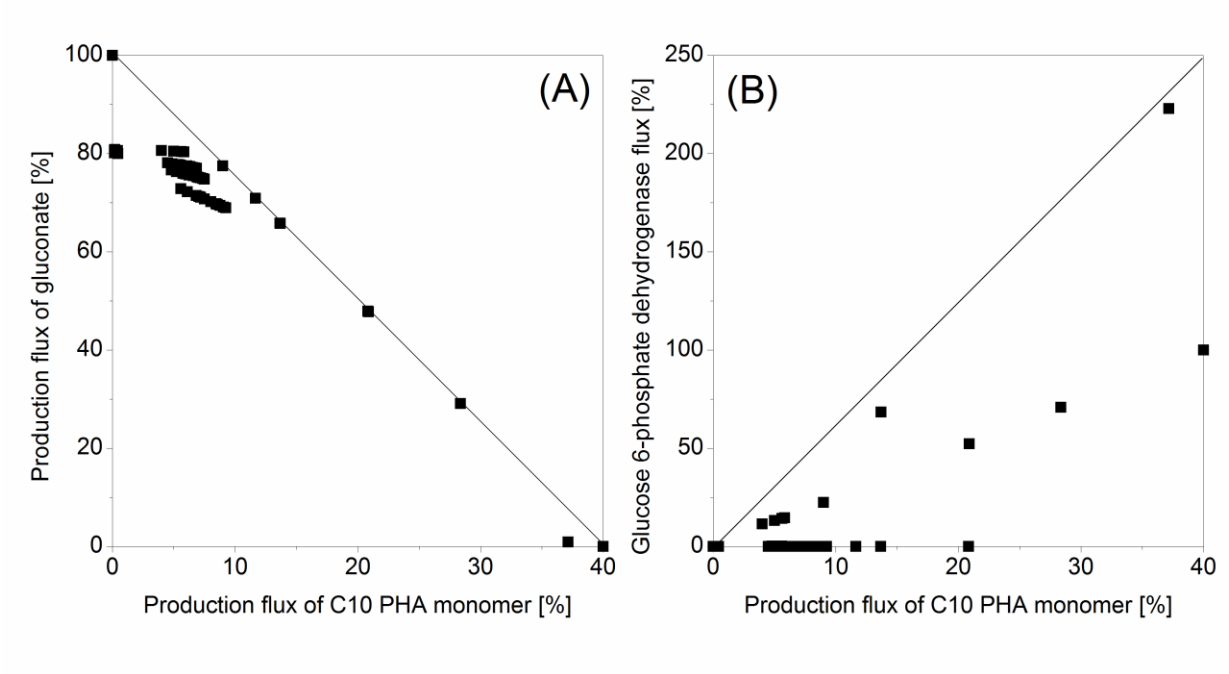

Figure 4. Metabolic pathway correlation of PHA production and (A) gluconate production or (B) glucose 6-phosphate dehydrogenase flux. Negative correlation for gluconate secretion indicates gluconate synthesis as promising deletion target for improved production. Contrarily, positive correlation for the glucose 6-phosphate dehydrogenase flux suggests amplification of the encoding gene. Data are given as relative molar fluxes normalized to the substrate influx.

4.4.5 Transcriptome profiling of the designed producing strains P. putida Δ*gcd* and *Δgcd-pgl*

To study the response of the complex glucose metabolism from a more global perspective, gene expression of the superior single mutant *P. putida* Δ*gcd* and the double mutant *P. putida* Δ*gcd-pgl* was compared to the parent wild type. Four biological replicates each were used for the analysis. Remarkably, both over-producing strains exhibited a rather unaffected expression of genes in the central metabolic pathways (Table 3). The network of *P. putida* thus seemed capable to fully redirect the fluxes towards the desirable compounds via the enzymatic set available, reflecting a high versatility. Concerning the PHA biosynthetic pathway, the ORFs PP5008 and PP5007, encoding for the phasin enzymes PhaI and PhaF, respectively, were up-regulated, whereas the other genes were unaffected. Overall, only 34 genes were differentially expressed (Table 2). More than 50% of the genes were hypothetical proteins (COG classification), whereas genes with known function belonged to energy metabolism, cell envelope, regulatory function, PHA metabolism, and transport and binding proteins (Table 2 and 3). The *lrgA* and *lrgB* genes were down regulated most (Table 2). Although their function is not fully understood, it is proposed that they act against cell death and lysis (Yamaguchi et al., 2011). The oxidative phosphorylation system, which provides the ATP, exhibited two genes with a lower transcript level (PP4650 and PP4651) relative to KT2440 (Table 2). Interestingly, Δ*gcd* also showed an up-regulation 3-hydroxybutyrate dehydrogenase (encoded by PP3073), which yields 3-hydroxybutyrate. One of the most important regulators for glucose metabolism, PtxS (encoded by PP3380), was found to be down-regulated.

Table 2. Genes differentially expressed in the metabolically engineered strains as compared to the wild type *Pseudomonas putida* KT2440.

Cellular role category	Locus tag	Description	Fold change	
			Δ*gcd*	Δ*gcd-pgl*
Energy metabolism				
	PP4650	Cytochrome *d* ubiquinol oxidase subunit II	-5.0	-1.4*
	PP4651	Ubiquinol oxidase subunit II	-3.8	-1.7*
	PP4655	Protocatechuate 3,4-dioxygenase	-4.1	-13.7*
	PP1444	Glucose dehydrogenase	-2.3	-2.9
	PP3161	Benzoate dioxygenase, alpha subunit	-2.2	-2.1
	PP5270	D-amino acid dehydrogenase	-2.0	-1.6
	PP1023	6-phosphogluconolactonase	-1.4	-3.8
	PP4666	3-hydroxybutyrate dehydrogenase	3.3	1.0
	PP4667	Methylmalonate dehydrogenase	3.6	1.1
Regulatory function				
	PP2695	LysR family transcriptional regulator	-4.7	-13.3
	PP3380	PtxS family transcriptional regulator	-2.2	-1.9*
Cell envelope				
	PP4626	LrgA family protein	-7.4	-2.9
	PP4625	LrgB family protein	-4.5	-3.4
	PP1185	Outer membrane protein H1	-1.9*	-2.2
Transport and binding proteins				
	PP0057	major facilitator family transporter	2.3	1.6
	PP1400	major facilitator superfamily (MFS)	2.4	1.3

* *p*-value > 0.05

Table 3. Expression profile of genes belonging to PHA biosynthesis and central metabolic pathways in the metabolically engineered strains as compared to wild type *Pseudomonas putida* KT2440.

Gene name	Locus tag	Description	Fold change	
			Δ*gcd*	Δ*gcd-pgl*
PHA synthesis				
phaI	PP5008	PHA granule-associated	2.4	1.7
phaF	PP5007	PHA granule-associated	2.5	1.6
phaC1	PP5003	PHA polymerase	1.4	1.4
phaC2	PP5005	PHA polymerase	1.1	1.0
phaZ	PP5004	PHA depolymerase	1.1	1.0
phaD	PP5006	Transcriptional regulator	1.3	1.2
phaG	PP1408	Acyl-transferase	1.5	*2.0
bdhA	PP3073	3-hydroxybutyrate dehydrogenase	2.0	1.2
Glycolysis/gluconeogenesis				
glk	PP1011	Glucokinase	-1.4	1.0
pgi	PP1808	Glucose-6-phosphate isomerase	1.1	1.0
fbp	PP5040	Fructose-1,6-bisphosphatase	1.1	1.1
fda	PP4960	Fructose-1,6-bisphosphate aldolase	1.0	1.0
tpiA	PP4715	Triosephosphate isomerase	-1.0	-1.0
gap1	PP1009	GAP dehydrogenase, type I	-1.1	-0.9
gap2	PP2149	GAP dehydrogenase, type II	1.0	-1.1
pgk	PP4963	Phosphoglycerate kinase	-1.0	-1.1
pgm	PP5056	Phosphoglyceromutase	1.0	1.1
eno	PP1612	Phosphopyruvate hydratase	-1.1	1.0
pyk	PP1362	Pyruvate kinase	-1.2	-1.5
Pentose phosphate pathways				
zwf1	PP1022	G6P dehydrogenase	-1.3	-0.7
zwf2	PP4042		-1.0	-1.0
zwf3	PP5351		1.0	1.1
gnd	PP4043	6-phosphogluconate dehydrogenase	-1.0	-1.0
gnuK	PP3416	Carbohydrate kinase	-1.1	-1.0

kguK	PP3378	Dehydroglucokinase	-1.5	-1.5
kguD	PP3376	2-Ketogluconate 6-phosphate reductase	-1.2	-1.2
rpiA	PP5150	Ribose-5-phosphate isomerase A	1.0	1.0
rpe	PP0415	Ribulose-phosphate 3-epimerase	1.0	-1.1
tktA	PP4965	Transketolase	1.0	-1.0
tal	PP2168	Transaldolase B	-1.2	-1.2
Entner-Doudoroff pathway				
edd	PP1010	6-Phosphogluconate dehydratase	1.4	1.0
eda	PP1024	KDPG aldolase	-1.7	-1.3
Pyruvate metabolism				
acoA	PP0555	Pyruvate dehydrogenase	1.0	1.0
	PP0545	Aldehyde dehydrogenase	1.2	1.1
acsA	PP4487	Acetyl-CoA synthetase	-1.0	-1.0
accC-2	PP5347	Pyruvate carboxylase	-1.3	1.0
ppsA	PP2082	Phosphoenolpyruvate synthase	-1.1	-1.1
ppc	PP1505	Phosphoenolpyruvate carboxylase	-1.0	1.1
TCA cycle				
gltA	PP4194	Citrate synthase	-1.0	1.1
acnA	PP2112	Aconitate hydratase	1.1	1.1
acnB	PP2339	Aconitate hydratase	-1.2	-1.1
icd	PP4011	Isocitrate dehydrogenase	1.0	1.1
sucA	PP4189	2-Oxoglutarate dehydrogenase	-1.1	-1.2
sucD	PP4185	Succinyl-CoA synthetase sub alpha	1.1	1.1
sucC	PP4186	Succinyl-CoA synthetase sub beta	1.0	1.1
sdh	PP4191	Succinate dehydrogenase	-1.3	-1.5
fumC	PP0944	Fumarate hydratase	-1.0	1.0
mdh	PP0654	Malate dehydrogenase	1.0	1.1
Glyoxylate shunt				
aceA	PP4116	Isocitrate lyase	1.3	1.1
glcB	PP356	Malate synthase	1.0	1.1

* *p*-value > 0.05

4.4.6 Evaluation of the designed PHA hyper-producer *P. putida* Δ*gcd* in batch bioreactors

It was now important to validate the potential for medium chain length PHA production of the designed strains in a sophisticated process environment in bioreactors that allowed controlling the process settings more precisely than it was possible in the initial shake flask studies (Figure 3). The culture profile of the parent strain *P. putida* KT2440 on glucose as the sole carbon and energy source is given in Figure 5 A. During the initial period of about 12-15 h, glucose and ammonium were depleted, which as accompanied by accumulation of gluconate. During this phase, the strain had a specific growth rate of 0.53 h^{-1} (Table 4 A). The PHA level began to increase, after ammonium was exhausted, and continuously increased up to a final value of 0.88 g L^{-1}. At the final stage of the process, the cells consisted of about 25 % of the polymer (Table 4 B). Gluconate and 2-ketogluconate were detected as by-products in the fermentation broth. The designer mutant, *P. putida* KT2440 Δ*gcd*, revealed a much higher synthesis of the desired polymer (Figure 5 B). The final PHA titer was 1.76 g L^{-1} and thus 100 % higher as compared to the parent strain. At the same time, also the cellular PHA content was substantially increased to more than 35 %, resulting in an almost doubled polymer yield (Tables 4 A and B). The deletion of glucose dehydrogenase did not substantially affect the value of μ_{max}, since the cells still grew rather fast (Table 4 A, Figure 5 B). Synthesis of both organic acids was completely abolished, which obviously supported the redirection of carbon to anabolism and PHA biosynthesis. The monomer composition of the produced PHAs did not differ significantly between the strains (Table 5). The major monomer was 3-hydroxy-decanoate (C_{10}), accounting for a fraction of more than 70%. In addition, also larger monomers up to C_{14} were incorporated.

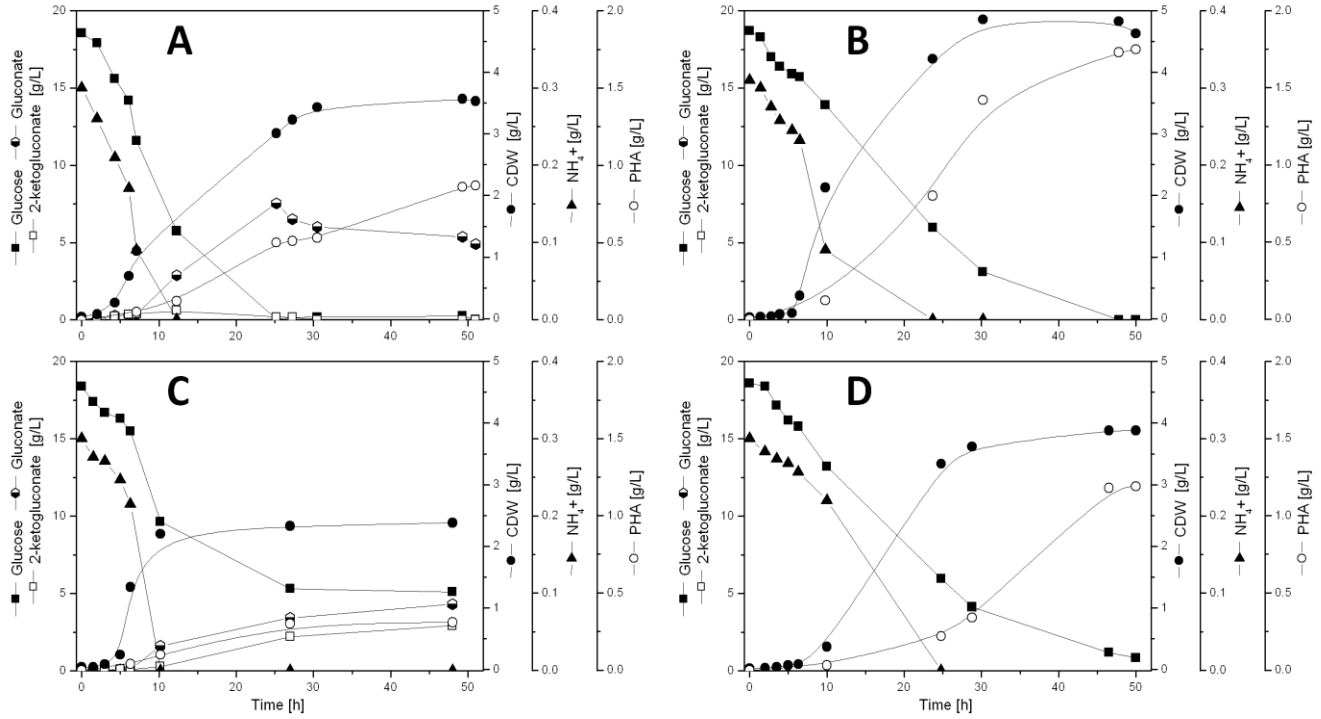

Figure 5. Growth and PHA production of the parent wild type *P. putida* KT2440 (A), and the deletion mutants *P. putida* KT2440 Δ*gcd* (B), Δ*pgl* (C), Δ*gcd-pgl* (D). Cells were grown in lab scale bioreactors containing minimal medium with 18.5 g L^{-1} glucose as carbon source. All data reflect the mean from two parallel cultivations.

Table 4 A. Physiological parameters of the wild type *P. putida* KT2440 and different metabolically engineered strains in batch cultures on glucose. All data reflect the mean and standard deviation from two parallel bioreactor cultivations (see Figure 5).

		KT2440	Δ*gcd*	Δ*pgl*	Δ*gcd-pgl*
μ_{max}	(h^{-1})	0.53 ± 0.02	0.45 ± 0.01	0.28 ± 0.01	0.31 ± 0.00
$Y_{X/S}$§	(g/g)	0.19 ± 0.04	0.25 ± 0.02	0.17 ± 0.02	0.21 ± 0.01
$Y_{Xr/S}$¤	(g/g)	0.14 ± 0.04	0.15 ± 0.02	0.15 ± 0.02	0.15 ± 0.00
$Y_{PHA/S}$	(g/g)	0.05 ± 0.00	0.09 ± 0.00	0.02 ± 0.04	0.06 ± 0.01

§Total cell dry weight yield on glucose.

¤Residual biomass yield on glucose.

Table 4 B. Final concentration of biomass (CDW), PHA, and secreted organic acids of the wild type *P. putida* KT2440 and different metabolically engineered strains in batch cultures on glucose. In addition, the PHA content of the cells is given. All data reflect the mean and standard deviation from two parallel bioreactor cultivations (see Figure 5) and the end of the process after 50 h.

	KT2440	Δ*gcd*	Δ*pgl*	Δ*gcd-pgl*
CDW (g/L)	3.6 ± 0.7	4.6 ± 0.3	2.4 ± 0.3	3.9 ± 0.3
PHA (wt%)	25.4 ± 0.9	38.0 ± 2.5	12.9 ± 3.3	29.5 ± 3.0
PHA (g/L)	0.9 ± 0.0	1.8 ± 0.0	0.3 ± 0.0	1.2 ± 0.2
Gluconate (g/L)	4.4 ± 0.3	n.d.	4.7 ± 0.2	n.d.
2-Ketogluconate(g/L)	n.d.	n.d.	2.8 ± 1.0	n.d.

n.d.: not detected, less than 0.05 g L^{-1}

4.4.7 Characteristics of *P. putida* strains deficient in 6-phosphoglucolactonase

The PPP enzyme 6-phosphoglucolactonase was deleted to test the model-based prediction that it is crucial for enhanced PHA production. The growth and production behavior of the corresponding deletion strain *P. putida* KT2440 Δ*gcd* fully confirmed this prediction (Figure 5 C). The growth of the mutant was significantly retarded (Table 4 A). Moreover, PHA production was reduced almost 100 % as compared to the wild type. In contrast, the deletion enhanced the final concentrations of the by-products gluconate and 2-ketogluconate in the process, which accumulated to high amounts, but obviously could not be re-utilized by the strain during the later process stages. The negative effects of the deletion of 6-phosphoglucolactonase were also obvious in the double mutant *P. putida* KT2440 Δ*gcd-pgl* (Figure 5 D). In terms of PHA production is was slightly better than the parent wild type, but by far did not reach the performance of the FluxDesign strain.

Table 5. Monomer composition of medium chain length PHA produced by metabolically engineered *P. putida* strains in bioreactors. The data were determined by GC/MS and are given as relative molar fraction (%) of C6: 3-hydroxyexanoate, C8: 3-hydroxyoctanoate, C10:3-hydroxydecanoate, C12: 3-hydroxydodecanoate, C12:1: 3-hydroxy-5-cis-dodecanoate, and C14: 3-hydroxytetradecanoate.

Strain	C6	C8	C10	C12	C12:1	C14
KT2440	n.d.	11.8 ± 0.2	73.0 ± 0.1	4.7 ± 0.2	9.4 ± 0.7	0.8 ± 0.3
Δ*gcd*	n.d.	14.0 ± 0.4	71.1 ± 0.8	4.6 ± 0.9	8.5 ± 0.4	1.1 ± 0.2
Δ*pgl*	n.d	8.6 ± 0.2	74.2 ± 1.0	4.8 ± 0.4	8.1± 0.7	6.5 ± 0.0
Δ*gcd-pgl*	n.d	12.2 ± 0.3	72.4 ± 0.6	5.3 ± 0.2	9.3 ± 0.1	0.8 ± 0.1

n.d. : not detected, less than 0.2%.

4.5 Discussion

Pseudomonas putida and related species are known as natural producers of medium chain length PHAs, a promising sustainable substitute of oil-based plastics. Over more than three decades, *P. putida* has been investigated as a model strain for PHA production. Excellent studies have elucidated pathway organization (Huijberts et al., 1992; Rehm et al., 1998) and regulation of the PHA machinery (de Eugenio et al., 2010b) and of PHA granule formation (Galan et al., 2011; Prieto et al., 2007). These were complemented by the development of polymers with improved properties (Hartmann et al., 2004; Liu et al., 2011) and the increase of the total accumulation of these polyesters (Poblete-Castro et al., 2012b; Sun et al., 2009). With regard to the last point, fatty acids have been the most used carbon source, since they promote rapid and high accumulation of the biopolymer. Metabolic engineering of genes belonging to the β-oxidation pathway has led to an increased accumulation of PHAs in comparison to the wild-type strain (Ouyang et al., 2007). Nevertheless, the still low PHA volumetric productivity by the metabolically engineered strains along with the high cost associated to the use of fatty acids limits the competiveness of such strains against established petroleum-based plastic production processes. In this regard, the use of

low cost sugars such as glucose - the carbon source of choice in industrial biotechnology (Straathof et al., 2002) - would open a new avenue to compete against petrochemical plastics.

In this work, we generated a metabolically engineered *P. putida* strain, which showed superior PHA accumulation. To achieve desirable features of the PHA-producer strain, we used a metabolic model and the FluxDesign framework to identify target genes to enhance the synthesis of medium chain length PHAs in *P. putida* KT2440 on glucose. With full consideration of network stoichiometry, glucose dehydrogenase (encoded by PP1444, *gcd*) was predicted as target with highest priority to be deleted for increased PHA synthesis (Figure 3), although the predicted mutation point seemed far away from the biosynthetic PHA pathway. The mutant *P. putida* KT2440 Δ*gcd* indeed showed superior production performance. Already in shake flask tests, the PHA content of the cells increased by 60 % as compared to the parent strain (Figure 2), whereby no more by-products were secreted. The industrial production performance was then assessed by well-controlled bioreactor fermentations. This further increased the PHA titer of the designed strain, *P. putida* KT2440 Δ*gcd* (Table 5 and Figure 5 A). Here, the single deletion of *gcd* allowed a remarkable increase of the PHA concentration of 100% as compared to KT2440 (Figure 5, Table 5). It is important to note that the deletion strain could almost maintain growth rate of the wild type strain (Table 4), a crucial feature, since this value will finally affect the total PHA volumetric productivity.

More than one decade ago, previous metabolic engineering of *P. putida* KT2442 was based on inactivating the enzyme isocitrate lyase (ICL) which consumes the main PHA precursor acetyl-CoA (Klinke et al., 2000). That obtained mutant strain (KT217) grew to a maximum specific growth rate of 0.25 h^{-1} and showed a PHA content of 0.34 g L^{-1} (Klinke et al., 2000). Those values are far below that of the novel over-producer strain *P. putida* KT2440 Δ*gcd,* which grows almost twice as fast and accumulates about 5-fold more PHA than KT217. It is interesting to note that the elimination of the glyoxylate shunt was also predicted by the model-based design, however, at a much reduced priority (Figure 2), which might explain the relatively weak improvement observed previously. The predictive

power of the model could be also verified by the second tested mutant strain (Δ*pgl*). The simulations in Figure 2 show that glucose 6-phosphate dehydrogenase (*pgl*), supplying 6-phosphogluconate (Daddaoua et al., 2010; del Castillo et al., 2007), should be amplified to redirect metabolic fluxes to PHA formation. Deleting this gene resulted in poor PHA production (Table 5 and Fig 4, 5C), but rather stimulated the secretion of gluconate and 2-ketogluconate at high concentration (Figure 5C), reducing carbon availability for biomass and PHA synthesis.

The generated double mutant (Δ*gcd-pgl*) synthesized slightly more PHA than KT2440, but suffered from weak growth. This indicates the basic potential of using genome-scale metabolic reconstruction models to enhance PHA production in *P. putida* (Puchalka et al., 2008), although this approach failed to predict the single gene deletion as most promising and even suggested to disrupt the obviously rather important 6-phospho-glucolactonase. One of the main reasons for the suboptimal outcome seems that the previous genome-scale model approximated PHA production by supply of its precursor acetyl-CoA. This neglected NADPH required for assembling the acetyl-CoA units into the building blocks of the polymer the long chain acyl units. Indeed, the two entry reactions into the PPP, predicted as amplification targets, supply NADPH, which is probably the major reason for their high importance. The full consideration of stoichiometry for the finally obtained product, as done here, seems therefore crucial in model-based design.

With regard to transcriptional regulation, LysR and PtxS showed reduced expression levels (Table 2). Recent studies revealed that PtxS controls the expression of the enzyme for oxidation of gluconate to 2-ketogluconate, its transport (del Castillo et al., 2008), and the compartmentalization of glucose metabolism in *P. putida* KT2440 (Daddaoua et al., 2010). Most likely due to the lack of carbon through the periplasm oxidation pathway in both mutants that lacked glucose dehydrogenase, this regulator was no longer active. LysR belongs to the largest family of transcriptional regulators in bacteria (Tropel and van der Meer, 2004). Nevertheless, we could not associate it to any specific pathway, although, operons from the benzoate pathway are under control of LysR-type regulators such as CatR and BenR (Cowles et

al., 2000; Rothmel et al., 1990). Concerning energy metabolism, the expression of genes belonging to the cytochrome ubiquinol oxidase in *P. putida* KT2442 were found to be up-regulated under high PHA-accumulating condition (Poblete-Castro et al., 2012b). This effect was because - as PHA is an energy-storage compound - the cell reorganizes the terminal oxidase accordingly, in order to generate enough ATP molecules for biomass and maintenance requirements. In this study, the repression of the cytochrome bd complex (PP4650-4651) (Table 2), could be assigned to normal operation of the cytochrome bo which is more effective in proton-pumping oxidase than bd, and thus better conserves the energy that is produced at the respiratory electron transport (D'mello et al., 1996). The phasin enzymes where the highest among expression levels of genes belonging to PHA metabolism (Table 2), as also previously reported (Poblete-Castro et al., 2012b) This confirms that these enzymes play a very important role in PHA formation not only when fatty acids are supplied as carbon source, but also in the presence of glucose. Interestingly, 3-hydroxybutyrate dehydrogenase (encoded by PP3073) was up-regulated in the single mutant strain. It has been shown by several reports that *P. putida* KT2442 cannot incorporate the monomer 3-hydroxybutyrate in the final monomer composition e.g. 3-hydroxydecanoate-co-3-hydroxyoctanoate, due to the specificity of PhaC synthase for monomers containing at least six carbon atoms in their chemical structure (Kessler and Witholt, 2001; Steinbüchel and Lutke-Eversloh, 2003). Thereby is seems a good target for increasing the available carbon for PHA synthesis.

4.6 Conclusion

The present work describes the successful application of *in silico* driven systems metabolic engineering to biopolymer over-production. The tailored approach allowed an almost doubled production performance by only one single gene deletion, apparently located in the metabolic network far away from the biosynthetic PHA chain, which had been the major focus of research in the past. The computational predictions from the systems-wide design strategy thus seem a nice complementation to be integrated with previous metabolic engineering of the terminal biosynthetic chain (Liu et al., 2011) to further

generating improved biocatalysts for enhanced synthesis of medium chain length PHAs. The excellent performance of the designed strain visualizes the truly predictive power of design-based systems metabolic engineering that integrates the full stoichiometry of the pathway repertoire for strain engineering. It will interesting to evaluate the potential of the generated hyper-producer strains in high cell density fed-batch processes to exploit their production capacity and further close the gap between synthetic and bio-based plastic production. So far only a few examples have really managed to successfully translate model-based predictions to direct strain engineering on a global scale, examples being succinate (Lee et al., 2006), 1,4 butandiol (Yim et al., 2011), sequipertenes (Asadollahi et al., 2009), bio-ethanol (Bro et al., 2006), and amino acids (Becker et al., 2011). However, we can expect that this powerful concept of design-based systems metabolic will be recruited far more in the future for the synthesis of valuable products.

4.7 Acknowledgments

All authors thank Bianka Karge for the excellent technical assistance during the construction of the plasmids and Yvonne Göcke for excellent support during HPLC analysis. Ignacio Poblete-Castro and Vitor Martins dos Santos acknowledge financial support by the German Federal Ministry of Education (BMBF) via the project “PSysMo” (FKZ 0313980) within the ERA-NET initiative “Systems Biology of Microorganisms” as well as the EU-FP7 project “Microme”. Christoph Wittmann and Judith Becker kindly acknowledge support by the German Federal Ministry of Education (BMBF) via the project “Systems biology of Pseudomonas and other uropathogenic bacteria” (FKZ 0315833D). André L. Rodrigues gratefully acknowledges financial support by the German Academic Exchange Service (A-08-71658) and by the Max-Buchner Foundation (Nr. 2924).

4.8 References

Asadollahi, M. A., et al., 2009. Enhancing sesquiterpene production in *Saccharomyces cerevisiae* through in silico driven metabolic engineering. Metabolic Engineering. 11**,** 328-334.

Bagdasarian, M., et al., 1981. Specific-purpose plasmid cloning vectors. II. Broad host range, high copy number, RSF 1010-derived vectors, and a host-vector system for gene cloning in Pseudomonas. Gene. 16**,** 237-247.

Becker, J., et al., 2011. From zero to hero - Design-based systems metabolic engineering of *Corynebacterium glutamicum* for l-lysine production. Metabolic Engineering. 13**,** 159-168.

Bro, C., et al., 2006. In silico aided metabolic engineering of *Saccharomyces cerevisiae* for improved bioethanol production. Metabolic Engineering. 8**,** 102-111.

Burgard, A. P., et al., 2003. Optknock: A bilevel programming framework for identifying gene knockout strategies for microbial strain optimization. Biotechnology and Bioengineering. 84**,** 647-657.

Chen, G.-Q., 2009. A microbial polyhydroxyalkanoates (PHA) based bio- and materials industry. Chemical Society Reviews. 38.

Chen, G.-Q., Wu, Q., 2005. Microbial production and applications of chiral hydroxyalkanoates. Applied Microbiology and Biotechnology. 67**,** 592-599.

Cowles, C. E., et al., 2000. BenR, a XylS Homologue, Regulates Three Different Pathways of Aromatic Acid Degradation in *Pseudomonas putida*. Journal of Bacteriology. 182**,** 6339-6346.

D'mello, R., et al., 1996. The cytochrome bd quinol oxidase in *Escherichia coli* has an extremely high oxygen affinity and two oxygen-binding haems: implications for regulation of activity in vivo by oxygen inhibition. Microbiology. 142**,** 755-763.

Daddaoua, A., et al., 2010. Compartmentalized Glucose Metabolism in *Pseudomonas putida* Is Controlled by the PtxS Repressor. Journal of Bacteriology. 192**,** 4357-4366.

de Eugenio, L. I., et al., 2010a. The turnover of medium-chain-length polyhydroxyalkanoates in *Pseudomonas putida* KT2442 and the fundamental role of PhaZ depolymerase for the metabolic balance. Environmental Microbiology. 12**,** 207-221.

de Eugenio, L. I., et al., 2010b. The PhaD regulator controls the simultaneous expression of the pha genes involved in polyhydroxyalkanoate metabolism and turnover in *Pseudomonas putida* KT2442. Environmental Microbiology. 12**,** 1591-1603.

de Lorenzo, V., Timmis, K. N., 1994. Analysis and construction of stable phenotypes in gram-negative bacteria with Tn5- and Tn10-derived minitransposons. Methods in Enzymology. 235**,** 386-405.

del Castillo, T., et al., 2008. A Set of Activators and Repressors Control Peripheral Glucose Pathways in *Pseudomonas putida* To Yield a Common Central Intermediate. Journal of Bacteriology. 190**,** 2331-2339.

del Castillo, T., et al., 2007. Convergent peripheral pathways catalyze initial glucose catabolism in *Pseudomonas putida*: Genomic and flux analysis. Journal of Bacteriology. 189**,** 5142-5152.

Driouch, H., et al., 2012. Integration of in vivo and in silico metabolic fluxes for improvement of recombinant protein production. Metabolic Engineering. 14**,** 47-58.

Galan, B., et al., 2011. Nucleoid-associated PhaF phasin drives intracellular location and segregation of polyhydroxyalkanoate granules in *Pseudomonas putida* KT2442. Molecular Microbiology. 79**,** 402-418.

Grage, K., et al., 2009. Bacterial Polyhydroxyalkanoate Granules: Biogenesis, Structure, and Potential Use as Nano-/Micro-Beads in Biotechnological and Biomedical Applications. Biomacromolecules. 10**,** 660-669.

Hartmann, R., et al., 2004. Tailored Biosynthesis of Olefinic Medium-Chain-Length Poly[(R)-3-hydroxyalkanoates] in *Pseudomonas putida* GPo1 with Improved Thermal Properties. Macromolecules. 37**,** 6780-6785.

Herrero, M., et al., 1990. Transposon vectors containing non-antibiotic resistance selection markers for cloning and stable chromosomal insertion of foreign genes in gram-negative bacteria. Journal of Bacteriology. 172**,** 6557-6567.

Huber, W., et al., 2002. Variance stabilization applied to microarray data calibration and to the quantification of differential expression. Bioinformatics. 18**,** S96-S104.

Huijberts, G. N. M., et al., 1992. *Pseudomonas putida* KT2442 cultivated on glucose accumulates poly(3-hydroxyalkanoates) consisting of saturated and unsaturated monomers. Applied and Environmental Microbiology. 58**,** 536-544.

Kauffmann, A., et al., 2009. arrayQualityMetrics - A bioconductor package for quality assessment of microarray data. Bioinformatics. 25**,** 415-416.

Kellerhals, M. B., et al., 2000. Renewable Long-Chain Fatty Acids for Production of Biodegradable Medium-Chain-Length Polyhydroxyalkanoates (mcl-PHAs) at Laboratory and Pilot Plant Scales. Macromolecules. 33**,** 4690-4698.

Kessler, B., Witholt, B., 2001. Factors involved in the regulatory network of polyhydroxyalkanoate metabolism. Journal of Biotechnology. 86**,** 97-104.

Kim, D. Y., et al., 2007. Biosynthesis, modification, and biodegradation of bacterial medium-chain-length polyhydroxyalkanoates. Journal of Microbiology. 45**,** 87-97.

Klinke, S., et al., 2000. Inactivation of isocitrate lyase leads to increased production of medium-chain-length poly(3-hydroxyalkanoates) in *Pseudomonas putida*. Applied and Environmental Microbiology. 66**,** 909-913.

Lee, S. J., et al., 2006. Genome-Based Metabolic Engineering of *Mannheimia succiniciproducens* for Succinic Acid Production. Applied and Environmental Microbiology. 72**,** 1939-1948.

Liu, Q., et al., 2011. Biosynthesis of poly(3-hydroxydecanoate) and 3-hydroxydodecanoate dominating polyhydroxyalkanoates by β-oxidation pathway inhibited *Pseudomonas putida*. Metabolic Engineering. 13**,** 11-17.

Madison, L. L., Huisman, G. W., 1999. Metabolic engineering of poly(3-hydroxyalkanoates): From DNA to plastic. Microbiology and Molecular Biology Reviews. 63**,** 21-53.

Martinez-Garcia, E., de Lorenzo, V., 2011. Engineering multiple genomic deletions in Gram-negative bacteria: Analysis of the multi-resistant antibiotic profile of *Pseudomonas putida* KT2440. Environmental Microbiology. 13**,** 2702-2716.

Melzer, G., et al., 2009. Flux Design: In silico design of cell factories based on correlation of pathway fluxes to desired properties. BMC Systems Biology. 3**,** 120.

Nelson, K. E., et al., 2002. Complete genome sequence and comparative analysis of the metabolically versatile *Pseudomonas putida* KT2440. Environmental Microbiology. 4**,** 799-808.

Nogales, J., et al., 2008. A genome-scale metabolic reconstruction of *Pseudomonas putida* KT2440: iJN746 as a cell factory. BMC Syst Biol. 2**,** 79.

Ouyang, S. P., et al., 2007. Production of polyhydroxyalkanoates with high 3-hydroxydodecanoate monomer content by fadB anf fadA knockout mutant of *Pseudomonas putida* KT2442. Biomacromolecules. 8**,** 2504-2511.

Park, J. H., et al., 2007. Metabolic engineering of *Escherichia coli* for the production of l-valine based on transcriptome analysis and in silico gene knockout simulation. Proceedings of the National Academy of Sciences. 104**,** 7797-7802.

Poblete-Castro, I., et al., 2012a. Industrial biotechnology of *Pseudomonas putida* and related species. Applied Microbiology and Biotechnology. 93**,** 2279-2290.

Poblete-Castro, I., et al., 2012b. The metabolic response of *P. putida* KT2442 producing high levels of polyhydroxyalkanoates under single- and multiple-nutrient-limited growth: Highlights from a multi-level omics approach. Microbial Cell Factories.

Prieto, M. A., et al., 2007. Synthesis and degradation of polyhydroxyalkanoates. In: Ramos, J.-L., Filloux, A., Eds.), Pseudomonas --- A Model in Systems Biology. vol. 5. Springer, pp. 409-410.

Puchalka, J., et al., 2008. Genome-scale reconstruction and analysis of the *Pseudomonas putida* KT2440 metabolic network facilitates applications in biotechnology. PLoS Comput Biol. 4**,** e1000210.

Regenhardt, D., et al., 2002. Pedigree and taxonomic credentials of *Pseudomonas putida strain* KT2440. Environmental Microbiology. 4**,** 912-915.

Rehm, B. H. A., 2003. Polyester synthases: Natural catalysts for plastics. Biochemical Journal. 376**,** 15-33.

Rehm, B. H. A., 2007. Biogenesis of microbial polyhydroxyalkanoate granules: A platform technology for the production of tailor-made bioparticles. Current Issues in Molecular Biology. 9**,** 41-62.

Rehm, B. H. A., et al., 1998. A new metabolic link between fatty acid de novo synthesis and polyhydroxyalkanoic acid synthesis. The phaG gene from *Pseudomonas putida* KT2440 encodes a 3-hydroxyacyl-acyl carrier protein-coenzyme a transferase. Journal of Biological Chemistry. 273**,** 24044-24051.

Ritchie, M. E., et al., 2007. A comparison of background correction methods for two-colour microarrays. Bioinformatics. 23**,** 2700-2707.

Rothmel, R. K., et al., 1990. Nucleotide sequencing and characterization of *Pseudomonas putida* catR: A positive regulator of the catBC operon is a member of the LysR family. Journal of Bacteriology. 172**,** 922-931.

Ryu, H. W., et al., 1997. Production of poly(3-hydroxybutyrate) by high cell density fed-batch culture of *Alcaligenes eutrophus* with phospate limitation. Biotechnology and Bioengineering. 55**,** 28-32.

Segre, D., et al., 2002. Analysis of optimality in natural and perturbed metabolic networks. Proceedings of the National Academy of Sciences. 99**,** 15112-15117.

Shevchuk, N. A., et al., 2004. Construction of long DNA molecules using long PCR-based fusion of several fragments simultaneously. Nucleic acids research. 32**,** e19.

Smyth, G. K., 2004. Linear models and empirical bayes methods for assessing differential expression in microarray experiments. Statistical Applications in Genetics and Molecular Biology. 3.

Sohn, S. B., et al., 2010. In silico genome-scale metabolic analysis of Pseudomonas putida KT2440 for polyhydroxyalkanoate synthesis, degradation of aromatics and anaerobic survival. Biotechnology Journal. 5**,** 739-750.

Steinbüchel, A., Lutke-Eversloh, T., 2003. Metabolic engineering and pathway construction for biotechnological production of relevant polyhydroxyalkanoates in microorganisms. Biochemical Engineering Journal. 16**,** 81-96.

Straathof, A. J. J., et al., 2002. The production of fine chemicals by biotransformations. Current Opinion in Biotechnology. 13**,** 548-556.

Sun, Z., et al., 2009. Fed-batch production of unsaturated medium-chain-length polyhydroxyalkanoates with controlled composition by *Pseudomonas putida* KT2440. Applied Microbiology and Biotechnology. 82**,** 657-662.

Sun, Z., et al., 2007. Carbon-limited fed-batch production of medium-chain-length polyhydroxyalkanoates from nonanoic acid by *Pseudomonas putida* KT2440. Applied Microbiology and Biotechnology. 74**,** 69-77.

Tang, H., et al., 2011. Genome Sequence of *Pseudomonas putida* Strain B6-2, a Superdegrader of Polycyclic Aromatic Hydrocarbons and Dioxin-Like Compounds. Journal of Bacteriology. 193**,** 6789-6790.

Tao, F., et al., 2011. Genome Sequence of *Pseudomonas putida* Idaho, a Unique Organic-Solvent-Tolerant Bacterium. Journal of Bacteriology. 193**,** 7011-7012.

Tropel, D., van der Meer, J. R., 2004. Bacterial Transcriptional Regulators for Degradation Pathways of Aromatic Compounds. Microbiology and Molecular Biology Reviews. 68**,** 474-500.

Vicente, M., Canovas, J. L., 1973. Glucolysis in Pseudomonas putida: Physiological Role of Alternative Routes from the Analysis of Defective Mutants. Journal of Bacteriology. 116**,** 908-914.

Wang, F., Lee, S. Y., 1997. Poly(3-hydroxybutyrate) production with high productivity and high polymer content by a fed-batch culture of *Alcaligenes latus* under nitrogen limitation. Applied and Environmental Microbiology. 63**,** 3703-3706.

Yamaguchi, M., et al., 2011. Loss of the plastid envelope protein AtLrgB causes spontaneous chlorotic cell death in *Arabidopsis thaliana*. Plant and Cell Physiology.

Yamane, T., 1993. Yield of poly-D(-)-3-hydroxybutyrate from various carbon sources: A theoretical study. Biotechnology and Bioengineering. 41**,** 165-170.

Yim, H., et al., 2011. Metabolic engineering of *Escherichia coli* for direct production of 1,4-butanediol. Nature Chemical Biology. 7**,** 445-452.

Zinn, M., et al., 2001. Occurrence, synthesis and medical application of bacterial polyhydroxyalkanoate. Adv Drug Deliv Rev. 53**,** 5-21.

CHAPTER V. Production of mcl(PHA) in high-cell-density cultures of metabolically engineered *P. putida* strains.

5.1 Abstract

Medium-chain-length polyhydroxyalkanoates mcl(PHAs) have become popular due to their similar properties to petroleum-based plastics, thus opening an alternative-sustainable option to obtain this highly demanded commodity. Nevertheless, the high costs associated with the production process of mcl(PHAs) using fatty acid as the carbon source make them not suitable yet for production at industrial scale. One possibility to address such drawback is the use of sugars as carbon sources. As shown in Chapter 4, we have created a metabolically engineered *P. putida* strain which can accumulate 60% more mcl(PHA) relative to its parental strain KT2440 in the presence of glucose using batch as the cultivation mode. Beyond this, the generated mutant strains were now challenged with the process of choice for industrial biotechnology — the fed-batch process. For the Δ*gcd* mutant and the wild-type strain, the imposed specific growth rate μ [0.25 h^{-1}] worked well, reaching 35 [g/L] of biomass in 15 hours. It was not the case for the double-deletion mutant, which the set μ evoked glucose accumulation during the exponential feeding phase, having a big impact on biomass and PHA synthesis. For the PHA accumulation process, two induction techniques were tested under nitrogen limitation — the substrate-pulse feeding was more efficient than the linear feeding to promote the accumulation of the desirable product within high cell density cultures. The total PHA accumulation was 0.44 and 0.19 [g/L·h] for *P. putida* KT2440 and Δ*gcd*, respectively. Although the mutant strain did not show improved accumulation of PHA in comparison to the wild-type strain, several drawbacks during the fed-batch process were observed for the engineered strain, concluding that the chose feeding-strategy but not its bio-production capacity was the main cause of such PHA accumulation within the process.

5.2 Materials and methods

Strains and growth medium

P. putida KT2440, Δ*gcd* , and Δ*gcd-pgl* mutant strains were used in this study. *P. putida* strains, kept as frozen stocks in 25% glycerol at -80°C, were straigthed in Luria Bertani agar dish plates to obtain single colonies after one day incubation at 30°C. Inocula were prepared by picking up one colony from the plate and inoculating it into a 50 mL shake flask containing 10 mL of the defined minimal medium (M9) consisting of (per liter) 12.8 g $Na_2HPO_4.7H_2O$, 3 g KH_2O_4, 4.7 g $(NH_4)_2SO_4$, 0.5 g NaCl. This medium was autoclaved and subsequently supplemented with 0.12 g of $MgSO_4.H_2O$, trace elements ($mg{\cdot}L^{-1}$): 6.0 $FeSO_4.7H_2O$, 2.7 $CaCO_3$, 2.0 $ZnSO_4.H2O$, 1.16 $MnSO_4.H_2O$, 0.37 $CoSO_4.7H_2O$, 0.33 $CuSO_4.5H_2O$, 0.08 H_3BO_3, and 3 g/L of glucose (all filter-sterilized) as the unique carbon source. The cells were grown under aerobic conditions at 30 °C in an Innova incubator shaker set at 180 rpm. By taking a calculated volume of the overnight-growth cell suspension from the pre-inoculum, 1000 mL baffled Erlenmeyer flasks containing 200 mL of culture medium were inoculated and placed in a rotary shaker under aerobic conditions. This second preculture was used as seed for the Fed-batch process. The starting medium (M9) in the Fed-batch process was supplemented with 3 g/L glucose, 0.12 g/L $MgSO_4.H_2O$, and 8 mL of trace element solution. Nitrogen source was supplied by using 14% (w/v) NH_4OH to control the pH for the batch and exponential feeding phase. For the PHA accumulation phase NH_4OH was replaced by NaOH 10%. Each liter of feeding medium contained 600 g glucose and 12 g $MgSO_4.H_2O$.

Fed-batch cultivations

Fermentations were carried out in a 10 L B10 stirred tank bioreactor (Biologische Verfahrenstechnik, Basel, Switzerland). The starting working volume was 4 L in all experiments. The temperature was controlled at 30°C, and the pH was set at 7.0 by controlled addition of H_2SO_4 (4%) or [NH_4OH or NaOH (see above)]. The dissolved oxygen partial pression (pO_2) was set at 20% by spargeding a mixture of air and pure oxygen at > 0.33 vvm and by adjusting the agitation speed up to 1000 rpm. A gas analyzer

(BlueSense, BCpreFerm, Germany) to record online the concentrations of carbon dioxide and oxygen in the course of the process was coupled to the gas outlet of the bioreactor.

Analytical procedures

Cell dry weight, ammonium, optical density, and PHA concentration were performed as described previously in the materials and methods section 4.3 in Chapter 4.

Calculations

In the C-limitied exponential phase of fed-batch cultures using glucose as the solely carbon source the volumetric feeding rate was calculated using the following equation:

$$F(t) = \left(\frac{\mu_{set}}{Y_{x/s}} + m \right) \frac{V_0 X_0 \cdot e^{\mu_{set}(t-t_0)}}{S_0} \qquad (1)$$

where

F(t) volumetric feeding rate [L/h]

S_0 concentration of the substrate in the feeding solution [g/L]

μ_{set} predetermined specific growth rate [1/h]

$Y_{x/s}$ yield coefficient of biomass from glucose [g/g]

m specific maitenence coefficient [g/g·h]

V_0 initial volume of the bioreactor [L]

X_0 initial biomass concentration [g/L]

t time [h]

5.3 Results

5.3.1 High-cell-density culture of *P. putida* KT2440

To develop a robust carbon-limited fed-batch fermentation process, an exponential feeding strategy was applied which allows setting a constant and a specific growth rate at will (Korz et al. 1995) by using glucose as the growth limiting nutrient. Maintenance and yield coefficients obtained from chemostat cultures (van Duuren 2011) were used to fill Eq. (1). The fermentor was inoculated with cells to reach an OD_{600} of 0.2. After 6 hours the initial glucose concentration [3 g/L] was totally consumed. In that stage (I), *P. putida* KT2440 was growing at a maximum specific growth rate of 0.56 h^{-1}. In the second stage (II), the exponential feeding started with a μ_{set} of 0.25 [h^{-1}]. After 10 hours of feeding, the process reached a biomass concentration of 51 g/L, where no glucose or another secondary metabolite was accumulated in the culture (Fig. 1). It reflects the successful application of the exponential feeding strategy at a constant μ of 0.25 [h^{-1}] to achieve a good biomass concentration in a short period of time. Similar concentrations have been achieved using the same feeding strategy on *P. putida* (Sun et al. 2006b).

5.3.2 Nitrogen limitation along with a linear feeding strategy induces PHA synthesis

As PHA accumulation is normally stimulated by the limitation of an inorganic nutrient while the carbon source is in excess (Hartmann et al. 2004). The stage III was conducted by stopping the exponential feeding and replacing NH_4OH by NaOH. This promoted rapid nitrogen consumption, making it undetectable after 6 hours. Glucose was supplied to the fermentor until 45 [g/L] of the sugar was accumulated in the process, followed by a linear feeding rate of 70 [g/h]. At 32 h glucose was still present in the medium, resulting in a slight rise in PHA concentration. Therefore, it was decided to stop the linear feeding and let the cells consume the remained sugar in the bioreactor. Surprisingly, this promoted rapid accumulation of the polyester. In order to test the influence of different feeding aproaches on the PHA

accumulation, a double feeding strategy (glucose- of 120 [g/h] and ammonium-feeding rate of 9.6 [g/h]), was set at 35 h. After 9 hours, this strategy did not bring any improvement on PHA synthesis. As done in part of stage III, glucose was not added anymore to the fermentor, as well as the ammonium to let the cells deplete the remained sugar. At that point glucose had a concentration of 52 [g/L]. In the next 6 hours most part of the glucose was converted to PHA, which finally reached a concentration of 21.3 [g/L] at 50 hours. It represents 38% of the CDW as PHA with a final PHA productivity of 0.44 [g/L·h].

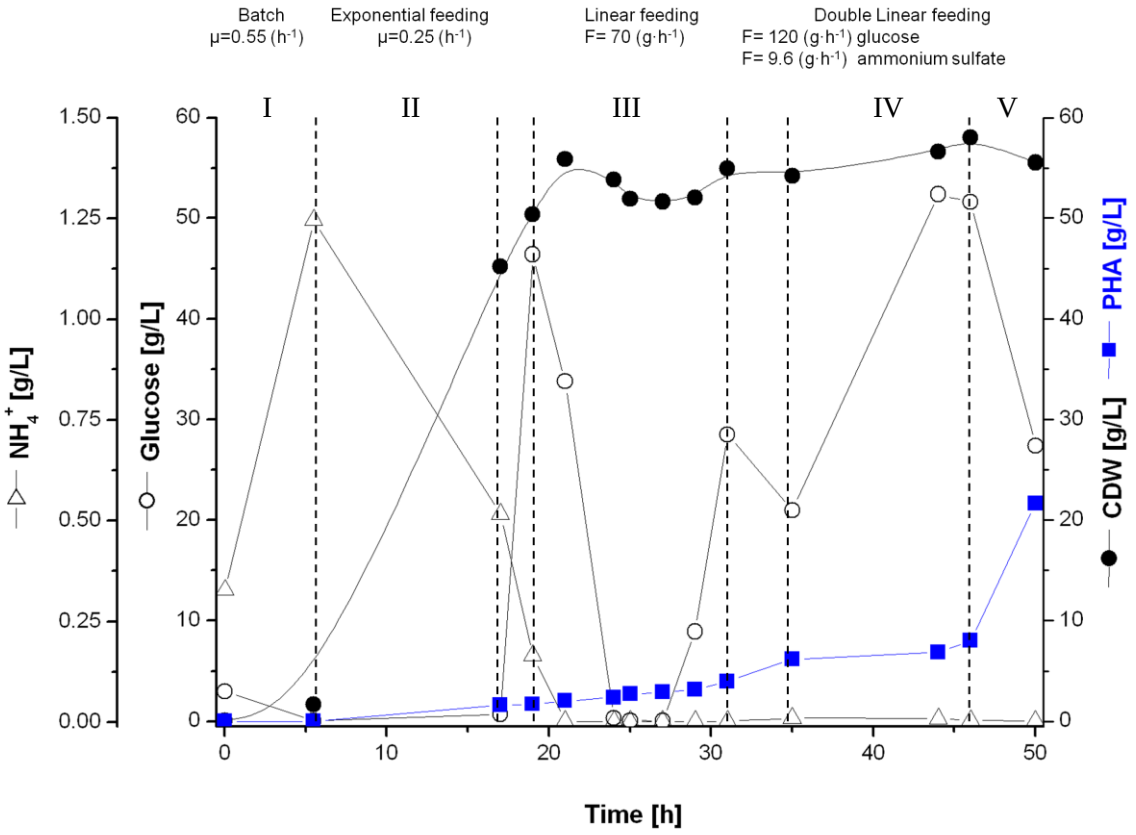

Figure 1. Fermentation profile of *P. putida* KT2440 during fed-batch process; batch (stage I), exponential feeding (II), Linear feeding (III), Double linear feeding (IV), no glucose or ammonium addition (V).

5.3.3 High-cell-density cultures of mutant strains

In order to compare the PHA productivity among the mutant strains and the wild type in fed-batch processes, first the Δ*gcd* mutant strain was subjected to a similar feeding profile as described above. Within the batch phase the mutant strain grew to a maximum specific growth rate of 0.44 [h^{-1}]. At 7 hours after inoculation, the exponential feeding was set at μ 0.25 [h^{-1}]. Glucose accumulation began after 15 hours of feeding, where at that time the biomass concentration was 34 [g/L]. As the μ_{set} was closer to μ_{max} for this mutant as compared to the wild type, it was not possible to keep the carbon-limited fed-batch to the desirable period of time. Once glucose reached 10 g/L within the culture broth, the feeding strategy was stopped, letting the cells to consume the accumulated carbon source. At 25 hours the linear feeding strategy began with a rate of 70 [g/h] of glucose. Unexpectedly, the mutant Δ*gcd* consumed all the supplied glucose during the following 10 hours, as well as showing a small PHA accumulation. At 35 hours the single linear feeding was shifted to a double one. After 10 hours, the glucose concentration reached a value of 30 [g/L]. As performed with the wild type, the feeding pumps were switched off to let the cell to uptake the accumulated sugar. Instead of synthesizing PHA, the mutant used mainly the glucose for biomass production reaching a total biomass of 60 [g/L] at 50 hours (Fig. 2A). Only 16% of the CDW was synthesized as PHA, resulting in a final PHA productivity of 0.19 [g/L·h].

The Δ*gcd-pgl* mutant strain showed a maximum specific growth rate of 0.33 [h^{-1}] within the batch phase. It was challenged to grow at a set μ of 0.25 [h^{-1}], as we performed with the other strains. The culture could not stand such imposed specific growth rate, showing through the exponential feeding glucose accumulation and low biomass production (data not shown). Therefore we started the exponential feeding with a μ of 0.1 [h^{-1}]. After 26 h of feeding, the culture reached a biomass concentration of 33 [g/L]. At that point the concentration of glucose was under the detection limit. To promote PHA accumulation within the process, a pulse of glucose was given to the bioreactor to reach a sugar concentration of 40 [g/L], following by a linear feeding of 70 [g/h] of the carbohydrate (Fig. 2B). This strategy did not promote PHA synthesis within the cell, resulting in glucose accumulation up to 49 [g/L]. Once the linear

feeding was stopped, the cells began to catabolize the available sugar to a rate of 2.5 [g/h]. The overall PHA productivity at 50 h was 0.063 [g/L·h].

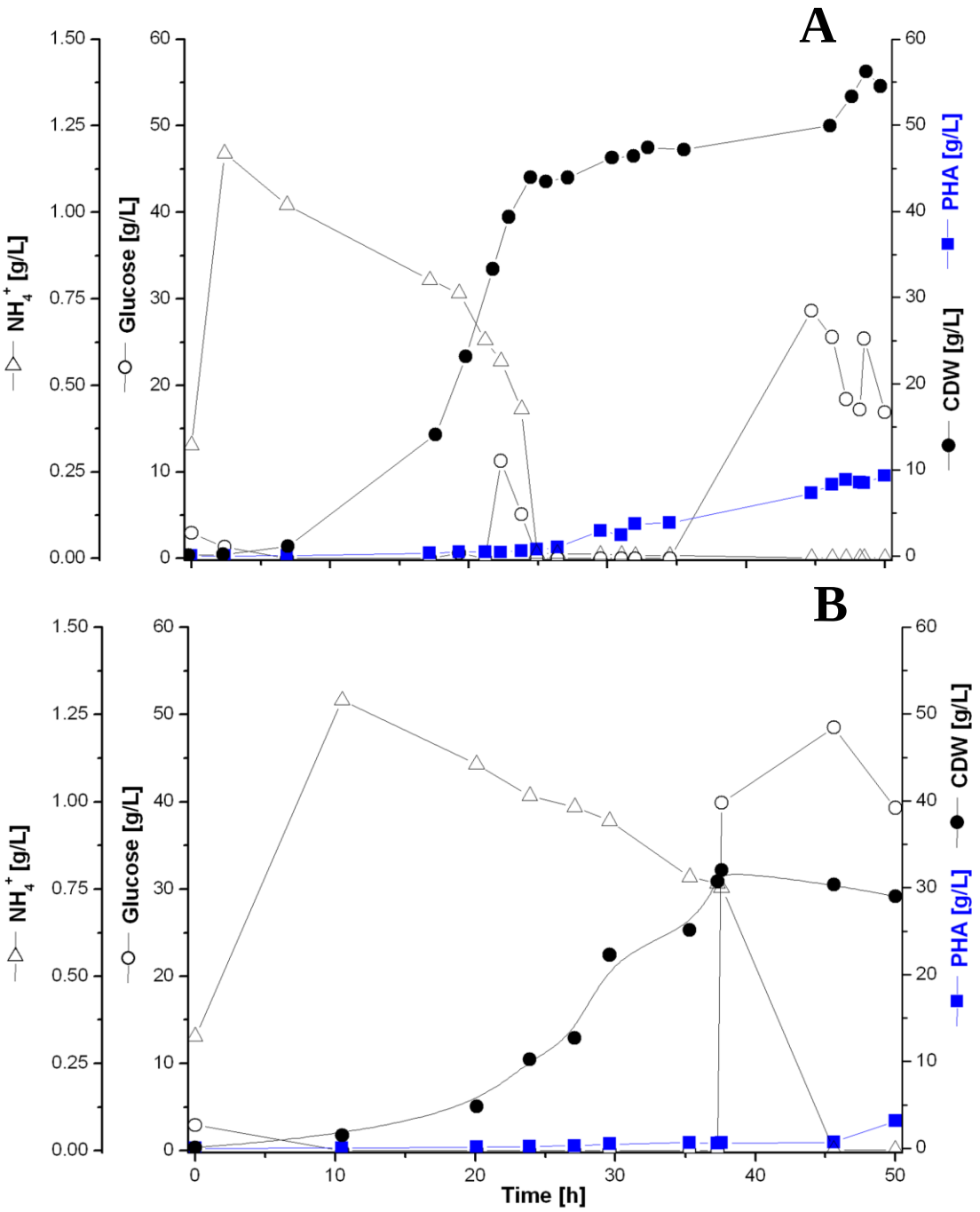

Figure 2. Fermentation profile of Δ*gcd* (A) and Δ*gcd-pgl* (B) mutant strains during fed-batch process.

Table 1. Summary of PHA production by *P. putida* strains in fed-batch process.

Strain	μ (h^{-1})	CDW (g/L)	PHA [ ] (g/L)	PHA content (%)	Productivity (g/L·h)
P. putida KT2440	0.25	56	22	38	0.44
Δgcd	0.25	60	9.6	16	0.19
Δgcd-pgl	0.10	33	3.15	10.5	0.06

5.4 Discussion

Commercialized PHAs (Mirel®, Metabolix, USA) are currently produced using fed-batch processes (Chen 2009), thus fed-batch is still the most employed technique to obtain both high cell and PHA concentration (Chen 2009; Sun et al. 2007c). In this study, it was demonstrated that *P. putida* KT2440 is a suitable microbial factory for the production of mcl(PHA). *P. putida* strains grew very well on glucose reaching more than 80 (g/L) at 20 hours in feed-batch processes (Sun et al. 2006a). Nevertheless, the key step to stimulate PHA synthesis is to shift from carbon-limitation to carbon-excess along with the limitation of an inorganic nutrient e.g. nitrogen (Lee et al. 1999). The commonly used two-step cultivation has yielded high PHA accumulation as impressively shown by *Alacaligenes latus* (5.13 [g/L·h]) (Wang and Lee 1997), *P. putida* (1.91 [g/L·h]) (Lee et al. 2000), and *Ralstonia. eutropha* (3.14 [g/L·h]) (Ryu et al. 1997), among others. The accumulation phase — inorganic nutrient limitation — can be done in many different ways: e.g. linear feeding where a constant feed-rate of the substrate is applied to the bioreactor (Wang and Lee 1997); via pulses by adding a known concentration of the substrate and then leaving the culture to metabolize it till the presence of the carbon source is very low within the culture, the procedure is further cyclically repeated to the end of the process (Ryu et al. 1997). By applying the first described strategy (above), Sun and coworkers produced 0.91 [g/L·h] in *P. putida* KT2440 using nonanoic acid as carbon source under nitrogen limitation (Sun et al. 2007b). We applied

the same procedure in KT2440 in the presence of glucose (Fig 1). It took 6 hours after the set feeding rate 70 [g/L] affected the culture as such that it could not metabolize more glucose, and progressively the sugar accumulated within the process. The PHA content did not substantially change (Fig. 1), demonstrating that the linear feeding strategy is not a good approach when glucose is used as carbon source. We next proceeded to increase the feeding rate to 120 [g/L] along with ammonium. This strategy was shown to be very promising for organisms that can accumulate PHAs even when all nutrients are in excess (Lee et al. 2000; Sun et al. 2007b). As *P. putida* has been shown to be one of them (Poblete-Castro et al. 2012b), we thought that it could highly promote the PHA synthesis. Nevertheless that was not the case since a only little rise in the PHA concentration was observed, thus confirming that linear feeding is not as efficient as when fatty acid is used as carbon source (Sun et al. 2007b). The glucose accumulated to a concentration of 53 [g/L] (Fig. 1), which normally inhibits growth and PHA synthesis (Kim et al. 1997). When we determined such glucose concentration within the culture broth, we stopped the feeding of glucose and ammonium. Surprisingly, once more *P. putida* showed its robustness by starting metabolizing the remaining glucose to a consumption rate of 2.5 [g/ L h], which led to a sharp increase of the PHA concentration at the end of the process (Fig. 1).

By comparing KT2440 against Δ*gcd* mutant strain, the latter did not accumulate more PHAs under the same fed-batch feeding approach (Fig. 1 and 2A). Although, the reached biomass concentration was pretty much the same value for both strains at 17 hours, the first drawback for the mutant started when the set feeding rate was not enough to promote glucose accumulation in the culture (Fig. 2A), thus delaying the induction of PHAs synthesis, which finally affects the overall productivity. It is interesting to see that when both strains had glucose in excess and sensed that glucose was provided, no PHA-accumulation was promoted, but as soon as glucose feeding stop rapidly, PHA accumulation was triggered by such environmental condition (Fig. 1 and 2A). As expected, the double-deletion mutant is a less efficient producer strain in comparison to the wild-type and the single-deletion mutant, since the reduced specific growth rate negatively influenced the overall PHA accumulation (Fig. 2B).

Several reports have shown to achieve high PHA concentration using *P. putida* (Kim et al. 1997; Lee et al. 2000; Sun et al. 2007b). The use of fatty acids has been the dominating practice in such processes. In this study we developed a fed-batch process where the cheap substrate glucose was used as carbon source. A total PHA productivity of 0.44 and 0.19 [g/L·h] was obtained with *P. putida* KT2440 and its mutant strain (Δ*gcd*), respectively. Although we were far from 0.7 [g/L·h], which is a needed value for making a process economically viable (Huijberts and Eggink 1996), we have gained deep knowledge concerning feeding strategies when glucose is the substrate. This work will serve as the base to lead further investigation in the metabolically engineered *P. putida* strain, which has very promising features for sustainable production of polyhydroxyalkanoates.

5.5 Acknowledgments

We thank to Wolfgang Kessler for allowing to performe the fed-bacth experiments in the fermentation facilities of the HZI. We also thank Reinhard Sterlinski, Axel Schulz, Burkhard Ebert, and Andrew Perreth for the excellent technical assistance on the preparation of the bioreactors and HPLC analysis.

5.6 References

Chen G-Q. 2009. A microbial polyhydroxyalkanoates (PHA) based bio- and materials industry. Chemical Society Reviews 38(8).

Hartmann R, Hany R, Geiger T, Egli T, Witholt B, Zinn M. 2004. Tailored Biosynthesis of Olefinic Medium-Chain-Length Poly[(R)-3-hydroxyalkanoates] in *Pseudomonas putida* GPo1 with Improved Thermal Properties. Macromolecules 37(18):6780-6785.

Huijberts GNM, Eggink G. 1996. Production of poly(3-hydroxyalkanoates) by *Pseudomonas putida* KT2442 in continuous cultures. Applied Microbiology and Biotechnology 46(3):233-239.

Kim GJ, Lee IY, Yoon SC, Shin YC, Park YH. 1997. Enhanced yield and a high production of medium-chain-length poly(3-hydroxyalkanoates) in a two-step fed-batch cultivation of *Pseudomonas putida* by combined use of glucose and octanoate. Enzyme and Microbial Technology 20(7):500-505.

Korz DJ, Rinas U, Hellmuth K, Sanders EA, Deckwer WD. 1995. Simple fed-batch technique for high cell density cultivation of *Escherichia coli*. Journal of Biotechnology 39(1):59-65.

Lee SY, Choi J-i, Wong HH. 1999. Recent advances in polyhydroxyalkanoate production by bacterial fermentation: mini-review. International Journal of Biological Macromolecules 25(1-3):31-36.

Lee SY, Wong HH, Choi JI, Lee SH, Lee SC, Han CS. 2000. Production of medium-chain-length polyhydroxyalkanoates by high-cell- density cultivation *Pseudomonas putida* under phosphorus limitation. Biotechnology and Bioengineering 68(4):466-470.

Poblete-Castro I, Escapa I, Jager C, Puchalka J, Lam C, Shomburg D, Prieto MA, dos Santos VAP. 2012. The metabolic response of *P. putida* KT2442 producing high levels of polyhydroxyalkanoates under single- and multiple-nutrient-limited growth: Highlights from a multi-level omics approach. Microbial Cell Factories.

Ryu HW, Hahn SK, Chang YK, Chang HN. 1997. Production of poly(3-hydroxybutyrate) by high cell density fed-batch culture of *Alcaligenes eutrophus* with phospate limitation. Biotechnology and Bioengineering 55(1):28-32.

Sun Z, Ramsay JA, Guay M, Ramsay BA. 2006. Automated feeding strategies for high-cell-density fed-batch cultivation of *Pseudomonas putida* KT2440. Applied Microbiology and Biotechnology 71(4):423-431.

Sun Z, Ramsay JA, Guay M, Ramsay BA. 2007a. Carbon-limited fed-batch production of medium-chain-length polyhydroxyalkanoates from nonanoic acid by *Pseudomonas putida* KT2440. Applied Microbiology and Biotechnology 74(1):69-77.

Sun Z, Ramsay JA, Guay M, Ramsay BA. 2007b. Fermentation process development for the production of medium-chain-length poly-3-hyroxyalkanoates. Applied Microbiology and Biotechnology 75(3):475-485.

van Duuren JBJH. 2011. Optimization of *Pseudomonas putida* KT2440 as host for the production of cis, cis-muconate from benzoate. Wageningen: Wageningen.

Wang F, Lee SY. 1997. Poly(3-hydroxybutyrate) production with high productivity and high polymer content by a fed-batch culture of *Alcaligenes latus* under nitrogen limitation. Applied and Environmental Microbiology 63(9):3703-3706.

CHAPTER VI. Summary and outlook

White Biotechnology is devoted to the industrial production of chemicals using living cells or their components (enzymes) to perform biotransformations towards a desired product. The application of such approaches at industrial scale aims at developing more cost-effective and environmental-friendly processes than conventional chemical conversions. As microorganisms have evolved through millions of years, their intrinsic metabolic repertoire has been continuously reshaped by the natural environment. Their capability to synthesize thousands of value-added compounds has served to solve a broad range of challenges in production processes in the modern society. Metabolic engineering marked a major turning point in white biotechnology when the application of recombinant DNA methods was proved to be extremely efficient to restructure metabolic networks and improve the yield of metabolite and protein products. This has brought many innovations to various industrial areas, especially concerning to the use of alternative substrates and energy sources. In this concern, a priority point on the agenda of industrial application of biotechnologies has been the replacement of oil-based plastics production. For more than 30 years, polyhydroxybutyrate (PHB) and its co-polymer polyhydroxybutyrate-co-valerate (PHBV) have been extensively produced to satisfy the demand of the biopolymer market. Nevertheless, these types of biopolymers have a slim range of applications because of their limited range of mechanical and physical properties. Medium-chain-length (mcl) polyhydroxyalkanoates (PHAs) have opened a new avenue to fulfill the gap between petroleum-based plastic and PHB (as shown in Chapter I). *Pseudomonas* species belonging to rRNA homology group I can naturally accumulate such polyesters as inclusion bodies in the cytoplasmic space of the cell, which can amass up to 60% of its dry weight as PHA in the presence of fatty acids as carbon sources. Nevertheless, production of mcl-PHA is currently restricted due to the high costs associated to the production process, as they are 5-10 times more expensive to obtain than conventional polymers. Therefore, whole-cell biocatalyst and process development for PHA synthesis requires in-depth understanding of the metabolic response of the cell at several omics levels to unravel the biological functions and regulations in a more systematic fashion. The application of a *systems*

biotechnology approach —combination of quantitative measurements (omics data) and *in silico* modeling of the cellular metabolism towards the improvement of a target compounds in a rational manner — appears to be powerful a tool to step ahead in the production of biopolymers along with the use of inexpensive substrates.

In *Chapter II*, *P. putida* and related species are shown to be suitable as whole-cell biocatalyzers for the production of several value-added compounds. Their enzymatic repertoire to carry out specific chemical conversions e.g., oxygenases and the naturally high tolerance along with their versatile metabolism appear as desirable features to develop a strong platform for obtaining *de novo* chemicals at industrial scale, among them sustainable biopolymers. In this concern, the study described in *Chapter III* attempted to highlight the differences between nutrient limitations and their impact on PHA synthesis under well-controlled conditions using a system-level approach. This allowed successful development of three different processes where carbon-, carbon-nitrogen-, and strict nitrogen-limitation led to 26, 62, and 81% of the cell dry weight as PHA, respectively. In order to consume all available carbon and nitrogen by the cells growing at a specific growth rate of 0.1 [h^{-1}] under steady-state condition, the culture should be supplied with a carbon/nitrogen (C/N) ratio lower than 20.5 [mol/mol]. A high specific PHA production rate of 0.43 [g/g·h] was obtained under nitrogen limitation, which is the highest ever achieved in chemostate cultures in comparison to other *P. putida* strains. Transcriptome, proteome, and metabolome analyses were employed to investigate the metabolic responses under such limiting conditions. Dual limitation showed different expression patterns in comparison to those observed under strict carbon- or nitrogen-limiting conditions. Energy metabolism, fatty acids metabolism, stress response, and proteins belonging to the transport system were the components of the cell which were highly affected by the imposed nutrient limitation. Driven by the top-down approach, it was possible to increase the PHA accumulation under dual limitation from 62 to 77% of the cell dry weight, which finally resulted in a specific accumulation rate of 0.34 [g/g·h]. Our study concluded that oxygen availability highly affects the PHA synthesis within continuous cultivation mode in *P. putida* KT2442 and the integration of

hightroughtput data is a powerful tool for process reengineering towards increasing biopolymer production.

Chapter IV describes the enhancement of PHA synthesis in *P. putida* KT2440 applying a model-driven metabolic engineering approach along with the use of the cheap carbon source glucose. From the *in silico* modeling using FluxDesign, glucose dehydrogenase (encoded by *gcd*) was predicted as a target with the highest priority to be deleted. The created Δ*gcd* mutant strain exhibited 60% increase in PHA accumulation as compared to the parental wild-type strain. The mutant maintained a high specific growth rate and exhibited an almost unaffected gene expression profile. To further develop an industrial-scale PHA production process, the generated mutant strain and its parental strain KT2440 were subjected to the industrial process of choice — the fed-batch cultivation (Chapter V). The wild-type reached a total PHA productivity of 0.44 [g/L·h] in the presence of glucose. It is concluded that linear feeding is not the best feeding strategy for PHA synthesis in *P. putida* within high cell cultivations. Instead, a pulse-feeding approach — to reach cyclically a concentration up to 40 g/L of glucose — is found to be more appropriate. The mutant strain (Δ*gcd-pgl*) did not accumulate more PHA than its parental wild-type strain due to the high uptake rate of glucose under the same linear-feeding conditions, thus delaying glucose accumulation in the fermentor which finally impacts the total PHA productivity. Further investigations of the metabolically engineered strain in the fed-batch process with higher feeding rates along with a pulse-feeding strategy are necessary in order to fully exploit the metabolic capacity of the mutant strain for the production PHAs.

In conclusion, the results described in this thesis have shown the strength of *in silico* modeling and integration of omics measurements to lead metabolic engineering works towards optimal performance of the cell and reengineering processes for the synthesis of polyhydroxyalkanoates. In addition, we have proved that inclusion of co-factors, e.g. NADPH, within the *in silico* metabolic network of *P. putida* is of great importance in allowing PHA synthesis; but maximizing only the availability of main precursors such as acetyl-CoA does not guarantee an increase in PHA yield without detrimental physiological

effects. Furthermore, NADPH appears to be key for mcl-PHAs synthesis in *P. putida* in the presence of glucose since the deletion of glucose-6P dehydrogenase (encoded by PP_1023) — which generates high levels of NADPH — lead to a decrease in PHA accumulation relative to KT2440. On the other hand, it is also known that NADPH is a needed co-factor in the synthesis of *de novo* fatty acids which generate intermediate PHA precursors (Fig. 6.1).

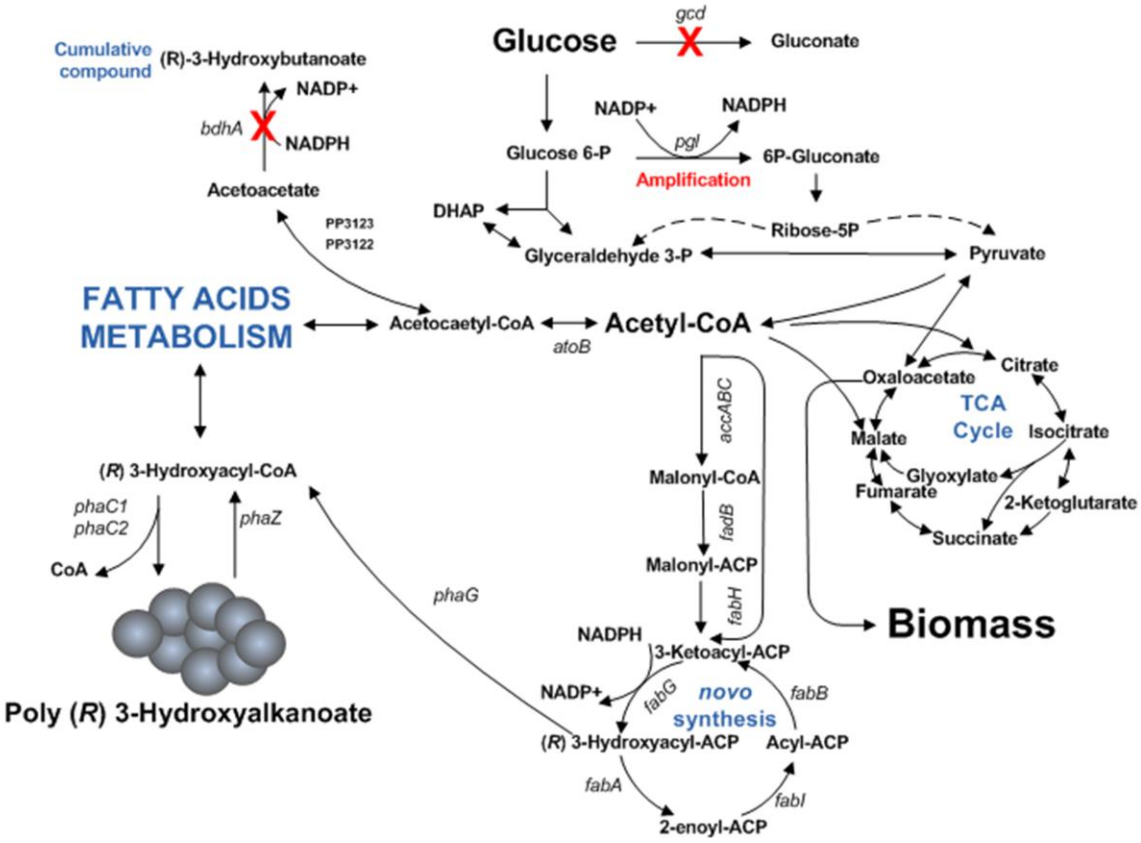

Figure 6.1. The sheme shows pathways for PHA synthesis and the requirement of NADPH for reduction of intermediates for its production. Different strategies (knockout/overexpression of genes, in red) for possible enahnicing of PHA synthesis.

In this concern, based on the transcriptome analysis of the PHA-overproducer strain (Δ*gcd*) a further promising deletion target would be the protein 3-hydroxybutyrate dehydrogenase (encoded by PP_3073) which shows a high mRNA expression level. This enzyme requires NADPH as a cofactor to yield (*R*)-3-

hydroxybutanoate from acetoacetate. (*R*)-3-hydroxybutanoate cannot be incorporated into the monomer composition of the resulted PHA due to the specificity of the PHA synthase PhaC (encoded by PP_5003) towards the carbon chain length of PHA precursors (C_6 hydroxy alkanoates or higher), and as shown by our metabolome analysis (*R*)-3-hydroxybutanoate is accumulated in the cell. Therefore, this engineering strategy might lead to an increase of available NADPH molecules which can be exploited for other metabolic functions such as PHA synthesis (Fig. 6.1).

This work has demonstrated the advantages of applying a systems biotechnology approach for the production of PHAs. The rational design of processes and superior strains is the base for making white-biotechnology an economically sustainable-viable alternative towards the synthesis of various industrially valuable compounds. Altough consirerable progesses have been made in increasing our understanding of the PHA synthesis taking into account of whole metabolic system of *P. putida* strains, continued effort to strengthen both fine-tuned strategies of systems metabolic engineering and process optimization are required to fully replace convetional oil-based plastic production processes.

CHAPTER VII. Supplementary material

Supplementary Table S1. Transcriptomic data of genes differentially expressed with a fold change above 2 and below -2 and a *P* value below 0.05. Comparison 1: CN- vs. C-limited cultures. Comparison 2: N- vs. C- limited cultures.

Comparison 1

Locus name	*Gene Name*	*Log change*	*Fold change*	*p-value*
PP_0555	acetoin dehydrogenase alpha subunit gb|AE015451.1|:c645014-644037	-3.12	**-8.68**	0.00
PP_4006	arginine-tRNA-protein transferase-related protein gb|AE015451.1|:4516135-4516842	-2.84	**-7.14**	0.00
PP_0600	ribosomal protein S20 gb|AE015451.1|:c707346-707068	-2.75	**-6.73**	0.00
PP_0556	acetoin catabolism protein gb|AE015451.1|:c646092-645037	-2.18	**-4.55**	0.00
PP_0554	acetoin dehydrogenase beta subunit gb|AE015451.1|:c644003-642981	-2.04	**-4.12**	0.00
PP_0553	acetoin dehydrogenase dihydrolipoamide acetyltransfe gb|AE015451.1|:c642984-641878	-2.01	**-4.03**	0.00
PP_1037	phosphoribosylformylglycinamidine synthase gb|AE015451.1|:1184794-1188693	-2.00	**-3.99**	0.01
PP_2297	integrative genetic element Ppu40 integrase gb|AE015451.1|:2624995-2625819	-1.99	**-3.97**	0.00
PP_2435	cysteine desulfurase gb|AE015451.1|:c2782362-2781145	-1.96	**-3.89**	0.00
PP_3504	conserved hypothetical protein gb|AE015451.1|:3974810-3975076	-1.96	**-3.88**	0.01
PP_2149	glyceraldehyde 3-phosphate dehydrogenase gb|AE015451.1|:2455283-2456746	-1.89	**-3.70**	0.00
PP_4872	conserved hypothetical protein gb|AE015451.1|:c5540982-5538628	-1.85	**-3.59**	0.00
PP_0557	acetoin catabolism regulatory protein gb|AE015451.1|:646376-648229	-1.81	**-3.50**	0.00
PP_2423	conserved hypothetical protein gb|AE015451.1|:c2771139-2770240	-1.75	**-3.37**	0.02
PP_4715	triosephosphate isomerase gb|AE015451.1|:c5362357-5361602	-1.72	**-3.29**	0.01
PP_4793	conserved hypothetical protein gb|AE015451.1|:c5456039-5455725	-1.72	**-3.28**	0.00
PP_0389	ribosomal protein S21 gb|AE015451.1|:c475503-475288	-1.71	**-3.28**	0.00
PP_5214	transcription termination factor Rho gb|AE015451.1|:c5948464-5947205	-1.71	**-3.27**	0.02
PP_4174	3-hydroxydecanoyl-(acyl-carrier-protein) dehydratase gb|AE015451.1|:4716908-4717423	-1.70	**-3.26**	0.01
PP_3954	periplasmic binding protein putative gb|AE015451.1|:4460534-4461484	-1.70	**-3.24**	0.04
PP_2437	acyl-CoA dehydrogenase putative gb|AE015451.1|:2783545-2784789	-1.68	**-3.20**	0.00

PP_1016	sugar ABC transporter permease protein gb|AE015451.1|:1159286-1160194	-1.67	**-3.17**	0.04
PP_0545	aldehyde dehydrogenase family protein gb|AE015451.1|:c633438-631918	-1.66	**-3.17**	0.01
PP_4737	D-lactate dehydrogenase putative gb|AE015451.1|:5386489-5389299	-1.66	**-3.15**	0.01
PP_2141	conserved hypothetical protein gb|AE015451.1|:2444126-2444359	-1.65	**-3.14**	0.00
PP_5224	conserved hypothetical protein gb|AE015451.1|:c5960294-5960070	-1.60	**-3.03**	0.01
PP_0469	ribosomal protein L6 gb|AE015451.1|:557869-558402	-1.59	**-3.02**	0.00
PP_5127	conserved hypothetical protein gb|AE015451.1|:5847820-5849016	-1.58	**-2.99**	0.03
PP_3560	transcriptional regulator LysR family gb|AE015451.1|:4039141-4040004	-1.55	**-2.93**	0.01
PP_1076	glycerol uptake facilitator protein gb|AE015451.1|:c1236186-1235335	-1.54	**-2.91**	0.03
PP_1083	bacterioferritin-associated ferredoxin putative gb|AE015451.1|:c1242882-1242664	-1.54	**-2.91**	0.01
PP_1430	alginate biosynthesis negative regulator serine prot gb|AE015451.1|:1629584-1631062	-1.53	**-2.89**	0.03
PP_0551	MORN domain protein gb|AE015451.1|:c640742-638814	-1.52	**-2.87**	0.04
PP_0765	conserved hypothetical protein gb|AE015451.1|:880484-882370	-1.46	**-2.74**	0.01
PP_0932	glutamyl-tRNA(Gln) amidotransferase C subunit gb|AE015451.1|:c1075177-1074869	-1.45	**-2.74**	0.01
PP_1099	cold-shock domain family protein gb|AE015451.1|:c1257128-1256919	-1.45	**-2.74**	0.01
PP_2086	crfX protein gb|AE015451.1|:2378443-2378715	-1.42	**-2.68**	0.02
PP_0974	hypothetical protein gb|AE015451.1|:1113202-1113531	-1.42	**-2.68**	0.01
PP_2088	RNA polymerase sigma factor SigX gb|AE015451.1|:2379632-2380222	-1.42	**-2.68**	0.01
PP_4517	conserved hypothetical protein gb|AE015451.1|:5131645-5132232	-1.41	**-2.65**	0.02
PP_3071	acetoacetyl-CoA synthetase putative gb|AE015451.1|:c3455887-3453935	-1.41	**-2.65**	0.01
PP_1766	initiation factor 2 subunit family gb|AE015451.1|:1969627-1970703	-1.40	**-2.65**	0.01
PP_2258	sensory box protein gb|AE015451.1|:2574821-2576509	-1.40	**-2.64**	0.04
PP_4147	peptide ABC transporter periplamic peptide-binding p gb|AE015451.1|:4685186-4687021	-1.40	**-2.64**	0.01
PP_2853	conserved hypothetical protein gb|AE015451.1|:c3257150-3255870	-1.39	**-2.63**	0.02
PP_1799	GDP-mannose 4 6 dehydratase gb|AE015451.1|:2021899-2022966	-1.39	**-2.63**	0.01
PP_4439	ISPpu14 transposase Orf3 gb|AE015451.1|:5033959-5035494	-1.39	**-2.62**	0.02
PP_3402	hypothetical protein gb|AE015451.1|:c3854191-3853796	-1.37	**-2.59**	0.01
PP_2874	hypothetical protein gb|AE015451.1|:3275984-3276295	-1.37	**-2.59**	0.01
PP_3557	methyl-accepting chemotaxis transducer gb|AE015451.1|:4034947-4037091	-1.36	**-2.56**	0.04
PP_5067	potassium efflux system protein KefA putative	-1.35	**-2.56**	0.04

	gb|AE015451.1|:5781517-5784825			
PP_5124	ferredoxin 4Fe-4S gb|AE015451.1|:5845668-5845919	-1.35	**-2.55**	0.04
PP_3319	sensory box protein/GGDEF domain protein gb|AE015451.1|:3754557-3756758	-1.35	**-2.55**	0.02
PP_4945	conserved hypothetical protein gb|AE015451.1|:c5628525-5627689	-1.35	**-2.55**	0.02
PP_0957	KpsF/GutQ family protein gb|AE015451.1|:c1099563-1098589	-1.35	**-2.55**	0.01
PP_1100	deoxycytidine triphosphate deaminase gb|AE015451.1|:1257456-1258022	-1.34	**-2.54**	0.01
PP_2006	hypothetical protein gb|AE015451.1|:c2277453-2275675	-1.34	**-2.53**	0.01
PP_4933	conserved hypothetical protein gb|AE015451.1|:5613045-5614013	-1.34	**-2.53**	0.01
PP_4938	glycosyl transferase putative gb|AE015451.1|:c5620495-5619356	-1.33	**-2.51**	0.01
PP_0441	preprotein translocase SecE subunit gb|AE015451.1|:534102-534470	-1.32	**-2.50**	0.04
PP_5392	conserved hypothetical protein gb|AE015451.1|:c6147451-6146318	-1.32	**-2.50**	0.01
PP_5391	hypothetical protein gb|AE015451.1|:c6146308-6145727	-1.32	**-2.49**	0.01
PP_3564	transcriptional regulator AraC family gb|AE015451.1|:c4043740-4042763	-1.31	**-2.49**	0.02
PP_5027	D-tyrosyl-tRNA(Tyr) deacylase gb|AE015451.1|:c5729389-5728952	-1.31	**-2.47**	0.01
PP_4852	transcriptional regulator AraC family gb|AE015451.1|:c5519726-5518938	-1.30	**-2.47**	0.01
PP_4736	L-lactate dehydrogenase gb|AE015451.1|:5385268-5386413	-1.30	**-2.47**	0.01
PP_4547	glutamine synthetase putative gb|AE015451.1|:5168381-5169745	-1.30	**-2.46**	0.04
PP_0559	acetyl-CoA carboxylase biotin carboxyl carrier prote gb|AE015451.1|:c650154-649693	-1.30	**-2.45**	0.01
PP_1073	glycerol-3-phosphate dehydrogenase gb|AE015451.1|:c1232710-1231166	-1.29	**-2.45**	0.04
PP_1659	conserved hypothetical protein gb|AE015451.1|:1854985-1856325	-1.29	**-2.44**	0.03
PP_3321	conserved hypothetical protein gb|AE015451.1|:3757176-3757688	-1.27	**-2.41**	0.02
PP_4636	beta-ketothiolase gb|AE015451.1|:5259457-5260635	-1.25	**-2.39**	0.03
PP_0453	ribosomal protein S10 gb|AE015451.1|:550659-550970	-1.25	**-2.38**	0.01
PP_1773	integration host factor beta subunit gb|AE015451.1|:1981358-1981660	-1.24	**-2.36**	0.01
PP_4192	succinate dehydrogenase hydrophobic membrane anchor gb|AE015451.1|:c4738740-4738372	-1.23	**-2.35**	0.04
PP_5091	conserved hypothetical protein gb|AE015451.1|:c5816017-5815598	-1.22	**-2.33**	0.01
nonsymbol	RNA polymerase sigma-54 factor gb|AE015451.1|:c1096058-1094565	-1.22	**-2.33**	0.02
PP_3981	ISPpu14 transposase Orf3 gb|AE015451.1|:4487111-4488646	-1.20	**-2.30**	0.01
PP_1661	dehydrogenase subunit putative gb|AE015451.1|:1856818-1859076	-1.20	**-2.30**	0.04

PP_5350	transcriptional regulator RpiR family gb|AE015451.1|:c6099078-6098212	-1.19	**-2.27**	0.03
PP_3693	transcriptional regulator MvaT P16 subunit putative gb|AE015451.1|:c4211487-4211122	-1.18	**-2.27**	0.01
PP_1609	hypothetical protein gb|AE015451.1|:1806092-1806232	-1.18	**-2.26**	0.04
PP_4731	outer membrane lipoprotein OmlA gb|AE015451.1|:5380697-5381233	-1.18	**-2.26**	0.02
PP_4958	conserved hypothetical protein gb|AE015451.1|:c5649060-5648521	-1.17	**-2.25**	0.01
PP_3663	GGDEF domain protein gb|AE015451.1|:c4162052-4160751	-1.16	**-2.23**	0.01
PP_4870	azurin gb|AE015451.1|:c5537572-5537123	-1.15	**-2.22**	0.04
PP_4193	succinate dehydrogenase cytochrome b556 subunit gb|AE015451.1|:c4739120-4738734	-1.15	**-2.22**	0.04
PP_4708	polyribonucleotide nucleotidyltransferase gb|AE015451.1|:c5354114-5352009	-1.15	**-2.22**	0.02
PP_3698	conserved hypothetical protein gb|AE015451.1|:c4219292-4217793	-1.15	**-2.21**	0.03
PP_1146	hypothetical protein gb|AE015451.1|:1314805-1315500	-1.15	**-2.21**	0.02
PP_3908	hypothetical protein gb|AE015451.1|:4418483-4418833	-1.14	**-2.21**	0.03
PP_5396	ISPpu14 transposase Orf3 gb|AE015451.1|:c6154464-6152929	-1.14	**-2.20**	0.03
PP_4476	conserved hypothetical protein gb|AE015451.1|:c5085956-5085666	-1.13	**-2.19**	0.05
PP_2313	conserved hypothetical protein gb|AE015451.1|:2643254-2643691	-1.13	**-2.19**	0.02
PP_4648	nucleotide methyltransferase putative gb|AE015451.1|:5272852-5273976	-1.13	**-2.19**	0.04
PP_3598	conserved hypothetical protein gb|AE015451.1|:4087773-4088582	-1.13	**-2.18**	0.02
PP_1714	peptidyl-prolyl cis-trans isomerase FKBP-type gb|AE015451.1|:1914817-1915569	-1.13	**-2.18**	0.03
PP_4839	membrane protein putative gb|AE015451.1|:5505171-5506538	-1.11	**-2.15**	0.04
PP_3747	glycolate oxidase iron-sulfur subunit gb|AE015451.1|:4276603-4277838	-1.11	**-2.15**	0.02
PP_0477	ribosomal protein S11 gb|AE015451.1|:561868-562257	-1.10	**-2.15**	0.01
PP_0468	ribosomal protein S8 gb|AE015451.1|:557464-557856	-1.10	**-2.14**	0.02
PP_0476	ribosomal protein S13 gb|AE015451.1|:561493-561849	-1.09	**-2.13**	0.01
PP_1642	conserved hypothetical protein gb|AE015451.1|:1837378-1838049	-1.09	**-2.12**	0.03
PP_0450	ribosomal protein S7 gb|AE015451.1|:546648-547118	-1.07	**-2.10**	0.04
PP_4346	D-alanine--D-alanine ligase A gb|AE015451.1|:c4938751-4937693	-1.07	**-2.10**	0.05
PP_0339	pyruvate dehydrogenase E1 component gb|AE015451.1|:c410662-408017	-1.07	**-2.09**	0.04
PP_5088	primosomal protein N` gb|AE015451.1|:5810664-5812883	-1.06	**-2.09**	0.03
PP_4624	hydrolase alpha/beta fold family gb|AE015451.1|:c5249813-5248914	-1.06	**-2.09**	0.02
PP_5054	glutaredoxin gb|AE015451.1|:c5760317-5760063	-1.06	**-2.09**	0.04
PP_5418	ATP synthase F0 C subunit gb|AE015451.1|:c6180422-6180165	-1.05	**-2.07**	0.03

PP_1212	conserved domain protein gb|AE015451.1|:1389877-1390098	-1.05	**-2.07**	0.04
PP_3839	alcohol dehydrogenase zinc-containing gb|AE015451.1|:4362913-4363923	-1.05	**-2.07**	0.02
PP_4714	conserved hypothetical protein gb|AE015451.1|:c5360836-5360327	-1.04	**-2.06**	0.01
PP_4724	carbamoyl-phosphate synthase small subunit gb|AE015451.1|:c5373167-5372031	-1.04	**-2.06**	0.02
PP_4652	membrane protein putative gb|AE015451.1|:5277038-5278258	-1.04	**-2.05**	0.02
PP_1749	acetyltransferase GNAT family gb|AE015451.1|:c1949651-1947906	-1.03	**-2.04**	0.02
PP_5324	response regulator gb|AE015451.1|:c6070635-6069745	-1.03	**-2.04**	0.02
PP_3043	hypothetical protein gb|AE015451.1|:3428087-3428293	-1.03	**-2.04**	0.02
PP_4811	gamma-glutamyl phosphate reductase gb|AE015451.1|:c5474791-5473520	-1.02	**-2.03**	0.04
PP_2324	phospho-2-dehydro-3-deoxyheptonate aldolase class I gb|AE015451.1|:c2652414-2651302	-1.02	**-2.03**	0.04
PP_1876	conserved hypothetical protein gb|AE015451.1|:2099932-2100978	-1.01	**-2.02**	0.05
PP_4788	conserved hypothetical protein TIGR00043 gb|AE015451.1|:5450121-5450594	-1.01	**-2.02**	0.04
PP_1365	exodeoxyribonuclease I gb|AE015451.1|:1553925-1555358	-1.01	**-2.01**	0.03
PP_1914	3-oxoacyl-(acyl-carrier-protein) reductase gb|AE015451.1|:2157648-2158388	-1.00	**-2.01**	0.02
PP_4283	transcriptional regulator GntR family gb|AE015451.1|:c4874531-4873776	-1.00	**-2.00**	0.03
PP_5298	conserved hypothetical protein gb|AE015451.1|:c6046101-6045334	1.01	**2.01**	0.02
PP_3513	transcriptional regulator LysR family gb|AE015451.1|:3984714-3985568	1.04	**2.05**	0.03
PP_0369	GGDEF domain protein gb|AE015451.1|:447502-448704	1.10	**2.14**	0.01
PP_4137	outer membrane siderophore receptor putative gb|AE015451.1|:4673226-4675298	1.10	**2.14**	0.02
PP_2843	urease gamma subunit gb|AE015451.1|:3247742-3248044	1.11	**2.15**	0.04
PP_3951	3-oxoadipate CoA-transferase subunit A gb|AE015451.1|:4457362-4458057	1.11	**2.16**	0.02
PP_3021	transporter LysE family gb|AE015451.1|:c3408540-3407926	1.12	**2.18**	0.02
PP_1408	acyl-transferase gb|AE015451.1|:c1607529-1606642	1.13	**2.18**	0.04
PP_2093	response regulator NasT gb|AE015451.1|:c2385874-2385299	1.16	**2.23**	0.05
PP_4311	D-amino acid dehydrogenase small subunit putative gb|AE015451.1|:c4904125-4902932	1.16	**2.23**	0.04
PP_5007	polyhydroxyalkanoate granule-associated protein GA2 gb|AE015451.1|:c5705363-5704578	1.20	**2.30**	0.01
PP_0759	conserved hypothetical protein gb|AE015451.1|:874420-875259	1.21	**2.31**	0.05
PP_4069	hypothetical protein gb|AE015451.1|:4594782-4595081	1.22	**2.33**	0.03
PP_2850	hypothetical protein gb|AE015451.1|:3252514-3252627	1.29	**2.44**	0.01
PP_2847	urease accessory protein UreJ	1.29	**2.44**	0.02

	gb|AE015451.1|:3250613-3251158			
PP_2689	endoribonuclease putative gb|AE015451.1|:c3080067-3079696	1.29	**2.45**	0.04
PP_3902	hypothetical protein gb|AE015451.1|:c4416483-4416175	1.33	**2.51**	0.02
PP_5008	polyhydroxyalkanoate granule-associated protein GA1 gb|AE015451.1|:c5705793-5705374	1.34	**2.54**	0.01
PP_2687	conserved hypothetical protein gb|AE015451.1|:c3077849-3076899	1.37	**2.58**	0.04
PP_2094	nitrate-binding protein NasS putative gb|AE015451.1|:c2387100-2385886	1.37	**2.58**	0.03
PP_5233	ammonium transporter gb|AE015451.1|:c5967683-5966352	1.38	**2.60**	0.01
PP_2846	urease accessory protein UreE gb|AE015451.1|:3250091-3250594	1.45	**2.74**	0.02
PP_1703	assimilatory nitrate reductase/sulfite reductase put gb|AE015451.1|:1899399-1903472	1.85	**3.61**	0.01
PP_2092	nitrate transporter gb|AE015451.1|:c2385138-2383903	1.85	**3.61**	0.01
PP_2685	conserved hypothetical protein gb|AE015451.1|:c3076049-3075327	1.99	**3.96**	0.01
PP_2638	cellulose synthase operon C protein putative gb|AE015451.1|:3019460-3022978	2.09	**4.26**	0.00
PP_4841	branched-chain amino acid ABC transporter periplasmi gb|AE015451.1|:5508393-5509658	2.16	**4.46**	0.02
PP_2686	transglutaminase-like superfamily domain protein gb|AE015451.1|:c3076902-3076123	2.19	**4.58**	0.01
PP_1705	nitrite reductase gb|AE015451.1|:1903743-1906295	2.38	**5.20**	0.04
PP_4842	branched-chain amino acid ABC transporter permease p gb|AE015451.1|:5510246-5511286	2.54	**5.82**	0.02
PP_5234	nitrogen regulatory protein P-II gb|AE015451.1|:c5968068-5967730	3.61	**12.22**	0.01

Comparison 2

Locus name	*Gene Name*	*Log change*	*Fold change*	*P-value*
PP_0555	acetoin dehydrogenase alpha subunit gb|AE015451.1|:c645014-644037	-3.98	**-15.76**	0.00
PP_0553	acetoin dehydrogenase dihydrolipoamide acetyltransfe gb|AE015451.1|:c642984-641878	-3.65	**-12.58**	0.00
PP_0556	acetoin catabolism protein gb|AE015451.1|:c646092-645037	-3.20	**-9.19**	0.01
PP_3504	conserved hypothetical protein gb|AE015451.1|:3974810-3975076	-3.08	**-8.48**	0.02
PP_0554	acetoin dehydrogenase beta subunit gb|AE015451.1|:c644003-642981	-2.86	**-7.27**	0.01
PP_0557	acetoin catabolism regulatory protein gb|AE015451.1|:646376-648229	-2.82	**-7.06**	0.00
PP_0765	conserved hypothetical protein gb|AE015451.1|:880484-882370	-2.79	**-6.94**	0.00
PP_4794	leucyl-tRNA synthetase gb|AE015451.1|:5456267-5458873	-2.63	**-6.20**	0.01

PP_1743	sodium:solute symporter family protein gb|AE015451.1|:1942832-1944496	-2.51	**-5.71**	0.03
PP_5324	response regulator gb|AE015451.1|:c6070635-6069745	-2.50	**-5.64**	0.00
PP_0765	conserved hypothetical protein gb|AE015451.1|:880484-882370	-2.49	**-5.62**	0.00
PP_1659	conserved hypothetical protein gb|AE015451.1|:1854985-1856325	-2.28	**-4.85**	0.05
PP_2437	acyl-CoA dehydrogenase putative gb|AE015451.1|:2783545-2784789	-2.15	**-4.43**	0.02
PP_0545	aldehyde dehydrogenase family protein gb|AE015451.1|:c633438-631918	-2.13	**-4.39**	0.04
PP_2141	conserved hypothetical protein gb|AE015451.1|:2444126-2444359	-1.98	**-3.96**	0.02
PP_4454	opine ABC transporter permease protein putative gb|AE015451.1|:c5055386-5054514	-1.80	**-3.49**	0.02
PP_2569	metabolite MFS transporter MHS family gb|AE015451.1|:2935964-2937640	-1.62	**-3.07**	0.05
PP_0469	ribosomal protein L6 gb|AE015451.1|:557869-558402	1.54	**2.91**	0.05
PP_4050	glycogen synthase gb|AE015451.1|:4564755-4566314	1.64	**3.12**	0.04
PP_5075	glutamate synthase small subunit gb|AE015451.1|:c5793321-5791903	1.76	**3.39**	0.04
PP_1360	chaperonin 10 kDa gb|AE015451.1|:1549256-1549549	1.78	**3.44**	0.04
PP_3951	3-oxoadipate CoA-transferase subunit A gb|AE015451.1|:4457362-4458057	1.87	**3.67**	0.04
PP_3105	hypothetical protein gb|AE015451.1|:3507649-3508344	1.96	**3.89**	0.05
PP_4573	ATPase AAA family gb|AE015451.1|:5192819-5193664	1.98	**3.95**	0.05
PP_1385	multidrug/solvent RND transporter TtgB gb|AE015451.1|:c1581392-1578240	2.01	**4.02**	0.01
PP_4550	long-chain-fatty-acid--CoA ligase gb|AE015451.1|:c5174977-5173289	2.07	**4.19**	0.04
PP_2074	transcriptional regulator LysR family gb|AE015451.1|:2359040-2359963	2.11	**4.33**	0.01
PP_0814	cytochrome o ubiquinol oxidase subunit III gb|AE015451.1|:953190-953813	2.12	**4.35**	0.05
PP_2688	conserved hypothetical protein gb|AE015451.1|:c3079262-3077853	2.14	**4.40**	0.00
PP_2094	nitrate-binding protein NasS putative gb|AE015451.1|:c2387100-2385886	2.16	**4.48**	0.00
PP_4308	transcriptional regulator AsnC family gb|AE015451.1|:4899601-4900038	2.19	**4.56**	0.02
PP_0153	conserved hypothetical protein gb|AE015451.1|:c161965-161750	2.23	**4.69**	0.04
PP_4054	conserved hypothetical protein gb|AE015451.1|:4572905-4573189	2.26	**4.80**	0.01
PP_1794	hypothetical protein gb|AE015451.1|:c2015484-2014042	2.27	**4.83**	0.04
PP_0813	cytochrome o ubiquinol oxidase subunit I gb|AE015451.1|:951168-953186	2.31	**4.95**	0.03

PP_1795	hypothetical protein gb|AE015451.1|:c2016389-2015502	2.32	**5.00**	0.04
PP_5008	polyhydroxyalkanoate granule-associated protein GA1 gb|AE015451.1|:c5705793-5705374	2.62	**6.14**	0.00
PP_0811	cyoups2 protein gb|AE015451.1|:949961-950197	2.63	**6.18**	0.00
PP_4204	transcriptional regulator Cro/CI family gb|AE015451.1|:c4750452-4750051	2.65	**6.29**	0.01
PP_3213	ABC transporter periplasmic binding component-relate gb|AE015451.1|:c3647060-3646032	2.66	**6.33**	0.05
PP_1185	outer membrane protein H1 gb|AE015451.1|:1360133-1360738	2.72	**6.57**	0.01
PP_2686	transglutaminase-like superfamily domain protein gb|AE015451.1|:c3076902-3076123	2.72	**6.57**	0.00
PP_2687	conserved hypothetical protein gb|AE015451.1|:c3077849-3076899	2.82	**7.07**	0.00
PP_4841	branched-chain amino acid ABC transporter periplasmi gb|AE015451.1|:5508393-5509658	2.87	**7.30**	0.00
PP_2638	cellulose synthase operon C protein putative gb|AE015451.1|:3019460-3022978	2.90	**7.45**	0.02
PP_3781	oxygen-independent Coproporphyrinogen III oxidase fam gb|AE015451.1|:4308593-4310008	2.91	**7.53**	0.00
PP_1690	conserved hypothetical protein gb|AE015451.1|:c1883189-1882707	3.10	**8.56**	0.00
PP_2051	acetyl-CoA acetyltransferase gb|AE015451.1|:2333066-2334250	3.27	**9.64**	0.04
PP_2685	conserved hypothetical protein gb|AE015451.1|:c3076049-3075327	3.48	**11.14**	0.00
PP_5233	ammonium transporter gb|AE015451.1|:c5967683-5966352	3.77	**13.67**	0.00
PP_0367	conserved hypothetical protein gb|AE015451.1|:444691-445026	3.78	**13.74**	0.00
PP_4842	branched-chain amino acid ABC transporter permease p gb|AE015451.1|:5510246-5511286	3.99	**15.91**	0.00
PP_2048	acyl-CoA dehydrogenase putative gb|AE015451.1|:2329570-2331420	4.31	**19.87**	0.00
PP_2047	3-hydroxyacyl-CoA dehydrogenase family protein gb|AE015451.1|:2328410-2329648	4.39	**20.91**	0.00
PP_5234	nitrogen regulatory protein P-II gb|AE015451.1|:c5968068-5967730	4.65	**25.10**	0.00
PP_2051	acetyl-CoA acetyltransferase gb|AE015451.1|:2333066-2334250	4.80	**27.95**	0.00
PP_2049	alcohol dehydrogenase iron-containing gb|AE015451.1|:2331454-2332617	4.82	**28.31**	0.00
PP_2050	conserved hypothetical protein TIGR00051 gb|AE015451.1|:2332617-2333069	4.83	**28.42**	0.00

Supplementary Table S2. Proteomics data of proteins that were differentially expressed.

SPOT NUMBER	ID	Enzyme name	Fold change
1	gi|26992090	F0F1 ATP synthase subunit alpha	91.70
2	gi|26991521	branched-chain amino acid ABC transporter, periplasmic amino acid-binding protein, putative	35.15
5	gi|26987038	glycine betaine/L-proline ABC transporter, periplasmic binding protein	4.88
6	gi|26991724	nitrogen metabolism transcriptional regulator NtrC	6.70
7	gi|26990756	glycogen debranching protein GlgX	4.48
8	gi|26990172	hypothetical protein PP_3459	5.47
9	gi|26987893	acetolactate synthase	3.46
10	gi|26988814	OmpF family protein	2.60
11	gi|26987941	outer membrane porin	2.68
12	gi|26991722	glutamine synthetase, type I	2.20
22	gi|26987192	elongation factor G	20.03
23	gi|26991722	glutamine synthetase, type I	15.80
24	gi|26990756	glycogen debranching protein GlgX	11.70
26	gi|26988775	hypothetical protein PP_2050	9.38
27	gi|26991001	hydantoin racemase, putative	8.77
28	gi|26991724	nitrogen metabolism transcriptional regulator NtrC	4.87
29	gi|26988814	OmpF family protein	5.43
30	gi|26987296	acetyl-CoA carboxylase biotin carboxylase subunit	8.34

31	gi|26987458	ribose-phosphate pyrophosphokinase	6.55
32	gi|26989406	hypothetical protein PP_2687	5.59
33	gi|26988830	hypothetical protein PP_2105	5.51
34	gi|26990895	electron-transferring-flavoprotein dehydrogenase	4.52
35	gi|26989812	hypothetical protein PP_3093	4.85
36	gi|26988035	general amino acid ABC transporter, ATP-binding protein	4.07
37	gi|26988772	3-hydroxyacyl-CoA dehydrogenase family protein	3.97
38	gi|26988860	multifunctional fatty acid oxidation complex subunit alpha	3.06
39	gi|26989257	hypothetical protein PP_2537	3.17
40	gi|26988861	3-ketoacyl-CoA thiolase	2.95
41	gi|26990883	succinate dehydrogenase flavoprotein subunit	3.93
43	gi|26988860	multifunctional fatty acid oxidation complex subunit alpha	3.06
44	gi|26990817	NADH dehydrogenase I subunit F	2.89
45	gi|26990754	malto-oligosyltrehalose synthase	2.56
46	gi|26988807	phosphoenolpyruvate synthase	2.35
13	gi|26991567	adenylosuccinate synthetase	0.23
14	gi|26990716	isocitrate dehydrogenase, NADP-dependent	0.20
15	gi|26987293	pyruvate dehydrogenase (acetyl-transferring)	0.25
16	gi|26987292	acetoin dehydrogenase, beta subunit	0.18
17	gi|26987291	branched-chain alpha-keto acid dehydrogenase subunit E2	0.27
18	gi|26989108	branched chain amino acid ABC transporter	0.36
19	gi|26987716	leucyl aminopeptidase	0.44
47	gi|26987024	amino acid ABC transporter, periplasmic amino acid-binding protein	0.03

48	gi|26988458	ABC transporter, periplasmic binding protein	0.04
49	gi|26991547	extracellular ligand-binding receptor	0.06
50	gi|26987651	superoxide dismutase	0.05
51	gi|26992051	LysR family transcriptional regulator	0.08
52	gi|26991377	C4-type zinc finger DksA/TraR family protein	0.09
54	gi|26991067	flagellin FliC	0.17
55	gi|26988588	elongation factor P	0.12
56	gi|26988743	BNR domain-containing protein	0.13
57	gi|26987098	malate synthase G	0.11
58	gi|26988076	cell division protein FtsZ	0.14
59	gi|26986857	metal ABC transporter periplasmic-binding protein	0.13
60	gi|26991413	ferric uptake regulator, Fur family	0.16
62	gi|26987621	dipeptide ABC transporter, periplasmic peptide-binding protein	0.20
63	gi|26987283	aldehyde dehydrogenase family protein	0.17
64	gi|26990223	branched-chain amino acid aminotransferase	0.32
65	gi|26991067	flagellin FliC	0.18
67	gi|26988032	general amino acid ABC transporter, periplasmic binding protein	0.16
68	gi|26990810	isocitrate lyase	0.24
69	gi|26990740	dihydropyrimidine dehydrogenase	0.29
70	gi|26990737	allantoate amidohydrolase	0.22
71	gi|26987501	hypothetical protein PP_0765	0.22
72	gi|26988094	co-chaperonin GroES	0.36
73	gi|26990893	electron transfer flavoprotein, alpha subunit	0.27

74	gi|26987098	malate synthase G	0.25
76	gi|26991857	putrescine ABC transporter, periplasmic putrescine-binding protein	0.33
77	gi|26991502	bifunctional phosphoribosylaminoimidazolecarboxamide formyltransferase/IMP cyclohydrolase	0.22
78	gi|26987250	hypothetical protein PP_0512	0.35
79	gi|26987499	acyl-CoA synthetase	0.27
80	gi|26987501	hypothetical protein PP_0765	0.37
81	gi|26987585	nucleoside-diphosphate kinase	0.30
83	gi|26987407	serine hydroxymethyltransferase	0.28
84	gi|161378124	flagellum-specific ATP synthase	0.44
85	gi|26987578	cysteine desulfurase IscS	0.35
86	gi|26990716	isocitrate dehydrogenase, NADP-dependent	0.48
20	gi|26987193	elongation factor Tu	Novo C/N-C (UP)
21	gi|26991910	nitrogen regulatory protein P-II	Novo C/N-C (UP)
87	gi|26988772	3-hydroxyacyl-CoA dehydrogenase family protein	Novo N-C (UP)
88	gi|26987920	outer membrane protein H1	Novo N-C (UP)
89	gi|26988776	acetyl-CoA acetyltransferase	Novo N-C (UP)
90	gi|26992090	F0F1 ATP synthase subunit alpha	Novo N-C (UP)
91	gi|26990877	succinyl-CoA synthetase subunit alpha	Novo N-C (UP)

92	gi|26989024	ATP-dependent Clp protease proteolytic subunit	**Novo N-C (UP)**
93	gi|26991544	branched chain amino acid ABC transporter ATP-binding protein	**Novo N-C (UP)**
94	gi|26987502	hypothetical protein PP_0766	**Novo N-C (DOWN)**
95	gi|26987877	extracellular ligand-binding receptor	**Novo N-C (DOWN)**
96	gi|26987807	amino acid ABC transporter, periplasmic amino acid-binding protein	**Novo N-C (DOWN)**
98	gi|26987292	acetoin dehydrogenase, beta subunit	**Novo N-C (DOWN)**
99	gi|26987291	branched-chain alpha-keto acid dehydrogenase subunit E2	**Novo N-C (DOWN)**

Supplementary Table S3. Transcriptomic data of genes differentially expressed with a fold change above 3 and a *P* value below 0.02. Nitrogen- vs. dual-nutrient-limited cultures.

Locus Name	**Gene Name**	Log change	Fold change	*p*-value
PP_0389	ribosomal protein S21 gb|AE015451.1|:c475503-475288	1.85	**3.62**	0.00
PP_1099	cold-shock domain family protein gb|AE015451.1|:c1257128-1256919	1.89	**3.72**	0.02
PP_0008	ribonuclease P protein component gb|AE015451.1|:c8798-8394	1.99	**3.98**	0.02
PP_1083	bacterioferritin-associated ferredoxin putative gb|AE015451.1|:c1242882-1242664	2.03	**4.09**	0.02
PP_2048	acyl-CoA dehydrogenase putative gb|AE015451.1|:2329570-2331420	3.32	**10.01**	0.00
PP_2051	acetyl-CoA acetyltransferase gb|AE015451.1|:2333066-2334250	3.37	**10.36**	0.01
PP_2050	conserved hypothetical protein TIGR00051 gb|AE015451.1|:2332617-2333069	3.64	**12.45**	0.00
PP_2049	alcohol dehydrogenase iron-containing gb|AE015451.1|:2331454-2332617	4.00	**16.05**	0.00
PP_2047	3-hydroxyacyl-CoA dehydrogenase family protein gb|AE015451.1|:2328410-2329648	4.69	**25.84**	0.00

Curriculum vitae

Name:	Ignacio Andrés Poblete Castro
Birth date and place:	December 28th 1981, Santiago, Chile.
Nationality:	Chilean
Address:	Wendenstrasse 48, 38100 Braunschweig, Germany.
E-mail:	ignaciopobletec@gmail.com

Education

2012 – 2008	Ph.D. thesis at the Helmholtz Centre for Infection Research and ***Technical University of Braunschweig***, Germany. Supervisors: Prof. Dr. Christoph Wittmann and Prof. Dr.-Ing. Vitor Martins dos Santos.
2006 – 2007	Master in Environmental Scince, ***Universidad de Santiago de Chile***, Chile.
2000 – 2005	Environmetal Engineering, ***Universidad Tecnológica Metropolitana***, Chile.
1996 – 1999	Technical Chemistry, Liceo Industrial Domingo Matte Perez, Chile.

Training

2011	Advanced Course Metabolomics for Microbial Systems Biology, ***Technical University of Delft***. Netherlands.
2009	MFCS/win 3.0 User training, ***Sartoriuos Stedim Systems GmbH***, Melsungen, Germany.

Ignacio Andrés Poblete Castro

April 16th 2012